

**University of Alberta**

**Application of Brønsted Acid-Catalyzed Allylboration toward a  
Stereodivergent Synthesis of Eupomatilone-6**

by

**Siu Hong Yu**

A thesis submitted to the Faculty of Graduate Studies and Research in partial fulfillment  
of the requirements for the degree of Master of Science

Department of Chemistry

Edmonton, Alberta

Spring 2006



Library and  
Archives Canada

Bibliothèque et  
Archives Canada

Published Heritage  
Branch

Direction du  
Patrimoine de l'édition

395 Wellington Street  
Ottawa ON K1A 0N4  
Canada

395, rue Wellington  
Ottawa ON K1A 0N4  
Canada

*Your file* *Votre référence*  
*ISBN: 0-494-13917-X*  
*Our file* *Notre référence*  
*ISBN: 0-494-13917-X*

**NOTICE:**

The author has granted a non-exclusive license allowing Library and Archives Canada to reproduce, publish, archive, preserve, conserve, communicate to the public by telecommunication or on the Internet, loan, distribute and sell theses worldwide, for commercial or non-commercial purposes, in microform, paper, electronic and/or any other formats.

The author retains copyright ownership and moral rights in this thesis. Neither the thesis nor substantial extracts from it may be printed or otherwise reproduced without the author's permission.

**AVIS:**

L'auteur a accordé une licence non exclusive permettant à la Bibliothèque et Archives Canada de reproduire, publier, archiver, sauvegarder, conserver, transmettre au public par télécommunication ou par l'Internet, prêter, distribuer et vendre des thèses partout dans le monde, à des fins commerciales ou autres, sur support microforme, papier, électronique et/ou autres formats.

L'auteur conserve la propriété du droit d'auteur et des droits moraux qui protègent cette thèse. Ni la thèse ni des extraits substantiels de celle-ci ne doivent être imprimés ou autrement reproduits sans son autorisation.

---

In compliance with the Canadian Privacy Act some supporting forms may have been removed from this thesis.

Conformément à la loi canadienne sur la protection de la vie privée, quelques formulaires secondaires ont été enlevés de cette thèse.

While these forms may be included in the document page count, their removal does not represent any loss of content from the thesis.

Bien que ces formulaires aient inclus dans la pagination, il n'y aura aucun contenu manquant.

  
**Canada**

# University of Alberta

## Library Release Form

**Name of Author:** *Siu Hong Yu*

**Title of Thesis:** *Application of Brønsted Acid-Catalyzed Allylboration toward a Stereodivergent Synthesis of Eupomatilone-6*

**Degree:** *Master of Science*

**Year this Degree Granted:** *2006*

Permission is hereby granted to the University of Alberta Library to reproduce single copies of this thesis and to lend or sell such copies for private, scholarly or scientific research purposes only.

The author reserves all other publication and other rights in association with the copyright in the thesis, and except as herein before provided, neither the thesis nor any substantial portion thereof may be printed or otherwise reproduced in any material form whatever without the author's prior written permission.

\_\_\_\_\_  
*Signature* *Dec 2, 2005*  
434 Stonehaven Place  
London, Ontario, N6H 5N3

University of Alberta

Faculty of Graduate Studies and Research

The undersigned certify that they have read, and recommend to the Faculty of Graduate Studies and Research for acceptance, a thesis entitled *Application of Brønsted Acid-Catalyzed Allylboration toward a Stereodivergent Synthesis of Eupomatilone-6* submitted by *Siu Hong Yu* in partial fulfillment of the requirements for the degree of *Master of Science*.

---

Professor Dennis G. Hall

---

Assistant Professor Peter E. Light

---

Professor Frederick G. West

*Supervisor writes the date that the thesis is approved by committee here* Nov. 29, 2005.

**Dedicated to my grandmas**

**Yu Lee Mei Siu**

**1911 – 2005**

**&**

**Ho Chung King Fun**

**for their love and lifelong lessons  
which I am still learning everyday**

## Abstract

---

Allylboration is one of the most important carbon-carbon bond formation reactions. Chapter 2 of this thesis describes a novel Brønsted acid-catalyzed allylboration variant applicable to the most difficult, electronically deactivated allylboronate and aldehyde substrates. The usefulness of this methodology was demonstrated with a four-step, stereodivergent synthesis of all four diastereomers of eupomatilone-6. The five X-ray crystallographic structures obtained brings an end to the ambiguity of the lactone's original stereochemical assignments.

To access homoallylic alcohols, Chapter 3 investigates the Lewis acid-catalyzed allylboration. An efficient synthetic route was developed for the achiral 2-*O*-TIPS ether allylboronate, which serves as a better allylboration substrate than the 2-alkoxycarbonyl analogue at subzero temperatures.

Chapter 4 examines the concept of "Lewis acid activation of a Lewis acid" using *ortho*-substituted arylboronates. The syntheses of the desired arylboronates were challenging. Various NMR experiments did not show the desired boronate-metal complexation, but an allylstannation model reaction revealed a promising synergetic effect.

## Acknowledgement

---

The completion of this thesis would not be possible without the support from the following people. First of all, I would like to sincerely thank my supervisor Professor Dennis Hall for his patience toward research and his insightful guidance. In retrospect, I can honestly say that joining his group was one of my wisest decisions thus far. Not only was I exposed to some of the most advanced and innovative research areas in organic chemistry, but I was also deeply inspired by all of the talented Hall group members, past and present. A special thank you goes to Dr. Jason Kennedy for his initial work on the Lewis acid-catalyzed allylboration, Hugo Lachance for all his scientific advice, Eric Pelletier and Lisa Carosi for the numerous trips to the Rockies, Maria David for taking over the solvent stills and Feng Peng and Vivek Rauniyar for just being there in the same lab. I would also like to acknowledge Yuichiro Arimura for providing me with an important starting material and Felicia Owokalu who I had the privilege to supervise during my studies.

Beyond the Hall group, the research support staff at the University of Alberta has undoubtedly simplified my work enormously. I am especially indebted to the expertise provided by Dr. Bob McDonald and Dr. Mike J. Ferguson in the X-ray Crystallography Laboratory, Glen Bigam, Lai Kong and Mark Miskolzie in the NMR Laboratory, Dr. Angie Morales-Izquierdo in the Mass Spectrometry Laboratory as well as all the dedicated technicians at the Analytical and Instrumentation Laboratory. In addition, I would like to express my heartfelt gratitude to all the support staff working at the Glassblowing, Electronics and Machine Shops, the General and Purchasing Offices with a special thank you to Graduate Services Coordinator Ilona Baker, Secretary Diane Dowhaniuk and last but not least Ken Jorgensen and Bernie Hippel at the Receiving and Chemical Store. All the assistance from faxing my resume to repairing my stir plate is gratefully appreciated.

I would also like to thank Undergraduate Laboratory Coordinators Dr. Norman Gee and Dr. Lois Browne for the enjoyable and invaluable teaching experience which completely altered my career plan. I would never have imagined how challenging but fulfilling it would be to make someone understand a concept or laboratory technique.

On this occasion, I would like to acknowledge University of Alberta for granting me a Graduate Entrance Scholarship back in 2002 and Alberta Learning for awarding me a Graduate Student Scholarship in 2004.

Throughout my graduate studies, I was very fortunate to come across many good friends and inspiring people but among them, two deserve a special salute. Thank you Tina and Vince for being there right from the very beginning. It is comforting to know that there are others who share the same pain and stress (Fine! A lot less stress for me as I didn't need to go through Cums and 502 but still...) while celebrating any achievement that comes along the way.

Thank you Dr. Monica Barra at the University of Waterloo for starting my love/hate affair with organic chemistry.

Finally, thank you Grandma, Mom, Dad and Sister for the endless care and support even though they usually do not have a clue about exactly what I am working on or my next move is toward the future. Yes mom, your worries are sometimes annoying but *always* appreciated after I hang up that phone.



# Table of Contents

---

<b>CHAPTER 1 INTRODUCTION: CURRENT ADVANCES OF CATALYSIS IN ORGANIC SYNTHESIS.....</b>	<b>1</b>
1.1 Introduction.....	1
1.2 Combined Acid Catalysis.....	1
1.2.1 Background.....	1
1.2.2 Brønsted acid assisted Lewis acid (BLA) catalysis.....	2
1.2.3 Lewis acid assisted Lewis acid (LLA) catalysis.....	5
1.2.4 Lewis acid assisted Brønsted acid (LBA) catalysis.....	7
1.3 Dual Activation Catalysis.....	8
1.3.1 Background.....	8
1.3.2 Bifunctional catalysts.....	9
1.3.3 Two-catalyst catalytic system.....	10
1.3.4 Lewis base activation of a Lewis acid.....	11
1.4 Organocatalysis.....	13
1.4.1 Background.....	13
1.4.2 Covalent transition complex catalysis.....	13
1.4.3 Noncovalent activation complex catalysis.....	14
1.5 Thesis Objectives: Examination of Boronate Activation Strategies And Their Practical Applications in Allylation Reactions.....	16
1.6 References.....	18
<b>CHAPTER 2 APPLICATION OF BRØNSTED ACID-CATALYZED ALLYLBORATION TO A CONCISE, STEREODIVERGENT SYNTHESIS OF EUPOMATILONE-6.....</b>	<b>21</b>
2.1 Introduction.....	21
2.1.1 Background.....	21

2.1.2	Brønsted acid catalysis.....	24
2.2	Optimization of Brønsted Acid-Catalyzed Allylboration.....	26
2.2.1	Synthesis of starting allylboronates.....	26
2.2.2	Catalyst screening.....	27
2.2.3	Optimization on other reaction parameters.....	28
2.3	Toward The Total Synthesis of Eupomatilone-6.....	29
2.3.1	Background.....	30
2.3.2	Retrosynthetic analysis.....	31
2.3.3	Model reaction with electron-rich aldehydes.....	32
2.3.4	Diastereoselective hydrogenation.....	34
2.3.5	Access of C4-C5 <i>cis</i> lactone adduct via thermal allylboration.....	36
2.3.6	Construction of the biaryl moiety by Suzuki-Miyaura coupling.....	37
2.3.7	Synthesis of the natural eupomatilone-6.....	39
2.3.8	Summary on the stereodivergent synthesis of eupomatilone-6 diastereomers.....	41
2.4	Preliminary Mechanistic Investigation on TfOH-Catalyzed Allylboration.....	43
2.5	Enantioselective Brønsted-Acid Catalyzed Allylboration.....	48
2.5.1	Synthesis of starting chiral alkynoate esters.....	48
2.5.2	Enantioselectivity of catalyzed allylboration.....	49
2.6	Conclusion And Future Work.....	50
2.7	Experimental.....	51
2.7.1	General.....	51
2.7.2	Preparation of 2-alkoxycarbonyl allylboronates <b>13a-e</b> .....	52
2.7.2.1	Ethyl 2-[(4,4,5,5-tetramethyl-1,3,2-dioxaborolan-2-yl) methyl]-3-methylbut-2-enoate ( <b>13a</b> ).....	52
2.7.2.2	2-[(4,4,5,5-Tetramethyl-1,3,2-dioxaborolan-2-yl)methyl]-3- methylbut-2-enoic acid, (-)-menthol ester ( <b>13b</b> ).....	53
2.7.2.3	2-[(4,4,5,5-Tetramethyl-1,3,2-dioxaborolan-2-yl)methyl]-3- methylbut-2-enoic acid, (-)-8-phenylmenthol ester ( <b>13c</b> ).....	53
2.7.2.4	( <i>2E</i> )-2-[(4,4,5,5-Tetramethyl-1,3,2-dioxaborolan-2-yl)	

	methyl]-but-2-enoic acid, (-)-8-phenylmenthol ester (13d).....	54
2.7.2.5	Methyl (2 <i>E</i> )-2-[(4,4,5,5-tetramethyl-1,3,2-dioxaborolan-2-yl)methyl]-but-2-enoate (13e).....	55
2.7.3	Preparation of 4,4-dimethyl-3-methylene-5-phenyl-dihydro-furan-2-one (14) under the optimal conditions.....	56
2.7.4	Preparation of <i>rac</i> -(4 <i>R</i> <sup>*</sup> , 5 <i>S</i> <sup>*</sup> )-5-(2-bromo-3,4,5-trimethoxyphenyl)-4-methyl-3-methylene-dihydro-furan-2-one (19b) by TfOH-catalyzed allylboration.....	56
2.7.5	Preparation of <i>rac</i> -(4 <i>S</i> <sup>*</sup> , 5 <i>S</i> <sup>*</sup> )-5-(2-bromo-3,4,5-trimethoxyphenyl)-4-methyl-3-methylene-dihydro-furan-2-one (23) by thermal allylboration.....	57
2.7.6	Diastereoselective hydrogenation.....	58
2.7.6.1	<i>rac</i> -(3 <i>S</i> <sup>*</sup> , 4 <i>S</i> <sup>*</sup> , 5 <i>S</i> <sup>*</sup> )-5-(2-Bromo-3,4,5-trimethoxyphenyl)-3,4-dimethyl-dihydro-furan-2-one (20).....	58
2.7.6.2	<i>rac</i> -(3 <i>R</i> <sup>*</sup> , 4 <i>S</i> <sup>*</sup> , 5 <i>S</i> <sup>*</sup> )-5-(2-Bromo-3,4,5-trimethoxyphenyl)-3,4-dimethyl-dihydro-furan-2-one (21).....	59
2.7.6.3	<i>rac</i> -(3 <i>S</i> <sup>*</sup> , 4 <i>R</i> <sup>*</sup> , 5 <i>S</i> <sup>*</sup> )-5-(2-Bromo-3,4,5-trimethoxyphenyl)-3,4-dimethyl-dihydro-furan-2-one (24).....	60
2.7.7	Biaryls construction with Buchwald's Suzuki-coupling conditions.....	61
2.7.7.1	3,4- <i>epi</i> -15.....	61
2.7.7.2	4- <i>epi</i> -15.....	62
2.7.7.3	3- <i>epi</i> -15.....	63
2.7.8	DBU-promoted epimerization of 3- <i>epi</i> -15 to eupomatilone-6 (15).....	63
2.7.9	Preliminary mechanistic investigations.....	64
2.7.9.1	Treatment of <i>E</i> -allylboronate 13e with TfOH.....	64
2.7.9.2	Treatment of thermal <i>cis</i> -lactone 23 with TfOH.....	64
2.7.9.3	Preparation of ethyl (2 <i>Z</i> )-2-[(4,4,5,5-tetramethyl-1,3,2-dioxaborolan-2-yl)methyl]-but-2-enoate (29).....	65
2.7.9.4	Preparation of <i>rac</i> -(4 <i>R</i> <sup>*</sup> , 5 <i>S</i> <sup>*</sup> )-5-(2-bromo-3,4,5-trimethoxyphenyl)-4-methyl-3-methylene-dihydro-furan-2-	

one (19b) by TfOH-catalyzed allylboration with Z-allylboronate 29.....	66
2.7.10 Preparation of 4,4-dimethyl-3-methylene-5-phenethyl-dihydro-furan-2-one (35) by asymmetric allylboration using chiral allylboronate 13c.....	66
2.8 References.....	67

**CHAPTER 3 ACCESS TO HOMOALLYLIC ALCOHOL PRODUCTS VIA LEWIS ACID-CATALYZED ALLYLBORATION USING 2-FUNCTIONALIZED ALLYLBORONATE REAGENTS.....69**

3.1 Introduction.....	69
3.2 Lewis Acid-Catalyzed Allylboration Using 2-Alkoxy carbonyl Allylboronates.....	70
3.2.1 Synthesis of allylboronates.....	70
3.2.2 Results from Lewis acid-catalyzed allylboration using 2-alkoxy carbonyl allylboronates.....	72
3.3 Allylboration Using 2-O-Protected Ether Allylboronates.....	74
3.3.1 Synthesis of achiral allylboronates.....	74
3.3.2 Results from Lewis acid-catalyzed allylboration using 2-O-protected ether allylboronates.....	75
3.3.3 Synthetic attempts to generate chiral 2-O-TIPS ether allylboronate.....	76
3.3.3.1 Diboron coupling.....	76
3.3.3.2 Platinum-catalyzed borylation.....	78
3.3.3.3 Lithium-halogen exchange.....	78
3.3.3.4 Grignard addition using allyl halides.....	79
3.3.3.5 Generation of vinylic synthetic intermediates.....	80
3.3.3.6 Other synthetic attempts.....	81
3.4 Conclusion.....	82
3.5 Experimental.....	83
3.5.1 General.....	83

3.5.2	Preparation of 2-[(4,4,5,5-tetramethyl-1,3,2-dioxaborolan-2-yl) methyl]-prop-2-enoic acid, (-)-8-phenylmenthol ester ( <b>5b</b> ).....	84
3.5.3	Lewis acid-catalyzed allylboration using 2-alkoxycarbonyl allylboronates.....	85
3.5.3.1	<i>rac</i> -Methyl 4-hydroxy-2-methylidene-4-phenylbutanoate ( <b>6a</b> ).....	85
3.5.3.2	Methyl 4-hydroxy-2-methylidene-4-phenethylbutanoate ( <b>6b</b> ).....	85
3.5.3.3	(-)-8-Phenylmenthyl 4-hydroxy-2-methylidene-4-phenylbutanoate ( <b>7a</b> ).....	86
3.5.3.4	(-)-8-Phenylmenthyl 4-hydroxy-2-methylidene-4-phenethylbutanoate ( <b>7b</b> ).....	87
3.5.4	Generation of 2- <i>O</i> -protected ether allylboronates.....	88
3.5.4.1	2-Triisopropylsilyloxymethyl-prop-2-en-1-ol ( <b>8a</b> ).....	88
3.5.4.2	Acetic acid 2-triisopropylsilyloxymethyl-allyl ester ( <b>9a</b> )...	88
3.5.4.3	4,4,5,5-Tetramethyl-2-(2-triisopropylsilyloxymethyl-allyl)-1,3,2-dioxaborolane ( <b>11a</b> ).....	89
3.5.4.4	2-Benzyloxymethyl-prop-2-en-1-ol ( <b>8b</b> ).....	89
3.5.4.5	Acetic acid 2-benzyloxymethyl-allyl ester ( <b>9b</b> ).....	90
3.5.4.6	2-(2-Benzyloxymethyl-allyl)-4,4,5,5-tetramethyl-1,3,2-dioxaborolane ( <b>11b</b> ).....	90
3.5.5	Lewis acid-catalyzed allylboration using 2- <i>O</i> -protected ether allylboronates.....	91
3.5.5.1	<i>rac</i> -4-Hydroxy-2-methylidene-4-phenylbutan-1-ol triisopropylsilyl ether ( <b>12a</b> ).....	91
3.5.5.2	<i>rac</i> -4-Hydroxy-2-methylidene-4-phenethylbutan-1-ol triisopropylsilyl ether ( <b>12b</b> ).....	92
3.5.6	Toward the attempted synthesis of chiral 2- <i>O</i> -TIPS ether allylboronate <b>15</b> .....	92
3.5.6.1	(2-Bromomethyl-allyloxy) triisopropylsilane ( <b>16a</b> ).....	92
3.5.6.2	(2-Chloromethyl-allyloxy) triisopropylsilane ( <b>16b</b> ).....	93
3.5.6.3	2,5-Bis-triisopropylsilyloxymethyl-hexa-1,5-diene ( <b>17</b> )...	93

3.5.6.4	(2-Bromo-allyloxy) triisopropylsilane (19).....	94
3.5.6.5	Triisopropyl-prop-2-ynylloxysilane (20).....	95
3.5.6.6	2-(2-Triisopropylsilyloxymethyl-allyl)-[1,3,6,2]- dioxaborocane (22).....	95
3.5.6.7	1,10,10-Trimethyl-2-phenyl-4-(2- triisopropylsilyloxymethyl-allyl)-3,5-dioxa-4-bora- tricyclo[5.2.1.0 <sup>2,6</sup> ]decane (15).....	96
3.5.6.8	Potassium 2-triisopropylsilyloxymethyl allyltrifluoroborate (23).....	96
3.6	References.....	97

**CHAPTER 4 EXPLORATION OF LEWIS ACID ACTIVATION OF A  
LEWIS ACID USING *ORTHO*-SUBSTITUTED  
ARYLBORONATES.....99**

4.1	Introduction.....	99
4.2	Attempted Synthesis of Various <i>Ortho</i> -Substituted Arylboronates.....	101
4.2.1	Oxazoline 5.....	101
4.2.2	Imine 7.....	103
4.2.3	Quinoline 9.....	104
4.2.4	Dimethylaniline 17.....	105
4.3	Results from Various NMR Experiments.....	107
4.3.1	Varying the amount of Lewis acid.....	107
4.3.2	Lowering the experimental temperature.....	108
4.4	Model Reaction Study.....	109
4.5	Conclusion And Future Work.....	111
4.6	Experimental.....	111
4.6.1	General.....	111
4.6.2	Toward the synthesis of arylboronic ester 5.....	112
4.6.2.1	2-(4,4,5,5-Tetramethyl-1,3,2-dioxaborolan-2-yl)benzoic acid (10).....	112

4.6.2.2	2-(2-Iodophenyl)-4,5-dihydro-oxazole (12).....	112
4.6.2.3	[2-(4,5-Dihydro-oxazol-2-yl)-phenyl]boronic acid (13).....	113
4.6.2.4	2-[2-(4,4,5,5-Tetramethyl-1,3,2-dioxaborolan-2-yl)- phenyl]-4,5-dihydro-oxazole (5).....	114
4.6.3	Toward the synthesis of arylboronic ester 7.....	114
4.6.3.1	2-(4,4,5,5-Tetramethyl-1,3,2-dioxaborolan-2-yl) phenylamine (16).....	114
4.6.4	Toward the synthesis of arylboronic ester 17.....	115
4.6.4.1	Methyl-[2-(4,4,5,5-tetramethyl-1,3,2-dioxaborolan-2-yl)- phenyl] amine (18).....	115
4.6.4.2	Trimethyl-[2-(4,4,5,5-tetramethyl-1,3,2-dioxaborolan-2-yl)- phenyl] ammonium iodide (19).....	115
4.6.4.3	(2-Iodophenyl)-dimethylamine (20).....	116
4.6.4.4	Dimethyl-[2-(4,4,5,5-tetramethyl-1,3,2-dioxaborolan-2-yl)- phenyl] amine (17).....	116
4.6.5	Model allylstannation: preparation of <i>rac</i> -1-phenyl-3-buten-1-ol (24).....	117
4.7	References.....	118
<b>CHAPTER 5 THESIS CONCLUSIONS.....</b>		<b>119</b>
<b>APPENDICES: X-RAY CRYSTALLOGRAPHY REPORTS.....</b>		<b>122</b>

## List of Tables

---

Table 2-1	Chemoselectivity reversal by the choice of acid catalyst in a Diels-Alder reaction.....	25
Table 2-2	Synthesis of various starting allylboronates.....	27
Table 2-3	Catalyst screening.....	28
Table 2-4	Further optimization of other reaction parameters.....	29
Table 2-5	Model reaction between <b>13d</b> and electron-rich aldehydes.....	32
Table 2-6	Summary table of <sup>1</sup> H NMR correspondences for the lactone moiety.....	43
Table 2-7	DCC-mediated esterification to generate chiral acetylenic esters.....	48
Table 2-8	Examination of enantioselectivity of catalyzed allylboration.....	50
— . . . —		
Table 3-1	Synthesis of various 2-alkoxycarbonyl allylboronates.....	70
Table 3-2	Conditions to generate chiral alkynoate ester <b>3b</b> .....	71
Table 3-3	Optimization of allylboration parameters.....	72
Table 3-4	Results from asymmetric allylboration using <b>5b</b> and <b>5c</b> .....	73
Table 3-5	Results from Lewis acid-catalyzed allylboration using <b>11a</b> and <b>11b</b> .....	76
— . . . —		
Table 4-1	Attempted synthesis of <b>17</b> via nucleophilic substitution.....	106
Table 4-2	NMR experiments varying the amount of Lewis acid.....	108
Table 4-3	Model reaction study.....	110



## List of Figures

---

Figure 1-1	General catalyst feature for a) BLA b) LLA c) LBA and d) BBA catalysis.....	2
Figure 1-2	General structure of CAB catalysts.....	2
Figure 1-3	General concept of two-center catalysis.....	8
Figure 1-4	Bifunctional catalysts developed by Shibasaki.....	9
Figure 1-5	LLA catalysis with Sc(OTf) <sub>3</sub> and arylboronates.....	18
— . . . —		
Figure 2-1	Eupomatilone-6 and its three unnatural diastereomers.....	30
Figure 2-2	Preliminary structural assignment based on <sup>1</sup> H nOe experiment.....	34
Figure 2-3	Intramolecular π-π interactions in phenylmenthyl ester chiral allylboronate.....	50
— . . . —		
Figure 4-1	Solvolysis as an origin of compound instability.....	105

## List of Schemes

---

Scheme 1-1	Various asymmetric reactions catalyzed by CAB catalysts.....	3
Scheme 1-2	Active cationic oxazaborolidines <b>3</b> generated by protonation with strong Brønsted acids (XH) and the proposed pre-transition-state assemblies for Diels-Alder reactions.....	4
Scheme 1-3	Diels-Alder reactions catalyzed by cationic oxazaborolidines.....	4
Scheme 1-4	Examples of CBS reduction and its transition state.....	5
Scheme 1-5	Asymmetric allylboration catalyzed by Sc(OTf) <sub>3</sub> .....	6
Scheme 1-6	Catalytic enantioselective protonation of silyl enol ether.....	7
Scheme 1-7	The general catalytic cycle of chiral protonation.....	7
Scheme 1-8	Direct aldol and Michael addition reactions catalyzed by bifunctional catalysts.....	9
Scheme 1-9	Catalytic cycle for Shibasaki's bifunctional catalysts.....	10
Scheme 1-10	Corey's two-catalyst catalytic system for asymmetric cyanosilylation.....	11
Scheme 1-11	Asymmetric allylation catalyzed by chiral phosphoramides.....	11
Scheme 1-12	Concept of Lewis base activation of a Lewis acid.....	12
Scheme 1-13	Catalytic cycle for Denmark's allylation.....	12
Scheme 1-14	L-Proline-mediated enamine-promoted catalytic cycle.....	14
Scheme 1-15	Proline-catalyzed cross-aldol reaction of aldehydes.....	14
Scheme 1-16	TADDOL-catalyzed Diels-Alder reactions.....	15
Scheme 1-17	TfOH-catalyzed allylboration toward a total synthesis of eupomatilone-6.....	17
Scheme 1-18	Sc(OTf) <sub>3</sub> -catalyzed allylboration to access homoallylic alcohol products.....	17

— . . . —

Scheme 2-1	Postulated mechanisms for Type I and II allylation reagents.....	21
Scheme 2-2	Diastereoselective additions with crotylboronates.....	22
Scheme 2-3	Lewis acid-catalyzed allylboration of <b>5</b> .....	23
Scheme 2-4	Preservation of stereospecificity of Lewis acid-catalyzed allylboration compared to the uncatalyzed reaction.....	23
Scheme 2-5	Closed transition structure with Lewis acid activation.....	23
Scheme 2-6	Brønsted acid-catalyzed aza-Darzens reaction.....	24
Scheme 2-7	Stereoselective Brønsted acid-catalyzed arene-ynamide Cyclization.....	26
Scheme 2-8	Retrosynthetic plan.....	31
Scheme 2-9	Activation of aldehyde <b>18b</b> by steric-induced deconjugation.....	33
Scheme 2-10	Switching plan to a racemic synthesis.....	33
Scheme 2-11	Diastereoselective hydrogenation of <b>19b</b> and the ORTEP diagrams for <b>20</b> and <b>21</b> .....	35
Scheme 2-12	Possible explanation for the diastereoselective hydrogenation of <b>19b</b> .....	36
Scheme 2-13	Thermal allylboration followed by homogeneous hydrogenation.....	37
Scheme 2-14	Biaryl construction under Buchwald's conditions.....	38
Scheme 2-15	Attempted methoxy-directed hydrogenation with Crabtree's catalyst.....	39
Scheme 2-16	Alternative Crabtree hydrogenation on open-chain homoallylic alcohol <b>22</b> .....	40
Scheme 2-17	DBU-promoted C3-epimerization of 3- <i>epi</i> - <b>15</b> to <b>15</b> .....	41
Scheme 2-18	Stereodivergent total synthesis of all four stereoisomers of <b>15</b> ....	42
Scheme 2-19	<i>E</i> -to- <i>Z</i> isomerization of the starting allylboronate <b>13e</b> .....	44
Scheme 2-20	<i>Cis</i> -to- <i>trans</i> isomerization of the thermal allylboration adduct <b>23</b> via benzylic carbocation <b>27</b> .....	44
Scheme 2-21	Mechanistic study with TfOH-induced lactonization.....	45
Scheme 2-22	Synthesis of <i>Z</i> -allylboronate <b>29</b> and the subsequent TfOH-catalyzed allylboration.....	46

Scheme 2-23	Stereoconvergently <i>cis</i> adducts obtained from both <i>E</i> - and <i>Z</i> -allylboronates via a Type II mechanism.....	46
Scheme 2-24	Tentative mechanistic explanation for the <i>trans</i> stereochemical outcome.....	47
Scheme 2-25	<i>p</i> TSA-catalyzed esterification.....	49

— . . . —

Scheme 3-1	Literature precedent for uncatalyzed allylboration using <b>1</b> .....	69
Scheme 3-2	Application of allylboronate <b>2</b> to the synthesis of (-)-( <i>R</i> )-ipsdienol.....	70
Scheme 3-3	Generation of two different <i>O</i> -protected ether allylboronates.....	75
Scheme 3-4	Attempted synthesis of <b>15</b> via Miyaura's diboron coupling and diol exchange.....	77
Scheme 3-5	Synthesis of allylic halides <b>16a</b> and <b>16b</b> .....	77
Scheme 3-6	Failed attempts of diboron coupling via borylcopper species.....	78
Scheme 3-7	Pt-catalyzed borylation using pinacolborane.....	78
Scheme 3-8	Attempted lithium-halogen exchange with allyl bromide <b>16a</b> .....	79
Scheme 3-9	Dimerization via attempted Grignard additions.....	79
Scheme 3-10	Synthesis of alkenyl bromide <b>19</b> .....	80
Scheme 3-11	Attempted synthesis of <b>11a</b> via vinylstannane intermediate <b>21</b> ....	81
Scheme 3-12	Attempted ester reduction in the presence of the boronate moiety.....	81
Scheme 3-13	Various diol exchange attempts.....	83

— . . . —

Scheme 4-1	Concept of Lewis acid activation of a Lewis acid using <i>ortho</i> -substituted arylboronate <b>1</b> .....	99
Scheme 4-2	Target arylboronates <b>5</b> , <b>7</b> , <b>9</b> and their corresponding commercially available starting materials.....	100
Scheme 4-3	First attempt to generate arylboronate <b>5</b> .....	101
Scheme 4-4	Attempted synthesis of <b>5</b> via amide coupling.....	101

Scheme 4-5	Attempted synthesis of <b>5</b> by Pd-catalyzed coupling.....	102
Scheme 4-6	Generation of <b>5</b> via lithium-halogen exchange.....	102
Scheme 4-7	Alternative synthesis of <b>5</b> avoiding the boronic acid intermediate.....	103
Scheme 4-8	Attempted synthesis of imine <b>7</b> .....	103
Scheme 4-9	Attempted synthesis of quinoline <b>9</b> .....	104
Scheme 4-10	Attempted reductive amination to generate <b>17</b> .....	105
Scheme 4-11	Last attempts to generate <b>17</b> from 2-iodoaniline.....	107
Scheme 4-12	VT NMR experiment with phenol <b>22</b> .....	109

## List of Abbreviations

---

Ac	Acetyl
AIBN	2,2'-Azobis(2-methylpropionitrile)
Anal.	Elemental analysis
app	Apparent
Ar	Aryl
B	Generic base
BBA	Brønsted acid assisted Brønsted acid
BINOL	1,1'-Bi-2-Naphthol
BLA	Brønsted acid assisted Lewis acid
BMS	Borane dimethyl sulfide
Bn	Benzyl
<i>i</i> Bu	Isobutyl
<i>n</i> Bu	<i>n</i> -Butyl
<i>s</i> Bu	<i>sec</i> -Butyl
<i>t</i> Bu	<i>tert</i> -Butyl
CAB	Chiral acyloxyborane
Calcd	Calculated
CBS	Corey, Bakshi and Shibata
Cy	Cyclohexyl
d (in <sup>1</sup> H NMR)	Doublet
dba	Dibenzylideneacetone
dd	Doublet of doublets
ddd	Doublet of doublets of doublets
DMSO	Dimethyl sulfoxide
dppf	1,1'-Bis(diphenylphosphino)ferrocene
dq	Doublet of quartets
dt	Doublet of triplets
DBU	1,8-Diazabicyclo[5.4.0]undec-7-ene

DCC	1,3-Dicyclohexylcarbodiimide
DEAM-PS	<i>N,N</i> -diethanolaminomethyl polystyrene
DIBALH	Diisobutylaluminum hydride
DMAP	4-( <i>N,N</i> -Dimethylamino)pyridine
DMF	<i>N,N</i> -Dimethylformamide
dr	Diastereomeric ratio
E	Generic electrophile
EDCI	<i>N</i> -(3-Dimethylaminopropyl)- <i>N'</i> -ethylcarbodiimide hydrochloride
ee	Enantiomeric excess
EI	Electron impact
equiv	Equivalents
ES	Electrospray
Et	Ethyl
EWG	Generic electron-withdrawing group
HIV	Human immunodeficiency virus
HMPA	Hexamethylphosphoramide
HOBT	1-Hydroxybenzotriazole
HPLC	High performance liquid chromatography
HRMS	High resolution mass spectrometry
IR	Infrared spectroscopy
LA	Generic Lewis acid
LAH	Lithium aluminum hydride
LB	Generic Lewis base
LBA	Lewis acid assisted Brønsted acid
LLA	Lewis acid assisted Lewis acid
m	Multiplet
Me	Methyl
ML <sub>n</sub>	Generic metal with ligands
Ms	Methanesulfonyl
ms	Molecular sieves

NMR	Nuclear magnetic resonance
nOe	Nuclear Overhauser effect
ORTEP	Oak Ridge thermal ellipsoid plot
PG	Generic protecting group
Ph	Phenyl
pin	Pinacol
PMP	1,2,2,6,6-Pentamethylpiperidine
<i>i</i> Pr	Isopropyl
q	Quartet
qt	Quartet of triplets
R	Generic alkyl group
rt	Room temperature
s	Singlet
SPhos	2-Dicyclohexylphosphino-2',6'-dimethoxy-1,1'-biphenyl
t	Triplet
TADDOL	$\alpha,\alpha,\alpha',\alpha'$ -Tetraaryl-1,3-dioxolan-4,5-dimethanol
td	Triplet of doublets
TBS	<i>tert</i> -Butyldimethylsilyl
Tf	Trifluoromethanesulfonyl
TFA	Trifluoroacetic acid
THF	Tetrahydrofuran
TIPS	Triisopropylsilyl
TLC	Thin layer chromatography
<i>p</i> TSA	<i>para</i> -Toluenesulfonic acid
UV	Ultraviolet
vac.	Vacuum
VT	Varying temperature



# Chapter 1 Introduction: Current Advances of Catalysis in Organic Synthesis

---

## 1.1 Introduction

In 1812, Kirchoff reported one of the first scientific observations of a catalytic transformation.<sup>1</sup> He showed that in hot water solution, starch was changed into dextrine and sugar in the presence of certain mineral acids while the acids themselves were not altered by the reaction. By definition, catalysis refers to a mechanism in which the reaction is caused or accelerated by substances that do not *appear* to take any part in the process.<sup>2</sup> Performing reactions catalytically is not only atom economical,<sup>3</sup> it more importantly provides an unique opportunity to make difficult transformations possible and practical. In modern chemistry, the role of catalysis on improving reactivity, selectivity and versatility of a wide variety of reactions is absolutely undeniable and pursuit of more efficient catalytic systems remains one of the main driving forces pushing the forefront of organic chemistry research. The catalysis topics presented in this chapter, which is categorized into combined acid, dual activation and organocatalysis with each subdivided into different underlying catalytic modes of action, are selected to highlight the current advances and practicality of using Lewis and Brønsted acid species in homogeneous catalysis.

## 1.2 Combined Acid Catalysis<sup>4</sup>

### 1.2.1 Background

In an excellent review, Yamamoto coined the term “designer acids” and identified four different modes of combined acid catalysis, namely Brønsted acid assisted Lewis acid (BLA), Lewis acid assisted Lewis acid (LLA), Lewis acid

assisted Brønsted acid (LBA) and Brønsted acid assisted Brønsted acid (BBA) catalysis (Figure 1-1).<sup>4</sup> By combining acids, the inherent reactivity of each acid could be brought out by associative interactions while an effective asymmetric environment could be generated by the more-organized transition state structure. The ultimate goal of such designer acids is to engineer a combination of acids with higher reactivity, selectivity and versatility than the individual acid catalysts alone. In order to follow the organization of this introduction, BBA catalysis will be discussed under organocatalysis (Section 1.4.3).

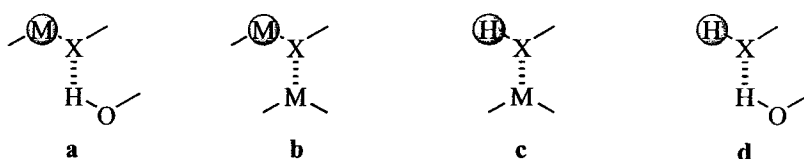
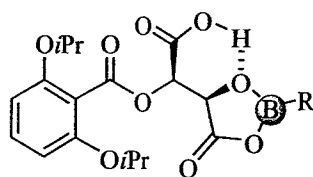


**Figure 1-1.** General catalyst feature for a) BLA b) LLA c) LBA and d) BBA catalysis.<sup>4</sup>

### 1.2.2 Brønsted acid assisted Lewis acid (BLA) catalysis

First reported in 1988 by Yamamoto and co-workers as an “activating device for carboxylic acids” because of borane’s unique electrophilicity,<sup>5</sup> chiral acyloxyborane (CAB) catalysts **1a-c** (Figure 1-2) have been demonstrated to be

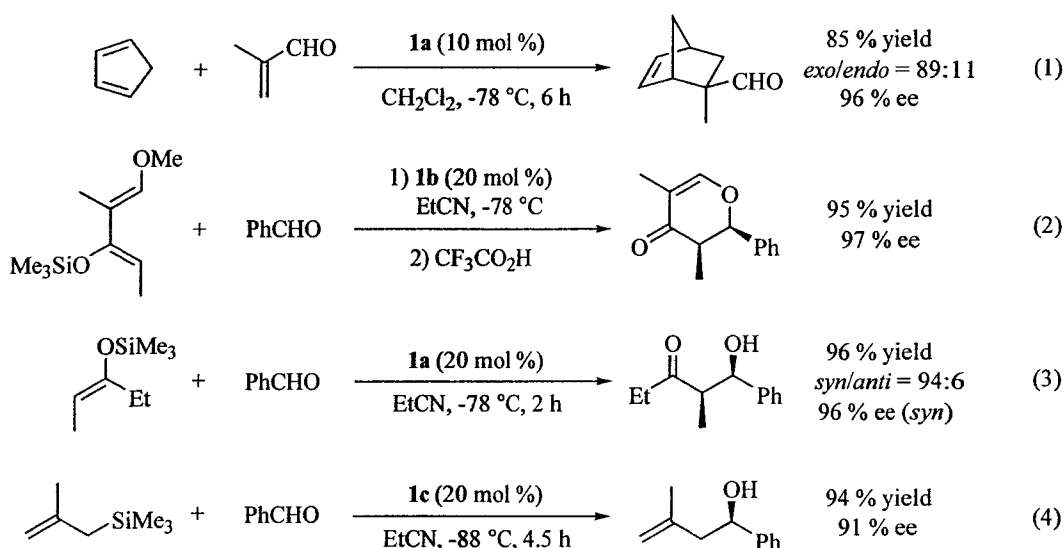


R = H (**1a**); 2-methoxyphenyl (**1b**); 3,5-bis(trifluoromethyl)phenyl (**1c**)

**Figure 1-2.** General structure of CAB catalysts.

uniformly effective for Diels-Alder (Equation 1),<sup>6</sup> hetero Diels-Alder (Equation 2),<sup>7</sup> aldol (Equation 3)<sup>8</sup> and Sakurai-Hosomi allylation (Equation 4)<sup>9</sup> reactions (Scheme 1-1). The high reactivity of CAB catalysts is originated from intramolecular hydrogen bonding of the internal carboxylic acid to the alkoxy

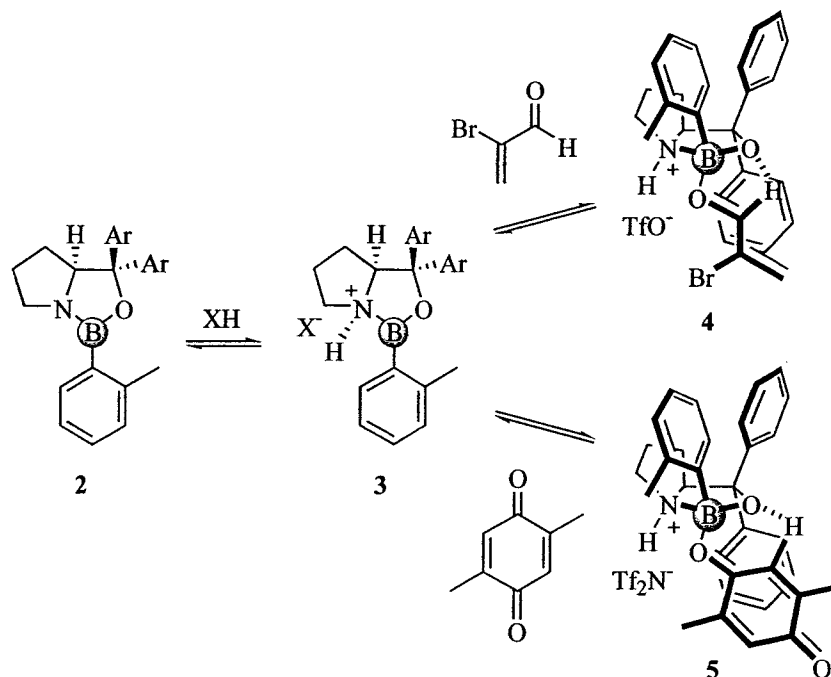
oxygen atom. Based on a series of *n*Oe experiments, the effective shielding of the CAB-activated aldehydes arises from  $\pi$ -stacking of the 2,6-diisopropoxyphenyl ring moiety with the  $\pi$  system of the aldehydes.<sup>10</sup> Despite the limited substrate scope and the need for relatively high catalyst loadings, the concept of BLA catalysis has paved a new avenue for asymmetric catalysis.



**Scheme 1-1.** Various asymmetric reactions catalyzed by CAB catalysts.

In 2002, Corey and co-workers reported an intermolecular variant of BLA catalysis for Diels-Alder reactions using chiral proline-derived oxazaborolidines **2** combined with triflic acid (Scheme 1-2).<sup>11</sup> In essence, triflic acid (TfOH) is used here as an external, strong Brønsted acid activator to generate a potent cationic Lewis acid **3**. Even using the least reactive 1,3-butadiene with catalyst loading as low as 6 mol %, the Diels-Alder reaction was carried out with high yield and enantioselectivity (Scheme 1-3, Equation 5). The same research group later reported that the use of triflimide (Tf<sub>2</sub>NH) in place of TfOH improves catalyst stability without losing potency and further expanded the reaction scope to enantioselective Diels-Alder reactions involving quinones as dienophiles (Equation 6).<sup>12</sup> Even though the exact mechanism was not addressed, these results illustrate that the role of the counter anion (*X*<sup>-</sup>) cannot be ignored in these systems. The absolute stereochemical outcomes for the two cases in Scheme 1-3

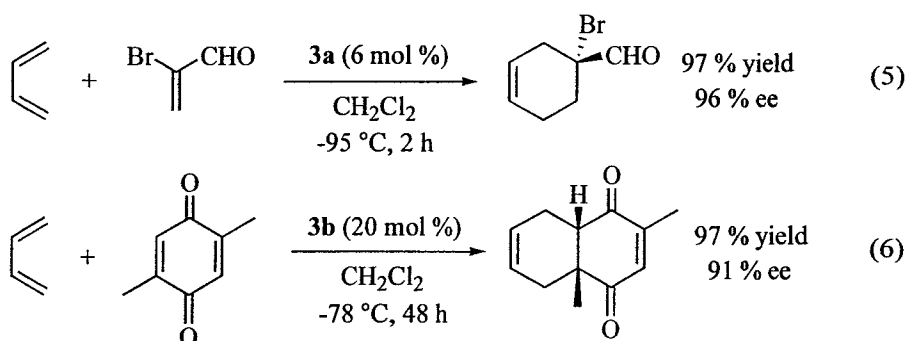
were explained on the basis of the pre-transition-state assemblies **4** and **5**, respectively (Scheme 1-2). The concept of BLA catalysis intrigues us and formulates the basis of the work done in Chapter 2 of this thesis.



**3a:** X = OTf, Ar = 3,5-dimethylphenyl (only the phenyl ring is shown for clarity);

**3b:** X = NTf<sub>2</sub>, Ar = Ph

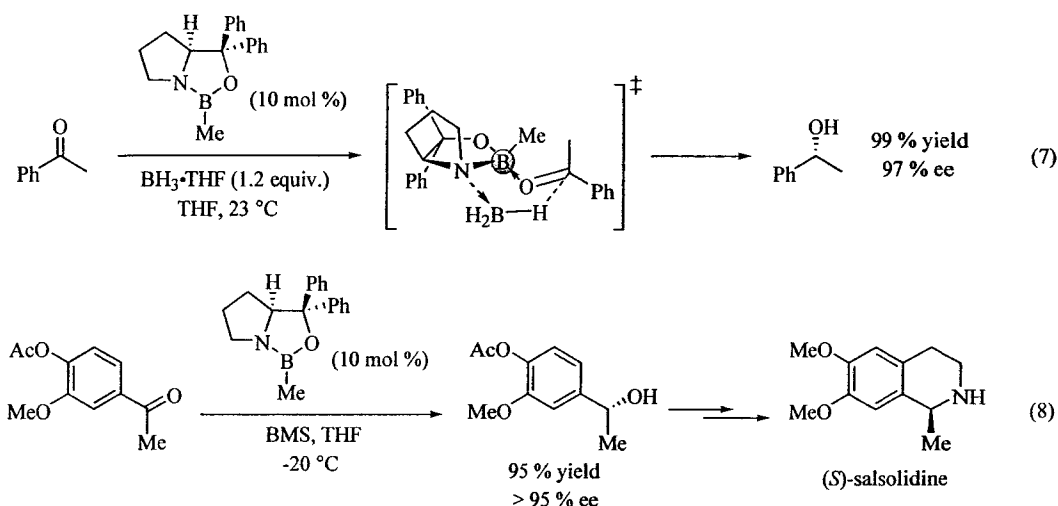
**Scheme 1-2.** Active cationic oxazaborolidines **3** generated by protonation with strong Brønsted acids (XH) and the proposed pre-transition-state assemblies for Diels-Alder reactions.



**Scheme 1-3.** Diels-Alder reactions catalyzed by cationic oxazaborolidines.

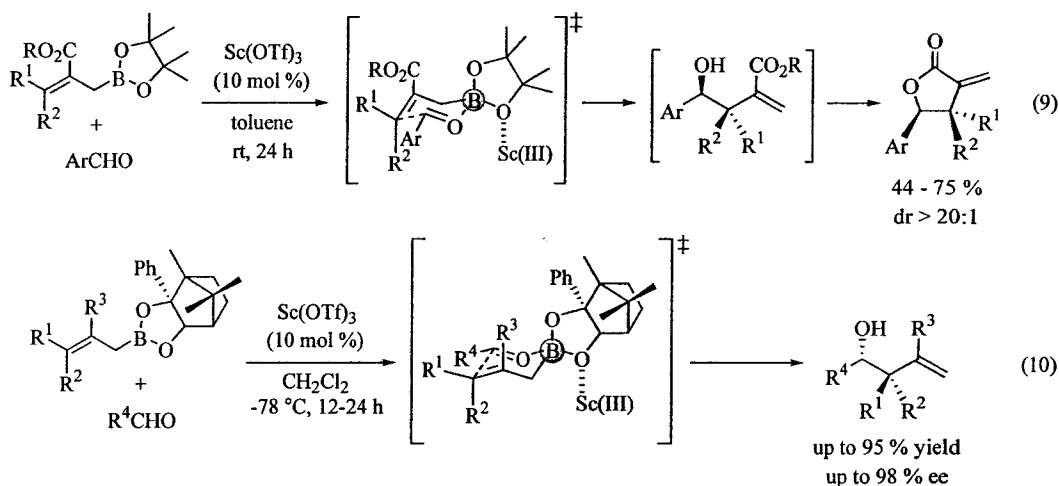
### 1.2.3 Lewis acid assisted Lewis acid (LLA) catalysis

Electron-deficient metal centers can be further activated to become even stronger electrophiles through homo- or heterobimetallic associative interactions and reactive LLA catalysts are relatively well known. Named after its developers Corey, Bakshi and Shibata, CBS reduction is one of the most efficient asymmetric catalytic methods for the reduction of unfunctionalized ketones<sup>13</sup> and the catalyst itself is a classic example of homobimetallic LLA catalyst. The general mechanism involves the coordination of the electrophilic BH<sub>3</sub> to the nitrogen atom of the oxazaborolidine, which serves to activate BH<sub>3</sub> as the hydride donor and also to increase the Lewis acidity of the endocyclic boron atom. The now stronger Lewis acidic complex then readily binds to the ketone at the more sterically accessible electron lone pair and *cis* to the vicinal BH<sub>3</sub> group (Scheme 1-4, Equation 7). As a result, the chiral catalyst is capable of both activating the ketone while assembling the hydride reagent for face-discrimination. In Equation 8, the synthesis of (*S*)-salsolidine is just one of the numerous examples of natural product syntheses making use of CBS reduction.<sup>14</sup>



**Scheme 1-4.** Examples of CBS reduction and its transition state.

As for an example of heterobimetallic LLA catalysis, our research group reported the first Lewis acid-catalyzed allylboration protocol (Scheme 1-5, Equation 9).<sup>15</sup> Based on the fact that the diastereospecificity of the uncatalyzed reaction is preserved and the results of a comprehensive mechanistic study,<sup>16c</sup> the allylboration is thought to proceed via the usual cyclic Zimmerman-Traxler transition state. With Lewis acid coordination to one of the boronate oxygen atoms, the electrophilic boron is further activated leading to the dramatic rate acceleration observed in the formation of the homoallylic alcohol intermediates. Upon *in situ* cyclization, the overall reaction provides  $\alpha$ -methylene- $\gamma$ -butyrolactone adducts which could be served as useful synthetic intermediates. It was found, however, that allylation between deactivated 2-alkoxycarbonyl allylboronates and electron-rich aromatic aldehydes gives only moderate yields and dual auxiliary approach is required to give high enantioselectivities.

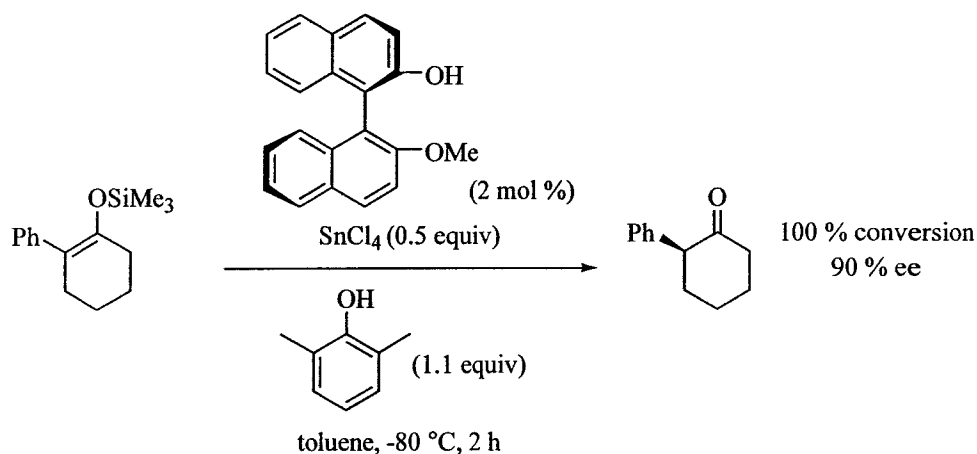


**Scheme 1-5.** Asymmetric allylboration catalyzed by Sc(OTf)<sub>3</sub>.

Using chiral allylboronates without the ester moiety, our group further extended the Lewis acid-catalyzed allylboration methodology to generate homoallylic alcohols in high yields and excellent enantioselectivities (Equation 10).<sup>16a,b</sup> Chapter 3 and 4 of this thesis will further explore the concept of LLA catalysis using boronate compounds.

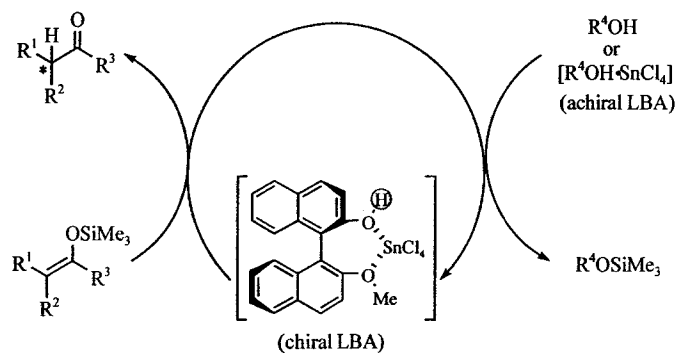
### 1.2.4 Lewis acid assisted Brønsted acid (LBA) catalysis

When Lewis acids are combined with Brønsted acids (e.g. anhydrous  $\text{HF}\cdot\text{BF}_3$  and  $\text{HCl}\cdot\text{AlCl}_3$ ), the resulting superacids effectively catalyze hydrocarbon transformations.<sup>17</sup> The chiral version based on this concept of LBA catalysis was utilized by Yamamoto in 1996 to perform catalytic enantioselective protonation of silyl enol ethers (Scheme 1-6).<sup>18</sup> The active catalyst (chiral LBA) is generated *in*



**Scheme 1-6.** Catalytic enantioselective protonation of silyl enol ether.

*situ* from optically pure monomethoxy-BINOL and  $\text{SnCl}_4$  in the presence of an achiral proton source (Scheme 1-7). The catalytic cycle presupposes the following



**Scheme 1-7.** The general catalytic cycle of chiral protonation.

features: 1) after protonation of silyl enol ethers with the chiral LBA, there requires an achiral proton source to regenerate the chiral proton reagent and this role is played by the phenol additive; 2)  $\text{SnCl}_4$  must be predominantly coordinated to the chiral proton source; 3) the reactivity of chiral LBA must be much higher than that of achiral LBA. In this practical application, the coordination of the Lewis acid to the heteroatom of the Brønsted acid is crucial for increasing the acidity of the latter.

### 1.3 Dual Activation Catalysis<sup>19, 20</sup>

#### 1.3.1 Background

The problem with classical catalysis, where an electrophile is activated by a Lewis acid or a nucleophile is activated by a Lewis base, is that many substrates are still not reactive enough for the desired reaction to occur. To further broaden the spectrum of catalysis from combined acid catalysis (Section 1.2), one obvious approach to this problem is the integration of Brønsted or Lewis base with Lewis acid working in concert to achieve “dual activation”.<sup>20</sup> Learning from nature’s enzymatic catalytic action, the idea is to use a catalyst that consists of a Lewis acid moiety that activates the electrophilic substrate while a basic site of the same catalyst (or catalytic system) activates the nucleophilic reagent (Figure 1-3). Three general strategies will be discussed in this section.

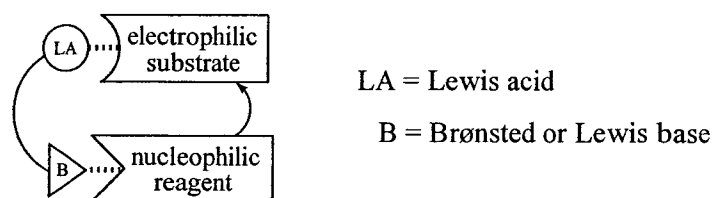


**Figure 1-3.** General concept of two-center catalysis.



### 1.3.2 Bifunctional catalysts

The design of bifunctional catalysts is to integrate two separate catalytic moieties into one molecule giving rise to a cooperative mode of action. The development of bifunctional catalysts **6**, **7** and **8** (Figure 1-4) by Shibasaki and co-

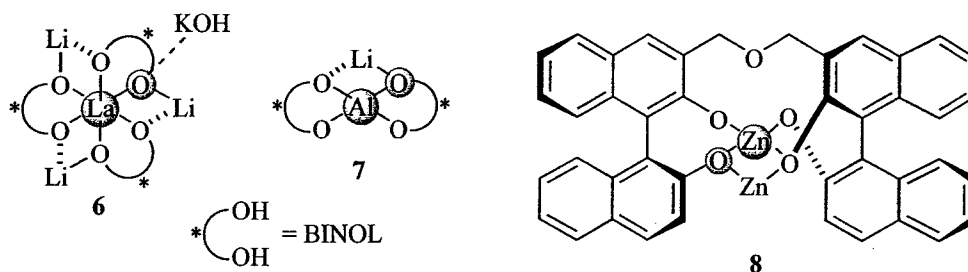
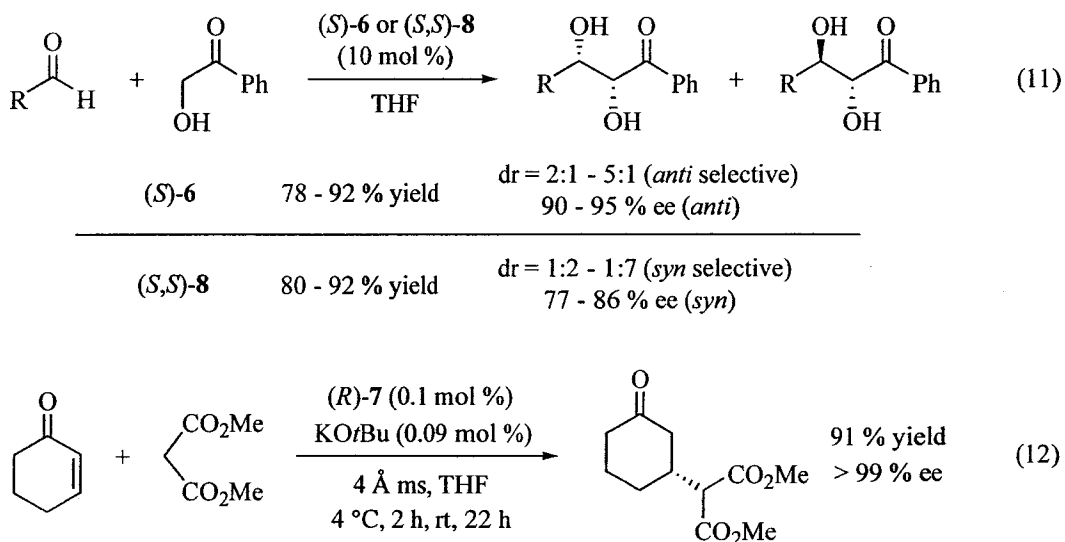


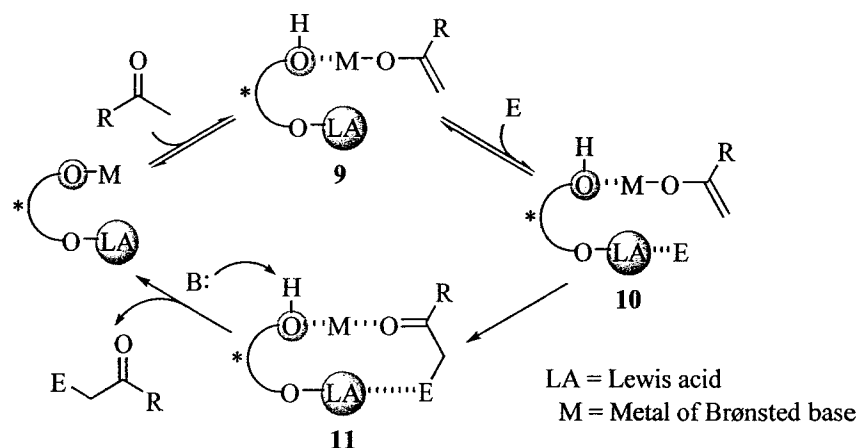
Figure 1-4. Bifunctional catalysts developed by Shibasaki.

workers represents a remarkable breakthrough in enantioselective direct aldol<sup>21</sup> and conjugate addition<sup>22</sup> reactions (Scheme 1-8 Equation 11 and 12, respectively).



Scheme 1-8. Direct aldol and Michael addition reactions catalyzed by bifunctional catalysts.

It is noteworthy to point out that **6** and **8** give complementary *anti/syn* selectivity and that the Michael addition using **7** was carried out on a kilogram scale. Both reactions are thought to be catalyzed mainly by the Brønsted basicity of the catalysts, whereas the Lewis acidity assists the catalysis by coordinating to the electrophile thus both activating and positioning the latter (Scheme 1-9). The first step is the rate-determining deprotonation of the  $\alpha$ -hydrogen to generate metal enolate **9** followed by the activation of electrophile (E) by the Lewis acid moiety (LA) to give intermediate **10**. The metal enolate then reacts with the activated electrophile in a chelation-controlled asymmetric environment to afford intermediate **11**. Upon deprotonation, the optically active reaction adduct is produced along with the regeneration of catalyst.

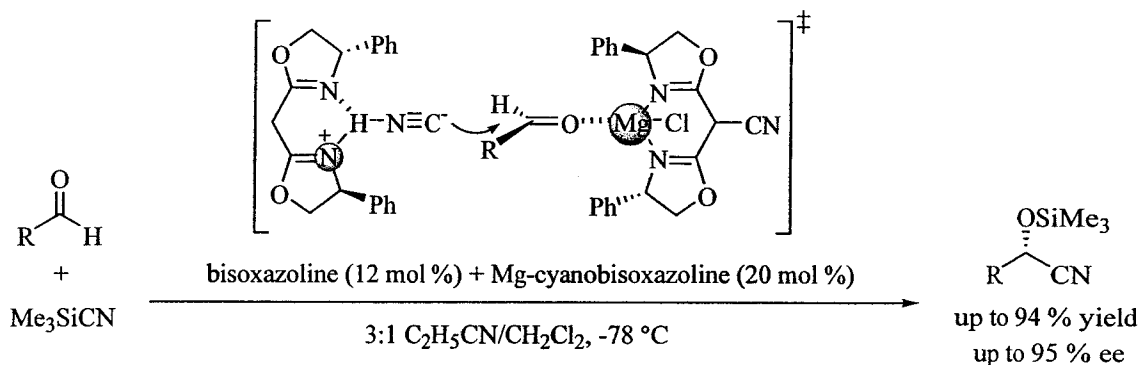


**Scheme 1-9.** Catalytic cycle for Shibasaki's bifunctional catalysts.

### 1.3.3 Two-catalyst catalytic system

While cyanosilylation can be catalyzed by either Lewis acids or Lewis bases, Corey and co-workers reported that the simultaneous use of both could generate a synergistic two-catalyst catalytic system efficient for the asymmetric addition of trimethylsilyl cyanide ( $\text{Me}_3\text{SiCN}$ ) to aldehydes (Scheme 1-10).<sup>23</sup> The metal-free bisoxazoline acts as a Brønsted base to activate the hydrogen cyanide, which is believed to be formed *in situ* from the hydrolysis of  $\text{Me}_3\text{SiCN}$  caused by

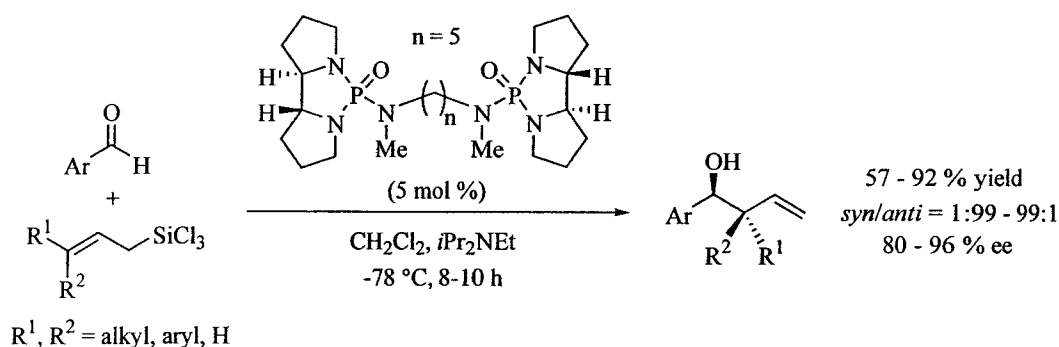
adventitious traces of water. Meanwhile, the magnesium cyanobisoxazoline serves as a Lewis acid to activate the aldehyde. Base on this pioneering work, most recently reported metal-catalyzed, enantioselective cyanosilylations operate under this double activation as a key feature.<sup>20</sup>



**Scheme 1-10.** Corey's two-catalyst catalytic system for asymmetric cyanosilylation.

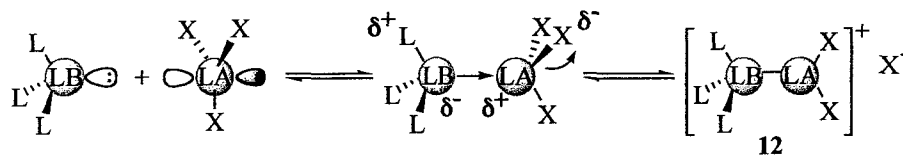
### 1.3.4 Lewis base activation of a Lewis acid<sup>24</sup>

Although it first appeared to contradict general chemical intuition, the concept of activation of Lewis acid by Lewis base was applied by Denmark and co-workers in their allylation chemistry using chiral phosphoramides (Scheme 1-11).<sup>24</sup> The key success of this catalysis concept relies on the fact that upon complexation with the Lewis base, electron transfer does not take place toward



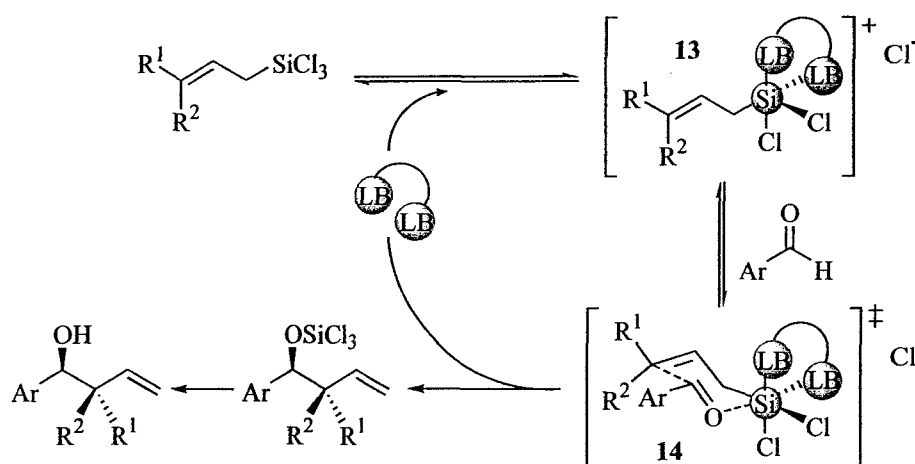
**Scheme 1-11.** Asymmetric allylation catalyzed by chiral phosphoramides.

the Lewis acid central atom, but rather toward its peripheral ligands generating a cationic species **12** with enhanced Lewis acidity (Scheme 1-12). The excellent



**Scheme 1-12.** Concept of Lewis base activation of a Lewis acid.

diastereoselectivity of these allylations can be explained by the closed, chair-like transition structure **14** depicted in Scheme 1-13.<sup>25</sup> In the mechanism, the Lewis base coordinates to the weakly Lewis acidic allylsilane to give hypervalent silicon species **13** which now acts as a strong Lewis acid to activate the aldehyde for allylation. This ligand-accelerated, dual activation strategy, which involves the tandem activation of electrophile via the reactive species generated from the activation of nucleophile, leads to the high reaction rates and excellent transfer of stereochemical information. As no transition metal is present in the phosphoramidate catalyst, this particular methodology was included in Dalako's recent review on organocatalysis<sup>26</sup> which will be discussed in the next section (Section 1.4).



**Scheme 1-13.** Catalytic cycle for Denmark's allylation.

## 1.4 Organocatalysis

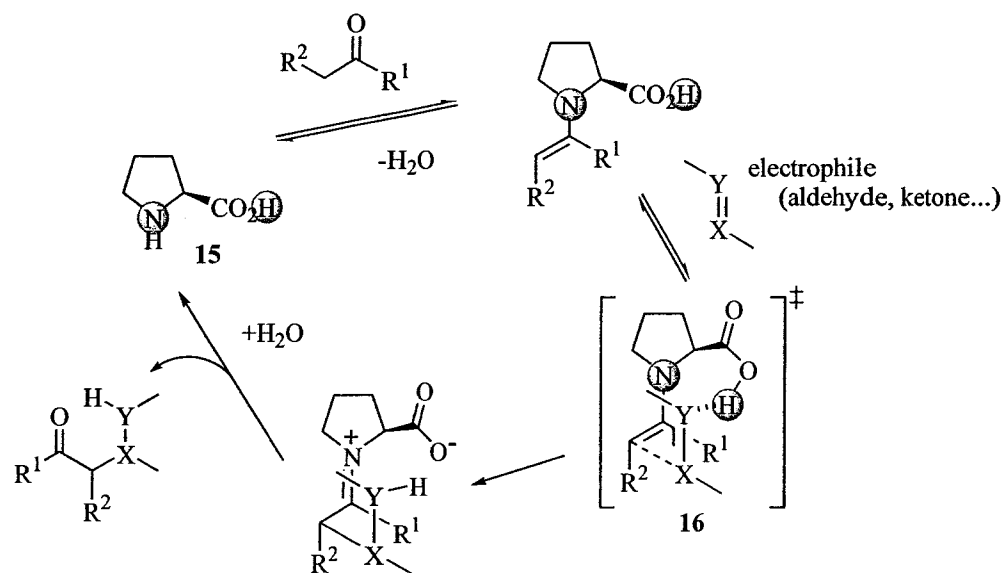
### 1.4.1 Background<sup>26</sup>

Many metals are toxic and their usage often poses a real challenge in terms of the production process in chemical and pharmaceutical industries. Organocatalysis refers to the acceleration of chemical reactions using a substoichiometric amount of a metal-free organic compound. In addition to being environmentally benign, recent evidence has revealed that this type of catalysis played a determinant role in the formation of prebiotic essential building blocks, such as sugars, and as a result allowed the introduction and spread of homochirality in living organisms.<sup>27</sup> In general, when an organocatalytic reaction proceeds via a covalent transition complex, the reaction is recognized to have a tighter transition state than those mediated by conventional metal catalysts. On the other hand, an organocatalytic reaction can also occur via a looser, noncovalent activation complex. Because of these “tighter” and “looser” transition states, improved or, in some cases, completely new chemistry could spring out when an organocatalyst is employed to catalyze a reaction.

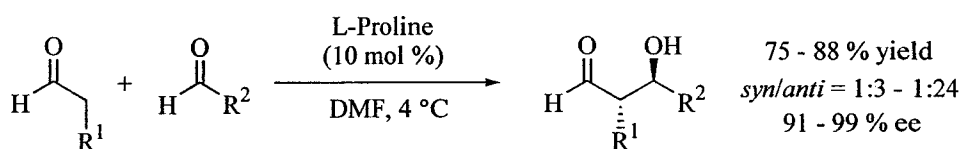
### 1.4.2 Covalent transition complex catalysis

Commonly consisted of a Lewis base and a Brønsted acid centers, most organocatalysts currently used are bifunctional (Section 1.3.2).<sup>20</sup> The vast majority involves amine-based chemistry<sup>28</sup> using amino acids, peptides, alkaloids or synthetic nitrogen-containing molecules as catalyst, with L-proline (**15**) being the most successful, and proceeds via the generalized enamine catalytic cycle shown in Scheme 1-14.<sup>26</sup> As the only natural amino acid that consists of a secondary amine functionality, proline's higher  $pK_a$  value and thus enhanced nucleophilicity relative to other amino acids make proline a good organocatalyst. It first reacts covalently as a nucleophile with carbonyl groups or Michael acceptors to form iminium ions or enamines, while the carboxylic acid moiety can

then act as a Brønsted acid to activate the electrophile. Because of this hydrogen-bonding network (structure **16**), which is crucial for charge stabilization and C-C bond formation in the highly organized transition state, proline-mediated reactions often give exceptional enantioselectivity. As an example, MacMillan and co-workers reported the first direct enantioselective cross-aldol reaction of aldehydes using L-proline (Scheme 1-15).<sup>29</sup>



**Scheme 1-14.** L-Proline-mediated enamine-promoted catalytic cycle.

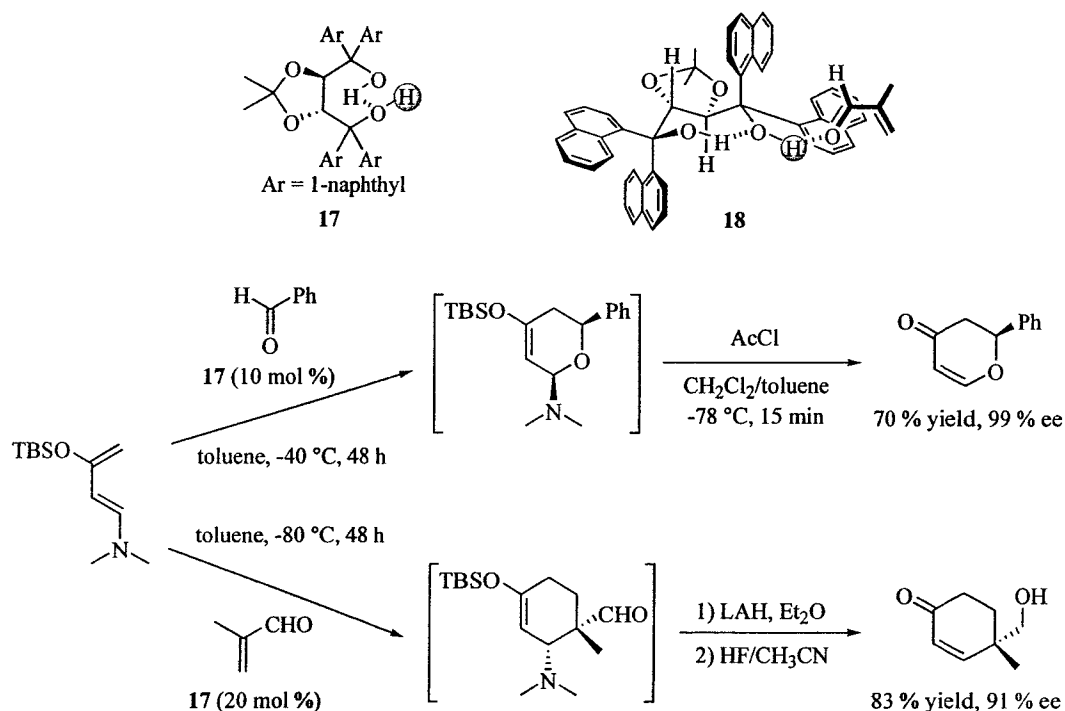


**Scheme 1-15.** Proline-catalyzed cross-aldol reaction of aldehydes.

### 1.4.3 Noncovalent activation complex catalysis

As demonstrated in the above proline-based catalytic cycle (Scheme 1-14), hydrogen bonding can play an important role in organizing the transition state structure of a reaction. Being one of the most efficient chiral backbones for asymmetric synthesis, intramolecular hydrogen bonding has been observed in

TADDOL.<sup>30</sup> In consequence, the non-hydrogen bonded proton becomes more Brønsted acidic and available for intermolecular interactions. Returning to the concept of combined acid catalysis (Section 1.2), Rawal and co-workers took advantage of this Brønsted acid assisted Brønsted acid (BBA) catalytic mode of action and developed a TADDOL-catalyzed Diels-Alder methodology using **17** (Scheme 1-16).<sup>31</sup> The initial cycloadducts in both cases can be further transformed into useful chiral building blocks for natural product synthesis. Based on the proposed pre-transition-state assembly **18**, well-defined intramolecular hydrogen bonding organizes TADDOL's chiral backbone while at the same time increases the Brønsted acidity of the free hydroxy proton which in turn activates the dienophile. This organocatalysis, which involves a noncovalent activated complex, effectively achieved what has previously only been accomplished by enzymes and antibodies and opened up broad potential for metal-free catalysis in asymmetric synthesis.



**Scheme 1-16.** TADDOL-catalyzed Diels-Alder reactions.

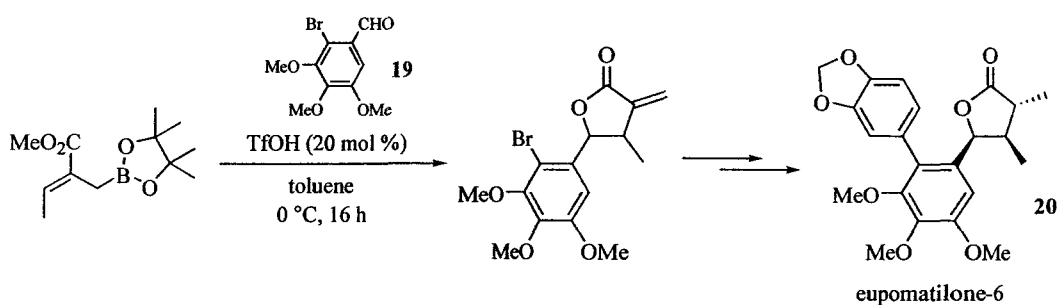
While the basic fundamental definition of catalysis stated at the beginning of this chapter has not changed over the years, new concepts have recently sprung up and enriched the field of organic chemistry. In addition to their interesting mechanisms, the above-mentioned catalytic methodologies using Brønsted or Lewis acid have more importantly demonstrated high practicality in terms of improving the scope of difficult transformations, reactivity and selectivity, large-scale chemical production and natural product synthesis.

### **1.5 Thesis Objectives: Examination of Boronate Activation Strategies And Their Practical Applications in Allylation Reactions**

In 2002, our laboratory reported the surprising findings that additions of allylboronates to aldehydes can be accelerated by Lewis acids.<sup>15</sup> While this important discovery has led to the uncovering of a new mode of boronate activation, the main focus of this thesis is to further explore the concepts of combined acid catalysis using boronate compounds. Making use of Yamamoto's terminology, the two catalytic modes of action of interest here are Brønsted acid assisted Lewis acid (BLA) and Lewis acid assisted Lewis acid (LLA) catalysis (Section 1.2.2 and 1.2.3, respectively).

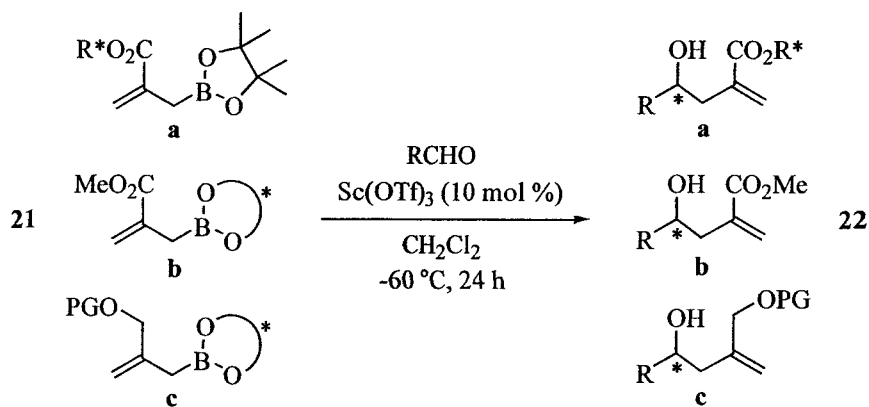
Chapter 2, which summarizes the most recent and positive results, examines the possibility of Brønsted acid-catalyzed allylboration. The chapter first describes the optimization process of TfOH-catalyzed allylboration and then in the second part, focuses on our effort to apply the methodology toward a total synthesis of eupomatilone-6 (**20**) using a very electron-rich, thus difficult, aldehyde **19** as the allylboration partner (Scheme 1-17). Four different stereoisomers of **20** were successfully synthesized in the aim to clear away the ambiguity of the structural assignment published in the original literature.





**Scheme 1-17.** TfOH-catalyzed allylboration toward a total synthesis of eupomatilone-6.

In an attempt to access homoallylic alcohol products **22a-c** enantioselectively, we explored the Lewis acid-catalyzed allylboration using allylboronates **21a-c** (Scheme 1-18). Synthesis of substrates **21a** and **21b**, the subsequent allylboration results as well as the laborious attempt to make **21c** will be discussed in Chapter 3 in full details.



**Scheme 1-18.** Sc(OTf)<sub>3</sub>-catalyzed allylboration to access homoallylic alcohol products.

Lastly, Chapter 4 looks into the intermolecular Lewis acid activation of Lewis acid via the complexation of Sc(OTf)<sub>3</sub> to *ortho*-substituted arylboronates as depicted in structure **23** (Figure 1-5). Full account of the synthesis of various *ortho*-substituted arylboronates, VT NMR experiment results and conclusions drawn from model allylstannations and allylsilylations reactions will be presented.

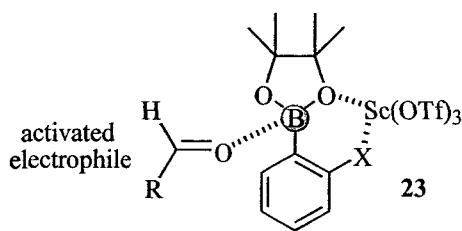


**Figure 1-5.** LLA catalysis with  $\text{Sc}(\text{OTf})_3$  and arylboronates.

## 1.6 References

1. Kirchhof, *Schweigger's Jour.* **1812**, *4*, 108.
2. Sabatier, P., Part II in *Catalysis Then And Now*, Franklin Publishing Company, Inc., Englewood, **1965**, pp 1.
3. Trost, B. M. *Science* **1991**, *254*, 1471-1477.
4. Yamamoto, H.; Futatsugi, K. *Angew. Chem. Int. Ed.* **2005**, *44*, 1924-1942.
5. Furuta, K.; Miwa, Y.; Iwanaga, K.; Yamamoto, H. *J. Am. Chem. Soc.* **1988**, *110*, 6254-6255.
6. Furuta, K.; Shimizu, S.; Miwa, Y.; Yamamoto, H. *J. Org. Chem.* **1989**, *54*, 1481-1483.
7. Gao, Q.; Maruyama, T.; Mouri, M.; Yamamoto, H. *J. Org. Chem.* **1992**, *57*, 1951-1952.
8. Furuta, K.; Maruyama, T.; Yamamoto, H. *J. Am. Chem. Soc.* **1991**, *113*, 1041-1042.
9. Ishihara, K.; Mouri, M.; Gao, Q.; Maruyama, T.; Furuta, K.; Yamamoto, H. *J. Am. Chem. Soc.* **1993**, *115*, 11490-11495.
10. Ishihara, K.; Gao, Q.; Yamamoto, H. *J. Am. Chem. Soc.* **1993**, *115*, 10412-10413.
11. a) Corey, E. J.; Shibata, T.; Lee, T. W. *J. Am. Chem. Soc.* **2002**, *124*, 3808-3809. b) Ryu, D. H.; Lee, T. W.; Corey, E. J. *J. Am. Chem. Soc.* **2002**, *124*, 9992-9993.
12. Ryu, D. H.; Corey, E. J. *J. Am. Chem. Soc.* **2003**, *125*, 6388-6390.

13. a) Corey, E. J.; Bakshi, R. K.; Shibata, S. *J. Am. Chem. Soc.* **1987**, *109*, 5551-5553. b) Corey, E. J.; Helal, C. J. *Angew. Chem. Int. Ed.* **1998**, *37*, 1986-2012.
14. Ponzio, V. L.; Kaufman, T. S. *Tetrahedron Lett.* **1995**, *36*, 9105-9108.
15. a) Kennedy, J. W. J.; Hall, D. G. *J. Am. Chem. Soc.* **2002**, *124*, 11586-11587. b) Kennedy, J. W. J.; Hall, D. G. *J. Org. Chem.* **2004**, *69*, 4412-4428.
16. a) Lachance, H.; Lu, X.; Gravel, M.; Hall, D. G. *J. Am. Chem. Soc.* **2003**, *125*, 10160-10161. b) Gravel, M.; Lachance, H.; Lu, X.; Hall, D. G. *Synthesis* **2004**, *8*, 1290-1302. c) Rauniyar, V.; Hall, D. G. *J. Am. Chem. Soc.* **2004**, *126*, 4518-4519.
17. Olah, G. A.; Prakash, G. K. S.; Sommer, J. *Science* **1979**, *206*, 13-20.
18. Ishihara, K.; Nakamura, S.; Kaneeda, M.; Yamamoto, H. *J. Am. Chem. Soc.* **1996**, *118*, 12854-12855.
19. Shibasaki, M.; Kanai, M.; Funabashi, K. *Chem. Commun.* **2002**, 1989-1999.
20. Ma, J.-A.; Cahard, D. *Angew. Chem. Int. Ed.* **2004**, *43*, 4566-4583.
21. a) Yoshikawa, N.; Yamada, Y. M. A.; Das, J.; Sasai, H.; Shibasaki, M. *J. Am. Chem. Soc.* **1999**, *121*, 4168-4178. b) Yoshikawa, N.; Kumagai, N.; Matsunaga, S.; Moll, G.; Ohshima, T.; Suzuki, T.; Shibasaki, M. *J. Am. Chem. Soc.* **2001**, *123*, 2466-2467.
22. a) Shimizu, S.; Ohori, K.; Arai, T.; Sasai, H.; Shibasaki, M. *J. Org. Chem.* **1998**, *63*, 7547-7551. b) Xu, Y.; Ohori, K.; Ohshima, T.; Shibasaki, M. *Tetrahedron* **2002**, *58*, 2585-2588.
23. Corey, E. J.; Wang, Z. *Tetrahedron Lett.* **1993**, *34*, 4001-4004.
24. a) Denmark, S. E.; Fu, J. *Chem. Rev.* **2003**, *103*, 2763-2794. b) Denmark, S. E.; Fu, J. *Chem. Commun.* **2003**, 167-170.
25. Denmark, S. E.; Fu, J. *J. Am. Chem. Soc.* **2003**, *125*, 2208-2216.
26. Dalko, P. I.; Moisan, L. *Angew. Chem. Int. Ed.* **2004**, *43*, 5138-5175.
27. Pizzarello, S.; Weber, A. L. *Science* **2004**, *303*, 1151.
28. Westermann, B. *Angew. Chem. Int. Ed.* **2003**, *42*, 151-153.

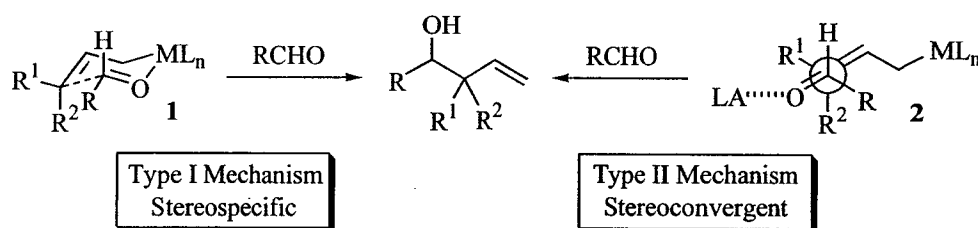
29. Northrup, A. B.; MacMillan, D. W. C. *J. Am. Chem. Soc.* **2002**, *124*, 6798-6799.
30. Seebach, D.; Beck, A. K.; Heckel, A. *Angew. Chem. Int. Ed.* **2001**, *40*, 92-138.
31. a) Huang, Y.; Unni, A. K.; Thadani, A. N.; Rawal, V. H. *Nature* **2003**, *424*, 146. b) Thadani, A. N.; Stankovic, A. R.; Rawal, V. H. *Proc. Natl. Acad. Sci. USA* **2004**, *101*, 5846-5850.

# Chapter 2 Application of Brønsted Acid-Catalyzed Allylboration to a Concise, Stereodivergent Synthesis of Eupomatilone-6

## 2.1 Introduction

### 2.1.1 Background

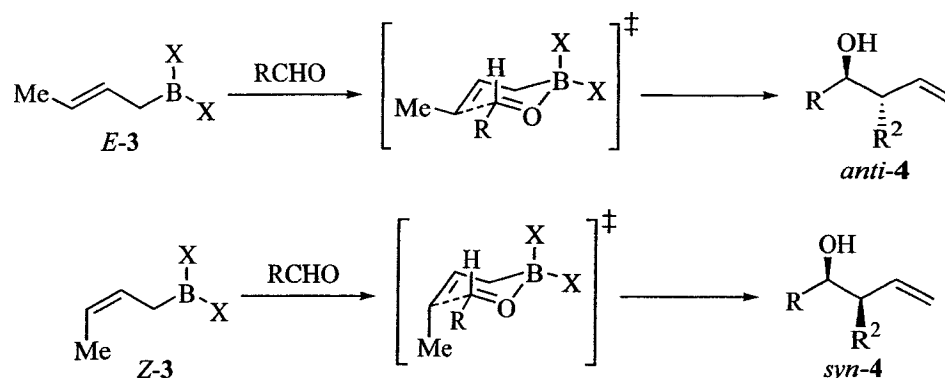
The addition of allylboronates to aldehydes is one of the most important carbon-carbon bond formation reactions.<sup>1</sup> The resulting homoallylic alcohol adducts stand for a highly prized class of synthetic intermediates for the construction of complex natural products. According to Denmark and Weber's classification,<sup>2</sup> carbonyl allylation with allylboronates proceeds via the Type I mechanism where a cyclic, chair-like transition state **1** characterized by internal activation of the carbonyl group by the boron atom is involved (Scheme 2-1, M =



**Scheme 2-1.** Postulated mechanisms for Type I and II allylation reagents.

B). As a result, the stereochemical outcome of aldehyde allylboration with  $\gamma$ -substituted reagents tend to be stereospecific with high predictability. For example, *E*- and *Z*-crotylboronates **3** reliably provide the *anti* and *syn* homoallylic alcohols **4**, respectively (Scheme 2-2). In contrast, Type II reagents, such as allyl trialkylsilanes and allyl trialkylstannanes (Scheme 2-1, M = Si or Sn), generally react with aldehydes under external Lewis acid activation and proceed via an open

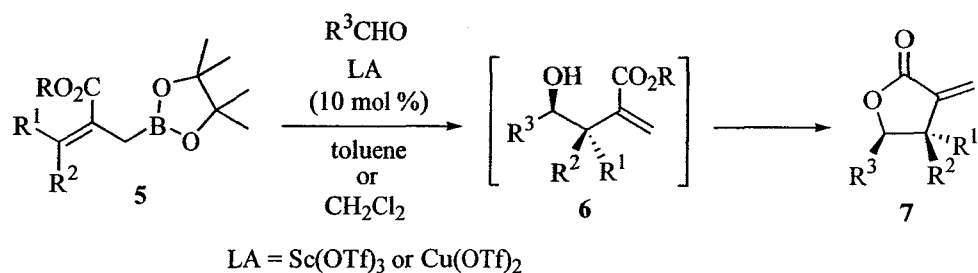
transition structure **2** giving stereoconvergent products usually with lower diastereoselectivity.



**Scheme 2-2.** Diastereoselective additions with crotylboronates.

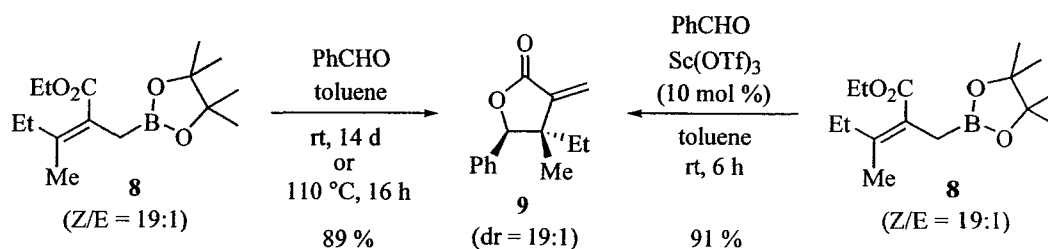
In addition to their superior diastereoselectivity, allylboronates are environmentally more benign than allylic tin reagents and their reactivity can be modulated more easily than allylic silicon reagents by varying the two remaining boron substituents (i.e., X in Scheme 2-2).<sup>3</sup> In terms of practicality, allylboronates are in general more air- and moisture-stable than their borane counterparts making the former more attractive to industrial applications.

As mentioned above, because of the internal activation of the aldehyde by the boron atom itself in the closed transition state, it was believed that acceleration of allylboration by an external Lewis acid was redundant and might even be detrimental to the diastereoselectivity by potentially disrupting the Type I mechanism. Since our group recently disclosed the first examples of Lewis acid-catalyzed allylboration,<sup>4</sup> however, these perspectives have been reconsidered. With isomerically pure tetrasubstituted 2-alkoxycarbonyl allylboronates **5**,<sup>5</sup> our group discovered that certain metal triflates catalyze the addition of **5** to aldehydes to give synthetically and biologically useful  $\alpha$ -exomethylene  $\gamma$ -lactone products **7** upon *in situ* lactonization of the homoallylic alcohol adducts **6** (Scheme 2-3). The reaction temperatures were almost 100 °C lower than the



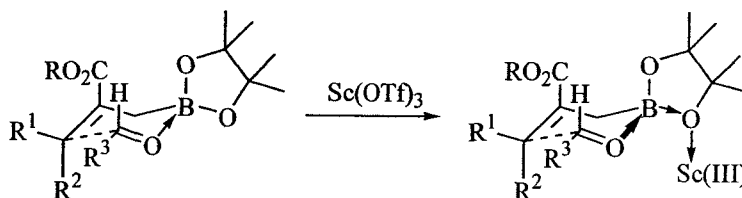
**Scheme 2-3.** Lewis acid-catalyzed allylboration of **5**.

uncatalyzed reactions and comparative kinetic experiments showed that Sc(OTf)<sub>3</sub>-catalysis provided at least a 35-fold acceleration in reaction rate for the reaction. More importantly, the stereospecificity observed in the uncatalyzed allylborations was preserved as demonstrated in Scheme 2-4 using allylboronate **8**.



**Scheme 2-4.** Preservation of stereospecificity of Lewis acid-catalyzed allylboration compared to the uncatalyzed reaction.

Based on the results of a comprehensive mechanistic study,<sup>6</sup> the allylboration is thought to proceed via the usual Type I mechanism with the Lewis acid coordinated to one of the boronate oxygen atoms (Scheme 2-5). The dramatic



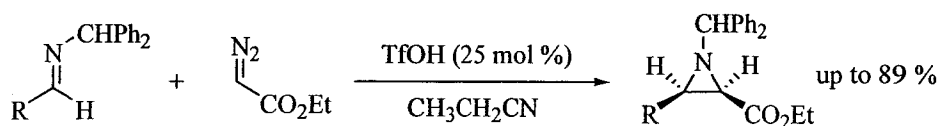
**Scheme 2-5.** Closed transition structure with Lewis acid activation.

rate acceleration observed is the consequence of a new catalytic motif where the electrophilicity of the boron atom is further increased by the Lewis acid coordination.

Despite the dramatic rate acceleration, however, this particular Lewis acid-catalyzed allylboration is limited to operate at room temperature which is a shortcoming that hampered the development of an enantioselective protocol using chiral allylboronates.<sup>4b</sup> Due to the inherent deactivation from the electron-withdrawing 2-carboxyester substituent present on the allylboronates, electron-rich aromatic aldehydes tend to be poor allylboration partners. In order to expand substrate scope and to allow absolute stereochemical control of products, the pursuit of a new catalytic method is essential. In this work, we sought to explore new catalytic mode of allylboration via Brønsted acid catalysis.

### 2.1.2 Brønsted acid catalysis

As exemplified in Chapter 1, a proton can introduce some very intriguing catalytic chemistry. More recently, Johnston and co-workers turned to Brønsted acid catalysis to expand the scope of Lewis acid-catalyzed aza-Darzens reactions and reported the first carbon-carbon bond-forming reaction using diazo compounds and a Schiff base in the presence of a Brønsted acid (Scheme 2-6).<sup>7</sup> Their initial catalyst screening revealed the superiority of triflic acid in terms of both reaction temperature (-78 °C compared to 25 °C for most other acids) and time (5 h instead of 18-24 h). Catalytic in protic acid despite the basic nature of the final aziridine product, the protocol could be scaled-up to 5 g with catalyst loading as low as 7 mol %.

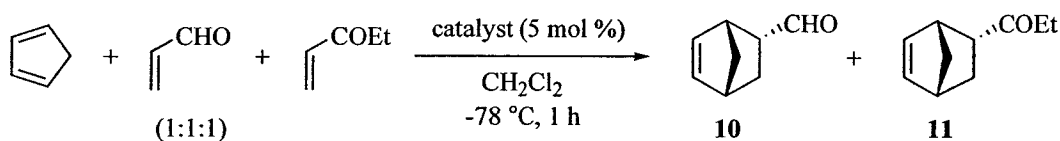


**Scheme 2-6.** Brønsted acid-catalyzed aza-Darzens reaction.



Earlier this year, Yamamoto and co-workers described a highly chemoselective Diels-Alder reaction catalyzed by Brønsted acid and the unprecedented reversal of chemoselectivity by the choice of acid catalyst (Table 2-1).<sup>8</sup> The excellent chemoselectivity can be explained by the steric demand of each catalyst. The proton of triflimide could be regarded as the smallest Lewis acid, thus would be insensitive to steric effects and selectively coordinates to the more basic  $\alpha,\beta$ -unsaturated ketone carbonyl group giving rise to Diels-Alder adduct **11**. Bulkier Lewis acids such as SnCl<sub>4</sub> on the other hand preferentially coordinate to the  $\alpha,\beta$ -unsaturated aldehyde generating adduct **10** due to the severe steric repulsion present in the competing  $\alpha,\beta$ -unsaturated ketone.

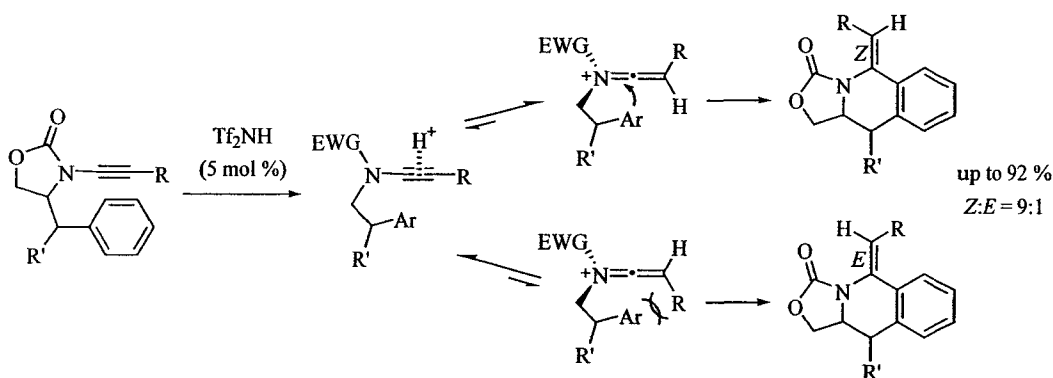
**Table 2-1.** Chemoselectivity reversal by the choice of acid catalyst in a Diels-Alder reaction.



Catalyst	Yield (%)	<b>10:11</b>
Tf <sub>2</sub> NH	93	5:95
SnCl <sub>4</sub>	73	97:3

Last but not least, Hsung and co-workers reported a highly stereoselective Brønsted acid-catalyzed arene-ynamide cyclization leading to an efficient synthesis of nitrogen heterocycles (Scheme 2-7).<sup>9</sup> The authors proposed that steric interactions between the R group and the incoming arene can account for the observed stereochemical outcome giving the *Z*-isomer as the major product.

With all the promising literature precedents showcasing the practicality, chemoselectivity and stereoselectivity in Brønsted acid catalysis, our initial goal was to explore the idea of using Brønsted acids to address some of the limitations of the Lewis acid-catalyzed allylboration alluded to in Section 2.1.1. As it turned



**Scheme 2-7.** Stereoselective Brønsted acid-catalyzed arene-ynamide cyclization.

out, after having successfully developed a Brønsted acid-catalyzed allylboration protocol (Sections 2.2 and 2.5), this project quickly evolved into applying the methodology to a natural product synthesis (Section 2.3 and 2.4). Under Yamamoto's terminology, Brønsted acid-catalyzed allylboration could be categorized as Brønsted acid assisted Lewis acid catalysis, a concept by which we were greatly inspired. For simplicity, and as a detailed mechanism has not yet been deduced, we would simply refer our methodology as Brønsted acid catalysis for the rest of the chapter.

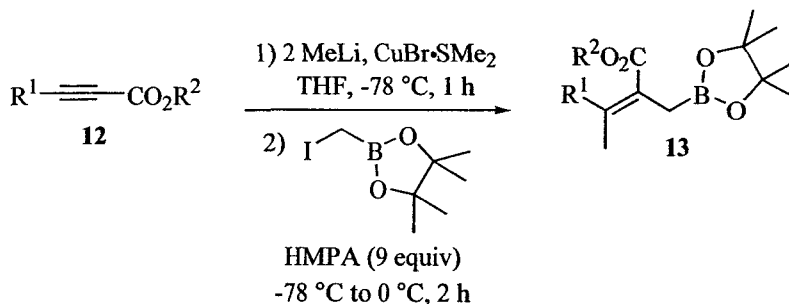
## 2.2 Optimization of Brønsted Acid-Catalyzed Allylboration

### 2.2.1 Synthesis of starting allylboronates

In order to carry out a study on allylboration, we first synthesized the desired allylboronates **13a-e** in good to excellent yields using the procedure developed by our group (Table 2-2).<sup>4b,5</sup> Since the project was first initiated as a methodology toward asymmetric allylboration, chiral auxiliaries were used in **13b-d** to test their stability, reactivity and enantioselectivity under Brønsted acid catalysis. Allylboronates **13d** and **13e** are used in Section 2.3.3 concerning the synthesis of the titled natural product eupomatilone-6. While chiral alkynoate esters **12b** and **12c** were synthesized according to literature procedures,<sup>4b</sup> an

improved synthesis of **12d**<sup>24</sup> as well as the results obtained from a preliminary study on asymmetric allylboration will be briefly discussed in Section 2.5.

**Table 2-2.** Synthesis of various starting allylboronates.

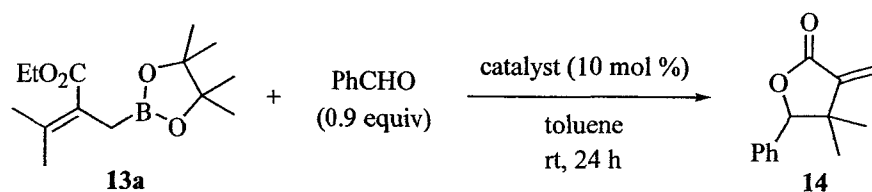


<b>13</b>	R <sup>1</sup>	R <sup>2</sup>	Yield (%) <sup>a</sup>
<b>a</b>	Me	Et	74
<b>b</b>	Me	(-)-menthyl	77
<b>c</b>	Me	(-)-8-phenylmenthyl	54
<b>d</b>	H	(-)-8-phenylmenthyl	87
<b>e</b>	H	Me	77

<sup>a</sup> Isolated yields.

### 2.2.2 Catalyst screening

With the desired allylboronates in hand, the next obvious step was to search for a promising Brønsted acid catalyst. Stirred for 24 h at room temperature, a solution of allylboronate **13a** and benzaldehyde in toluene was treated with 10 mol % of acid catalyst (Table 2-3). The 3,3-dimethyl group was selected to ensure lactonization (*gem*-dialkyl effect<sup>10</sup>) and to simplify characterization of the lactone product **14** by removing one stereogenic center. Furthermore, **13a** is more sterically demanding thus less reactive compared to its crotyl analogues and would serve as a good test for the reactivity under Brønsted acid catalysis. As shown in Table 2-3, both triflimide and triflic acid provided superior conversions. However, as triflimide is a fuming solid that quickly melts

**Table 2-3.** Catalyst screening.

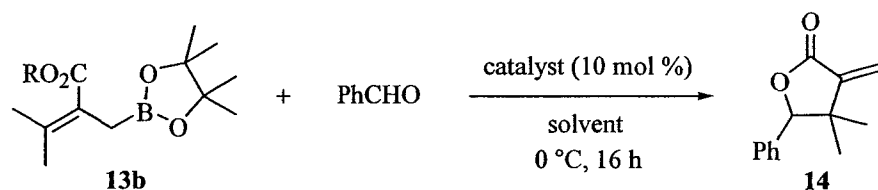
Catalyst	Yield (%) <sup>a</sup>
None	< 5 <sup>b</sup>
TFA	77
TfOH	99
Tf <sub>2</sub> NH	99

<sup>a</sup> Isolated yields. <sup>b</sup> Based on <sup>1</sup>H NMR analysis of crude reaction mixture.

upon exposure to air, triflic acid was selected owing to its easier handling for further optimization. In addition, some preliminary experiments done by another group member later on have shown that triflic acid is more efficient than triflimide for catalyzing the allylboration of interest at lower temperatures. Since complete consumption of the aldehyde was thought to be crucial for an eventual enantioselective allylboration protocol, and reductive workup is not viable here due to the presence of a lactone functionality in the product, only 0.9 equivalents of aldehyde was used during the initial optimization stage.

### 2.2.3 Optimization on other reaction parameters

In order to further improve the efficiency of the TfOH-catalyzed allylboration protocol, optimization on reaction solvent and amount of aldehyde used was undertaken (Table 2-4). Dichloromethane and toluene, which are the two solvents of choice for allylboration,<sup>3</sup> were tested and toluene gave moderately better results. It is noteworthy to highlight that the reaction temperature was lowered to 0 °C and reaction time shortened to 16 h where Sc(OTf)<sub>3</sub> was found to be inefficient (Entry 2), illustrating the superior rate acceleration provided by

**Table 2-4.** Further optimization of other reaction parameters.

Entry	Amount of PhCHO (equiv)	Catalyst	Solvent <sup>a</sup>	Yield (%) <sup>b</sup>
1	0.9	TfOH	CH <sub>2</sub> Cl <sub>2</sub>	64
2	0.9	Sc(OTf) <sub>3</sub>	toluene	< 5 <sup>c</sup>
3	0.9	TfOH	toluene	78
4	1.5	TfOH	toluene	96
5	2.0	TfOH	toluene	99

<sup>a</sup> 1 M solution of allylboronate. <sup>b</sup> Isolated yields. <sup>c</sup> From <sup>1</sup>H NMR analysis of crude reaction mixture.

Brønsted acid catalysis. In terms of the amount of aldehyde used, excess aldehyde gave higher yields and we settled at 2 equivalents as the optimum. During the course of reaction optimization, it was also found that the concentration of the reaction mixture is crucial and 1 M solution with respect to the starting allylboronate was recognized to be the most practical.

### 2.3 Toward The Total Synthesis of Eupomatilone-6

Over the progress of this methodology development, it did not take long for us to realize the potential of applying the Brønsted acid-catalyzed allylboronation protocol to natural product synthesis. Sections 2.3 and 2.4 present the full account of a concise, stereodivergent total synthesis of all four diastereomers of eupomatilone-6.

### 2.3.1 Background

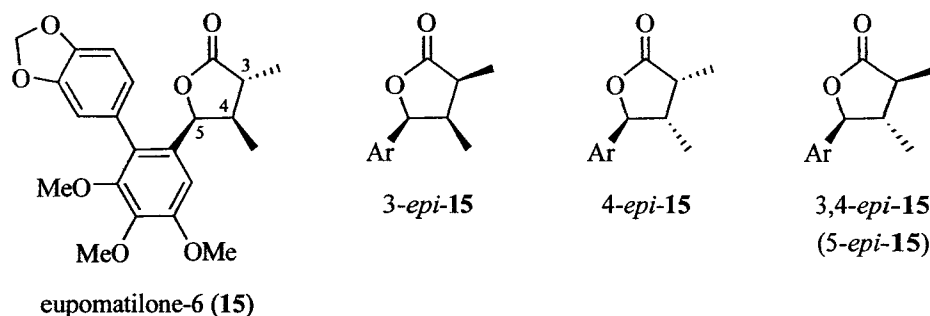


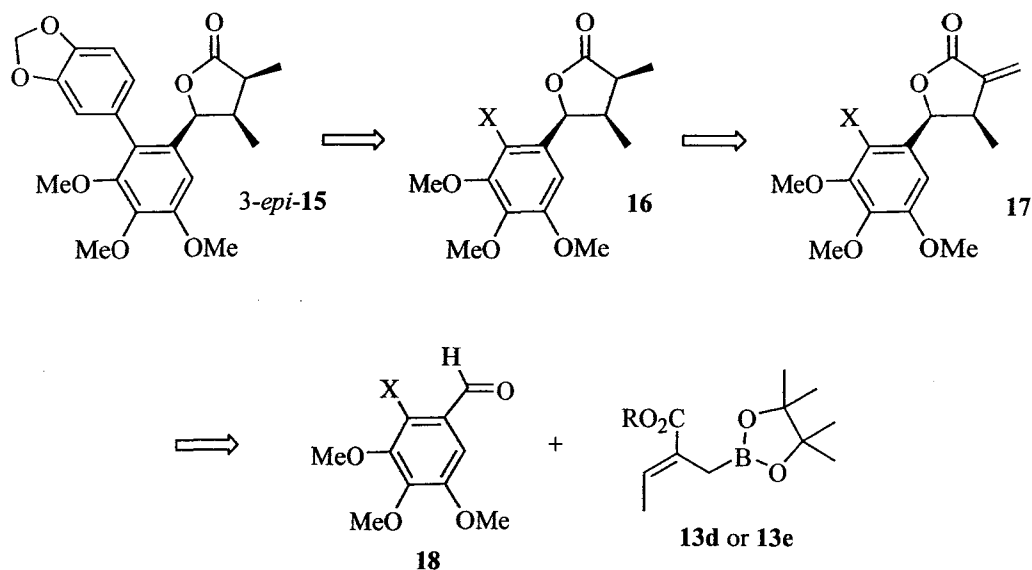
**Figure 2-1.** Eupomatilone-6 and its three unnatural diastereomers.

Eupomatilone-6 (**15**, Figure 2-1) belongs to a family of lignans isolated from the indigenous Australian shrub *Eupomatia bennettii*.<sup>11</sup> Under ambient conditions, eupomatilone-6 exist as an equilibrating mixture of biaryl atropisomers. The biological activities of lignans, among which anticancer, anti-HIV, antifungal activities and specific inhibition to certain enzymes are the most prominent, have been well documented.<sup>12</sup> There have been three synthetic studies<sup>13-15</sup> reported in the literature with Coleman's<sup>15</sup> being the shortest (seven linear steps) and most efficient (33 % overall yield). Having three contiguous stereogenic centers (as numbered 3-5 in Figure 2-1) in the lactone moiety, there exist four possible diastereomers, namely 3-*epi*-**15** (all-*cis*), 3,4-*epi*-**15** (all-*trans*), 4-*epi*-**15** (*cis-trans*) and **15** (*trans-cis*). Due to difficult configuration analysis of five-membered rings, eupomatilone-6's stereochemical assignments were still debated at the start of this project.

The first synthetic attempt was accomplished by McIntosh and co-workers using an Ireland-Claisen approach to give 4-*epi*-**15**.<sup>13</sup> Gurjar and co-workers later reported a synthesis based on an intramolecular Horner-Wadsworth-Emmons reaction<sup>14</sup> and found out that their final product did not match spectroscopically with Taylor's original structure<sup>11</sup> which has now been revised by Coleman<sup>15</sup> as 3-*epi*-**15**. Unaware of Coleman's work at the time, however, we devised our synthetic plan based on 3-*epi*-**15**. In retrospect, it was not of serious consequence due to our surprising discovery of the unexpected stereochemical outcomes

obtained from the TfOH-catalyzed allylboration and steric-controlled hydrogenations (Section 2.3.3 and Section 2.3.4, respectively).

### 2.3.2 Retrosynthetic analysis



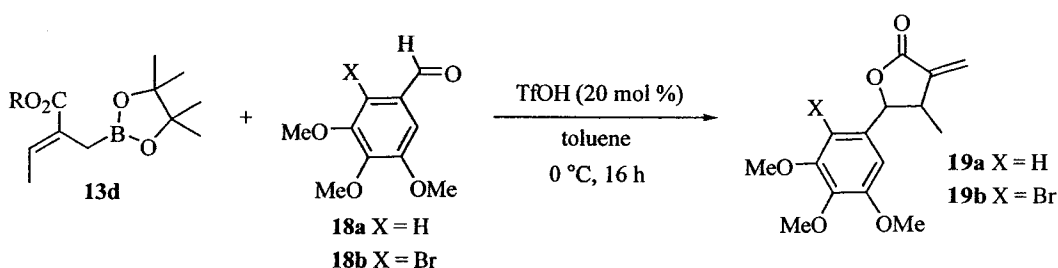
Scheme 2-8. Retrosynthetic plan.

The key step in the synthetic strategy to reach our initial target 3-epi-15 was to apply the TfOH-catalyzed allylboration between allylboronate **13d** or **13e** and aldehyde **18** to generate the lactone adduct **17** (Scheme 2-8). Based on the cyclic Zimmerman-Traxler transition state discussed in this chapter's introduction for the Type I stereospecific mechanism (Section 2.1), the *E* double bond geometry in **13d** or **13e** would provide the desired *cis* substitution pattern in **17**. For steric reasons, we expected hydrogen atoms to be delivered from the face opposite to the substituents on C4 and C5 obtaining intermediate **16** in the following hydrogenation. The biaryl functionality of the target compound would then be generated by Suzuki coupling in the last step. As a potential Michael acceptor, we decided to hydrogenate intermediate **17** first to avoid side reactions under the usually high temperature and basic conditions of Suzuki couplings. With plenty of alternative Suzuki coupling conditions available in the literature,

saving this step last would assure the completion of the synthesis. In this short synthetic sequence, the lactone moiety would be generated in one step with two of the stereogenic centers set in place. With the subsequent hydrogenation's stereoselectivity sterically controlled by the lactone's rigid cyclic structure, we wished to improve the overall yield compared to the literature precedents and more importantly to verify the structural assignment of eupomatilone-6.

### 2.3.3 Model reactions with electron-rich aldehydes

**Table 2-5.** Model reaction between **13d** and electron-rich aldehydes.



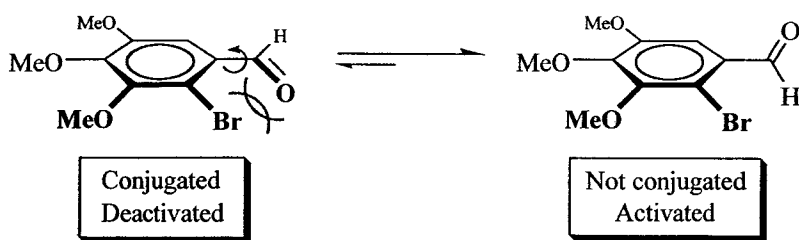
Aldehyde	X	Product	Yield (%) <sup>a</sup>
<b>18a</b>	H	<b>19a</b>	not observed
<b>18b</b>	Br	<b>19b</b>	57

<sup>a</sup> Isolated yields.

Although it requires a 2-halogen or triflate substituted benzaldehyde according to our synthetic plan, we first tested the TfOH catalysis using the commercially available 3,4,5-trimethoxybenzaldehyde (**18a**, Table 2-5). Catalyst loading was increased from 10 to 20 mol % to further promote the desired reaction. Not too unexpectedly however, this electron-rich, highly deactivated aldehyde was found to be inert even under the TfOH-catalyzed allylboration protocol. To our delight, the 2-bromo analogue **18b**<sup>16</sup> reacted smoothly to give a moderate yield of lactone **19b**. We believe that this key result cannot be fully explained by electron-withdrawing effect alone from the *ortho*-bromo substituent, and speculate that this very substituent increases the electrophilicity of aldehyde

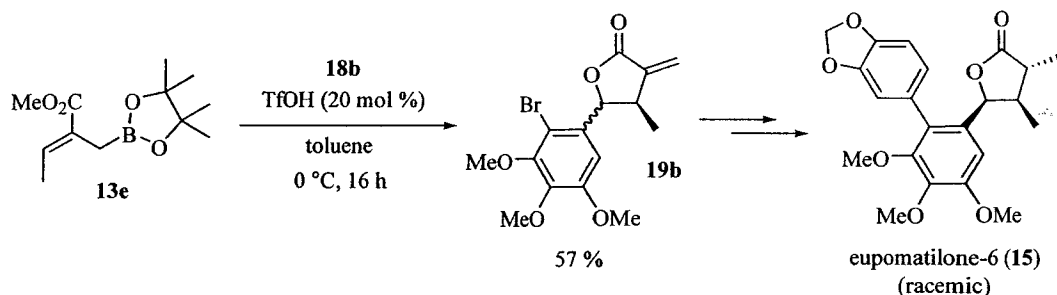


**18b** by twisting the carbonyl group out of conjugation with the aromatic  $\pi$  system (Scheme 2-9).



**Scheme 2-9.** Activation of aldehyde **18b** by steric-induced deconjugation.

From this point on, in the interest of material cost (chiral auxiliaries are expensive) and more pressingly to complete the project within a reasonable time frame, we devoted our effort to focus on a racemic but diastereoselective total synthesis of eupomatilone-6 using achiral allylboronate **13e** as the key starting material (Scheme 2-10).



**Scheme 2-10.** Switching plan to a racemic synthesis.

Preliminary  $^1\text{H}$  nOe experiment on allylboration adduct **19b**, where irradiation of the 4-methyl group resulted in signal enhancement of both H-4 and H-5, indicates that 4-methyl and 5-aryl groups may be *trans* to each other (Figure 2-2). This would contradict the expected *cis* relationship arisen from the *E*-allylboronate! However inconclusive due to the unavailability (at the time) of the other diastereomer for comparison and the inherent difficulties in determining a five-membered ring's stable conformation, this intriguing result gave us the first clue that some other mechanisms might be dictating the stereochemical outcome of this particular Brønsted acid-catalyzed allylboration.

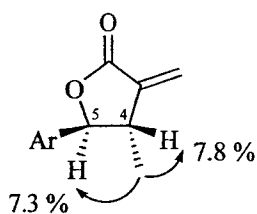


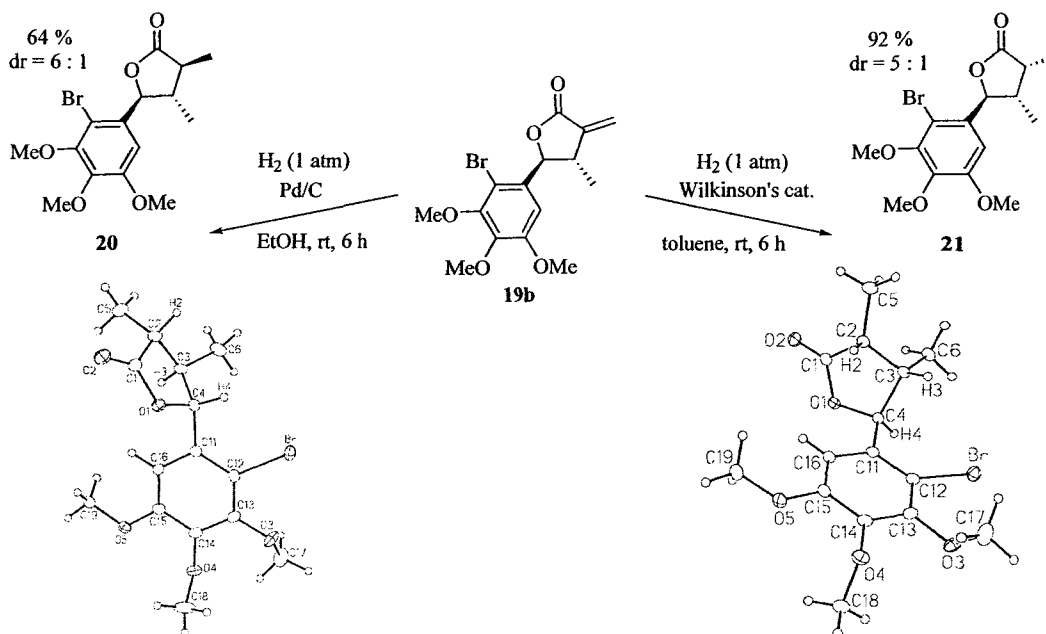
**Figure 2-2.** Preliminary structural assignment based on  $^1\text{H}$  nOe experiment.

### 2.3.4 Diastereoselective hydrogenation

Based on published results from our group, the hydrogenation of the exocyclic double bond could be highly diastereoselective because of the lactone's cyclic structure.<sup>4b</sup> Moreover, solid material could be obtained for X-ray crystallography. We therefore decided to carry on with this olefin reduction without fully resolving the stereochemistry of allylboration adduct **19b**. We first explored hydrogenation using palladium on charcoal and obtained **20** with 64 % yield (Scheme 2-11). This moderate result might be due to benzylic C-O bond cleavage under the heterogeneous hydrogenation conditions, although no identifiable by-product could be isolated. In an attempt to increase the yield of the desired product, we shortened the reaction time from 12 to 6 hours without any improvement. As Lowary and co-workers reported a chemo and stereoselective hydrogenation on an *O*-benzyl protected sugar derivative using Wilkinson's catalyst,<sup>17</sup> we decided to experiment with this homogeneous hydrogenation and gratifyingly obtained **21** with 92 % yield.

More detailed analysis on the  $^1\text{H}$  NMR spectra fascinatingly disclosed that the two hydrogenation conditions gave complementary diastereoselectivity. In both cases, the major diastereomers can be purely separated from the minor ones with simple silica gel chromatography. As **20** and **21** indeed turned out to be solid material, we were fortunate to obtain single crystals for X-ray crystallographic analyses which unambiguously revealed the relative stereochemistry of the three contiguous stereogenic centers in the lactone moiety. As shown in the ORTEP diagrams, the 4-methyl and 5-aryl groups indeed share a *trans* relationship. The

issues of this unexpected stereochemical outcome from TfOH-catalyzed allylboration will be addressed in Section 2.4.

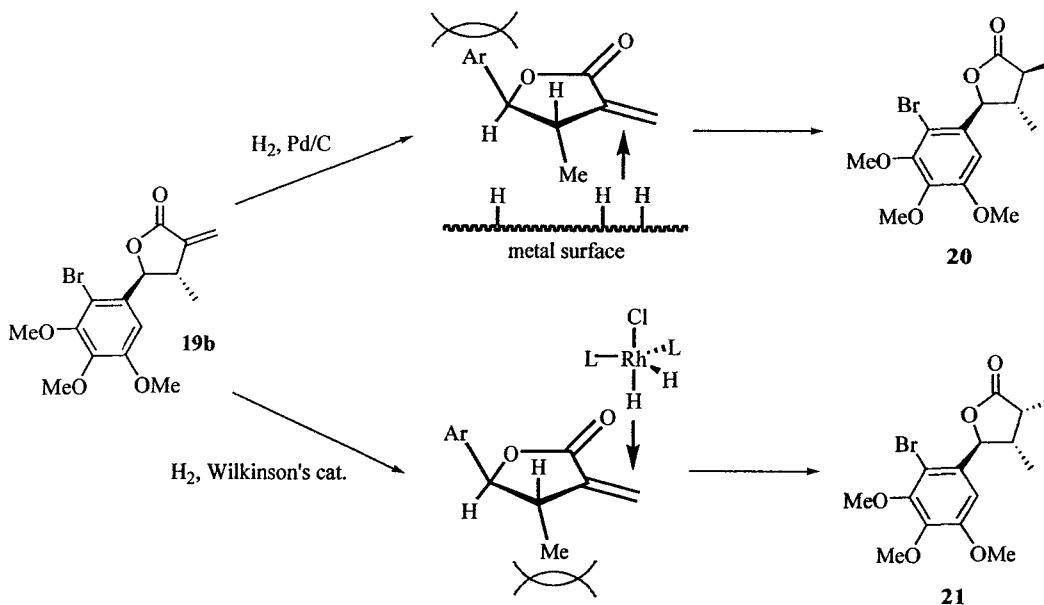


**Scheme 2-11.** Diastereoselective hydrogenation of **19b** and the ORTEP diagrams for **20** and **21**.

Having deduced the C4-C5 *trans* stereochemistry, the hydrogenation's diastereoselectivity can be explained by the steric demand of each catalyst (Scheme 2-12). In the case of heterogeneous conditions, the catalyst's surface avoids the face of the molecule bearing the remote but larger C5-aryl group to give product **20**. With homogeneous conditions using the relatively smaller Wilkinson's catalyst, the facial selectivity is in contrast controlled by the adjacent C4-methyl group giving rise to diastereomer **21**.

With the unforeseen stereochemical outcome obtained from TfOH-catalyzed allylboration and the consequential steric-controlled hydrogenation results, we promptly recognized the potential of applying our original synthetic route to access not only one but all four eupomatilone-6 diastereomers. The gift of having access to X-ray quality crystals provided us with an opportunity to close

the case concerning the uncertainties in the natural product's stereochemical assignments.

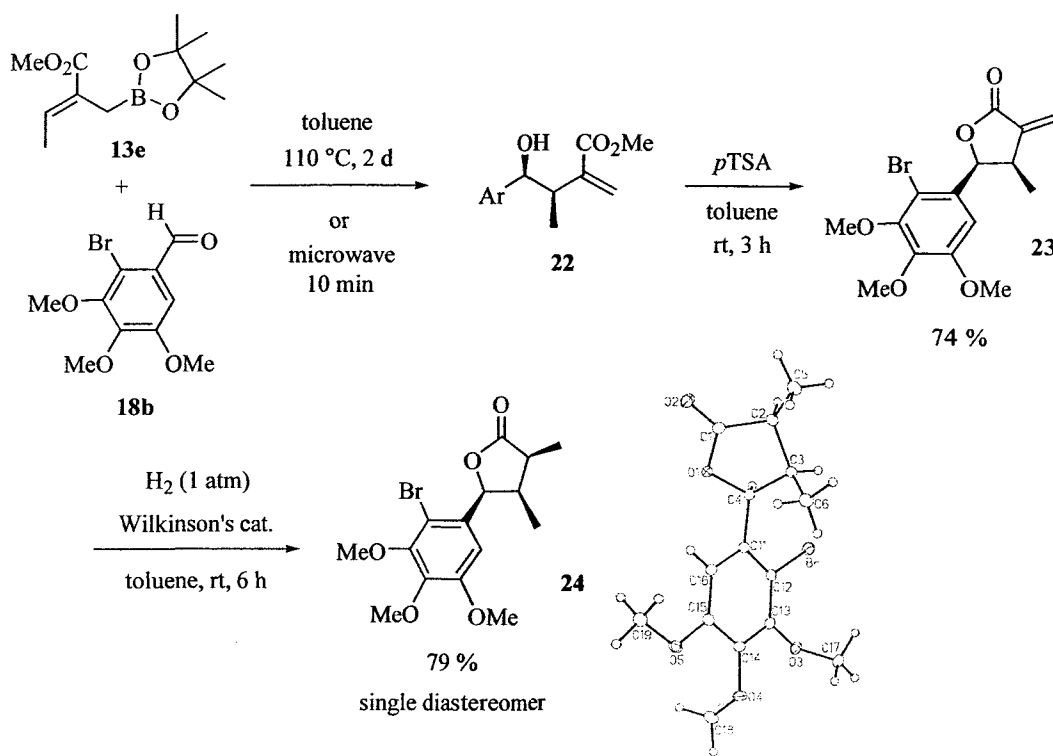


**Scheme 2-12.** Possible explanation for the diastereoselective hydrogenation of **19b**.

### 2.3.5 Access of C4-C5 *cis* lactone adduct via thermal allylboration

In order to access the C4-C5 *cis* lactone adduct, we reverted to thermal allylboration where the cyclic Zimmerman-Traxler transition state is well established (Section 2.1).<sup>4b</sup> Under this uncatalyzed allylboration, allylboronate **13e** and aldehyde **18b** were refluxed in toluene for 2 days (Scheme 2-13). Unlike the TfOH-catalyzed variant, it was necessary to induce lactonization of the *syn* hydroxy-ester adduct **22** under mildly acidic conditions using *p*TSA to give the final allylboration adduct **23**. The same thermal allylboration was also tried under microwave conditions in toluene using DMF as a co-solvent and similar results were obtained upon induced cyclization. In the subsequent hydrogenation step, we chose the higher yielding homogeneous conditions using Wilkinson's catalyst to give 79 % of **24** as a single diastereomer. The excellent diastereoselectivity can be explained by the fact that the 4-methyl and 5-aryl groups are now *cis* to each other and hydrogen atoms are most likely to be delivered from the more accessible

opposite face. The stereochemistry of hydrogenated product **24** was also unambiguously determined by X-ray crystallography.

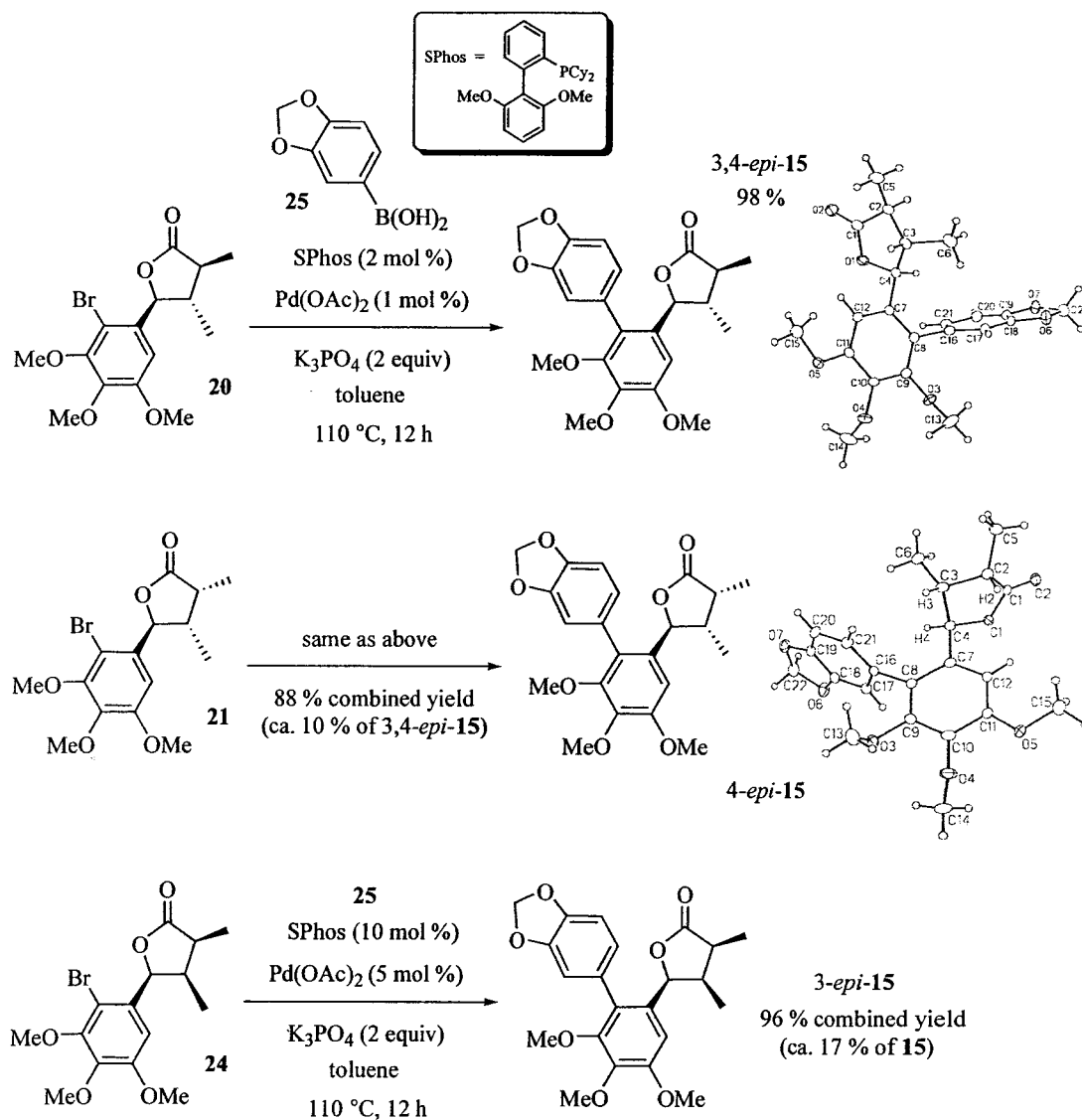


Scheme 2-13. Thermal allylboration followed by homogeneous hydrogenation.

### 2.3.6 Construction of the biaryl moiety by Suzuki-Miyaura coupling

Assessing the structure and functionalities of hydrogenated products **20**, **21** and **24**, they doubtlessly represent a rather challenging substrate for Suzuki biaryl cross-coupling reaction. First of all, the arylbromides are doubly *ortho*-substituted thus imposing a high steric hindrance. Secondly, both the arylbromides as well as the desired coupling partner arylboronic acid **25** are highly electron-rich. This electronic demand could potentially lead to aryl-aryl exchange side reactions with phosphine ligands on the palladium catalyst.<sup>18</sup> Faced with these anticipated problems, Buchwald's conditions, which confer unprecedented activity on preparing extremely hindered biaryls at low catalyst loadings and mild conditions,<sup>19</sup> provided us with the optimal solution.

Under Buchwald's conditions using the commercial SPhos ligand, hydrogenated products **20**, **21** and **24** were coupled very efficiently with commercial boronic acid **25** to give the desired eupomatilone-6's stereoisomers 3,4-*epi*-**15**, 4-*epi*-**15** and 3-*epi*-**15**, respectively (Scheme 2-14). According to  $^1\text{H}$



**Scheme 2-14.** Biaryl construction under Buchwald's conditions.

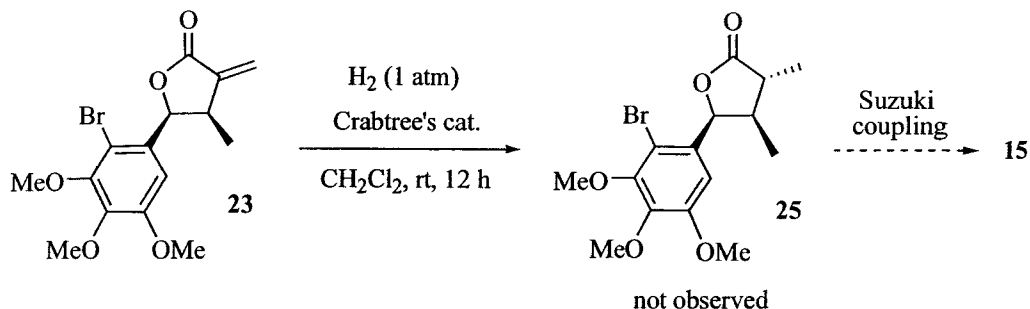
and  $^{13}\text{C}$  NMR analysis, all the coupling products exist as a mixture of biaryl atropisomers. To further confirm our stereochemical assignments, we were fortunate to obtain X-ray quality single crystals for one of the atropisomers for both 3,4-*epi*-**15** and 4-*epi*-**15**. Due to the hindered C3-C4 *cis* stereochemical

relationship, it was not too surprising to find out that 4-*epi*-**15** and 3-*epi*-**15** were contaminated respectively with ca. 10 % of 3,4-*epi*-**15** and ca. 17 % of **15** obtained from the epimerization of the alpha C3 center under Suzuki coupling's high heat, basic conditions. Although never explored, lowering the temperature with shortened reaction time should suppress this side reaction.

Being the first final product generated from our synthetic sequence, 3,4-*epi*-**15** is an eupomatilone-6 stereoisomer that had never been reported in the literature. We confirmed the structural assignment of McIntosh's 4-epimer with our X-ray crystallographic data of 4-*epi*-**15**. Table 2-6 in Section 2.3.8 summarizes all the <sup>1</sup>H NMR correspondences for the lactone moiety. Having our original target 3-*epi*-**15** in hand, we set out to verify the literature's characterization of the natural eupomatilone-6 and arrived at the same conclusion as Gurjar that a structural revision was warranted. On a side note, it was around this time that we came across Coleman's structural revision.

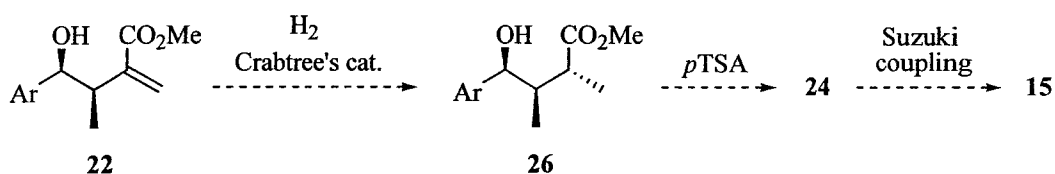
### 2.3.7 Synthesis of the natural eupomatilone-6

With Coleman's revised structure **15** and our goal set to synthesize the natural eupomatilone-6 with minor modification in our original sequence, we first decided to explore different homogeneous hydrogenation conditions using Crabtree's catalyst of which stereocontrol via ligating group coordination is well documented.<sup>20</sup> With 3 mol % catalyst under an atmosphere of hydrogen at room temperature, we were hoping that the methoxy groups on the aryl moiety of the



**Scheme 2-15.** Attempted methoxy-directed hydrogenation with Crabtree's catalyst.

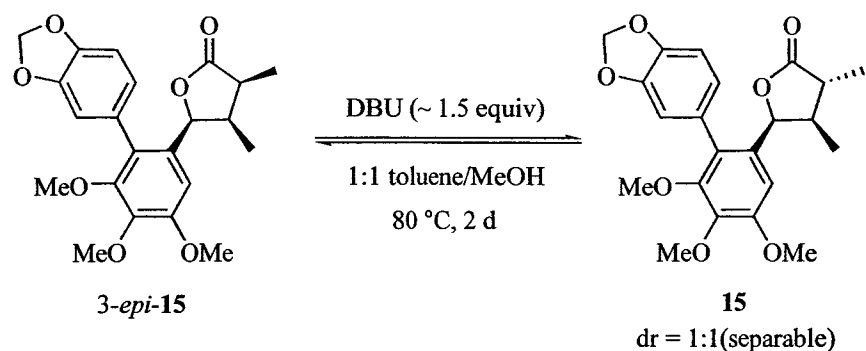
thermal allylboration adduct **23** could direct the hydrogen atom delivery to generate intermediate **25**, which could lead to the natural eupomatilone-6 upon Suzuki coupling (Scheme 2-15).  $^1\text{H}$  NMR analysis of the crude reaction mixture, however, revealed that the all-*cis* isomer **24** was generated as the only product. An alternative Crabtree hydrogenation on the open-chain homoallylic alcohol adduct **22** obtained via thermal allylboration before induced lactonization was also brought up (Scheme 2-16) but due to limitation on the availability of **22** and the catalyst, we turned our attention to focus on C3-epimerization of 3-*epi*-**15** instead.



**Scheme 2-16.** Alternative Crabtree hydrogenation on open-chain homoallylic alcohol **22**.

As mentioned in Section 2.3.6 concerning the Suzuki coupling step, epimerization of 3-*epi*-**15** at the C3 position is possible under basic conditions due to the inherent steric hindrance. To promote this epimerization, we tried different basic conditions including aqueous potassium carbonate, aqueous sodium hydroxide and sodium hydride in methanol with all leading to various degree of decomposition according to  $^1\text{H}$  NMR analysis of the crude reaction mixtures. As a last resort, the desired epimerization was effected with DBU<sup>21</sup> in heating 1:1 toluene/MeOH to give a ca. 1:1 mixture of 3-*epi*-**15** and eupomatilone-6 (**15**) without decomposition (Scheme 2-17). The two epimers were separated by preparative TLC with multiple developments and an analytically pure sample of **15** was thus obtained.

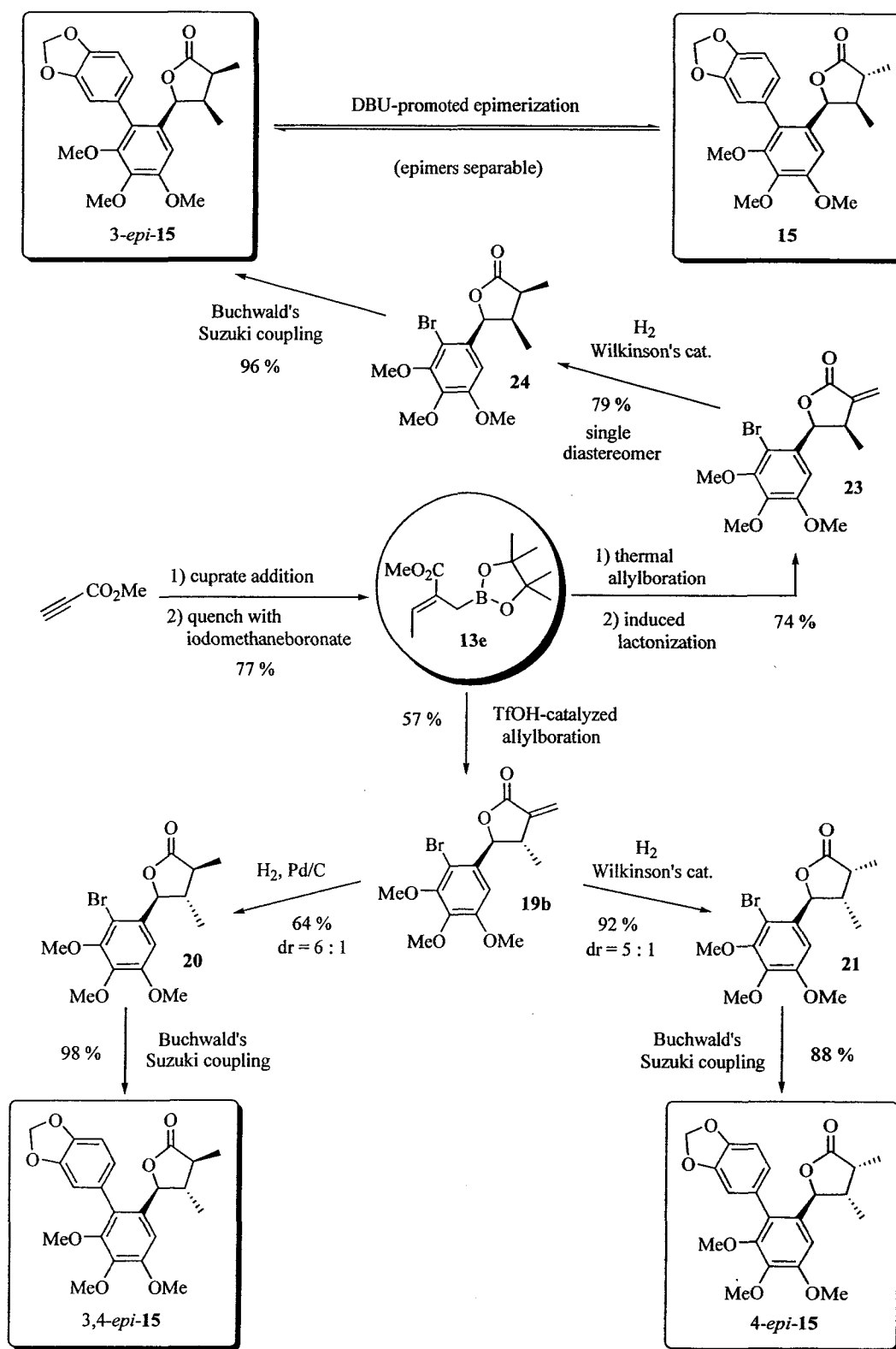




**Scheme 2-17.** DBU-promoted C3-epimerization of 3-*epi*-15 to 15.

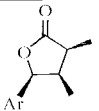
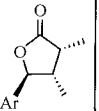
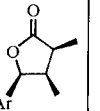
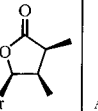
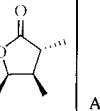
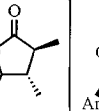
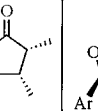
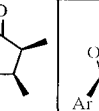
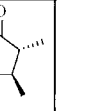
### 2.3.8 Summary on the stereodivergent synthesis of eupomatilone-6 diastereomers

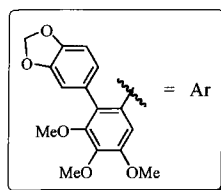
To sum up, a concise, stereodivergent total synthesis reaching all four diastereomers of eupomatilone-6 in only four or five steps with up to 43 % overall yield had been achieved starting from common allylboronate **13e** (Scheme 2-18). As one of the key steps, TfOH-catalyzed allylboration gave rise to an unexpected stereochemical outcome of which we took full advantage to control the diastereoselectivity of the subsequent hydrogenation using different catalysts. The generation of the natural **15** relied on a thermal, uncatalyzed allylboration protocol and a DBU-promoted epimerization. The biaryl constructions using Buchwald's conditions convincingly demonstrated its effectiveness. The stereochemistry of arylbromides **20**, **21** and **24** as well as 3,4-*epi*-**15** and 4-*epi*-**15** was unambiguously determined by X-ray crystallographic analyses. As summarized in Table 2-6, our stereochemical assignments were all correlated with the previously reported NMR spectroscopic data,<sup>13-15</sup> and further confirmed Coleman's recent structural revision of **15**<sup>15</sup> putting an end to the ambiguity in the original stereochemical assignments.



Scheme 2-18. Stereodivergent total synthesis of all four stereoisomers of 15.

**Table 2-6.** Summary table of  $^1\text{H}$  NMR correspondences for the lactone moiety.

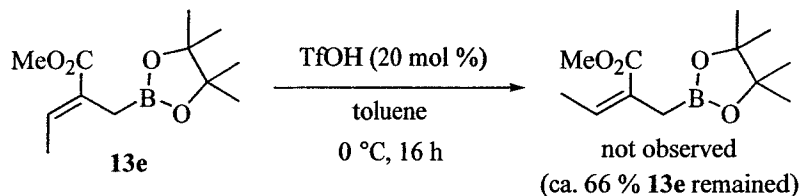
									
	Original 15 (Taylor <sup>13</sup> )	4- <i>epi</i> -15 (McIntosh <sup>15</sup> )	3- <i>epi</i> -15 (Gurjar <sup>14</sup> )	3- <i>epi</i> -15 (Coleman <sup>15</sup> )	Revised 15 (Coleman <sup>15</sup> )	3,4- <i>epi</i> -15 (this work)	4- <i>epi</i> -15 (this work)	3- <i>epi</i> -15 (this work)	15 (this work)
H-3	$\delta$ 2.36, 2.37, m, $J = 7.0, 5.2$	$\delta$ 2.75, m	$\delta$ 2.74, m	$\delta$ 2.74, app sextet, $J = 7.0$	$\delta$ 2.37, sextet, $J = 7.2$	$\delta$ 2.14, m	$\delta$ 2.75, m	$\delta$ 2.75, m	$\delta$ 2.36, m
H-4	$\delta$ 2.02, 1.97, m, $J = 7.0, 7.0, 5.2$	$\delta$ 2.36, m	$\delta$ 2.20, m	$\delta$ 2.20-2.10, m	$\delta$ 2.05-1.96, m	$\delta$ 2.03, m	$\delta$ 2.39, m	$\delta$ 2.20, m	$\delta$ 2.05-1.96, m
H-5	$\delta$ 5.54, 5.65, d, $J = 7.0$	$\delta$ 5.00, d, $J = 4.35$ ; $\delta$ 5.10, d, $J = 4.35$	$\delta$ 5.32, 5.41, d, $J = 5.0$	$\delta$ 5.32, 5.40, d, $J = 4.9$	$\delta$ 5.54, 5.65, d, $J = 6.9$	$\delta$ 4.78, 4.80, d, $J = 9.8$	$\delta$ 5.01, d, $J = 4.5$ ; $\delta$ 5.11, d, $J = 4.5$	$\delta$ 5.32, 5.41, d, $J = 4.9$	$\delta$ 5.53, 5.65, d, $J = 7.0$
3-Me	$\delta$ 1.20, 1.19, d, $J = 7.0$	$\delta$ 1.06, d, $J = 7.51$ ; $\delta$ 1.07, d, $J = 7.53$	$\delta$ 1.13, d, $J = 7.2$	$\delta$ 1.12, d, $J = 7.3$	$\delta$ 1.19, 1.20, d, $J = 7.4$	$\delta$ 1.23, d, $J = 6.9$	$\delta$ 1.07, d, $J = 7.3$ ; $\delta$ 1.08, d, $J = 7.3$	$\delta$ 1.12, d, $J = 7.2$	$\delta$ 1.19, 1.20, d, $J = 7.6$
4-Me	$\delta$ 0.70, 0.73, d, $J = 7.0$	$\delta$ 0.65, d, $J = 6.93$ ; $\delta$ 0.67, d, $J = 6.73$	$\delta$ 0.54, 0.56, d, $J = 7.2$	$\delta$ 0.54, 0.56, d, $J = 7.3$	$\delta$ 0.70, 0.73, d, $J = 7.1$	$\delta$ 0.86, 0.87, d, $J = 6.4$	$\delta$ 0.66, d, $J = 7.1$ ; $\delta$ 0.69, d, $J = 7.1$	$\delta$ 0.56, app triplet, $J = 7.2$	$\delta$ 0.70, 0.73, d, $J = 7.2$



## 2.4 Preliminary Mechanistic Investigation on TfOH-Catalyzed Allylboration

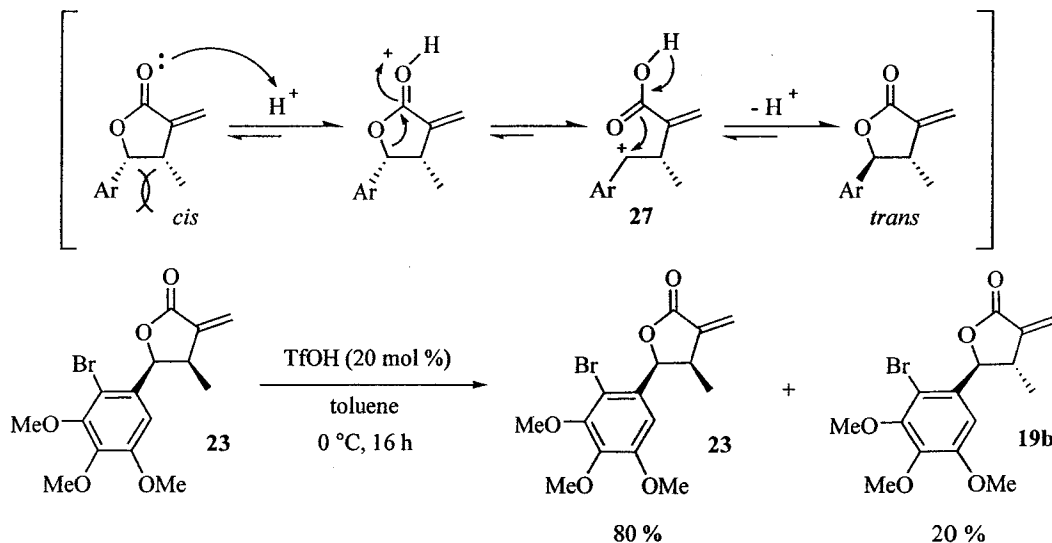
The unexpected stereochemical outcome from the TfOH-catalyzed allylboration intrigues us and raises a fundamental question. Does the allylboration of interest still undergo the Type I mechanism? To address this enquiry, we first investigated the possibility of starting material or product undergoing isomerization in the presence of the strong acid. With the absence of an aldehyde, *E*-allylboronate **13e** and thermal allylboration adduct **23** were submitted to the exact conditions as running a TfOH-catalyzed allylboration

(Scheme 2-19 and 2-20, respectively). According to  $^1\text{H}$  NMR analysis of the crude, worked up mixture, ca. 66 % of the starting *E*-allylboronate remained along with other unidentified side products but no *Z*-isomer was observed.



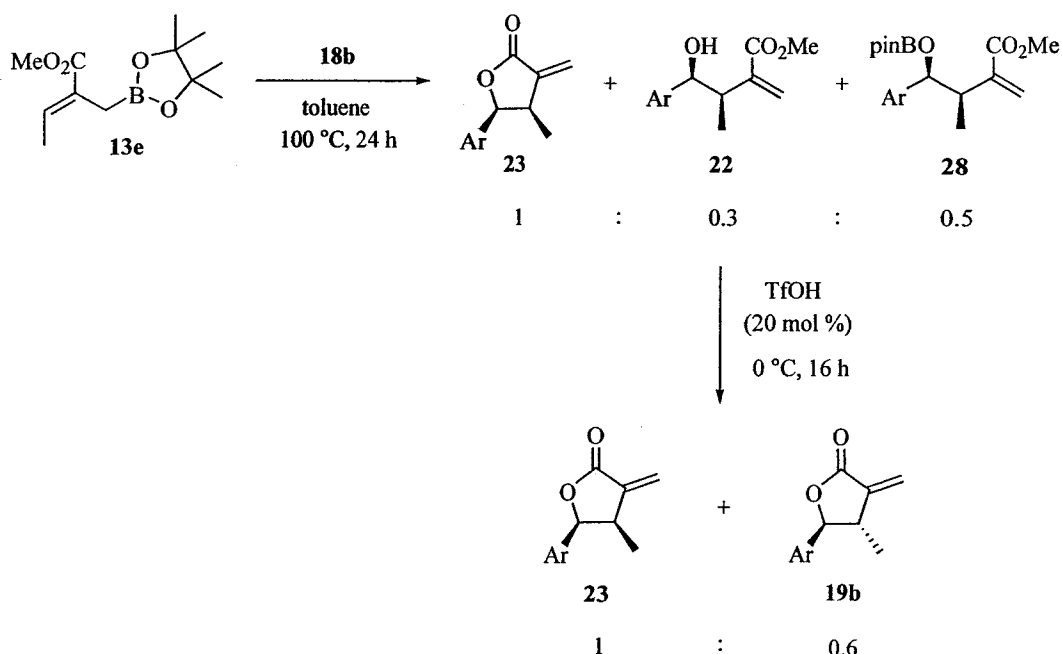
**Scheme 2-19.** *E*-to-*Z* isomerization of the starting allylboronate **13e**.

As for thermal adduct **23**, the depicted *cis*-to-*trans* isomerization did occur, presumably via the benzylic carbocation **27**. However, with only about 20 % conversion, this isomerization is much too slow to account for the complete *trans* stereochemistry observed in the normal TfOH-catalyzed allylboration case. As a result, a thermodynamic reaction control can putatively be ruled out.



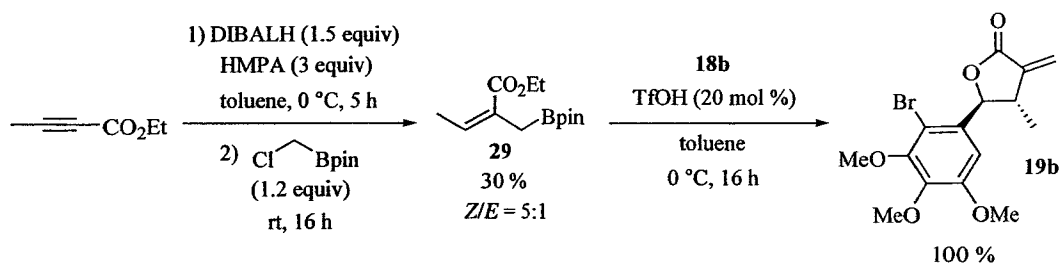
**Scheme 2-20.** *Cis*-to-*trans* isomerization of the thermal allylboration adduct **23** via benzylic carbocation **27**.

Since complete isomerization did not seem to take place either at the starting material or product level, we speculated that it would occur at the borate intermediate. Using TfOH instead of *p*TSA to induce lactonization (Scheme 2-21), we were hoping to gain more mechanistic insight on where the isomerization occurs if at all. Based on <sup>1</sup>H NMR analysis, a mixture of lactone **23**, free alcohol **22** and borate intermediate **28** were observed before the treatment of TfOH. Consequently, the final results might not be very conclusive and more sophisticated real-time NMR experiments may be required to resolve this disarray.



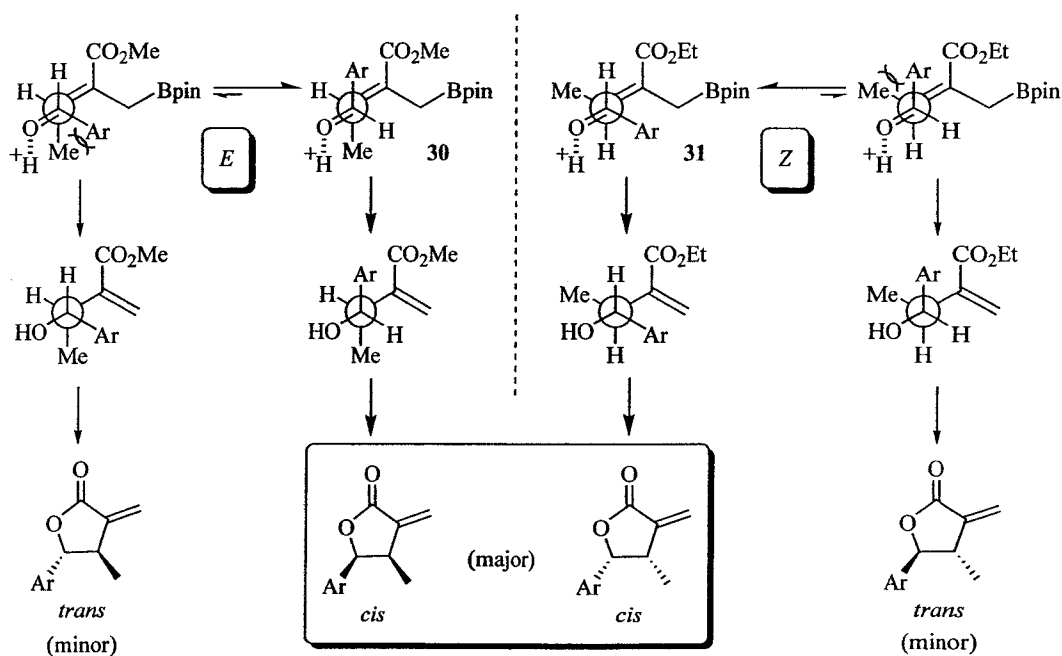
**Scheme 2-21.** Mechanistic study with TfOH-induced lactonization.

In our final attempt to probe the origin of the unexpected stereochemical outcome, we decided to independently generate the *Z*-allylboronate to examine whether the Brønsted acid-catalyzed allylboration is stereospecific or stereoconvergent. DIBALH-hydroalumination<sup>22</sup> of ethyl 2-butynoate followed by electrophile trapping with a chloromethaneboronate<sup>23</sup> provided the desired *Z*-allylboronate **29** with a *Z/E* ratio of 5:1 (Scheme 2-22). Upon TfOH-catalyzed allylboration, the same lactone adduct (**19b**) obtained from the *E*-allylboronate was isolated quantitatively. With both *E*- and *Z*-allylboronates leading to the same



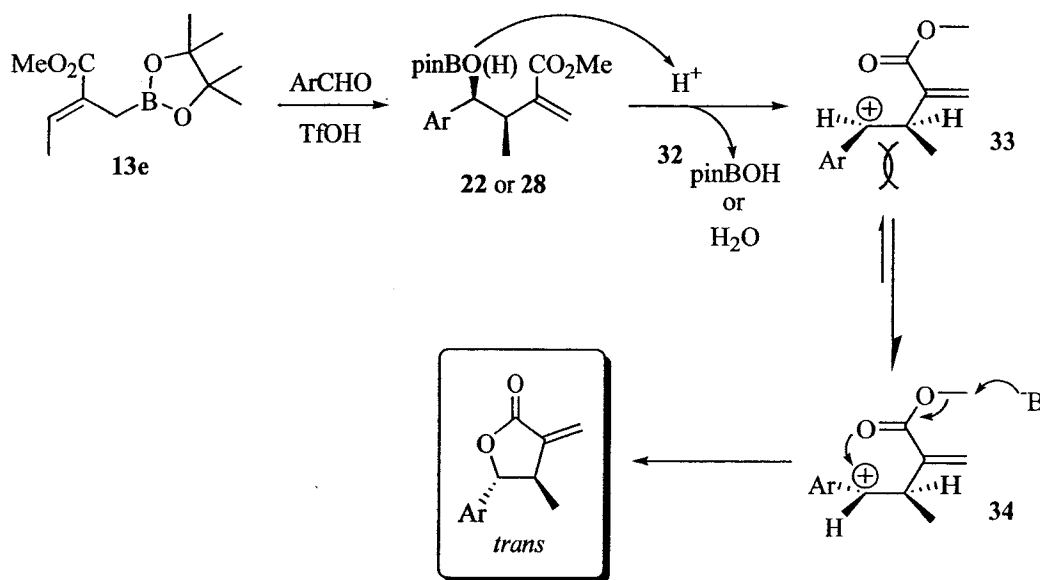
**Scheme 2-22.** Synthesis of Z-allylboronate **29** and the subsequent TfOH-catalyzed allylboration.

stereochemistry in the product, the allylboration of interest may appear to be stereoconvergent, indicating that a Type II mechanism may be at play. Close examination of the possible open transition structures, however, suggests otherwise (Scheme 2-23). Based on steric hindrance, transition states **30** and **31**, respectively arisen from the *E*- and *Z*-allylboronates, should be more favorable and both would stereoconvergently lead to the *cis* adducts. We therefore preliminarily ruled out this mechanistic pathway.



**Scheme 2-23.** Stereoconvergently *cis* adducts obtained from both *E*- and *Z*-allylboronates via a Type II mechanism.

Based on Bach and co-workers' recent work on chiral benzylic carbocation chemistry,<sup>25</sup> we tentatively favor the mechanism depicted in Scheme 2-24 to explain the unexpected *trans* stereochemical outcome. Under strong acidic conditions, benzylic carbocation **33** would be generated by the loss of water or boron species **32** from allylboration adduct **22** or **28**, respectively. An equilibrium should then favor the formation of conformer **34** to minimize the 1,3-allylic strain. In consequence, lactonization should be directed to the back of the carbenium ion giving the *trans* product.



**Scheme 2-24.** Tentative mechanistic explanation for the *trans* stereochemical outcome.

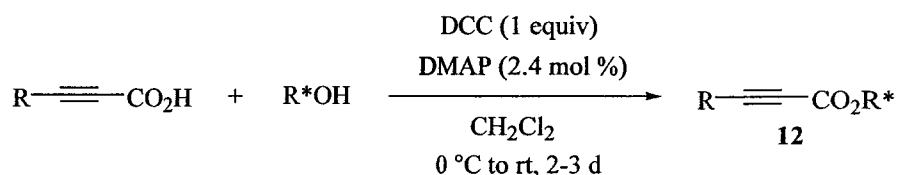
Last but not least, with respect to the rate acceleration of the Brønsted acid catalysis, we speculate that an electrophilic boronate activation similar to that of the  $\text{Sc}(\text{OTf})_3$ -catalyzed variant is at play (Scheme 2-5).<sup>6</sup> Since no material evidence was gathered, however, we cannot yet draw any further conclusion at this point.

## 2.5 Enantioselective Brønsted-Acid Catalyzed Allylboration

### 2.5.1 Synthesis of starting chiral alkynoate esters

In order to generate the desired chiral allylboronates **13b-d** mentioned in Section 2.2.1, we first needed to prepare the corresponding chiral alkynoate esters **12b-d**. Using literature procedure reported by our group,<sup>4b</sup> chiral butynoates **12b** and **12c** were generated under DCC-mediated esterification without incident (Table 2-7, Entries 1 and 2). With the presence of an acetylenic proton however,

**Table 2-7.** DCC-mediated esterification to generate chiral acetylenic esters.



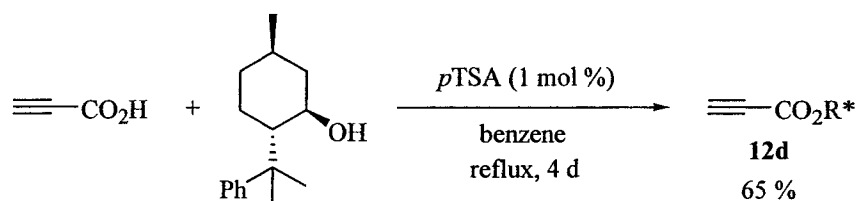
Entry	R	R*OH	Product	Yield (%) <sup>a</sup>
1	Me	(-)-menthol	<b>12b</b>	95
2	Me	(-)-8-phenylmenthol	<b>12c</b>	90
3	H	(-)-8-phenylmenthol	<b>12d</b>	20

<sup>a</sup> Isolated yields.

the synthesis of chiral propiolate **12d** under the same conditions was found to be problematic (Entry 3). The same low-yielding result was also encountered during an earlier project (Chapter 3, Section 3.2.1), and increasing the amount of DCC and DMAP did not resolve the problem. To our delight, Moyano and co-workers reported the synthesis of our exact desired compound.<sup>24</sup> In the presence of 1 mol % *p*TSA monohydrate, a benzene solution of propiolic acid and (-)-8-phenylmenthol was refluxed in a Dean-Stark apparatus for 4 days giving **12d** more than tripling the yield compared to the DCC reaction (Scheme 2-25). Although allylboronate **13d** was not included in the following asymmetric



allylboration study, its improved synthesis will definitely be invaluable for the future development of any enantioselective methodologies.



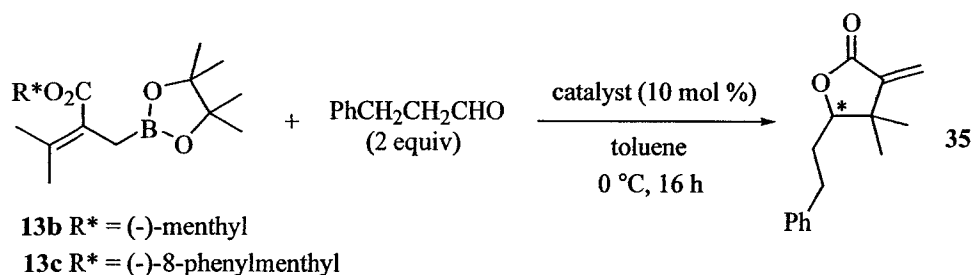
**Scheme 2-25.** *p*TSA-catalyzed esterification.

### 2.5.2 Enantioselectivity of catalyzed allylborations

Having synthesized the desired chiral allylboronates **13b-c** (Section 2.2.1) from the corresponding chiral alkynoate esters, asymmetric allylborations were carried out based on the optimized conditions established in Section 2.2.3. Even though the enantioselectivity of the catalyzed allylboration was only briefly examined here (Table 2-8) since the goal of the project had been shifted toward the total synthesis of eupomatilone-6, some interesting preliminary results were observed nonetheless. Most noteworthy was that Lewis acid catalysis was demonstrated to be ineffective under the reaction conditions (Entries 3-6). This important early result justified our further investigation to focus on Brønsted acid-catalysis.

As reported before by our group for the room temperature  $\text{Sc}(\text{OTf})_3$ -catalyzed allylboration,<sup>4b</sup> 8-phenylmenthyl ester is a better chiral auxiliary than menthyl ester in terms of stereinduction (compare Entries 1 and 2). Although never explored, we should be able to further improve the enantioselectivity in Entry 2 by lowering the reaction temperature. The effectiveness of phenylmenthyl ester can be attributed to the ability of its phenyl ring to shield off one face of the reacting allyl group through  $\pi$ - $\pi$  interactions as depicted in Figure 2-3.<sup>28</sup> In this study, benzaldehyde was also tested as one of the substrates, but we were unable to determine the chiral HPLC conditions after numerous attempts to measure the enantiomeric excess of the lactone adduct.

**Table 2-8.** Examination of enantioselectivity of catalyzed allylboration.



Entry	Allylboronate	Catalyst	Yield (%)	ee (%) <sup>c</sup>
1	<b>13b</b>	TfOH	99 <sup>a</sup>	7
2	<b>13c</b>	TfOH	78 <sup>a</sup>	62
3	<b>13c</b>	Sc(OTf) <sub>3</sub>	< 5 <sup>b</sup>	-
4	<b>13c</b>	AlCl <sub>3</sub>	< 5 <sup>b</sup>	-
5	<b>13c</b>	TiCl <sub>4</sub>	< 5 <sup>b</sup>	-
6	<b>13c</b>	BF <sub>3</sub> ·OEt <sub>2</sub>	< 5 <sup>b</sup>	-

<sup>a</sup> Isolated yields. <sup>b</sup> Based on <sup>1</sup>H NMR analysis of crude reaction mixture. <sup>c</sup> Determined by chiral HPLC.

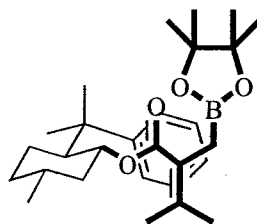


**Figure 2-3.** Intramolecular  $\pi$ - $\pi$  interactions in phenylmenthyl ester chiral allylboronate.

## 2.6 Conclusion And Future Work

In conclusion, a novel Brønsted acid-catalyzed allylboration methodology amenable to the most difficult, electronically deactivated allylboronate and aldehyde substrates was developed. Circumventing the use of metal ions, this protocol employs a simple and cheap catalyst, triflic acid, and its usefulness was

highlighted in the stereodivergent synthesis of eupomatilone-6 and its stereoisomers. In terms of future work, exploring the aldehyde substrate scope and determining the exact mechanism of the Brønsted acid-catalyzed allylboration would definitely be illuminating for the potential extension of an asymmetric variant.

## 2.7 Experimental

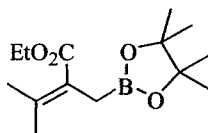
### 2.7.1 General

Unless otherwise noted, all reactions were performed under an argon atmosphere using flame-dried glassware. Tetrahydrofuran was distilled over sodium-benzophenone ketyl. Toluene, CH<sub>2</sub>Cl<sub>2</sub> and HMPA were distilled over CaH<sub>2</sub> before use. NH<sub>4</sub>Cl<sub>(aq)</sub> and NaHCO<sub>3(aq)</sub> refer to saturated aqueous solutions. All liquid aldehydes were purified by Kugelrohr distillation prior to use. Methylolithium was titrated according to the Gilman double titration method.<sup>26</sup> Chiral alkynoate esters **12b-c**,<sup>4b</sup> **12d**,<sup>24</sup> iodomethaneboronate,<sup>27</sup> chloromethaneboronate<sup>23</sup> and 2-bromo-3,4,5-trimethoxybenzaldehyde<sup>16</sup> were prepared according to literature procedures. TfOH was stored in a closed pear-shaped flask under Ar and placed in a jar filled with anhydrous calcium sulfate (Drierite<sup>®</sup>), which was then stored at 0 °C. All other chemicals were used as received from commercial sources. Thin layer chromatography (TLC) was performed on Silica Gel 60 F<sub>254</sub> plates and were visualized with UV light and aqueous KMnO<sub>4</sub> solution. NMR spectra were recorded on 300, 400 or 500 MHz instruments. The residual solvent protons (<sup>1</sup>H) or the solvent carbons (<sup>13</sup>C) were used as internal standards. <sup>1</sup>H NMR data are presented as follows: chemical shift in ppm downfield from tetramethylsilane (multiplicity, integration, coupling constant). The following abbreviations are used in reporting NMR data: s, singlet; d, doublet; t, triplet; q, quartet; dd, doublet of doublets; ddd, doublet of doublets of doublets; dq, doublet of quartets; dt, doublet of triplets; qt, quartet of triplets; m, multiplet; td, triplet of doublets. High resolution mass spectra were recorded

by the University of Alberta Mass Spectrometry Services Laboratory using electron impact (EI) or electrospray (ES) ionization techniques. Elemental analyses were performed by the University of Alberta Micro-Analytical Lab. Infrared spectra and X-ray diffraction data were collected by the University of Alberta Spectral Services and X-Ray Crystallography Laboratory, respectively. Chiral HPLC analysis was performed using a Chiralpak AD-RHCD-CC012 column (0.46 cm × 15 cm) with UV detection at 210 nm at 25 °C.

## 2.7.2 Preparation of 2-alkoxycarbonyl allylboronates 13a-e

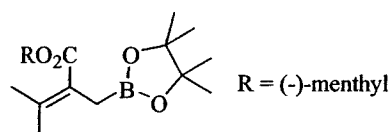
### 2.7.2.1 Ethyl 2-[(4,4,5,5-tetramethyl-1,3,2-dioxaborolan-2-yl)methyl]-3-methylbut-2-enoate (13a)



A slurry of recrystallized  $\text{CuBr}\cdot\text{SMe}_2$  (480 mg, 2.33 mmol) in anhydrous THF (5.5 mL) at 0 °C under Ar atmosphere was treated with MeLi (1.62 M in  $\text{Et}_2\text{O}$ , 2.88 mL, 4.66 mmol) using an air-tight syringe. An orange precipitate was formed initially then disappeared as the addition proceeded. The resulting clear colourless solution was stirred at 0 °C for an additional 10 min and then cooled to -78 °C in an acetone/ $\text{CO}_2$  bath. A -78 °C solution of ethyl 2-butynoate (0.266 mL, 2.29 mmol) in THF (1 mL) was added via cannulation with THF rinse (2 × 0.5 mL). The resulting light brown mixture was stirred at -78 °C for 1 h and then injected with a -78 °C solution of freshly distilled iodomethaneboronate<sup>27</sup> (1.72 g, 6.42 mmol) in THF (2 mL) via cannulation with THF rinse (3 × 1 mL). HMPA (3.65 mL, 21.0 mmol) was quickly added. Stirring continued at -78 °C for another 10 min. The mixture was then brought to 0 °C, stirred for 1 h and finally brought to rt, stirred for 1 h. The milky slurry was quenched with  $\text{NH}_4\text{Cl}_{(\text{aq})}$  (10 mL). The layers were separated and the aqueous layer was extracted with  $\text{Et}_2\text{O}$  (4 × 10 mL). The combined organic layers were washed with water (6 × 10 mL) and brine (1 × 10 mL), dried with anhydrous  $\text{Na}_2\text{SO}_4$ , filtered and concentrated. Flash

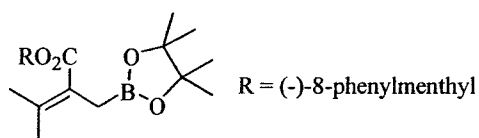
chromatography (25 % Et<sub>2</sub>O/hexane) gave the product as a clear colourless liquid (453 mg, 1.69 mmol, 74 %). This material possessed identical spectroscopic characteristics to those reported in the literature.<sup>4b</sup>

**2.7.2.2 2-[(4,4,5,5-Tetramethyl-1,3,2-dioxaborolan-2-yl)methyl]-3-methylbut-2-enoic acid, (-)-menthol ester (13b)**



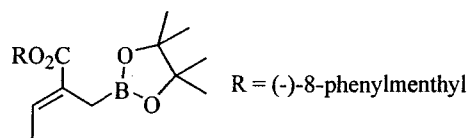
A slurry of recrystallized CuBr·SMe<sub>2</sub> (475 mg, 2.31 mmol) in anhydrous THF (5.5 mL) at 0 °C under Ar atmosphere was treated with MeLi (1.62 M in Et<sub>2</sub>O, 2.85 mL, 4.62 mmol) using an air-tight syringe. An orange precipitate was formed initially then disappeared as the addition proceeded. The resulting clear colourless solution was stirred at 0 °C for an additional 10 min and then cooled to -78 °C in an acetone/CO<sub>2</sub> bath. A -78 °C solution of (-)-menthol butynoate **12b**<sup>4b</sup> (508 mg, 2.29 mmol) in THF (1.5 mL) was added via cannulation with THF rinse (2 × 1 mL). The resulting light brown mixture was stirred at -78 °C for 1 h and then injected with a -78 °C solution of freshly distilled iodomethaneboronate<sup>27</sup> (1.7 g, 6.3 mmol) in THF (1 mL) via cannulation with THF rinse (2 × 0.5 mL). HMPA (3.6 mL, 20.7 mmol) was quickly added. Stirring continued at -78 °C for another 10 min. The mixture was then brought to 0 °C, stirred for 1 h and finally brought to rt, stirred for 1 h. Workup as Section 2.7.2.1. Flash chromatography (20 % Et<sub>2</sub>O/hexane) gave the product as a clear liquid (677 mg, 1.79 mmol, 77 %). This material possessed identical spectroscopic characteristics to those reported in the literature.<sup>4b</sup>

**2.7.2.3 2-[(4,4,5,5-Tetramethyl-1,3,2-dioxaborolan-2-yl)methyl]-3-methylbut-2-enoic acid, (-)-8-phenylmenthol ester (13c)**



A slurry of recrystallized  $\text{CuBr}\cdot\text{SMe}_2$  (410 mg, 1.99 mmol) in anhydrous THF (5.5 mL) at 0 °C under Ar atmosphere was treated with MeLi (1.62 M in  $\text{Et}_2\text{O}$ , 2.46 mL, 3.98 mmol) using an air-tight syringe. An orange precipitate was formed initially then disappeared as the addition proceeded. The resulting clear colourless solution was stirred at 0 °C for an additional 10 min and then cooled to -78 °C in an acetone/ $\text{CO}_2$  bath. A -78 °C solution of (-)-8-phenylmenthol butynoate **12c**<sup>4b</sup> (595 mg, 1.99 mmol) in THF (1.5 mL) was added via cannulation with THF rinse (2 × 0.5 mL). The resulting light brown mixture was stirred at -78 °C for 1 h and then injected with a -78 °C solution of freshly distilled iodomethaneboronate<sup>27</sup> (1.47 g, 5.49 mmol) in THF (1 mL) via cannulation with THF rinse (2 × 0.5 mL). HMPA (3.12 mL, 17.9 mmol) was quickly added. Stirring continued at -78 °C for another 10 min. The mixture was then brought to 0 °C, stirred for 1 h and finally brought to rt, stirred for 1 h. Workup as Section 2.7.2.1. Flash chromatography (10 % EtOAc/hexane) gave the product as a clear liquid (491 mg, 1.08 mmol, 54 %). This material possessed identical spectroscopic characteristics to those reported in the literature.<sup>4b</sup>

**2.7.2.4 (2E)-2-[(4,4,5,5-Tetramethyl-1,3,2-dioxaborolan-2-yl)methyl]-but-2-enoic acid, (-)-8-phenylmenthol ester (13d)**

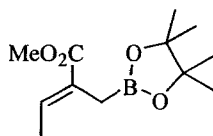


A slurry of recrystallized  $\text{CuBr}\cdot\text{SMe}_2$  (260 mg, 1.26 mmol) in anhydrous THF (3.5 mL) at 0 °C under Ar atmosphere was treated with MeLi (1.60 M in  $\text{Et}_2\text{O}$ , 1.58 mL, 2.53 mmol) using an air-tight syringe. An orange precipitate was formed initially then disappeared as the addition proceeded. The resulting clear colourless solution was stirred at 0 °C for an additional 10 min and then cooled to -78 °C in an acetone/ $\text{CO}_2$  bath. A -78 °C solution of (-)-8-phenylmenthol propiolate **12d**<sup>24</sup> (359 mg, 1.26 mmol) in THF (1 mL) was added via cannulation with THF rinse (2 × 0.3 mL). The resulting light brown mixture was stirred at -78 °C for 1 h and then injected with a -78 °C solution of freshly distilled

iodomethaneboronate<sup>27</sup> (930 mg, 3.47 mmol) in THF (0.6 mL) via cannulation with THF rinse (2 × 0.3 mL). HMPA (1.98 mL, 11.4 mmol) was quickly added. Stirring continued at -78 °C for another 10 min. The mixture was then brought to 0 °C, stirred for 1 h and finally brought to rt, stirred for 1 h. Workup as Section 2.7.2.1. Flash chromatography (10 % Et<sub>2</sub>O/hexane) gave the product as a clear liquid (483 mg, 1.10 mmol, 87 %).

<sup>1</sup>H NMR (500 MHz, CDCl<sub>3</sub>): δ 7.25 (m, 4H), 7.10 (m, 1H), 6.08 (q, 1H, *J* = 7.0 Hz), 4.89 (dt, 1H, *J* = 4.4, 10.7 Hz), 2.03 (m, 1H), 1.92 (m, 1H), 1.75 (d, 1H, *J* = 15.8 Hz), 1.68 (d, 1H, *J* = 15.8 Hz), 1.62 (d, 3H, *J* = 7.1 Hz), 1.61-1.54 (m, 2H), 1.52-1.42 (m, 1H), 1.31 (s, 3H), 1.24 (s, 12H), 1.22 (s, 3H), 1.06 (m, 1H), 0.97 (m, 1H), 0.85 (d, 3H, *J* = 6.5 Hz), 0.85-0.82 (m, 1H); <sup>13</sup>C NMR (125 MHz, CDCl<sub>3</sub>): δ 167.0, 151.6, 134.9, 130.4, 127.9, 125.5, 124.7, 83.1, 74.3, 50.6, 41.8, 39.8, 34.6, 31.3, 26.8, 26.3, 24.8, 24.7, 21.8, 14.4; IR (CH<sub>2</sub>Cl<sub>2</sub> cast film, cm<sup>-1</sup>): 3341 (broad), 2955, 1694, 1379, 1270, 1146, 700; HRMS (EI, *m/z*) Calcd for C<sub>27</sub>H<sub>41</sub><sup>11</sup>BO<sub>4</sub>: 440.30978. Found: 440.30964.

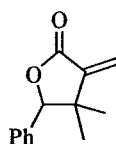
#### 2.7.2.5 Methyl (2*E*)-2-[(4,4,5,5-tetramethyl-1,3,2-dioxaborolan-2-yl)methyl]-but-2-enoate (13e)



A slurry of recrystallized CuBr·SMe<sub>2</sub> (833 mg, 4.05 mmol) in anhydrous THF (11 mL) at 0 °C under Ar atmosphere was treated with MeLi (1.60 M in Et<sub>2</sub>O, 5.1 mL, 8.1 mmol) using an air-tight syringe. An orange precipitate was formed initially then disappeared as the addition proceeded. The resulting clear colourless solution was stirred at 0 °C for an additional 10 min and then cooled to -78 °C in an acetone/CO<sub>2</sub> bath. A -78 °C solution of methyl propiolate (0.36 mL, 4.0 mmol) in THF (1 mL) was added via cannulation with THF rinse (3 × 1 mL). The resulting light brown mixture was stirred at -78 °C for 1 h and then injected with a -78 °C solution of freshly distilled iodomethaneboronate<sup>27</sup> (2.99 g, 11.2 mmol) in THF (2 mL) via cannulation with THF rinse (3 × 1 mL). HMPA (6.35

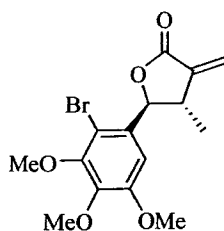
mL, 36.4 mmol) was quickly added. Stirring continued at  $-78\text{ }^{\circ}\text{C}$  for another 10 min. The mixture was then brought to  $0\text{ }^{\circ}\text{C}$ , stirred for 1 h and finally brought to rt, stirred for 1 h. Workup as Section 2.7.2.1 using 20 mL aliquots. Flash chromatography (25 %  $\text{Et}_2\text{O}$ /hexane) gave the product as a yellowish liquid (740 mg, 3.12 mmol, 77 %). This material possessed identical spectroscopic characteristics to those reported in the literature.<sup>4b</sup>

### 2.7.3 Preparation of 4,4-dimethyl-3-methylene-5-phenyl-dihydro-furan-2-one (14) under the optimal conditions



A solution of allylboronate **13b** (71.1 mg, 0.188 mmol) and benzaldehyde (38  $\mu\text{L}$ , 0.37 mmol) in toluene (0.2 mL) was treated with TfOH (1.7  $\mu\text{L}$ , 0.019 mmol) and stirred at  $0\text{ }^{\circ}\text{C}$  under Ar atmosphere for 16 h. The mixture was then diluted with  $\text{NH}_4\text{Cl}_{(\text{aq})}/\text{NH}_4\text{OH}$  (9:1 v/v, 3 mL) and extracted with  $\text{Et}_2\text{O}$  (3  $\times$  3 mL). The combined extracts were washed with brine (2  $\times$  3 mL), dried with anhydrous  $\text{Na}_2\text{SO}_4$  and concentrated. Flash chromatography (15 %  $\text{Et}_2\text{O}$ /hexane) gave the lactone product **14** (38 mg, 0.19 mmol, 99 %). This material possessed identical spectroscopic characteristics to those reported in the literature.<sup>4b</sup>

### 2.7.4 Preparation of *rac*-(4R\*, 5S\*)-5-(2-bromo-3,4,5-trimethoxyphenyl)-4-methyl-3-methylene-dihydro-furan-2-one (19b) by TfOH-catalyzed allylboration



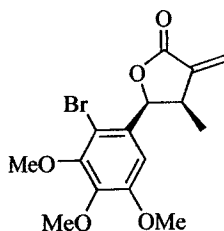
A slurry of allylboronate **13e** (323 mg, 1.34 mmol) and 2-bromo-3,4,5-trimethoxybenzaldehyde **18b**<sup>16</sup> (740 mg, 2.69 mmol) in toluene (1.34 mL) at  $0\text{ }^{\circ}\text{C}$  was treated with TfOH (24  $\mu\text{L}$ , 0.27 mmol) and stirred at  $0\text{ }^{\circ}\text{C}$  under Ar



atmosphere for 16 h. Workup as Section 2.7.3 using 20 mL aliquots. Flash chromatography (25 % EtOAc/hexane) gave the lactone product **19b** (272 mg, 0.762 mmol, 57 %).

$^1\text{H}$  NMR (500 MHz,  $\text{CDCl}_3$ ):  $\delta$  6.63 (s, 1H), 6.32 (d, 1H,  $J = 2.7$  Hz), 5.62 (d, 1H,  $J = 2.4$  Hz), 5.44 (d, 1H,  $J = 5.3$  Hz), 3.91 (s, 3H), 3.89 (s, 3H), 3.84 (s, 3H), 2.98 (m, 1H), 1.46 (d, 3H,  $J = 7.0$ );  $^{13}\text{C}$  NMR (100 MHz,  $\text{CDCl}_3$ ):  $\delta$  170.2, 153.3, 151.0, 143.1, 139.8, 134.0, 129.0, 122.1, 108.2, 105.4, 83.9, 61.0, 56.2, 43.5, 18.6; IR ( $\text{CH}_2\text{Cl}_2$  cast film,  $\text{cm}^{-1}$ ): 2969, 2938, 1769, 1485, 1396, 1325, 1248, 1107, 1000; HRMS (EI,  $m/z$ ) Calcd for  $\text{C}_{15}\text{H}_{17}^{81}\text{BrO}_5$ : 358.02390. Found: 358.02432.

### 2.7.5 Preparation of *rac*-(4S\*, 5S\*)-5-(2-bromo-3,4,5-trimethoxyphenyl)-4-methyl-3-methylene-dihydro-furan-2-one (**23**) by thermal allylboration



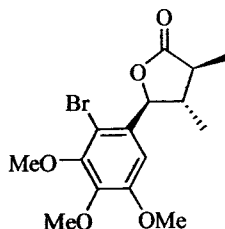
A slurry of allylboronate **13e** (358 mg, 1.49 mmol) and 2-bromo-3,4,5-trimethoxybenzaldehyde **18b**<sup>16</sup> (410 mg, 1.49 mmol) in toluene (1.5 mL) was heated at 110 °C under Ar atmosphere for 72 h. A spatula tip of *p*TSA·H<sub>2</sub>O was then added and the mixture was stirred for 3 h at rt. The reaction was quenched with  $\text{NaHCO}_3(\text{aq})$  (20 mL) and extracted with  $\text{Et}_2\text{O}$  (3 × 20 mL). The combined extracts were washed with brine (20 mL), dried with anhydrous  $\text{Na}_2\text{SO}_4$  and concentrated. Flash chromatography (35 % EtOAc/hexane) gave the lactone product **23** (394 mg, 1.10 mmol, 74 %).

$^1\text{H}$  NMR (300 MHz,  $\text{CDCl}_3$ ):  $\delta$  6.69 (s, 1H), 6.32 (d, 1H,  $J = 2.3$  Hz), 5.82 (dd, 1H,  $J = 0.6, 7.3$  Hz), 5.66 (d, 1H,  $J = 2.0$  Hz), 3.89 (s, 3H), 3.88 (s, 3H), 3.83 (s, 3H), 3.68 (m, 1H), 0.78 (d, 3H,  $J = 7.3$ );  $^{13}\text{C}$  NMR (100 MHz,  $\text{CDCl}_3$ ):  $\delta$  169.8, 152.9, 150.6, 142.6, 140.3, 131.2, 122.7, 107.3, 105.8, 80.7, 60.9, 56.1, 37.1, 16.6; IR ( $\text{CH}_2\text{Cl}_2$  cast film,  $\text{cm}^{-1}$ ): 2971, 2938, 1772, 1484, 1397, 1324,

1244, 1108, 1004; HRMS (EI, m/z) Calcd for C<sub>15</sub>H<sub>17</sub><sup>79</sup>BrO<sub>5</sub>: 356.02594. Found: 356.02523. Calcd for C<sub>15</sub>H<sub>17</sub><sup>81</sup>BrO<sub>5</sub>: 358.0290. Found: 358.02347.

## 2.7.6 Diastereoselective hydrogenation

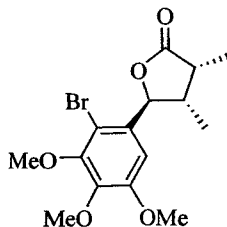
### 2.7.6.1 *rac*-(3S\*, 4S\*, 5S\*)-5-(2-Bromo-3,4,5-trimethoxyphenyl)-3,4-dimethyl-dihydro-furan-2-one (**20**)



A solution of lactone **19b** (78 mg, 0.22 mmol) in EtOH (2.4 mL) was hydrogenated at 1 atm with 10 % Pd/C (7 mg) for 6 h. The mixture was then filtered through Celite<sup>®</sup> 545 with EtOH rinse followed by solvent removal to give hydrogenated product **20** as the major diastereomer (6:1 dr). Flash chromatography (35 % EtOAc/hexane) separated the diastereomers and yielded the pure **20** (49 mg, 0.14 mmol, 64 %). Single crystals suitable for X-ray diffraction were obtained by dissolving **20** in hot pentane followed by storing the resulting solution at 0 °C in a closed vial.

<sup>1</sup>H NMR (300 MHz, CDCl<sub>3</sub>): δ 6.70 (s, 1H), 5.44 (d, 1H, *J* = 9.5 Hz), 3.91 (s, 3H), 3.90 (s, 3H), 3.87 (s, 3H), 2.40 (dq, 1H, *J* = 11.5, 7.0 Hz), 2.01 (m, 1H), 1.31 (d, 3H, *J* = 7.0 Hz), 1.23 (d, 3H, *J* = 6.6 Hz); <sup>13</sup>C NMR (125 MHz, CDCl<sub>3</sub>): δ 178.4, 153.3, 150.6, 143.4, 132.5, 109.6, 106.1, 83.9, 61.0, 60.9, 56.2, 48.6, 43.3, 14.9, 12.9; IR (CH<sub>2</sub>Cl<sub>2</sub> cast film, cm<sup>-1</sup>): 2968, 2937, 1776, 1486, 1397, 1333, 1241, 1169, 1107, 1002; HRMS (EI, m/z) Calcd for C<sub>15</sub>H<sub>19</sub><sup>79</sup>BrO<sub>5</sub>: 358.04160. Found: 358.04184. Calcd for C<sub>15</sub>H<sub>19</sub><sup>81</sup>BrO<sub>5</sub>: 360.03955. Found: 360.03992; Anal. Calcd for C<sub>15</sub>H<sub>19</sub>BrO<sub>5</sub>: C, 50.16; H, 5.33. Found: C, 50.17; H, 5.35. X-ray crystallographic data can be found in Appendix A.

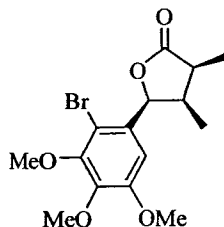
2.7.6.2 *rac*-(3R\*, 4S\*, 5S\*)-5-(2-Bromo-3,4,5-trimethoxyphenyl)-3,4-dimethyl-dihydro-furan-2-one (**21**)



A solution of lactone **19b** (86 mg, 0.24 mmol) in toluene (12.5 mL) was treated with Wilkinson's catalyst (56 mg, 0.060 mmol) and hydrogenated at 1 atm for 6 h. Solvent removal gave the hydrogenated product **21** as the major diastereomer (5:1 dr). Flash chromatography (35 % EtOAc/hexane) separated the diastereomers and yielded the pure **21** (80 mg, 0.22 mmol, 92 %). Single crystals suitable for X-ray diffraction were obtained by dissolving **21** in hot pentane followed by storing the resulting solution at 0 °C in a closed vial.

<sup>1</sup>H NMR (300 MHz, CDCl<sub>3</sub>): δ 6.63 (s, 1H), 5.34 (d, 1H, *J* = 2.5 Hz), 3.91 (s, 3H), 3.88 (s, 3H), 3.85 (s, 3H), 2.74 (app quintet, 1H, *J* = 7.5 Hz), 2.58 (m, 1H), 1.24 (d, 3H, *J* = 7.2 Hz), 1.19 (d, 3H, *J* = 7.3 Hz); <sup>13</sup>C NMR (125 MHz, CDCl<sub>3</sub>): δ 179.7, 153.1, 151.2, 142.7, 133.8, 107.4, 104.7, 84.2, 61.0, 56.2, 41.1, 36.3, 14.2, 9.5; IR (CH<sub>2</sub>Cl<sub>2</sub> cast film, cm<sup>-1</sup>): 2973, 2939, 1779, 1483, 1396, 1330, 1240, 1168, 1110, 1000; HRMS (EI, *m/z*) Calcd for C<sub>15</sub>H<sub>19</sub><sup>79</sup>BrO<sub>5</sub>: 358.04160. Found: 358.04156. Calcd for C<sub>15</sub>H<sub>19</sub><sup>81</sup>BrO<sub>5</sub>: 360.03955. Found: 360.04031; Anal. Calcd for C<sub>15</sub>H<sub>19</sub>BrO<sub>5</sub>: C, 50.16; H, 5.33. Found: C, 49.91; H, 5.32. X-ray crystallographic data can be found in Appendix B.

**2.7.6.3 *rac*-(3*S*\*, 4*R*\*, 5*S*\*)-5-(2-Bromo-3,4,5-trimethoxyphenyl)-3,4-dimethyl-dihydro-furan-2-one (24)**

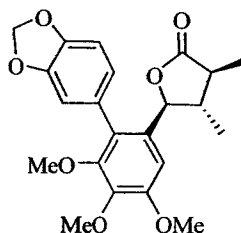


A solution of lactone **23** (55 mg, 0.16 mmol) in toluene (8 mL) was treated with Wilkinson's catalyst (36 mg, 0.039 mmol) and hydrogenated at 1 atm for 6 h. Solvent removal followed by flash chromatography (35 % EtOAc/hexane) gave the hydrogenated product **24** as the only diastereomer observed (44 mg, 0.13 mmol, 79 %). Single crystals suitable for X-ray diffraction were obtained by dissolving **24** in hot pentane followed by storing the resulting solution at 0 °C in a closed vial.

$^1\text{H}$  NMR (300 MHz,  $\text{CDCl}_3$ ):  $\delta$  6.81 (s, 1H), 5.63 (dd, 1H,  $J = 0.6, 5.0$  Hz), 3.90 (s, 3H), 3.88 (s, 3H), 3.85 (s, 3H), 3.21 (m, 1H), 3.03 (app quintet, 1H,  $J = 7.2$  Hz), 1.22 (d, 3H,  $J = 7.2$  Hz), 0.52 (d, 3H,  $J = 7.3$  Hz);  $^{13}\text{C}$  NMR (125 MHz,  $\text{CDCl}_3$ ):  $\delta$  178.5, 153.0, 150.8, 142.5, 131.1, 106.6, 106.3, 81.9, 61.1, 61.0, 56.3, 40.5, 37.3, 10.0, 9.7; IR ( $\text{CH}_2\text{Cl}_2$  cast film,  $\text{cm}^{-1}$ ): 2974, 2939, 1780, 1484, 1396, 1338, 1242, 1170, 1108, 997; HRMS (EI,  $m/z$ ) Calcd for  $\text{C}_{15}\text{H}_{19}^{79}\text{BrO}_5$ : 358.04160. Found: 358.04174. Calcd for  $\text{C}_{15}\text{H}_{19}^{81}\text{BrO}_5$ : 360.03955. Found: 360.03961; Anal. Calcd for  $\text{C}_{15}\text{H}_{19}\text{BrO}_5$ : C, 50.16; H, 5.33. Found: C, 49.63; H, 5.33. X-ray crystallographic data can be found in Appendix C.

## 2.7.7 Biaryls construction with Buchwald's Suzuki-coupling conditions<sup>19</sup>

### 2.7.7.1 3,4-*epi*-15

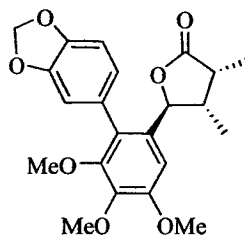


An oven-dried resealable Schlenk tube containing a magnetic stir bar was charged with arylbromide **20** (90 mg, 0.25 mmol), boronic acid **25** (62 mg, 0.38 mmol),  $K_3PO_4$  (106 mg, 0.5 mmol),  $Pd(OAc)_2$  (0.6 mg, 0.0025 mmol) and SPhos ligand (2.3 mg, 0.005 mmol). Capped with a rubber septum, the Schlenk tube was evacuated and backfilled with Ar (this sequence was repeated four times). Toluene (0.5 mL) was then added and the resulting mixture was degassed. Backfilled with Ar, the Schlenk tube was quickly sealed with a Teflon<sup>®</sup> screwcap. The mixture was heated at 110 °C with vigorous stirring for 12 h. Cooled to rt, the mixture was diluted with  $Et_2O$  followed by filtration through a thin pad of silica gel with  $Et_2O$  rinse. Solvent evaporation followed by flash chromatography (40 % EtOAc/hexane) gave 3,4-*epi*-**15** as the only diastereomer observed (96 mg, 0.24 mmol, 98 %). Single crystals suitable for X-ray diffraction were obtained by dissolving 3,4-*epi*-**15** in hot  $Et_2O$  followed by storing the resulting solution at rt in a bigger, screwcapped vial containing hexane.

<sup>1</sup>H NMR (500 MHz,  $CDCl_3$ , two atropisomers):  $\delta$  6.85 (s, 1H), 6.84 (s, 1H), 6.72 (d, 1H,  $J = 1.6$  Hz), 6.71-6.68 (m, 4H), 6.64 (dd, 1H,  $J = 1.7, 7.9$  Hz), 6.00 (m, 2H), 5.99 (m, 2H), 4.80 (d, 1H,  $J = 9.8$  Hz), 4.78 (d, 1H,  $J = 9.8$  Hz), 3.90 (s, 6H), 3.89 (s, 6H), 3.62 (s, 3H), 3.61 (s, 3H), 2.14 (m, 2H), 2.03 (m, 2H), 1.23 (d, 6H,  $J = 6.9$  Hz), 0.87 (d, 3H,  $J = 6.4$  Hz), 0.86 (d, 3H,  $J = 6.4$  Hz); <sup>13</sup>C NMR (125 MHz,  $CDCl_3$ ):  $\delta$  178.5, 178.4, 153.2, 151.2, 151.1, 147.4, 147.3, 146.8, 142.5, 130.7, 130.6, 129.8, 128.9, 128.8, 124.2, 123.3, 111.3, 110.5, 108.0, 107.8, 105.2, 105.1, 101.1, 101.0, 82.6, 82.5, 61.0, 60.9, 60.7, 56.1, 47.4, 43.2, 14.2, 12.8; IR ( $CH_2Cl_2$  cast film,  $cm^{-1}$ ): 2966, 2935, 1774, 1484, 1459, 1324, 1238, 1039, 982; HRMS (EI,  $m/z$ ) Calcd for  $C_{22}H_{24}O_7$ : 400.15219. Found:

400.15220. X-ray crystallographic data can be found in Appendix D. The compound crystallized into a single atropisomer.

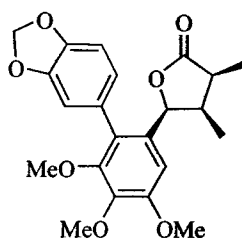
#### 2.7.7.2 4-*epi*-15



Same procedure as Section 2.7.7.1 using arylbromide **21** (90 mg, 0.25 mmol), boronic acid **25** (62 mg, 0.38 mmol),  $K_3PO_4$  (106 mg, 0.5 mmol),  $Pd(OAc)_2$  (0.6 mg, 0.0025 mmol) and SPhos ligand (2.3 mg, 0.005 mmol). After workup, solvent evaporation followed by flash chromatography (40 % EtOAc/hexane) gave 4-*epi*-**15** along with ca. 10 % of 3,4-*epi*-**15** (88 mg, 0.22 mmol, 88 % total yield). The major diastereomer 4-*epi*-**15** possessed identical spectroscopic characteristics to those reported in the literature.<sup>13</sup> Single crystals suitable for X-ray diffraction were obtained by dissolving 4-*epi*-**15** in hot  $Et_2O$  followed by storing the resulting solution at rt in a bigger, screwcapped vial containing hexane.

$^1H$  NMR (500 MHz,  $CDCl_3$ , two atropisomers):  $\delta$  6.90 (s, 1H), 6.88 (s, 1H), 6.75-6.61 (m, 6H), 6.02 (m, 4H), 5.11 (d, 1H,  $J = 4.5$  Hz), 5.01 (d, 1H,  $J = 4.5$  Hz), 3.90 (s, 6H), 3.88 (s, 6H), 3.65 (s, 3H), 3.64 (s, 3H), 2.75 (m, 2H), 2.39 (m, 2H), 1.08 (d, 3H,  $J = 7.3$  Hz), 1.07 (d, 3H,  $J = 7.3$  Hz), 0.69 (d, 3H,  $J = 7.1$  Hz), 0.66 (d, 3H,  $J = 7.1$  Hz);  $^{13}C$  NMR (125 MHz,  $CDCl_3$ ):  $\delta$  179.9, 153.1, 153.0, 151.8, 151.7, 147.7, 146.9, 146.8, 142.0, 132.8, 129.0, 128.9, 124.1, 122.9, 111.2, 110.1, 108.4, 108.2, 103.6, 101.2, 101.1, 82.8, 61.1, 61.0, 60.8, 56.2, 41.6, 41.5, 37.1, 13.3, 9.8. X-ray crystallographic data can be found in Appendix E. The compound crystallized into a single atropisomer.

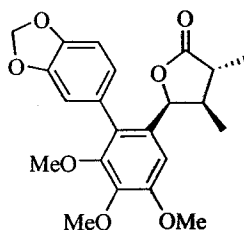
### 2.7.7.3 3-*epi*-15



Same procedure as Section 2.7.7.1 using arylbromide **24** (92 mg, 0.26 mmol), boronic acid **25** (63 mg, 0.38 mmol),  $K_3PO_4$  (108 mg, 0.51 mmol),  $Pd(OAc)_2$  (2.8 mg, 0.012 mmol) and SPhos ligand (12 mg, 0.026 mmol). After workup, solvent evaporation followed by flash chromatography (35 % EtOAc/hexane) gave 3-*epi*-**15** along with ca. 17 % of **15** (100 mg, 0.25 mmol, 96 % total yield). The major diastereomer 3-*epi*-**15** possessed identical spectroscopic characteristics to those reported in the literature.<sup>14, 15</sup>

$^1H$  NMR (300 MHz,  $CDCl_3$ , two atropisomers):  $\delta$  6.88 (s, 1H), 6.86 (s, 1H), 6.84 (s, 1H), 6.82 (s, 1H), 6.73 (d, 1H,  $J = 1.6$  Hz), 6.70 (dd, 1H,  $J = 1.6, 7.8$  Hz), 6.62 (d, 1H,  $J = 1.6$  Hz), 6.58 (dd, 1H,  $J = 1.7, 7.9$  Hz), 6.04 (m, 2H), 6.02 (m, 2H), 5.41 (d, 1H,  $J = 4.9$  Hz), 5.32 (d, 1H,  $J = 4.9$  Hz), 3.91 (s, 12H), 3.66 (s, 3H), 3.65 (s, 3H), 2.75 (m, 2H), 2.20 (m, 2H), 1.12 (d, 6H,  $J = 7.2$  Hz), 0.56 (app triplet, 6H,  $J = 7.2$  Hz);  $^{13}C$  NMR (125 MHz,  $CDCl_3$ ):  $\delta$  178.6, 152.7, 151.4, 147.6, 147.5, 146.9, 146.8, 141.4, 130.1, 129.1, 129.0, 126.3, 126.2, 123.4, 122.2, 110.5, 109.5, 108.3, 108.1, 104.8, 104.7, 101.1, 80.4, 80.3, 61.1, 61.0, 60.7, 56.1, 40.6, 38.7, 38.5, 9.8, 9.7, 9.6.

### 2.7.8 DBU-promoted epimerization<sup>21</sup> of 3-*epi*-15 to eupomatilone-6 (**15**)



In a resealable Schlenk tube, a small mixture which contained mainly 3-*epi*-**15** in 1:1 toluene/MeOH (2 mL) was treated with DBU (~ 1.5 equiv.). The Schlenk tube was sealed with a Teflon<sup>®</sup> screwcap and the mixture was heated at

80 °C with vigorous stirring for 2 days. The now almost 1:1 (based on  $^1\text{H}$  NMR) mixture of 3-*epi*-**15** and eupomatilone-6 (**15**) was submitted to preparative TLC (20 % EtOAc/hexane with multiple developments)<sup>15</sup> and an analytically pure sample of **15** was obtained by de-absorption with  $\text{CH}_2\text{Cl}_2$ , filtration and concentration. This material possessed identical spectroscopic characteristics to those reported in the literature.<sup>15</sup>

$^1\text{H}$  NMR (500 MHz,  $\text{CDCl}_3$ , two atropisomers):  $\delta$  6.88 (d, 1H,  $J = 8.1$  Hz), 6.87 (d, 1H,  $J = 8.1$  Hz), 6.73 (d, 1H,  $J = 1.4$  Hz), 6.70 (dd, 1H,  $J = 1.6, 7.8$  Hz), 6.67 (s, 1H), 6.66 (s, 1H), 6.65 (d, 1H,  $J = 1.4$  Hz), 6.59 (dd, 1H,  $J = 1.6, 8.1$  Hz), 6.03 (m, 2H), 6.02 (m, 2H), 5.65 (d, 1H,  $J = 7.0$  Hz), 5.53 (d, 1H,  $J = 7.0$  Hz), 3.91 (s, 6H), 3.89 (s, 6H), 3.65 (s, 3H), 3.64 (s, 3H), 2.36 (m, 2H), 2.05-1.96 (m, 2H), 1.20 (d, 3H,  $J = 7.6$  Hz), 1.19 (d, 3H,  $J = 7.6$  Hz), 0.73 (d, 3H,  $J = 7.2$  Hz), 0.70 (d, 3H,  $J = 7.2$  Hz).

## 2.7.9 Preliminary mechanistic investigations

### 2.7.9.1 Treatment of *E*-allylboronate **13e** with TfOH

Isomerically pure *E*-allylboronate **13e** (23 mg, 0.096 mmol) was dissolved in toluene (0.1 mL), cooled to 0 °C, treated with TfOH (1.7  $\mu\text{L}$ , 0.019 mmol) and stirred at 0 °C under Ar atmosphere for 16 h. Workup as Section 2.7.3 using 2 mL aliquots.  $^1\text{H}$  NMR analysis of the crude reaction mixture showed mainly starting *E*-allylboronate **13e** (ca. 66 %) along with other unidentified side products. No *Z*-isomer was observed.

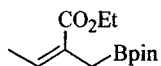
### 2.7.9.2 Treatment of thermal *cis*-lactone **23** with TfOH

Diastereomerically pure *cis*-lactone **23** (34 mg, 0.095 mmol) was dissolved in toluene (0.1 mL), cooled to 0 °C, treated with TfOH (1.7  $\mu\text{L}$ , 0.019 mmol) and stirred at 0 °C under Ar atmosphere for 16 h. Workup as Section 2.7.3



using 2 mL aliquots.  $^1\text{H}$  NMR analysis of the crude reaction mixture showed mainly starting lactone **23** (ca. 80 %) along with ca. 20 % of lactone **19b**.

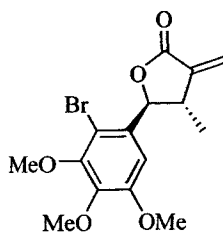
### 2.7.9.3 Preparation of ethyl (2*Z*)-2-[(4,4,5,5-tetramethyl-1,3,2-dioxaborolan-2-yl)methyl] but-2-enoate (**29**)<sup>22</sup>



To a stirring solution of HMPA (1.56 mL, 8.97 mmol) in toluene (9 mL) under Ar atmosphere at 0 °C, DIBALH (1.0 M in toluene, 4.48 mL, 4.48 mmol) was added dropwise. After stirring at 0 °C for 1 h, freshly distilled ethyl 2-butynoate (0.35 mL, 3.0 mmol) was added and stirring continued at 0 °C for another 5 h. Freshly distilled chloromethaneboronate<sup>23</sup> (632 mg, 3.58 mmol) in toluene (2 mL) was added via cannulation with toluene rinse (3 × 1 mL) and the resulting mixture was allowed to warm up to rt and stirred under Ar atmosphere for 16 h. The reaction was then quenched with 1 M HCl (16 mL) and extracted with Et<sub>2</sub>O (4 × 20 mL). The combined organic phase was washed with 1 M HCl (3 × 16 mL), NaHCO<sub>3(aq)</sub> (1 × 16 mL), water (1 × 16 mL), brine (1 × 16 mL), dried with anhydrous Na<sub>2</sub>SO<sub>4</sub>, filtered and concentrated. Flash chromatography (25 % Et<sub>2</sub>O/hexane) gave the product along with ca. 17 % of the *E*-isomer (224 mg, 0.882 mmol, 30 % combined yield).

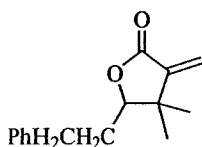
$^1\text{H}$  NMR (300 MHz, CDCl<sub>3</sub>):  $\delta$  6.04 (qt, 1H,  $J = 7.2, 1.3$  Hz), 4.20 (q, 2H,  $J = 7.1$  Hz), 2.00 (dt, 3H,  $J = 7.2, 1.3$  Hz), 1.84 (s, 2H), 1.30 (t, 3H,  $J = 7.1$  Hz), 1.24 (s, 12H);  $^{13}\text{C}$  NMR (125 MHz, CDCl<sub>3</sub>):  $\delta$  168.0, 136.8, 129.1, 83.2, 60.0, 24.7, 15.8, 14.2; IR (microscope, cm<sup>-1</sup>): 2980, 1717, 1353, 1323, 1146, 968, 847; HRMS (EI,  $m/z$ ) Calcd for C<sub>13</sub>H<sub>23</sub><sup>11</sup>BO<sub>4</sub>: 254.16985. Found: 254.16918.

**2.7.9.4 Preparation of *rac*-(4R\*, 5S\*)-5-(2-bromo-3,4,5-trimethoxyphenyl)-4-methyl-3-methylene-dihydro-furan-2-one (19b) by TfOH-catalyzed allylboration with *Z*-allylboronate 29**



A slurry of *Z*-allylboronate **29** (*Z/E* = 5:1, 60.4 mg, 0.238 mmol) and 2-bromo-3,4,5-trimethoxybenzaldehyde **18b**<sup>16</sup> (131 mg, 0.476 mmol) in toluene (0.24 mL) at 0 °C was treated with TfOH (4.2  $\mu$ L, 0.048 mmol) and stirred at 0 °C under Ar atmosphere for 16 h. Workup as Section 2.7.3 using 4 mL aliquots. Flash chromatography (25 % EtOAc/hexane) gave the diastereomerically pure lactone product **19b** (85 mg, 0.238 mmol, 100 %). This material possessed identical spectroscopic characteristics to those reported above for **19b**.

**2.7.10 Preparation of 4,4-dimethyl-3-methylene-5-phenethyl-dihydro-furan-2-one (35) by asymmetric allylboration using chiral allylboronate 13c**



A solution of chiral allylboronate **13c** (52.2 mg, 0.115 mmol) and hydrocinnamaldehyde (30  $\mu$ L, 0.23 mmol) in toluene (0.1 mL) was treated with TfOH (1.0  $\mu$ L, 0.011 mmol) and stirred at 0 °C under Ar atmosphere for 16 h. Workup as Section 2.7.3 using 3 mL aliquots. Flash chromatography (15 % Et<sub>2</sub>O/hexane) gave the lactone product **35** (23 mg, 0.10 mmol, 87 %, 62 % ee). Enantiomeric excess was determined by chiral HPLC using 45 % *i*PrOH and 55 % water as eluent at 0.3 mL/min.

<sup>1</sup>H NMR (500 MHz, CDCl<sub>3</sub>):  $\delta$  7.31 (m, 2H), 7.22 (m, 3H), 6.17 (s, 1H), 5.48 (s, 1H), 4.05 (m, 1H), 2.98 (m, 1H), 2.72 (dt, 1H, *J* = 13.9, 8.3 Hz), 1.85 (m, 2H), 1.20 (s, 3H), 1.10 (s, 3H); <sup>13</sup>C NMR (125 MHz, CDCl<sub>3</sub>):  $\delta$  170.2, 146.0, 141.0, 128.5, 128.4, 126.1, 119.3, 86.2, 41.8, 32.4, 32.1, 25.6, 22.8; IR (CHCl<sub>3</sub>

cast film,  $\text{cm}^{-1}$ ): 2942, 1755, 1454, 1026, 950, 757, 701; HRMS (EI,  $m/z$ ) Calcd for  $\text{C}_{15}\text{H}_{18}\text{O}_2$ : 230.13068. Found: 230.13059. Anal. Calcd for  $\text{C}_{15}\text{H}_{18}\text{O}_2$ : C, 78.23; H, 7.88. Found: C, 78.26; H, 7.94.

## 2.8 References

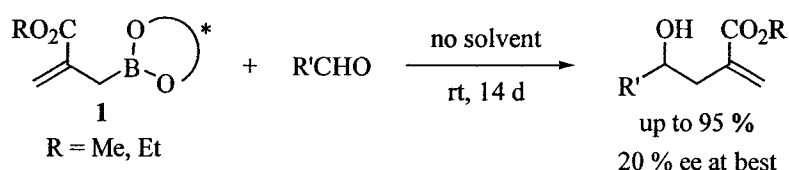
1. a) Denmark, S. E.; Almstead, N. G. in *Modern Carbonyl Chemistry* (Ed.: Otera, J.), Wiley-VCH, Weinheim, **2000**, pp 299-401. b) Chemler, S. R.; Roush, W. R. in *Modern Carbonyl Chemistry* (Ed.: Otera, J.), Wiley-VCH, Weinheim, **2000**, pp 403-490.
2. Denmark, S. E.; Weber, E. J. *Helv. Chim. Acta* **1983**, *66*, 1655-1660.
3. Kennedy, J. W. J.; Hall, D. G. *Angew. Chem. Int. Ed.* **2003**, *42*, 4732-4739.
4. a) Kennedy, J. W. J.; Hall, D. G. *J. Am. Chem. Soc.* **2002**, *124*, 11586-11587. b) Kennedy, J. W. J.; Hall, D. G. *J. Org. Chem.* **2004**, *69*, 4412-4428.
5. Kennedy, J. W. J.; Hall, D. G. *J. Am. Chem. Soc.* **2002**, *124*, 898-899.
6. Rauniyar, V.; Hall, D. G. *J. Am. Chem. Soc.* **2004**, *126*, 4518-4519.
7. Williams, A. L.; Johnston, J. N. *J. Am. Chem. Soc.* **2004**, *126*, 1612-1613.
8. Nakashima, D.; Yamamoto, H. *Org. Lett.* **2005**, *7*, 1251-1253.
9. Zhang, Y.; Hsung, R. P.; Zhang, X.; Huang, J.; Slafer, B. W.; Davis, A. *Org. Lett.* **2005**, *7*, 1047-1050.
10. Jung, M. E.; Gervay, J. *J. Am. Chem. Soc.* **1991**, *113*, 224-232.
11. Carroll, A. R.; Taylor, W. C. *Aust. J. Chem.* **1991**, *44*, 1615-1626.
12. a) MacRae, W. D.; Towers, G. H. N. *Phytochemistry* **1984**, *23*, 1207-1220. b) Ward, R. S. *Nat. Prod. Rep.* **1997**, *14*, 43-74.
13. Hutchison, J. M.; Hong, S.-P.; McIntosh, M. C. *J. Org. Chem.* **2004**, *69*, 4185-4191.
14. Gurjar, M. K.; Cherian, J.; Ramana, C. V. *Org. Lett.* **2004**, *6*, 317-319.
15. Coleman, R. S.; Gurrula, S. R. *Org. Lett.* **2004**, *6*, 4025-4028.

16. Molander, G. A.; George, K. M.; Monovich, L. G. *J. Org. Chem.* **2003**, *68*, 9533-9540.
17. Callam, C. S.; Lowary, T. L. *J. Org. Chem.* **2001**, *66*, 8961-8972.
18. Miyaura, N.; Suzuki, A. *Chem. Rev.* **1995**, *95*, 2457-2483.
19. Barder, T. E.; Walker, S. D.; Martinelli, J. R.; Buchwald, S. L. *J. Am. Chem. Soc.* **2005**, *127*, 4685-4696.
20. Crabtree, R. H.; Davis, M. W. *J. Org. Chem.* **1986**, *51*, 2655-2661.
21. Pinto, A. C.; Freitas, C. B. L.; Dias, A. G.; Pereira, V. L. P.; Tinant, B.; Declercq, J.-P.; Costa, P. R. R. *Tetrahedron: Asymmetry* **2002**, *13*, 1025-1031.
22. a) Ramachandran, P. V.; Pratihari, D.; Biswas, D.; Srivastava, A.; Reddy, M. V. R. *Org. Lett.* **2004**, *6*, 481-484. b) Nyzam, V.; Belaud, C.; Villiéras, J. *Tetrahedron Lett.* **1993**, *34*, 6899-6902.
23. Whiting, A. *Tetrahedron Lett.* **1991**, *32*, 1503-1506.
24. Fonquerna, S.; Moyano, A.; Pericàs, M. A.; Riera, A. *Tetrahedron* **1995**, *51*, 4239-4254.
25. Mühlthau, F.; Schuster, O.; Bach, T. *J. Am. Chem. Soc.* **2005**, *127*, 9348-9349.
26. Taylor, R. K.; Casy, G. In *Organocopper Reagents: A Practical Approach*; Taylor, R. K., Ed.; Oxford University Press: New York, **1994**, pp 53-72.
27. Phillion, D. P.; Neubauer, R.; Andrew, S. S. *J. Org. Chem.* **1986**, *51*, 1610-1612.
28. a) Mezrhab, B.; Dumas, F.; d'Angelo, J.; Riche, C. *J. Org. Chem.* **1994**, *59*, 500-503. b) Dumas, F.; Mezrhab, B.; d'Angelo, J.; Riche, C.; Chiaroni, A. *J. Org. Chem.* **1996**, *61*, 2293-2304.

# Chapter 3 Access to Homoallylic Alcohol Products via Lewis Acid-Catalyzed Allylboration Using 2-Functionalized Allylboronate Reagents

## 3.1 Introduction

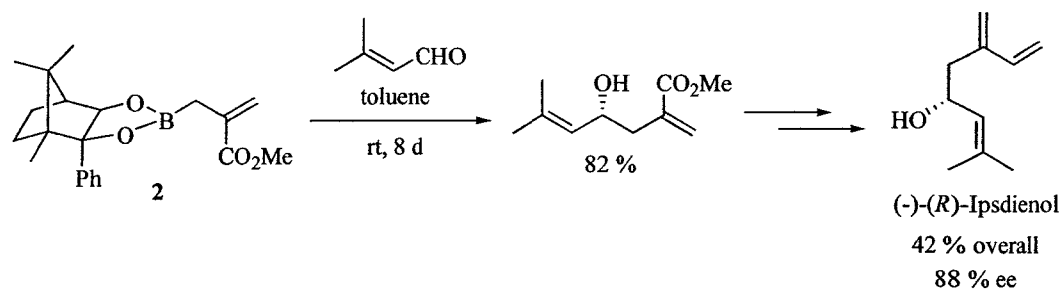
Over the development of an efficient, asymmetric allylboration methodology, Villieras and co-workers had demonstrated the usefulness of 2-alkoxycarbonyl allylboronates of type **1**.<sup>1</sup> In their original report using various chiral diol auxiliaries, excellent yields could be obtained for the homoallylic alcohol products but the enantioselectivity was quite poor (Scheme 3-1).<sup>1a</sup> Upon



**Scheme 3-1.** Literature precedent for uncatalyzed allylboration using **1**.

further investigation, they discovered that Hoffmann's diol provided a considerable improvement bringing the stereoselectivity to a more practical level (up to 82 % ee).<sup>1b</sup> Later on, making use of allylboronate **2**, Villieras and co-workers applied their optimal allylboration protocol as the key stereoinduction step to a synthesis of the unnatural enantiomer of (+)-(*S*)-ipsdienol with an enantiomeric excess of 88 % (Scheme 3-2).<sup>1c</sup> Despite the improved enantioselectivity, the major limitation in all these uncatalyzed allylborations was the sluggish reaction rate leading to prolonged reaction times. As our group had reported the unprecedented Lewis acid-catalyzed allylborations (Section 2.1.1),<sup>2</sup> we became interested in applying the Lewis acid catalytic protocol to

allylboration using 2-functionalized allylboronates to access synthetically useful homoallylic alcohol products.

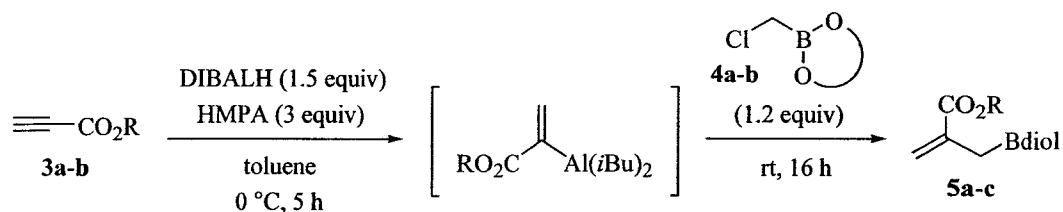


Scheme 3-2. Application of allylboronate **2** to the synthesis of (-)-(R)-ipsdienol.<sup>1c</sup>

## 3.2 Lewis Acid-Catalyzed Allylboration Using 2-Alkoxy carbonyl Allylboronates

### 3.2.1 Synthesis of allylboronates

Table 3-1. Synthesis of various 2-alkoxycarbonyl allylboronates.



3	4	Product	Yield (%) <sup>a</sup>
<b>a</b> (R = Me)	<b>a</b> (diol = pinacol)	<b>5a</b>	86
<b>b</b> (R = (-)-8-phenylmenthyl)	<b>a</b> (diol = pinacol)	<b>5b</b>	49
<b>a</b> (R = Me)	<b>b</b> (diol = Hoffmann <sup>10</sup> )	<b>5c</b> (same as <b>2</b> )	79

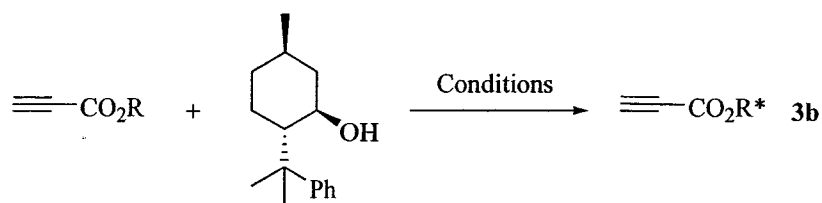
<sup>a</sup> Isolated yields.

During this first stage of the project, the generation of the required allylboronates was relatively straightforward. Following the hydroalumination/electrophile trapping protocol utilized by Villieras and co-

workers,<sup>1d</sup> achiral (**5a**) and chiral (**5b** and **5c**) allylboronates were synthesized in moderate to good yields (Table 3-1). Chloromethaneboronates **4a** and **4b** were synthesized based on Whiting's procedure.<sup>3</sup> At 0 °C in 5 hours, the chemoselective DIBALH-HMPA conjugate reduction proceeded smoothly without incident.

Although never explored by Villiéras, the introduction of a chiral auxiliary on the ester moiety might provide higher enantioselectivity in the subsequent asymmetric allylboration as demonstrated by our group.<sup>2b</sup> We therefore decided to make chiral allylboronate **5b**, but the synthesis of the required alkynoate ester **3b** turned out to be more difficult than expected. As shown in Table 3-2, both DCC-mediated esterification<sup>2b</sup> and AlMe<sub>3</sub>-promoted transesterification<sup>4</sup> were found to be low-yielding after several attempts with increased amount of DCC and DMAP, as well as with the use of a brand new bottle of AlMe<sub>3</sub> reagent. Since the

**Table 3-2.** Conditions to generate chiral alkynoate ester **3b**.



R	amount of phenylmenthol (equiv)	Conditions	Yield (%) <sup>a</sup>
H	1	DCC (4.4 equiv) DMAP (20 mol %) CH <sub>2</sub> Cl <sub>2</sub> 0 °C to rt, 12 h	20
Me	2.1	AlMe <sub>3</sub> (2.2 equiv) toluene 60 °C, 12 h	17

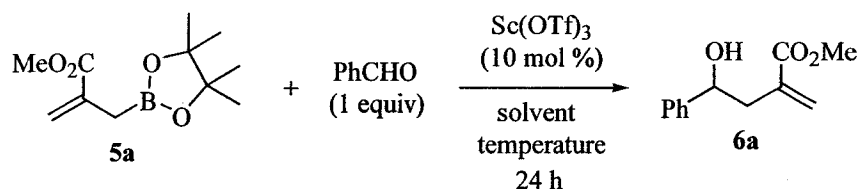
<sup>a</sup> Best isolated yields after several attempts.

unreacted chiral alcohol could be recovered, we managed to generate enough **3b** to carry on with the synthesis of **5b**. Later on for a different project, however, we were delighted to find an improved synthesis of **3b** via *p*TSA-catalyzed transesterification<sup>5</sup> (Section 2.5.1).

### 3.2.2 Results from Lewis acid-catalyzed allylboration using 2-alkoxycarbonyl allylboronates

Having the desired allylboronates in hand, we set out to optimize the Sc(OTf)<sub>3</sub>-catalyzed allylboration protocol. As suggested in Table 3-3, dichloromethane (Entries 1 and 2) was found to be a better solvent than toluene. It is noteworthy to highlight the significant rate acceleration provided by Sc(OTf)<sub>3</sub>. Compared to room temperature or reflux in toluene for 1 to 2 weeks as reported by Villi ras,<sup>1</sup> we were able to perform the desired allylboration at subzero temperatures (-60  C as the optimal, Entry 2) in only one day! Unlike using 3-substituted allylboronates as in Chapter 2, lactonization does not occur spontaneously under the current allylboration conditions.

**Table 3-3.** Optimization of allylboration parameters.



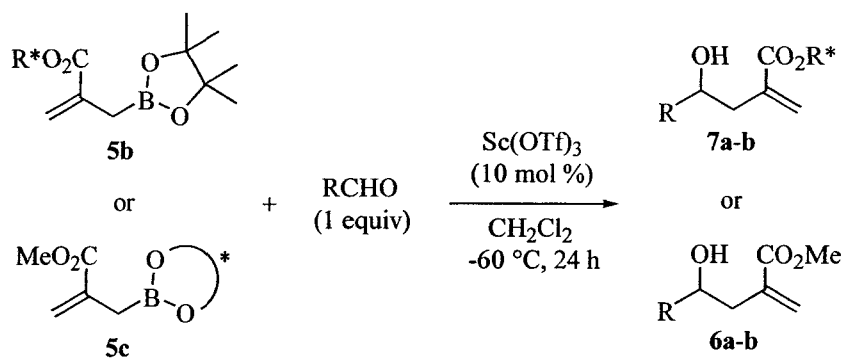
Entry	Solvent	Temperature (�C)	Yield (%) <sup>a</sup>
1	CH <sub>2</sub> Cl <sub>2</sub>	-78	60
2		-60	87
3	toluene	-78	45
4		-60	79

<sup>a</sup> Isolated yields.



With these promising results, asymmetric allylboration was then carried out using allylboronates **5b** and **5c** with both aromatic and aliphatic aldehydes (Table 3-4). Under the optimized conditions, aliphatic aldehyde seemed to be a better substrate than the aromatic one (compare Entries 2 to 1 and 4 to 3). Without lactonization, the phenylmenthyl chiral auxiliary remained in the final products **7a** and **7b** owning 1.2:1 and 1.5:1 dr, respectively. Using allylboronate **5c**, the desired product was not observed when benzaldehyde was used whereas hydrocinnamaldehyde gave the homoallylic alcohol adduct in 45 % yield with a decent 80 % ee, which is in the same range with those reported by Villieras.<sup>1b</sup> As most yields and stereoselectivities were rather disappointing, we reasoned that having the electron-withdrawing, deactivating carboxyester functionality might be the root of the problem and decided to replace it with a more electron-rich *O*-protected ether moiety.

**Table 3-4.** Results from asymmetric allylboration using **5b** and **5c**.



Entry	5	Aldehyde	Product	Yield (%)	Stereoselectivity
1	<b>b</b>	PhCHO	<b>7a</b>	57 <sup>a</sup>	1.2:1 dr <sup>c</sup>
2		PhCH <sub>2</sub> CH <sub>2</sub> CHO	<b>7b</b>	99 <sup>a</sup>	1.5:1 dr <sup>c</sup>
3	<b>c</b>	PhCHO	<b>6a</b>	not observed	-
4		PhCH <sub>2</sub> CH <sub>2</sub> CHO	<b>6b</b>	45 <sup>b</sup>	80 % ee <sup>d</sup>

<sup>a</sup> Combined yields of purified diastereomers. <sup>b</sup> Isolated yield. <sup>c</sup> Based on <sup>1</sup>H NMR analysis of the crude reaction mixture. <sup>d</sup> Determined by chiral HPLC.

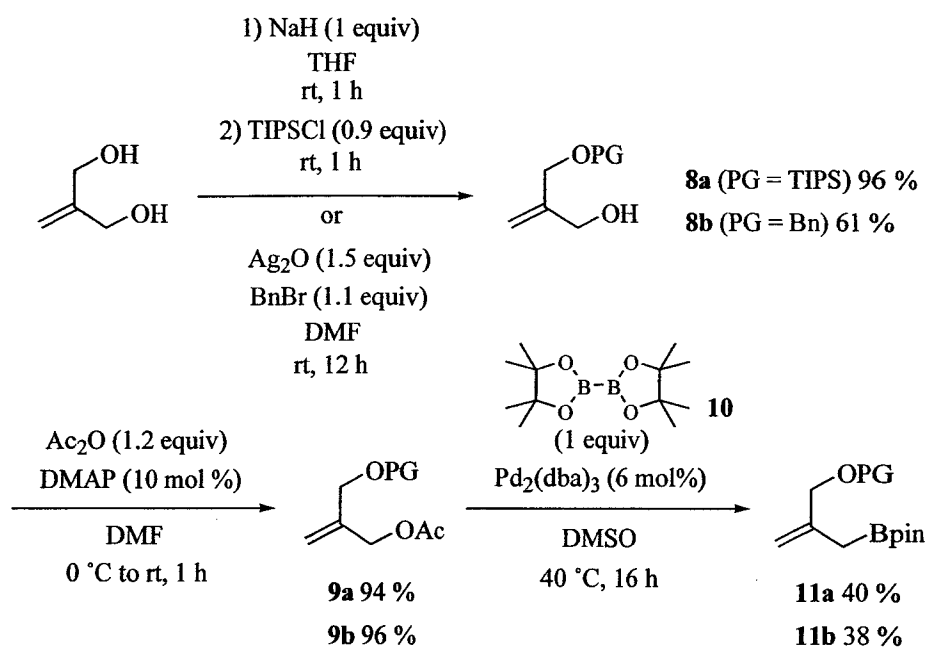
### 3.3 Allylboration Using 2-*O*-Protected Ether Allylboronates

With the aim to generate a more active and hopefully more stereoselective allylboronate reagent, 2-*O*-protected ether allylboronates were particularly attractive. In addition to fulfilling the electron-donating requirement, like the carboxyester functionality, the deprotected alcohol could undergo further transformations making the resulting allylboration adducts useful synthetic intermediates.

#### 3.3.1 Synthesis of achiral allylboronates

To synthesize the desired achiral allylboronates **11a** and **11b**, we started with the monoprotection of 2-methylene-1,3-propanediol (Scheme 3-3). Two electronically different classes, namely silyl and benzyl ethers, were selected in the aim to test the resulting allylboronates' reactivity in the Lewis acid-catalyzed allylboration. While the simple benzyl group was chosen, we decided to use the bulky triisopropylsilyl group because of its possible sterically-controlled regio and stereodirecting effects according to literature precedents.<sup>6</sup> With one equivalent of sodium hydride and TIPSCl as the limiting reagent,<sup>7</sup> monoprotected diol **8a** was obtained in 96 % yield. Monoprotection to generate **8b** was on the other hand more problematic. After several attempts, the NaH/BnBr protocol only gave **8b** in 49 % yield at best and the results were not consistent due to the formation of various amount of the undesired diprotected product. At the end, we settled with Sauv e's selective silver(I) oxide-mediated monoprotection protocol for symmetrical diols<sup>8</sup> to obtain **8b** in 61 % yield.

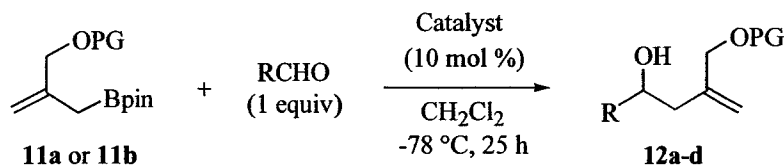
The subsequent acetylation was straightforward and provided both acetates **9a** and **9b** in almost quantitative yields. With the acetates in hand, allylboronates **11a** and **11b** were synthesized using Miyaura's procedure for palladium(0)-catalyzed cross-coupling reaction between bis(pinacolato)diboron (**10**) and allylic acetate.<sup>9</sup> Albeit low yielding, we were able to generate enough material to test the allylboration of interest.



**Scheme 3-3.** Generation of two different *O*-protected ether allylboronates.

### 3.3.2 Results from Lewis acid-catalyzed allylboration using 2-*O*-protected ether allylboronates

Using the optimized conditions from Section 3.2.2, Lewis acid-catalyzed allylborations were tested at -78 °C (instead of -60 °C) anticipating that **11a** and **11b** would be more reactive than their 2-alkoxycarbonyl analogues. As summarized in Table 3-5, it was indeed the case when using a silyl ether as protecting group under Sc(OTf)<sub>3</sub> catalysis (Entries 1 and 2). Surprisingly, the *O*-benzyl analogue did not lead to any allylboration adduct. After workup, the <sup>1</sup>H NMR spectra showed a complex mixture and neither starting material nor desired product could be isolated from a careful flash silica gel column. We also tried using milder Lewis acids such as Cu(OTf)<sub>2</sub> and Yb(OTf)<sub>3</sub> (Entries 5 and 6) without success. Based on these preliminary results, we decided to devote our effort to generate the chiral variant of 2-*O*-TIPS ether allylboronate to examine the enantioselectivity from the corresponding asymmetric allylboration.

**Table 3-5.** Results from Lewis acid-catalyzed allylboration using **11a** and **11b**.

Entry	PG	R	Catalyst	Product	Yield (%) <sup>a</sup>
1	TIPS	Ph	Sc(OTf) <sub>3</sub>	<b>12a</b>	99
2	TIPS	PhCH <sub>2</sub> CH <sub>2</sub>	Sc(OTf) <sub>3</sub>	<b>12b</b>	81
3	Bn	Ph	Sc(OTf) <sub>3</sub>	<b>12c</b>	-
4	Bn	PhCH <sub>2</sub> CH <sub>2</sub>	Sc(OTf) <sub>3</sub>	<b>12d</b>	-
5	Bn	PhCH <sub>2</sub> CH <sub>2</sub>	Cu(OTf) <sub>2</sub>	<b>12d</b>	-
6	Bn	PhCH <sub>2</sub> CH <sub>2</sub>	Yb(OTf) <sub>3</sub>	<b>12d</b>	-

<sup>a</sup> Isolated yields.

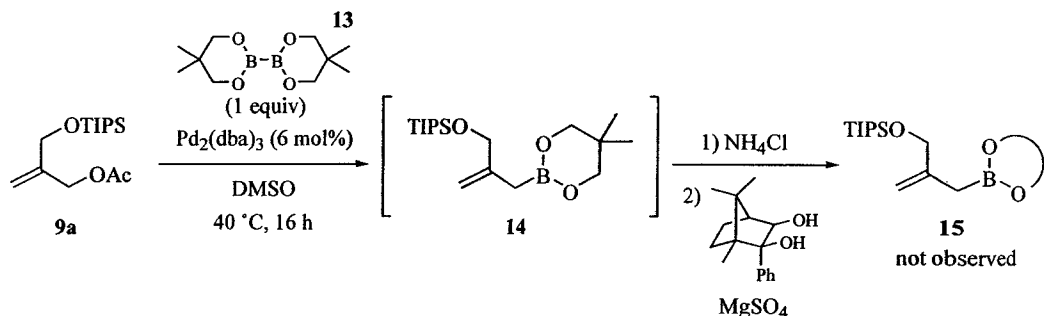
### 3.3.3 Synthetic attempts to generate chiral 2-*O*-TIPS ether allylboronate

As Hoffmann's diol<sup>10</sup> is not commercially available, most of the synthetic attempts summarized in this section were tested first in generating the achiral allylboronate **11a**.

#### 3.3.3.1 Diboron coupling

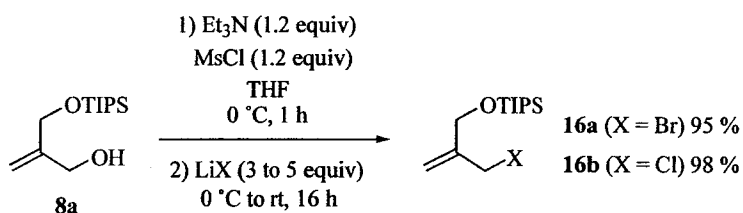
The first attempt to generate the desired chiral allylboronate **15** was to employ the same Miyaura's diboron coupling protocol used in Section 3.3.1 for the synthesis of **11**. Replacing the diboron species with bis(neopentyl glycolato)diboron (**13**, Scheme 3-4), the coupled product should more easily undergo a diol exchange. We first tried to isolate intermediate **14** without success. As neopentyl glycolate is a more labile ester than pinacolate, **14** may be prone to hydrolysis so we decided to generate the corresponding boronic acid *in situ* followed by esterification with Hoffmann's diol. Under this procedure, however,

only starting material **9a** (ca. 20 %) could be isolated and no desired product was observed.



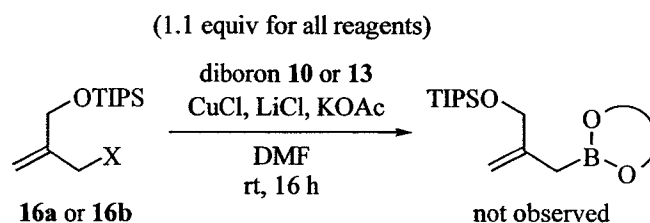
**Scheme 3-4.** Attempted synthesis of **15** via Miyaura's diboron coupling and diol exchange.

Based on another variant developed by Miyaura, allyl halides could be coupled with diboron compounds via a nucleophilic borylcopper species.<sup>11</sup> We therefore decided to synthesize the allylic halide precursors. Using Meyers' method,<sup>12</sup> mesylation of the monoprotected alcohol **8a** followed by *in-situ* nucleophilic displacement furnished allylic halides **16a** and **16b** in excellent yields (Scheme 3-5).



**Scheme 3-5.** Synthesis of allylic halides **16a** and **16b**.

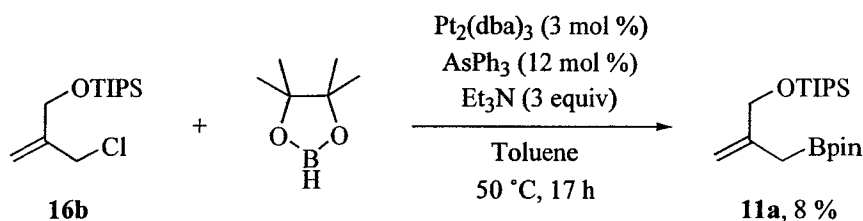
In the presence of CuCl, KOAc and LiCl (Scheme 3-6), both allyl halides **16a** and **16b** unfortunately failed to undergo the desired coupling with either diboron **10** (served as control) or **13** (potentially useful for diol exchange). In all cases, allylic chloride **16b** was isolated (or recovered) as the major product along with ca. 15 to 30 % allylic acetate **9a** as a side product.



**Scheme 3-6.** Failed attempts of diboron coupling via borylcopper species.

### 3.3.3.2 Platinum-catalyzed borylation

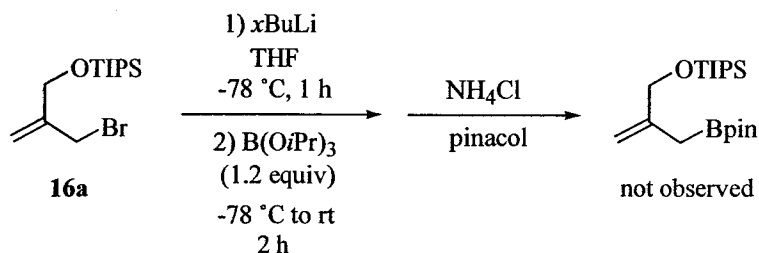
With the versatile allyl halides in hand, the next option was to try platinum-catalyzed borylation using Masuda's method.<sup>13</sup> In the presence of Et<sub>3</sub>N and a catalytic amount of Pt(dba)<sub>2</sub> and AsPh<sub>3</sub>, only trace amount of **11a** was isolated from the reaction with allyl chloride **16b** (Scheme 3-7). Since additional control experiments using simpler substrates such as allyl bromide and β-methallyl chloride could not reproduce the literature results, we decided to abandon this method



**Scheme 3-7.** Pt-catalyzed borylation using pinacolborane.

### 3.3.3.3 Lithium-halogen exchange

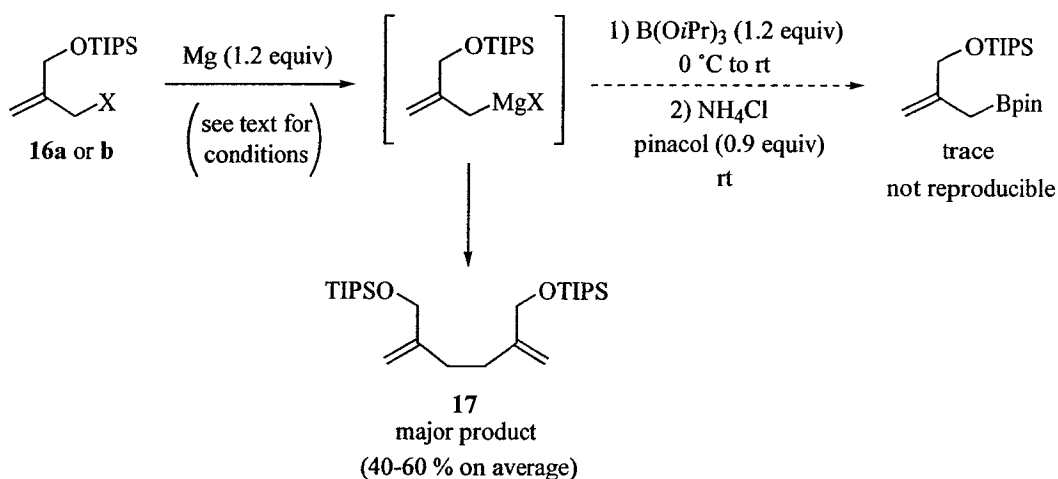
Using allyl bromide **16a**, lithium-halogen exchange (Scheme 3-8) was tried with *n*BuLi (1.2 equiv), *s*BuLi (1.2 equiv) and *t*BuLi (2 equiv). No desired product was observed in all cases according to <sup>1</sup>H NMR analysis of the crude reaction mixtures, and an *in-situ* trapping procedure with borate present in the first step did not provide any improvement.



**Scheme 3-8.** Attempted lithium-halogen exchange with allyl bromide **16a**.

### 3.3.3.4 Grignard addition using allyl halides

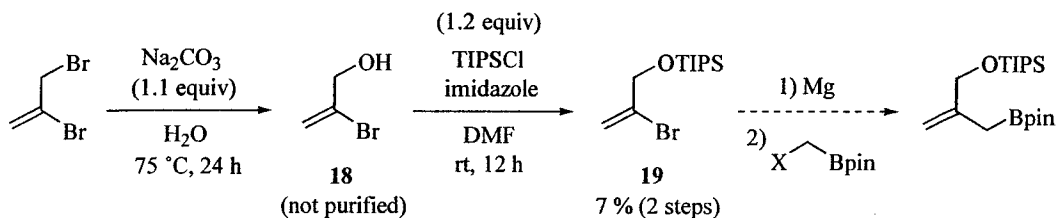
As the last alternative employing the allyl halides **16**, a laborious optimization of Grignard additions was carried out with both allyl chloride and bromide (Scheme 3-9). In terms of reaction conditions, different combinations of solvents (THF and Et<sub>2</sub>O), temperatures (0, rt, 50 and 70 °C) and catalytic promoters (I<sub>2</sub> and 1,2-dibromoethane) were tried, with most leading to dimer **17** as the major isolated product. At 0 °C, reactions usually did not take place and starting material was recovered. To minimize the extent of dimerization, we also experimented with high dilution, slow addition of the allyl halide, and varied the reaction time from 15 minutes to 2 h with no significant amelioration. Based on the results summarized so far in this section, it was apparent that allylic intermediates might not be the most suitable substrates to generate our target compound.



**Scheme 3-9.** Dimerization via attempted Grignard additions.

### 3.3.3.5 Generation of vinylic synthetic intermediates

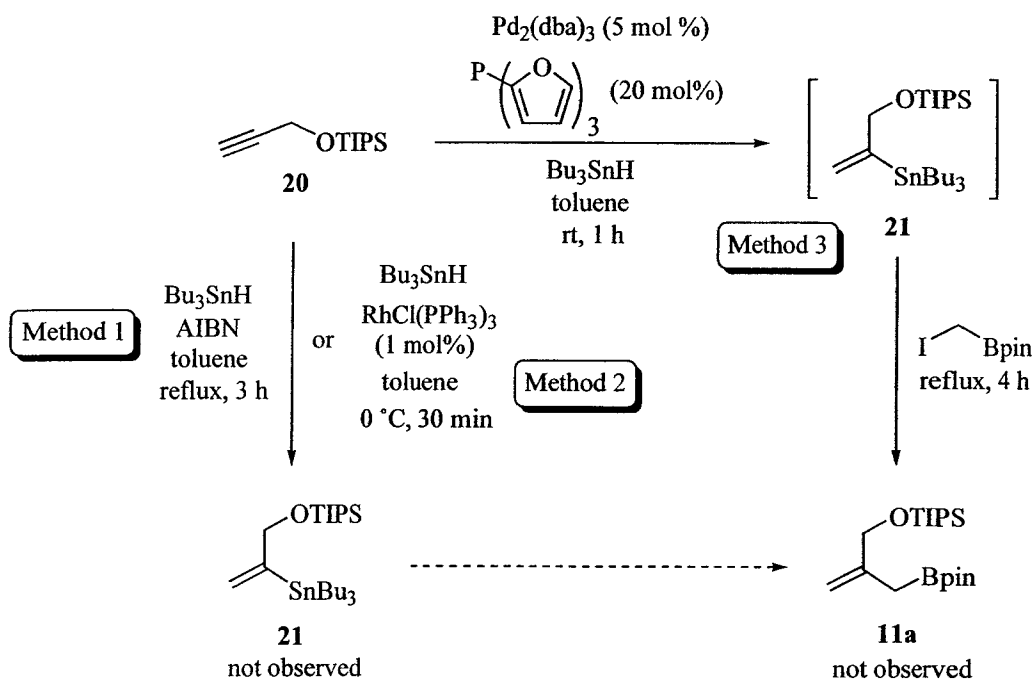
As an alternative approach, we started to look into using vinylic synthetic intermediates. Toward this goal, we first attempted to make alkenyl bromide **19**. Hydrolysis of 1,3-dibromopropene followed by protection of the resulting crude allylic alcohol **18** only gave the desired product in very low yield (Scheme 3-10). Both allylic alcohol **18** and alkenyl bromide **19** with a different silyl ether protecting group have been synthesized in the literature, but unfortunately, the detailed experimental procedures were not reported.<sup>14</sup> We suspected that the problem could arise from the fact that alcohol **18** might be water soluble and volatile. In an attempt to solve this problem, we had tried to deprotonate triisopropylsilanol with both *n*BuLi and NaH followed by *in situ* nucleophilic displacement of the 1,3-dibromopropene but without success.



Scheme 3-10. Synthesis of alkenyl bromide **19**.

Next, we decided to explore utilizing an alkenylstannane as intermediate. As shown in Scheme 3-11, we tried three different methods but none led to the desired product. Starting with the protected propargyl alcohol **20**, we first attempted to synthesize alkenylstannane **21** by radical<sup>15</sup> (Method 1) and Rh-catalyzed regioselective<sup>16</sup> (Method 2) hydrostannations without success. Inspired by Grigg's Pd-catalyzed cascade hydrostannation-anion capture methodology,<sup>17</sup> we were hoping to generate **21** in the presence of  $\text{Pd}_2(\text{dba})_3$  and tri-2-furylphosphine ligand followed by *in situ* Stille coupling with iodomethaneboronate exploiting the same palladium catalytic system (Method 3).

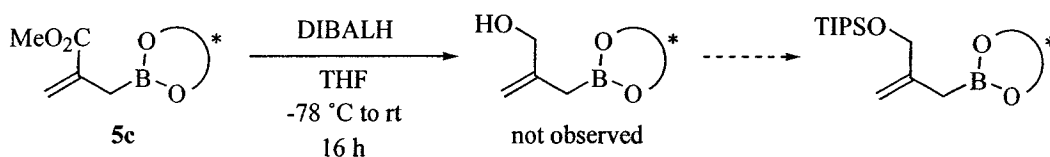




Scheme 3-11. Attempted synthesis of **11a** via vinylstannane intermediate **21**.

### 3.3.3.6 Other synthetic attempts

As Pietruszka reported that a boronate functionality could tolerate hydride reduction conditions,<sup>18</sup> we decided to make use of the readily available chiral allylboronate **5c**. Using DIBALH as the hydride source (Scheme 3-12), ester reduction of **5c**, however, only led to cleavage of the chiral diol along with ca. 14 % recovery of the starting material.



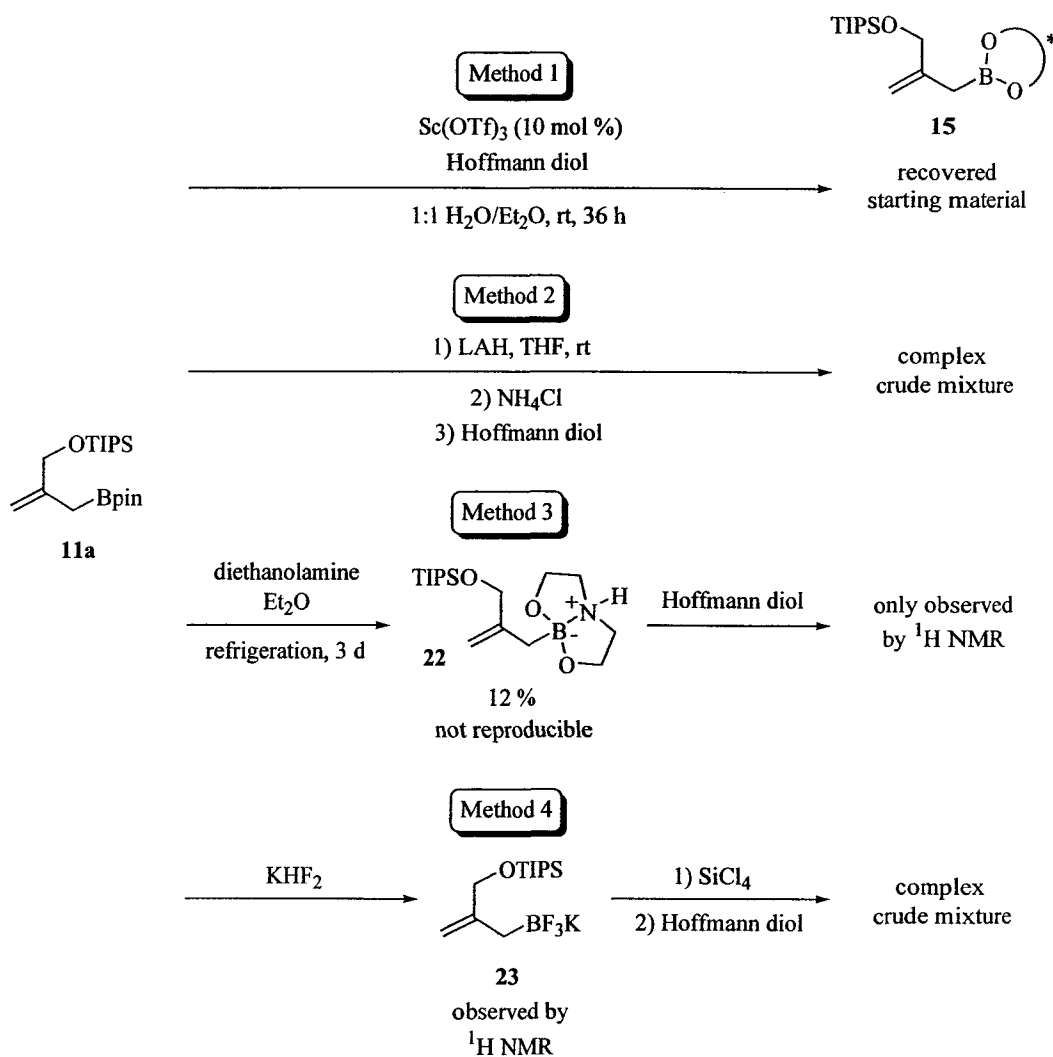
Scheme 3-12. Attempted ester reduction in the presence of the boronate moiety.

Lastly, various diol exchange experiments were investigated with achiral allylboronate **11a** (Scheme 3-13).  $\text{Sc}(\text{OTf})_3$ -catalyzed transesterification (Method 1), LAH-reductive cleavage followed by re-esterification (Method 2),

diethanolamine-mediated transesterification<sup>19</sup> (Method 3) and finally transesterification via Matteson's trifluoroborate/dichloroborane protocol<sup>20</sup> (Method 4) were all tried but none provided a promising solution. It is noteworthy to mention that we did observe the desired chiral allylboronate **15** by <sup>1</sup>H NMR in Method 3. However, since the only way to isolate the intermediate complex **22** was by crystallization, which was low yielding and not reproducible, we did not further optimize this alternative. As for Method 4, <sup>1</sup>H NMR analysis of the crude trifluoroborate intermediate **23** indicated different olefinic proton chemical shifts and the absence of the pinacolate signal, but the subsequent chlorination and re-esterification only gave disappointing results.

### 3.4 Conclusion

In conclusion, Sc(OTf)<sub>3</sub> was demonstrated to catalyze the desired allylboration generating homoallylic alcohol products at subzero temperatures within a much shortened reaction time. Due to the presence of an electron-withdrawing, deactivating ester functionality, 2-alkoxycarbonyl allylboronates were found to be not ideal for allylboration under Lewis acid catalysis. As we turned our attention to the more electron-rich 2-*O*-protected ether allylboronates, an efficient synthetic route was developed for the achiral variants. Using triisopropylsilyl ether as the protecting group, the corresponding allylborations indeed proceeded smoothly at -78 °C with both aromatic and aliphatic aldehydes. Unfortunately, after laborious experimentation with a wide range of different methods, we were unable to efficiently synthesize the desired chiral allylboronate to test the enantioselectivity of the subsequent asymmetric allylboration. As a result, we switched our focus toward other research projects described in this thesis.



Scheme 3-13. Various diol exchange attempts.

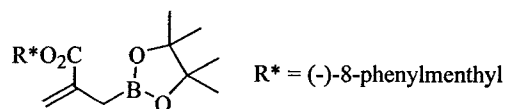
## 3.5 Experimental

### 3.5.1 General

The general experimental procedures described in Section 2.7.1 also apply here, with the following additions. DMSO was distilled over  $\text{CaH}_2$  before use. Propargyl alcohol and 1,3-dibromopropene were purified by Kugelrohr distillation prior to use. Hoffmann's diol<sup>10</sup> was prepared by a co-worker. Chiral

alkynoate ester **3b**,<sup>2b or 4</sup> chloromethaneboronate **4a-b**<sup>3</sup> and allylboronates **5a** and **5c**<sup>1d</sup> were prepared according to literature procedures.

### 3.5.2 Preparation of 2-[(4,4,5,5-tetramethyl-1,3,2-dioxaborolan-2-yl)methyl]prop-2-enoic acid, (-)-8-phenylmenthol ester (**5b**)

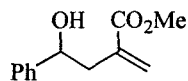


To a stirring solution of HMPA (92  $\mu\text{L}$ , 0.53 mmol) in toluene (0.5 mL) under Ar atmosphere at 0 °C, DIBALH (1.0 M in toluene, 0.26 mL, 0.26 mmol) was added dropwise. After stirring at 0 °C for 1 h, **3b**<sup>2b or 4</sup> (50 mg, 0.18 mmol) in toluene (0.5 mL) was added via cannulation with toluene rinse (2  $\times$  0.25 mL) and stirring continued at 0 °C for another 5 h. Chloromethaneboronate **4a**<sup>3</sup> (37 mg, 0.21 mmol) was added via cannulation with toluene rinse (1  $\times$  0.5 mL) and the resulting mixture was allowed to warm up to rt and stirred under Ar atmosphere for 16 h. The reaction was then quenched with 1 M HCl (1 mL) and extracted with Et<sub>2</sub>O (1  $\times$  5 mL). The organic phase was washed with 1 M HCl (3  $\times$  1 mL), NaHCO<sub>3(aq)</sub> (1  $\times$  1 mL), water (1  $\times$  1 mL), dried with anhydrous MgSO<sub>4</sub>, filtered and concentrated. Flash chromatography (20 % Et<sub>2</sub>O/hexane) gave the desired product **5b** (37.4 mg, 0.0877 mmol, 49 %).

<sup>1</sup>H NMR (500 MHz, CDCl<sub>3</sub>):  $\delta$  7.30-7.23 (m, 4H), 7.11 (m, 1H), 5.58 (d, 1H,  $J = 1.5$  Hz), 5.35 (d, 1H,  $J = 1.5$  Hz), 4.90 (td, 1H,  $J = 10.8, 4.5$  Hz), 2.07-1.88 (m, 2H), 1.78 (s, 2H), 1.63-1.40 (m, 5H), 1.33 (s, 3H), 1.29-1.20 (m, 14H), 1.10-0.92 (m, 2H), 0.85 (d, 3H,  $J = 6.4$  Hz); <sup>13</sup>C NMR (125 MHz, CDCl<sub>3</sub>):  $\delta$  166.7, 151.4, 137.9, 128.0, 125.6, 125.1, 123.9, 83.4, 74.9, 50.7, 41.8, 40.0, 34.6, 31.3, 27.4, 27.0, 26.0, 24.8, 21.8; IR (CHCl<sub>3</sub> cast film, cm<sup>-1</sup>): 2955, 1704, 1320, 1178, 1145, 971, 762, 700; HRMS (EI, m/z) Calcd for C<sub>26</sub>H<sub>39</sub><sup>11</sup>BO<sub>4</sub>: 426.29413. Found: 426.29457.

### 3.5.3 Lewis acid-catalyzed allylboration using 2-alkoxycarbonyl allylboronates

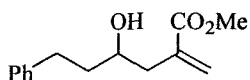
#### 3.5.3.1 *rac*-Methyl 4-hydroxy-2-methylidene-4-phenylbutanoate (6a)



To a suspension of  $\text{Sc}(\text{OTf})_3$  (143 mg, 0.29 mmol) in  $\text{CH}_2\text{Cl}_2$  (5 mL) at  $-60\text{ }^\circ\text{C}$ , freshly distilled benzaldehyde (0.295 mL, 2.90 mmol) was added. The resulting mixture was stirred for 10 min. followed by addition of allylboronate **5a**<sup>1d</sup> (656 mg, 2.90 mmol) in  $\text{CH}_2\text{Cl}_2$  (1 mL) via cannulation with  $\text{CH}_2\text{Cl}_2$  rinse ( $2 \times 0.5$  mL). Stirring continued under Ar atmosphere for 24 h at  $-60\text{ }^\circ\text{C}$ . The reaction was quenched by addition of  $\text{NaHCO}_3(\text{aq})$  (5 mL) followed by extraction with  $\text{CH}_2\text{Cl}_2$  ( $3 \times 10$  mL), dried with anhydrous  $\text{MgSO}_4$ , filtered and concentrated. Flash chromatography (25 % EtOAc/hexane) gave the desired racemic product **6a** (518 mg, 2.51 mmol, 87 %).

$^1\text{H}$  NMR (300 MHz,  $\text{CDCl}_3$ ):  $\delta$  7.40-7.20 (m, 5H), 6.25 (d, 1H,  $J = 1.4$  Hz), 5.62 (d, 1H,  $J = 1.0$  Hz), 4.90 (m, 1H), 3.78 (s, 3H), 2.81 (dd, 1H,  $J = 14.1$ , 4.5 Hz), 2.69 (dd, 1H,  $J = 14.1$ , 8.4 Hz), 2.56 (s, 1H);  $^{13}\text{C}$  NMR (100 MHz,  $\text{CDCl}_3$ ):  $\delta$  168.0, 143.8, 136.7, 128.2, 127.3, 125.6, 72.8, 51.9, 42.2, 24.5; IR ( $\text{CHCl}_3$  cast film,  $\text{cm}^{-1}$ ): 3447, 2951, 1718, 1439, 1203, 1144, 950, 702; HRMS (EI,  $m/z$ ) Calcd for  $\text{C}_{12}\text{H}_{14}\text{O}_3$ : 206.09430. Found: 206.09338.

#### 3.5.3.2 Methyl 4-hydroxy-2-methylidene-4-phenethylbutanoate (6b)



To a solution of chiral allylboronate **5c**<sup>1d</sup> (36 mg, 0.10 mmol) in  $\text{CH}_2\text{Cl}_2$  (1 mL) at  $-60\text{ }^\circ\text{C}$ , freshly distilled hydrocinnamaldehyde (13.4  $\mu\text{L}$ , 0.10 mmol) was added followed by addition of  $\text{Sc}(\text{OTf})_3$  (5.0 mg, 0.010 mmol). The resulting mixture was stirred at  $-60\text{ }^\circ\text{C}$  for 24 h and the reaction was quenched by adding  $\text{NaHCO}_3(\text{aq})$  (2 mL) followed by extraction with  $\text{CH}_2\text{Cl}_2$  ( $3 \times 5$  mL). The organic phase was dried with anhydrous  $\text{MgSO}_4$ , filtered and concentrated. Flash

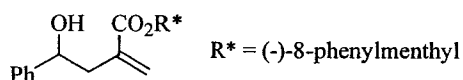
chromatography (20 % EtOAc/hexane) gave the desired product **6b** (10.6 mg, 0.045 mmol, 45 %, 80 % ee). Enantiomeric excess was determined by chiral HPLC using 35 % *i*PrOH and 65 % water as eluent at 0.35 mL/min.

$^1\text{H}$  NMR (400 MHz,  $\text{CDCl}_3$ ):  $\delta$  7.32-7.26 (m, 2H), 7.24-7.16 (m, 3H), 6.26 (d, 1H,  $J = 1.5$  Hz), 5.67 (d, 1H,  $J = 1.5$  Hz), 3.79 (m, 1H), 3.76 (s, 3H), 2.84 (m, 1H), 2.70 (m, 1H), 2.62 (ddd, 1H,  $J = 14.0, 3.7, 1.1$  Hz), 2.41 (ddd, 1H,  $J = 14.0, 8.3, 0.9$  Hz), 2.32 (s, 1H), 1.80 (m, 2H);  $^{13}\text{C}$  NMR (100 MHz,  $\text{CDCl}_3$ ):  $\delta$  168.1, 142.0, 137.2, 128.4, 128.3, 127.9, 125.7, 69.9, 52.0, 40.4, 38.8, 32.0; IR ( $\text{CHCl}_3$  cast film,  $\text{cm}^{-1}$ ): 3434, 2949, 1718, 1439, 1206, 1141, 947, 700; HRMS (EI,  $m/z$ ) Calcd for  $\text{C}_{14}\text{H}_{18}\text{O}_3$ : 234.12560. Found: 234.12493.

### 3.5.3.3 (-)-8-Phenylmenthyl 4-hydroxy-2-methylidene-4-phenylbutanoate

$\text{R}^* = (-)\text{-}8\text{-phenylmenthyl}$

(**7a**)

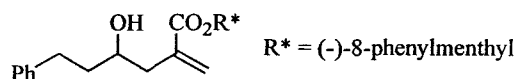


To a solution of chiral allylboronate **5b** (32.2 mg, 0.075 mmol) in  $\text{CH}_2\text{Cl}_2$  (1 mL) at  $-60$  °C, freshly distilled benzaldehyde (7.7  $\mu\text{L}$ , 0.076 mmol) was added followed by addition of  $\text{Sc}(\text{OTf})_3$  (3.7 mg, 0.0075 mmol). The resulting mixture was stirred at  $-60$  °C for 24 h and workup followed as Section 3.5.3.2. Flash chromatography (25 %  $\text{Et}_2\text{O}$ /hexane) gave the desired product **7a** as an inseparable mixture of diastereomers (17.5 mg, 0.043 mmol, 57 % combined yield, 1.2:1 dr).

$^1\text{H}$  NMR (300 MHz,  $\text{CDCl}_3$ , two diastereomers):  $\delta$  7.40-7.18 (m, 20H), 5.62 (m, 1H), 5.55 (m, 1H), 5.32 (s, 1H), 5.28 (s, 1H), 4.92 (m, 2H), 4.78 (m, 2H), 2.72 (broad s, 2H), 2.64-2.32 (m, 4H), 2.16-2.03 (m, 2H), 1.96-1.84 (m, 2H), 1.74-1.61 (m, 4H), 1.59-1.44 (m, 4H), 1.31 (s, 3H), 1.30 (s, 3H), 1.22 (s, 3H), 1.21 (s, 3H), 1.18-0.93 (m, 4H), 0.89 (d, 6H,  $J = 6.6$  Hz);  $^{13}\text{C}$  NMR (100 MHz,  $\text{CDCl}_3$ , [same carbon of different diastereomers]):  $\delta$  [167.0, 166.8], [151.8, 151.6], 144.0, [136.9, 136.8], 128.4, 128.1, 127.4, [125.8, 125.7], [125.5, 125.4], 125.1, [75.4, 75.3], [73.4, 73.0], 50.5, [42.6, 42.4], 41.7, [39.8, 39.7], 34.6, 31.4, [28.2, 27.8], [26.8, 26.7], 25.6, [24.9, 24.8], 21.8; IR ( $\text{CHCl}_3$  cast film,  $\text{cm}^{-1}$ ):

3481, 2923, 1705, 1322, 1195, 1145, 762, 700; HRMS (EI, m/z) Calcd for C<sub>27</sub>H<sub>34</sub>O<sub>3</sub>: 406.25079. Found: 406.25052.

### 3.5.3.4 (-)-8-Phenylmenthyl 4-hydroxy-2-methylidene-4-phenethyl butanoate (7b)



To a solution of chiral allylboronate **5b** (26.1 mg, 0.0612 mmol) in CH<sub>2</sub>Cl<sub>2</sub> (1 mL) at -60 °C, freshly distilled hydrocinnamaldehyde (8.1 μL, 0.061 mmol) was added followed by addition of Sc(OTf)<sub>3</sub> (3.0 mg, 0.0061 mmol). The resulting mixture was stirred at -60 °C for 24 h and workup followed as Section 3.5.3.2. Flash chromatography (25 % Et<sub>2</sub>O/hexane) provided the desired product **7b** with some separation of the diastereomers (26.3 mg, 0.0605 mmol, 99 % combined yield, 1.5:1 dr).

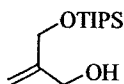
Diastereomer A: <sup>1</sup>H NMR (300 MHz, CDCl<sub>3</sub>): δ 7.32-7.04 (m, 10H), 5.59 (m, 1H), 5.34 (s, 1H), 4.90 (td, 1H, *J* = 10.6, 4.4 Hz), 3.68 (m, 1H), 2.81 (m, 1H), 2.67 (m, 1H), 2.36 (dd, 1H, *J* = 14.1, 3.8 Hz), 2.18 (dd, 1H, *J* = 14.1, 7.9 Hz), 2.09 (m, 1H), 1.87 (m, 1H), 1.77-1.61 (m, 4H), 1.59-1.40 (m, 2H), 1.30 (s, 3H), 1.20 (s, 3H), 1.16-0.92 (m, 2H), 0.88 (d, 3H, *J* = 6.7 Hz); <sup>13</sup>C NMR (100 MHz, CDCl<sub>3</sub>): δ 167.0, 151.7, 142.2, 137.3, 128.4, 128.1, 127.7, 125.8, 125.4, 125.1, 75.3, 70.2, 50.4, 41.7, 40.3, 39.7, 38.9, 34.6, 32.1, 31.4, 28.0, 26.7, 25.3, 21.8; IR (CHCl<sub>3</sub> cast film, cm<sup>-1</sup>): 3462, 2923, 1705, 1456, 1325, 1171, 700; HRMS (EI, m/z) Calcd for C<sub>29</sub>H<sub>38</sub>O<sub>3</sub>: 434.28210. Found: 434.28197.

Diastereomer B: <sup>1</sup>H NMR (300 MHz, CDCl<sub>3</sub>): δ 7.36-7.02 (m, 10H), 5.64 (m, 1H), 5.33 (s, 1H), 4.88 (td, 1H, *J* = 10.7, 4.4 Hz), 3.59 (m, 1H), 2.87-2.61 (m, 2H), 2.36 (m, 1H), 2.13-2.01 (m, 2H), 1.85 (m, 1H), 1.79-1.61 (m, 4H), 1.59-1.39 (m, 2H), 1.29 (s, 3H), 1.19 (s, 3H), 1.17-1.05 (m, 1H), 0.99-0.89 (m, 1H), 0.88 (d, 3H, *J* = 6.5 Hz); <sup>13</sup>C NMR (100 MHz, CDCl<sub>3</sub>): δ 166.6, 151.9, 142.2, 137.3, 128.5, 128.0, 125.8, 125.4, 125.1, 75.2, 69.7, 50.3, 41.6, 40.3, 39.6, 38.8, 34.6, 32.1, 31.4, 29.8, 28.5, 26.6, 24.7, 21.8; IR (CHCl<sub>3</sub> cast film, cm<sup>-1</sup>): 3462, 2924,

1707, 1456, 1323, 1174, 700; HRMS (EI, m/z) Calcd for C<sub>29</sub>H<sub>38</sub>O<sub>3</sub>: 434.28210. Found: 434.28089.

### 3.5.4 Generation of 2-*O*-protected ether allylboronates

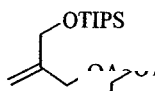
#### 3.5.4.1 2-Triisopropylsilyloxymethyl-prop-2-en-1-ol (**8a**)



To a suspension of NaH (60 % dispersion in mineral oil, 94 mg, 2.3 mmol) in THF (5 mL), 2-methylene-1,3-propanediol (0.185 mL, 2.27 mmol) was added. Formation of a gas and white precipitate were observed immediately while the reaction mixture was let stirred under Ar atmosphere at rt for 1 h. With vigorous stirring, TIPSCl (0.43 mL, 2.0 mmol) was added dropwise. Capped with a drying tube packed with anhydrous calcium sulfate (Drierite<sup>®</sup>), the reaction mixture was stirred at rt for another hour followed by quenching with 10 % K<sub>2</sub>CO<sub>3(aq)</sub> (10 mL), extracted with Et<sub>2</sub>O (20 mL), washed with brine (10 mL), dried with anhydrous MgSO<sub>4</sub>, filtered and concentrated. Flash chromatography (20 % EtOAc/hexane) gave the monoprotected diol **8a** (470 mg, 1.92 mmol, 96 %).

<sup>1</sup>H NMR (300 MHz, CDCl<sub>3</sub>): δ 5.13 (m, 1H), 5.09 (m, 1H), 4.35 (s, 2H), 4.20 (s, 2H), 1.93 (broad s, 1H), 1.20-1.00 (m, 21H); <sup>13</sup>C NMR (100 MHz, CDCl<sub>3</sub>): δ 147.4, 110.8, 65.4, 64.7, 17.9, 11.9; IR (CHCl<sub>3</sub> cast film, cm<sup>-1</sup>): 3327, 2943, 2866, 1463, 1120, 1066, 882, 809, 682; HRMS (ES, m/z) Calcd for C<sub>13</sub>H<sub>29</sub>O<sub>2</sub>Si: 245.19314. Found: 245.19304.

#### 3.5.4.2 Acetic acid 2-triisopropylsilyloxymethyl-allyl ester (**9a**)



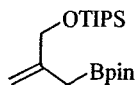
A solution of monoprotected diol **8a** (63 mg, 1.90 mmol) in anhydrous DMF (30 mL) was treated with DMAP (23 mg, 0.19 mmol). Cooled to 0 °C, Ac<sub>2</sub>O (0.216 mL, 2.27 mmol) was added dropwise and the resulting clear



colourless solution was stirred at 0 °C under Ar atmosphere for 15 min. Lifted up from the ice-water bath, stirring continued at rt for another hour. Dilution with MeOH (10 mL) followed by solvent evaporation and flash chromatography (40 % EtOAc/hexane) to give acetate **9a** (512 mg, 1.79 mmol, 94 %).

<sup>1</sup>H NMR (300 MHz, CDCl<sub>3</sub>): δ 5.28 (s, 1H), 5.14 (m, 1H), 4.60 (s, 2H), 4.25 (s, 2H), 2.08 (s, 3H), 1.08 (m, 21H); <sup>13</sup>C NMR (100 MHz, CDCl<sub>3</sub>): δ 143.3, 129.3, 112.6, 64.7, 64.0, 20.9, 17.9, 12.0; IR (CHCl<sub>3</sub> cast film, cm<sup>-1</sup>): 2943, 2866, 1747, 1463, 1373, 1238, 1121, 882, 808, 683; HRMS (ES, m/z) Calcd for C<sub>15</sub>H<sub>30</sub>O<sub>3</sub>SiNa: 309.18565. Found: 309.18583.

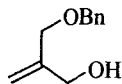
#### 3.5.4.3 4,4,5,5-Tetramethyl-2-(2-triisopropylsilyloxyethyl-allyl)-1,3,2-dioxaborolane (**11a**)



To a mixture of Pd<sub>2</sub>(dba)<sub>3</sub> (97 mg, 0.11 mmol) and bis(pinacolato)diboron (450 mg, 1.77 mmol) in freshly distilled DMSO (20 mL), acetate **9a** (506 mg, 1.77 mmol) in DMSO (3 mL) was cannulated in followed by DMSO rinse (5 mL). The resulting mixture was degassed for 2 min. and then stirred at 40 °C under an Ar atmosphere for 16 h. Cooled to rt, the mixture was diluted with benzene, washed with brine, dried with anhydrous MgSO<sub>4</sub>, filtered and concentrated. Flash chromatography (10 % Et<sub>2</sub>O/hexane) gave the desired allylboronate **11a** (249 mg, 0.702 mmol, 40 %).

<sup>1</sup>H NMR (300 MHz, CDCl<sub>3</sub>): δ 5.08 (s, 1H), 4.82 (s, 1H), 4.16 (s, 2H), 1.67 (s, 2H), 1.24 (s, 12H), 1.09 (m, 21H); HRMS (ES, m/z) Calcd for C<sub>19</sub>H<sub>39</sub>O<sub>3</sub>BSiNa: 377.26538. Found: 377.26571.

#### 3.5.4.4 2-Benzyloxymethyl-prop-2-en-1-ol (**8b**)

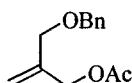


A solution 2-methylene-1,3-propanediol (0.10 mL, 1.2 mmol) in anhydrous DMF (5 mL) was treated with Ag<sub>2</sub>O (430 mg, 1.86 mmol) and BnBr

(0.16 mL, 1.3 mmol). The reaction mixture was stirred at rt under Ar atmosphere for 12 h. After filtration through a pad of silica gel with EtOAc rinse, solvent was evaporated followed by flash chromatography (40 % EtOAc/hexane) to give the monoprotected diol **8b** (130 mg, 0.730 mmol, 61 %).

$^1\text{H NMR}$  (500 MHz,  $\text{CDCl}_3$ ):  $\delta$  7.40-7.20 (m, 5H), 5.22 (m, 1H), 5.17 (m, 1H), 4.53 (s, 2H), 4.21 (s, 2H), 4.11 (s, 2H), 1.80 (s, 1H).

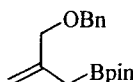
#### 3.5.4.5 Acetic acid 2-benzyloxymethyl-allyl ester (**9b**)



A solution of monoprotected diol **8b** (258 mg, 1.45 mmol) in anhydrous DMF (25 mL) was treated with DMAP (18 mg, 0.15 mmol). Cooled to 0 °C,  $\text{Ac}_2\text{O}$  (0.170 mL, 1.78 mmol) was added dropwise and the resulting clear colourless solution was stirred at 0 °C under Ar atmosphere for 15 min. Lifted up from the ice-water bath, stirring was continued at rt for another 40 min. Dilution with MeOH (10 mL) followed by solvent evaporation and flash chromatography (40 % EtOAc/hexane) to give acetate **9b** (306 mg, 1.39 mmol, 96 %).

$^1\text{H NMR}$  (300 MHz,  $\text{CDCl}_3$ ):  $\delta$  7.40-7.25 (m, 5H), 5.27 (s, 1H), 5.25 (s, 1H), 4.64 (s, 2H), 4.52 (s, 2H), 4.05 (s, 2H), 2.08 (s, 3H).

#### 3.5.4.6 2-(2-Benzyloxymethyl-allyl)-4,4,5,5-tetramethyl-1,3,2-dioxaborolane (**11b**)



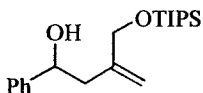
To a mixture of  $\text{Pd}_2(\text{dba})_3$  (31 mg, 0.034 mmol) and bis(pinacolato)diboron (142 mg, 0.559 mmol) in freshly distilled DMSO (7 mL), acetate **9b** (123 mg, 0.558 mmol) in DMSO (1 mL) was cannulated in followed by DMSO rinse (3 mL). The resulting mixture was degassed for 2 min. and then stirred at 40 °C under an Ar atmosphere for 16 h. Cooled to rt, the mixture was diluted with benzene, washed with brine, dried with anhydrous  $\text{MgSO}_4$ , filtered

and concentrated. Flash chromatography (20 % EtOAc/hexane) gave the desired allylboronate **11b** (61.6 mg, 0.214 mmol, 38 %).

$^1\text{H}$  NMR (300 MHz,  $\text{CDCl}_3$ ):  $\delta$  7.40-7.20 (m, 5H), 5.01 (s, 1H), 4.92 (s, 1H), 4.50 (s, 2H), 3.97 (s, 2H), 1.76 (s, 2H), 1.20 (s, 12H).

### 3.5.5 Lewis acid-catalyzed allylboration using 2-*O*-protected ether allylboronates

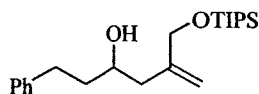
#### 3.5.5.1 *rac*-4-Hydroxy-2-methylidene-4-phenylbutan-1-ol triisopropylsilyl ether (**12a**)



To a suspension of  $\text{Sc}(\text{OTf})_3$  (5 mg, 0.01 mmol) in  $\text{CH}_2\text{Cl}_2$  (0.5 mL) at  $-78$  °C, freshly distilled benzaldehyde (10  $\mu\text{L}$ , 0.098 mmol) was added. The resulting mixture was stirred for 10 min. followed by addition of allylboronate **11a** (34.9 mg, 0.0985 mmol) via cannulation with  $\text{CH}_2\text{Cl}_2$  rinse ( $3 \times 0.5$  mL). Stirring continued under Ar atmosphere for 25 h at  $-78$  °C. Workup was done as in Section 3.5.3.1 using 2 mL aliquots. Pure desired product **12a** (33 mg, 0.098 mmol, 99 %) was obtained without further purification.

$^1\text{H}$  NMR (300 MHz,  $\text{CDCl}_3$ ):  $\delta$  7.42-7.31 (m, 4H), 7.29-7.23 (m, 1H), 5.21 (m, 1H), 5.00 (m, 1H), 4.84 (dd, 1H,  $J = 9.2, 3.8$  Hz), 4.21 (s, 2H), 3.18 (s, 1H), 2.58 (dd, 1H,  $J = 14.0, 3.8$  Hz), 2.45 (dd, 1H,  $J = 14.0, 9.2$  Hz), 1.25-1.05 (m, 21 H);  $^{13}\text{C}$  NMR (100 MHz,  $\text{CDCl}_3$ ):  $\delta$  145.2, 144.4, 128.3, 127.2, 125.7, 114.0, 73.0, 66.9, 44.4, 18.0, 12.0; IR ( $\text{CHCl}_3$  cast film,  $\text{cm}^{-1}$ ): 3414, 2942, 2865, 1463, 1113, 883, 807, 683; HRMS (ES,  $m/z$ ) Calcd for  $\text{C}_{20}\text{H}_{34}\text{O}_2\text{SiNa}$ : 357.22203. Found: 357.22214.

### 3.5.5.2 *rac*-4-Hydroxy-2-methylidene-4-phenethylbutan-1-ol triisopropylsilyl ether (**12b**)

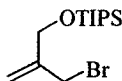


To a suspension of Sc(OTf)<sub>3</sub> (4 mg, 0.008 mmol) in CH<sub>2</sub>Cl<sub>2</sub> (0.5 mL) at -78 °C, freshly distilled hydrocinnamaldehyde (10 μL, 0.076 mmol) was added. The resulting mixture was stirred for 10 min. followed by addition of allylboronate **11a** (26.5 mg, 0.0748 mmol) via cannulation with CH<sub>2</sub>Cl<sub>2</sub> rinse (3 × 0.5 mL). Stirring was continued under Ar atmosphere for 25 h at -78 °C. Workup was done as in Section 3.5.3.1 using 2 mL aliquots. Flash chromatography (20 % Et<sub>2</sub>O/hexane) gave the desired product **12b** (22 mg, 0.061 mmol, 81 %).

<sup>1</sup>H NMR (300 MHz, CDCl<sub>3</sub>): δ 7.32-7.14 (m, 5H), 5.18 (m, 1H), 4.96 (m, 1H), 4.18 (s, 2H), 3.76 (m, 1H), 2.90-2.60 (m, 3H), 2.36 (dd, 1H, *J* = 13.9, 3.4 Hz), 2.18 (dd, 1H, *J* = 13.9, 9.0 Hz), 1.80 (m, 2H), 1.4-0.9 (m, 21 H); <sup>13</sup>C NMR (125 MHz, CDCl<sub>3</sub>): δ 145.4, 142.3, 128.4, 128.3, 125.7, 113.6, 69.3, 66.8, 42.3, 38.9, 32.1, 18.0, 12.0; IR (CHCl<sub>3</sub> cast film, cm<sup>-1</sup>): 3434, 2942, 2865, 1462, 1114, 1068, 882, 807, 683; HRMS (ES, *m/z*) Calcd for C<sub>22</sub>H<sub>39</sub>O<sub>2</sub>Si: 363.27139. Found: 363.27121.

### 3.5.6 Toward the attempted synthesis of chiral 2-*O*-TIPS ether allylboronate **15**

#### 3.5.6.1 (2-Bromomethyl-allyloxy) triisopropylsilane (**16a**)

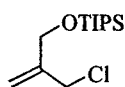


To a solution of monoprotected diol **8a** (286 mg, 1.17 mmol) in THF (6 mL), Et<sub>3</sub>N (0.196 mL, 1.41 mmol) was added and the reaction mixture was cooled to 0 °C, MsCl (0.109 mL, 1.41 mmol) was then added dropwise and formation of a white precipitate was observed. Stirring was continued at 0 °C for 1 h. LiBr (305 mg, 3.51 mmol) was then added and the resulting mixture was gradually warmed up to rt with stirring continued for 16 h. Workup was done by Et<sub>2</sub>O

extraction with H<sub>2</sub>O wash. The organic phase was dried with anhydrous MgSO<sub>4</sub>, filtered and concentrated. Kugelrohr distillation (180 °C/high vac.) gave allylic bromide **16a** (341 mg, 1.11 mmol, 95 %).

<sup>1</sup>H NMR (300 MHz, CDCl<sub>3</sub>): δ 5.29 (m, 1H), 5.26 (m, 1H), 4.36 (m, 2H), 4.02 (s, 2H), 1.09 (m, 21H); <sup>13</sup>C NMR (100 MHz, CDCl<sub>3</sub>): δ 144.9, 114.4, 63.7, 32.8, 18.0, 12.0; IR (CHCl<sub>3</sub> cast film, cm<sup>-1</sup>): 2943, 2866, 1463, 1104, 882, 805, 683; HRMS (ES, m/z) Calcd for C<sub>13</sub>H<sub>28</sub>BrOSi: 307.10873. Found: 307.10837.

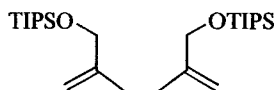
### 3.5.6.2 (2-Chloromethyl-allyloxy) triisopropylsilane (16b)



To a solution of monoprotected diol **8a** (460 mg, 1.88 mmol) in THF (12 mL), Et<sub>3</sub>N (0.32 mL, 2.3 mmol) was added and the reaction mixture was cooled to 0 °C. MsCl (0.18 mL, 2.3 mmol) was then added dropwise and formation of a white precipitate was observed. Stirring was continued at 0 °C for 1 h. LiCl (400 mg, 9.4 mmol) was then added and the resulting mixture was gradually warmed up to rt with stirring continued for 16 h. Workup was done as in Section 3.5.6.1 to give allylic chloride **16b** (484 mg, 1.84 mmol, 98 %).

<sup>1</sup>H NMR (300 MHz, CDCl<sub>3</sub>): δ 5.29 (m, 1H), 5.22 (m, 1H), 4.33 (m, 2H), 4.12 (s, 2H), 1.10 (m, 21H); <sup>13</sup>C NMR (100 MHz, CDCl<sub>3</sub>): δ 144.6, 114.0, 63.6, 45.0, 18.0, 12.0; IR (CHCl<sub>3</sub> cast film, cm<sup>-1</sup>): 2944, 2866, 1463, 1118, 882, 806, 683; HRMS (ES, m/z) Calcd for C<sub>13</sub>H<sub>28</sub>ClOSi: 263.15925. Found: 263.15954.

### 3.5.6.3 2,5-Bis-triisopropylsilyloxymethyl-hexa-1,5-diene (17)

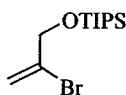


Oven-dried Mg pieces (9 mg, 0.4 mmol) was placed in a flame-dried round-bottom flask containing a magnetic stir bar. Anhydrous THF was added just enough to cover the metal followed by addition of a crystal of I<sub>2</sub>. Neat allylic bromide **16a** (98.5 mg, 0.320 mmol) was then added dropwise using an air-tight syringe. After stirring at rt for 30 min. under Ar atmosphere, the resulting mixture

was cooled to 0 °C followed by addition of B(OiPr)<sub>3</sub> (89 mL, 0.39 mmol). Stirring was continued for another 40 min. with temperature gradually warmed up to rt. NH<sub>4</sub>Cl<sub>(aq)</sub> (2 mL) was then added followed by the addition of pinacol (34 mg, 0.29 mmol) and stirring continued for 1 h. Workup was done by Et<sub>2</sub>O extraction with brine wash. The organic phase was dried with anhydrous MgSO<sub>4</sub>, filtered and concentrated. Flash chromatography (10 % Et<sub>2</sub>O/hexane) gave dimer **17** (68.5 mg, 0.151 mmol, 52 %) as the major product.

<sup>1</sup>H NMR (400 MHz, CDCl<sub>3</sub>): δ 5.10 (m, 2H), 4.85 (s, 2H), 4.18 (m, 4H), 2.20 (s, 4H), 1.10 (m, 42H); <sup>13</sup>C NMR (100 MHz, CDCl<sub>3</sub>): δ 148.4, 108.2, 66.0, 31.1, 18.0, 12.0; IR (neat film microscope, cm<sup>-1</sup>): 2943, 2866, 1655, 1463, 1114, 883; HRMS (ES, m/z) Calcd for C<sub>26</sub>H<sub>54</sub>O<sub>2</sub>Si<sub>2</sub>Na: 477.35546. Found: 477.35587.

#### 3.5.6.4 (2-Bromo-allyloxy) triisopropylsilane (**19**)

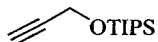


To a solution of Na<sub>2</sub>CO<sub>3</sub> (113 mg, 1.07 mmol) in water (25 mL), freshly distilled 1,3-dibromopropene (0.10 mL, 0.97 mmol) was added and the resulting clear colourless solution was refluxed at 75 °C for 24 h under Ar atmosphere. Cooled to rt, the reaction mixture was then acidified with 1 N HCl until pH 4 followed by Et<sub>2</sub>O and EtOAc extractions. The combined organic phase was washed with brine, dried with anhydrous MgSO<sub>4</sub>, filtered and concentrated. The crude allylic alcohol **18** (40 mg, 0.29 mmol) was then dissolved in anhydrous DMF (3 mL) followed by addition of imidazole (24 mg, 0.35 mmol) and TIPSCl (73 μL, 0.34). Capped with a drying tube packed with anhydrous calcium sulfate (Drierite<sup>®</sup>), the reaction mixture was stirred at rt for 12 hour. Workup was done by quenching with NaHCO<sub>3(aq)</sub>, extracted with Et<sub>2</sub>O and brine wash. The organic phase was then dried with anhydrous MgSO<sub>4</sub>, filtered and concentrated. Kugelrohr distillation gave vinyl bromide **19** (20 mg, 0.068 mmol, 7 %).

<sup>1</sup>H NMR (300 MHz, CDCl<sub>3</sub>): δ 6.04 (m, 1H), 5.55 (m, 1H), 4.29 (m, 2H), 1.10 (m, 21H); <sup>13</sup>C NMR (100 MHz, CDCl<sub>3</sub>): δ 131.6, 67.6, 29.8, 18.0, 12.0; IR (CH<sub>2</sub>Cl<sub>2</sub> cast film microscope, cm<sup>-1</sup>): 2926, 2867, 1739, 1641, 1464, 1098, 884;

HRMS (EI, m/z) Calcd for C<sub>12</sub>H<sub>25</sub><sup>79</sup>BrOSi: 292.08582. Found: 292.08573. Calcd for C<sub>12</sub>H<sub>25</sub><sup>81</sup>BrOSi: 294.08377. Found: 294.08317.

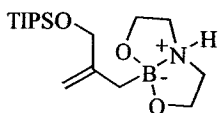
### 3.5.6.5 Triisopropyl-prop-2-ynyloxysilane (20)



To a solution of imidazole (210 mg, 3.1 mmol) in anhydrous DMF (20 mL), freshly distilled propargyl alcohol (0.15 mL, 2.6 mmol) was added followed by addition of TIPSCl (0.66 mL, 3.1 mmol). Capped with a drying tube packed with anhydrous calcium sulfate (Drierite<sup>®</sup>), the reaction mixture was stirred at rt for 2 hour. Workup was done by dilution with Et<sub>2</sub>O (40 mL) followed by NaHCO<sub>3(aq)</sub> wash (20 mL) and brine wash (2 × 20 mL). The organic phase was then dried with anhydrous MgSO<sub>4</sub>, filtered and concentrated. Flash chromatography (10 % Et<sub>2</sub>O/hexane) furnished the protected alcohol **20** (406 mg, 1.91 mmol, 74 %).

<sup>1</sup>H NMR (300 MHz, CDCl<sub>3</sub>): δ 4.39 (d, 2H, *J* = 2.5 Hz), 2.39 (t, 1H, *J* = 2.5 Hz), 1.10 (m, 21H); <sup>13</sup>C NMR (100 MHz, CDCl<sub>3</sub>): δ 82.4, 72.5, 51.7, 17.9, 12.0; IR (CHCl<sub>3</sub> cast film, cm<sup>-1</sup>): 3313, 2944, 2867, 2123, 1464, 1102, 882, 683; HRMS (ES, m/z) Calcd for C<sub>12</sub>H<sub>25</sub>OSi: 213.16692. Found: 213.16697.

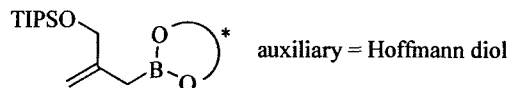
### 3.5.6.6 2-(2-Triisopropylsilanyloxymethyl-allyl)-[1,3,6,2]-dioxazaborocane (22)



To a solution of **11a** (43 mg, 0.12 mmol) in Et<sub>2</sub>O (0.3 mL), diethanolamine (2 M in isopropanol, 61 μL, 0.12 mmol) was added dropwise. The mixture was stirred at rt for 30 min. followed by refrigeration at 0 °C for 3 days. Vacuum filtration of the resulting crystals with ice-cold hexane rinse gave complex **22** (4.7 mg, 0.014 mmol, 12 %).

<sup>1</sup>H NMR (300 MHz, CDCl<sub>3</sub>): δ 5.88 (broad s, 1H), 4.86 (m, 1H), 4.79 (m, 1H), 4.19 (s, 2H), 4.00 (m, 2H), 3.87 (m, 2H), 3.16 (m, 2H), 2.74 (m, 2H), 1.52 (s, 2H), 1.12 (m, 21H).

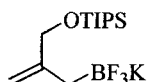
**3.5.6.7 1,10,10-Trimethyl-2-phenyl-4-(2-triisopropylsilanyloxymethyl-allyl)-3,5-dioxa-4-bora-tricyclo[5.2.1.0<sup>2,6</sup>]decane (15)**



To a solution of complex **22** (4.7 mg, 0.014 mmol) in  $\text{CHCl}_3$  (0.2 mL), Hoffmann's diol<sup>10</sup> (4 mg, 0.016 mmol) was added followed by the addition of HCl (0.04 M aqueous solution, 0.34 mL, 0.014). The resulting biphasic mixture was stirred vigorously for 1 h at rt. Workup was then done by dilution with  $\text{CHCl}_3$  and the organic phase was washed with water, dried with anhydrous  $\text{MgSO}_4$ , filtered and concentrated to give **15** (16 mg) as a crude analytical sample.

$^1\text{H}$  NMR (300 MHz,  $\text{CDCl}_3$ ):  $\delta$  7.44-7.24 (m, 5H), 5.04 (m, 1H), 4.74 (m, 1H), 4.71 (s, 1H), 4.13 (m, 2H), 2.13 (d, 1H,  $J = 4.9$  Hz), 1.80 (m, 1H), 1.69 (s, 2H), 1.22 (s, 3H), 1.20-1.08 (m, 2H), 1.04 (m, 22H), 0.95 (s, 3H), 0.93 (s, 3H); HRMS (ES,  $m/z$ ) Calcd for  $\text{C}_{29}\text{H}_{47}\text{BO}_3\text{SiNa}$ : 505.32798. Found: 505.32767.

**3.5.6.8 Potassium 2-triisopropylsilanyloxymethyl allyltrifluoroborate (23)**



To a solution of **11a** (91 mg, 0.26 mmol) in MeOH (2 mL),  $\text{KHF}_2$  (4.5 M aqueous solution, 0.40 mL, 1.8 mmol) was added. The resulting solution was stirred at rt for 2 h followed by solvent evaporation. Acetonitrile was then added followed by pentane wash and concentration of the acetonitrile layer gave the crude **23** (37 mg) which was used in the subsequent chlorination and esterification.

$^1\text{H}$  NMR (300 MHz,  $\text{CDCl}_3$ ):  $\delta$  4.79 (m, 1H), 4.49 (m, 1H), 4.12 (m, 2H), 1.92 (m, 2H), 1.07 (m, 21H).



### 3.6 References

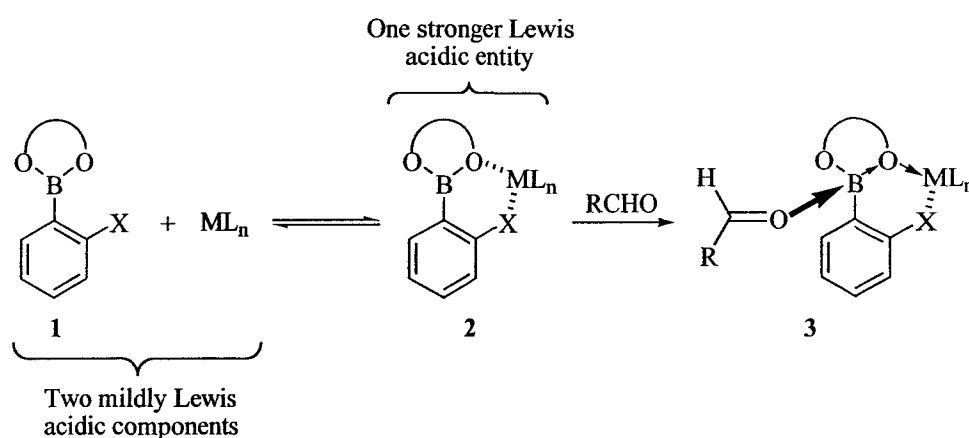
1. a) Nyzam, V.; Belaud, C.; Zammattio, F.; Villieras, J. *Bull. Soc. Chim. Fr.* **1997**, *134*, 583-592. b) Chataigner, I.; Lebreton, J.; Zammattio, F.; Villieras, J. *Tetrahedron Lett.* **1997**, *38*, 3719-3722. c) Draillard, K.; Lebreton, J.; Villieras, J. *Tetrahedron: Asymmetry* **1999**, *10*, 4281-4284. d) Nyzam, V.; Belaud, C.; Zammattio, F.; Villieras, J. *Tetrahedron Lett.* **1993**, *34*, 6899-6902.
2. a) Kennedy, J. W. J.; Hall, D. G. *J. Am. Chem. Soc.* **2002**, *124*, 11586-11587. b) Kennedy, J. W. J.; Hall, D. G. *J. Org. Chem.* **2004**, *69*, 4412-4428.
3. Whiting, A. *Tetrahedron Lett.* **1991**, *32*, 1503-1506.
4. Alvarez-Ibarra, C.; Csákÿ, A. G.; Martin, M. E.; Quiroga, M. L. *Tetrahedron* **1999**, *55*, 7319-7330.
5. Fonquerna, S.; Moyano, A.; Pericàs, M. A.; Riera, A. *Tetrahedron* **1995**, *51*, 4239-4254.
6. Rücker, C. *Chem. Rev.* **1995**, *95*, 1009-1064.
7. Zhang, Q.; Rivkin, A.; Curran, D. P. *J. Am. Chem. Soc.* **2002**, *124*, 5774-5781.
8. Bouzide, A.; Sauvé, G. *Tetrahedron Lett.* **1997**, *38*, 5945-5948.
9. Ishiyama, T.; Ahiko, T.; Miyaura, N. *Tetrahedron Lett.* **1996**, *37*, 6889-6892.
10. Herold, T.; Schrott, U.; Hoffmann, R. W. *Chem. Ber.* **1981**, *114*, 359-374.
11. Takahashi, K.; Ishiyama, T.; Miyaura, N. *J. Organomet. Chem.* **2001**, *625*, 47-53.
12. Collington, E. W.; Meyers, A. I. *J. Org. Chem.* **1971**, *36*, 3044-3046.
13. Murata, M.; Watanabe, S.; Masuda, Y. *Tetrahedron Lett.* **2000**, *41*, 5877-5880.
14. a) Hatch, L. F.; Harwell, K. E. *J. Am. Chem. Soc.* **1953**, *75*, 6002-6005. b) White, J. D.; Choi, Y. *Helv. Chim. Acta* **2002**, *85*, 4306-4327.

15. Ardisson, J.; Férézou, J. P.; Julia, M.; Li, Y.; Liu, L. W.; Pancrazi, A. *Bull. Soc. Chim. Fr.* **1992**, *129*, 387-400.
16. Kikukawa, K.; Umekawa, H.; Wada, F.; Matsuda, T. *Chem. Lett.* **1988**, 881-884.
17. Casaschi, A.; Grigg, R.; Sansano, J. M.; *Tetrahedron*, **2000**, *56*, 7553-7560.
18. Luithle, J. E. A.; Pietruszka, J. *J. Org. Chem.* **2000**, *65*, 9194-9200.
19. Mears, R. J.; Sailes, H. E.; Watts, J. P.; Whiting, A. *J. Chem. Soc., Perkin Trans.* **2000**, 3250-3263.
20. a) Kim, B. J.; Matteson, D. S. *Angew. Chem. Int. Ed.* **2004**, *43*, 3056-3058.  
b) Kanth, J. V. B.; Brown, H. C. *J. Org. Chem.* **2001**, *66*, 5359-5365.

# Chapter 4 Exploration of Lewis Acid Activation of a Lewis Acid Using *Ortho*-Substituted Arylboronates

## 4.1 Introduction

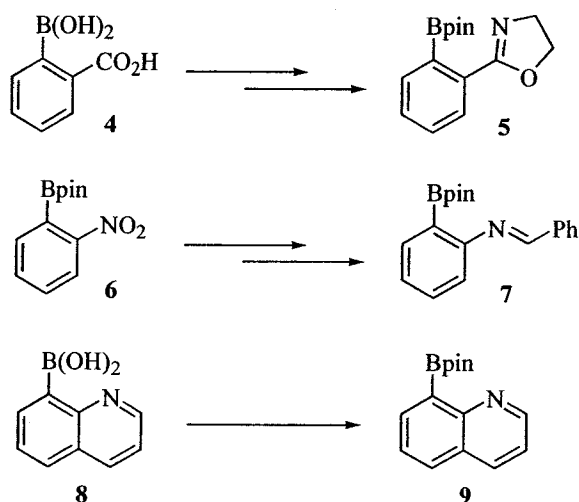
In the past two decades, the field of asymmetric synthesis has progressed tremendously and Chapter 1 of this thesis has briefly appraised several current advances in enantioselective catalysis using Lewis acids. Yet, an efficient asymmetric variant or a suitable chiral catalyst is still lacking for many important organic reactions. While a strong Lewis acid may offer the optimal activity for catalysis, its consequent instability toward air and water may on the other hand impede its industrial applications. Rooting back to the ideas of LLA (Section 1.2.3) and bifunctional catalysis (Section 1.3.2), we became interested to further explore the concept of Lewis acid activation of a Lewis acid using *ortho*-substituted arylboronates. Extending from the mechanistic insight gained for our group's first Lewis acid-catalyzed allylboration (Section 2.1.1, Scheme 2.5),<sup>1</sup> our catalyst design here was based on the electrophilic activation of the boron center in arylboronate **1** with an external metal via a putative complex **2** (Scheme 4-1).



**Scheme 4-1.** Concept of Lewis acid activation of a Lewis acid using *ortho*-substituted arylboronate **1**.

By intermolecularly combining two mildly Lewis acidic thus stable components to generate a stronger Lewis acidic entity *in situ*, we hoped to attain a cooperative, highly active catalyst system that concurrently circumvents the impractical handling of air and water sensitive reagents. Upon activation, the boron center could then in turn activate an aldehyde (via structure 3) to promote known classes of reactions such as allylsilylations or allylstannations (Section 4.4). Last but not least, the bidentate chelation depicted in complex 2 would provide an organized structure potentially useful for asymmetric catalysis if a chiral diol was employed in the boronate precursor. Alternatively, a chiral ligand ( $L_n$ ) on the external metal would also induce a chiral environment, so the system would be flexible for fine-tuning.

Our catalyst model was designed based on *ortho*-substituted phenylboronates because arylboronic esters are in general stable to air and water. For the initial studies conducted here, we focused on achiral systems where pinacol was used since the corresponding pinacolates should be stable enough to be isolated and characterized. Several NMR experiments were performed in Section 4.3 to detect the formation of the desired complex. As illustrated in Scheme 4-2, our original model targets included oxazoline 5, imine 7 and quinoline 9, which should all be easily accessible from commercially available starting materials 4, 6 and 8, respectively.

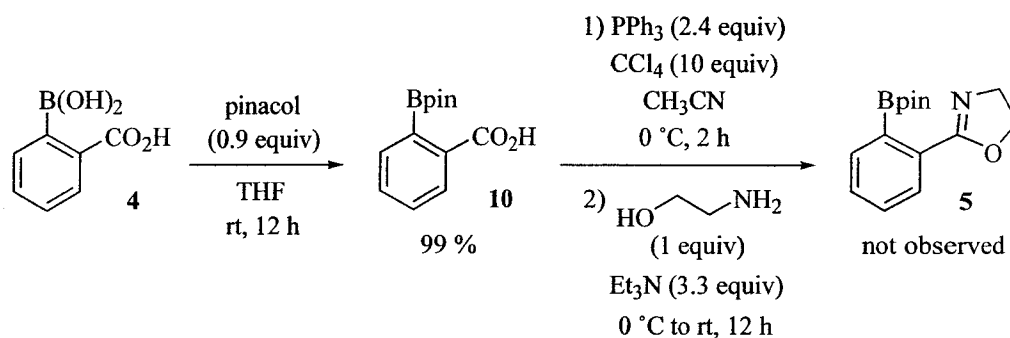


**Scheme 4-2.** Target arylboronates 5, 7, 9 and their corresponding commercially available starting materials.

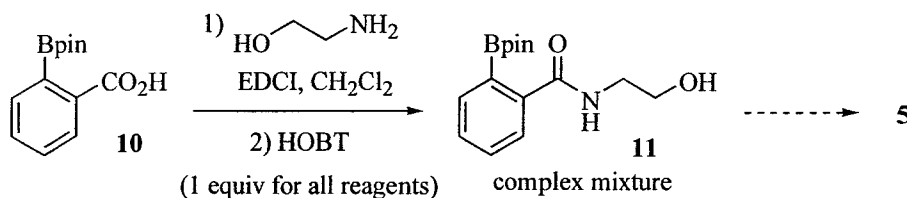
## 4.2 Attempted Synthesis of Various *Ortho*-Substituted Arylboronates

### 4.2.1 Oxazoline 5

To synthesize our first target arylboronate **5**, (2-carboxylphenyl)boronic acid (**4**) was treated with pinacol to generate the corresponding boronic ester **10** (Scheme 4-3). The resulting benzoic acid was then converted to the acid chloride *in situ* using triphenylphosphine- $\text{CCl}_4$  followed by nucleophilic substitution with ethanolamine in the presence of triethylamine.<sup>2a</sup> Upon workup and purification, however, only triphenylphosphine oxide was isolated and the pinacolate  $^1\text{H}$  NMR signal could not be found in any of the isolated material. We then decided to try presumably milder amide coupling protocol using EDCI and HOBT,<sup>3</sup> but only a complex mixture was obtained (Scheme 4-4).



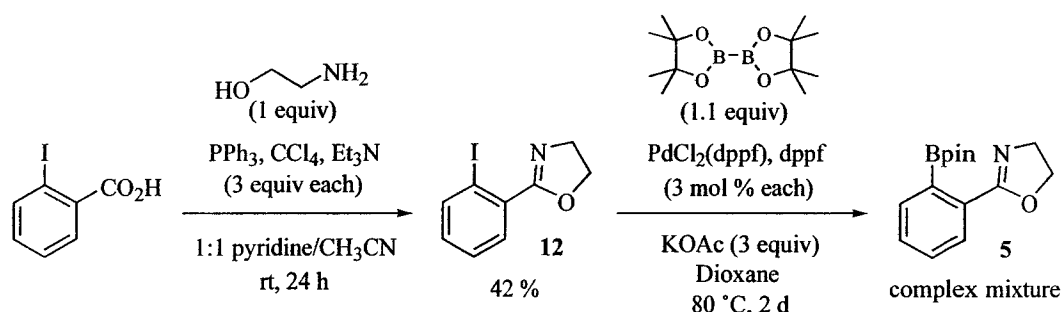
Scheme 4-3. First attempt to generate arylboronate **5**.



Scheme 4-4. Attempted synthesis of **5** via amide coupling.

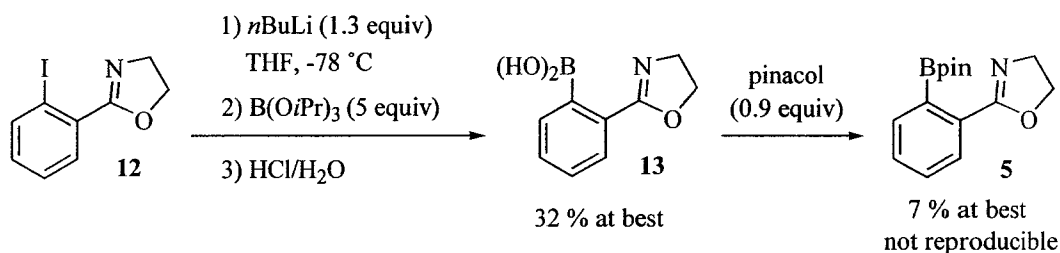
As an alternative approach, we decided to install the desired oxazoline moiety prior to the generation of the boronic ester. Under similar conditions as

above,<sup>2b</sup> 2-iodobenzoic acid was transformed to oxazoline **12** in 42 % yield (Scheme 4-5). Using a palladium-catalyzed diboron coupling protocol,<sup>4</sup> the subsequent synthesis of **5** was tried but without success.



**Scheme 4-5.** Attempted synthesis of **5** by Pd-catalyzed coupling.

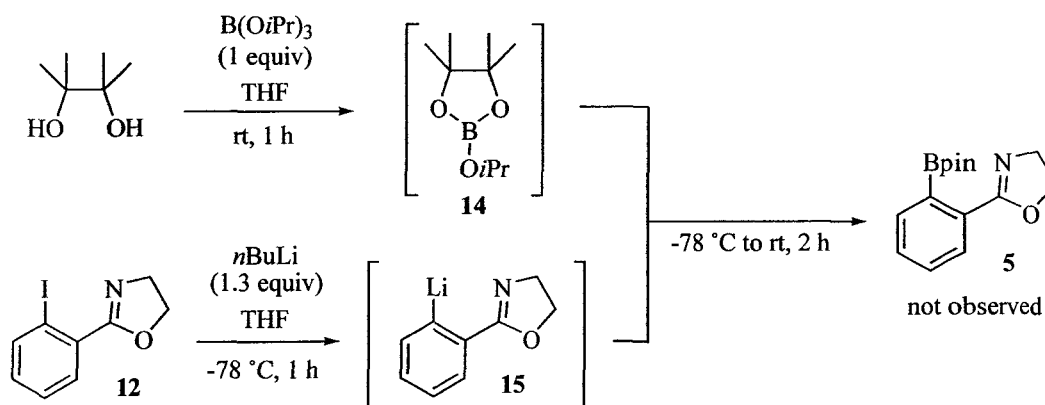
With the aryl iodide **12** in hand, we turned our attention to lithium-halogen exchange as the last resort. Using a conventional procedure with *n*BuLi and borate quench (Scheme 4-6),<sup>5</sup> the first problem we encountered was that the boronic acid intermediate **13** was found to be more soluble in aqueous solution



**Scheme 4-6.** Generation of **5** via lithium-halogen exchange.

than in organic extracts, even after careful neutralization, salting out and extensive extractions with both Et<sub>2</sub>O and EtOAc during workup. As our group had developed an universal solid-phase approach for immobilizing boronic acids,<sup>6</sup> we decided to isolate **13** using the DEAM-PS resin which afforded the desired boronic acid, albeit in low yield. In an unsuccessful attempt to improve the yield, we reverted to the lithium-halogen exchange step, and tried cannulating the lithiated intermediate into a solution of B(O*i*Pr)<sub>3</sub> instead of directly adding a

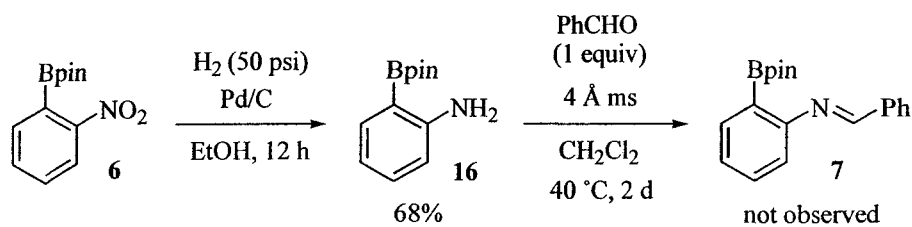
solution of the latter into the former. The results were even more disappointing when we carried on to make the pinacol boronic ester **5**. Toward this end, we also tried not to isolate the boronic acid intermediate hoping to improve the overall yield but in vain. As the last alternative, we decided to combine the two *in-situ* generated borate **14** and lithiated species **15** to synthesize our target without success (Scheme 4-7).



**Scheme 4-7.** Alternative synthesis of **5** avoiding the boronic acid intermediate.

#### 4.2.2 Imine **7**

To generate our second target, imine **7**, the commercial 2-nitrophenylboronic ester (**6**) was first hydrogenated under 50 psi of hydrogen gas to give aniline intermediate **16** (Scheme 4-8). On a side note, this particular



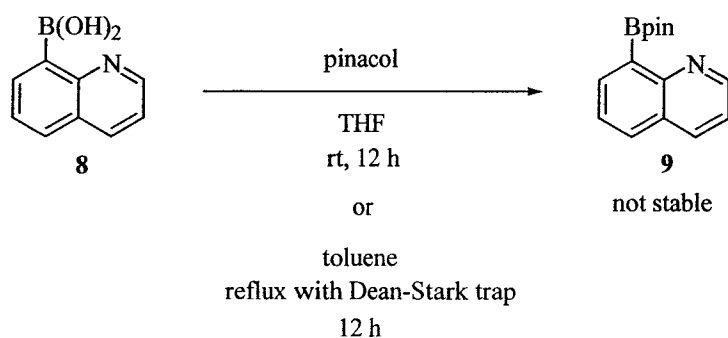
**Scheme 4-8.** Attempted synthesis of imine **7**.

hydrogenation could be achieved under atmospheric hydrogen with similar yields as was found by another group member.<sup>7</sup> In the presence of 4 Å molecular sieves,

aniline **16** was refluxed with benzaldehyde at 40 °C in dichloromethane for 2 days, but no desired product was observed. In order to increase the reaction temperature, we replaced dichloromethane with the higher boiling 1,2-dichloroethane. Using anhydrous MgSO<sub>4</sub> as the dehydrating agent, the last reaction was done at 80 °C for 3 days without any improvement.

#### 4.2.3 Quinoline **9**

Down to our third target, quinoline **9**, just the simple pinacol boronic ester formation was found to be difficult (Scheme 4-9). As the starting boronic acid **8**



**Scheme 4-9.** Attempted synthesis of quinoline **9**.

was not very soluble in THF even after the addition of pinacol, we changed solvent to toluene. Under reflux in a Dean-Stark apparatus, we did observe the desired product according to mass spectrometric analysis. However, compound **9** was found to be not particularly stable as even preparing a NMR sample was problematic. A precipitate was formed when CDCl<sub>3</sub> was used and dissolving **9** in CD<sub>3</sub>OD regenerated the starting boronic acid. With the presence of a sp<sup>2</sup> nitrogen atom at the *ortho* position, hydrolysis or alcoholysis as depicted in Figure 4-1 could possibly be the origin of the compound's instability. This would also explain why the syntheses of oxazoline **5** and imine **7** were not as straightforward as anticipated.



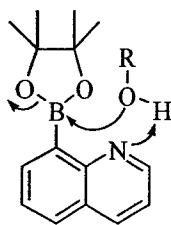
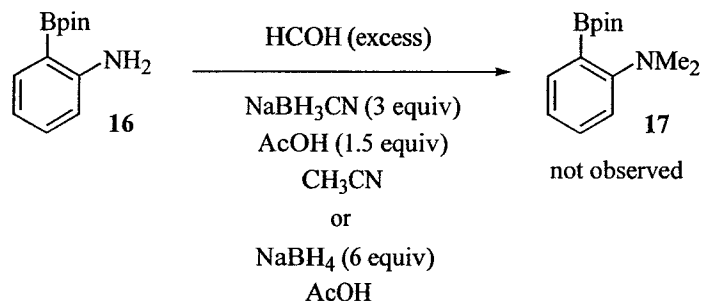


**Figure 4-1.** Solvolysis as an origin of compound instability.

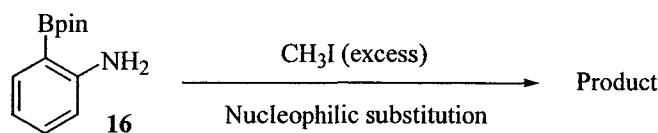
#### 4.2.4 Dimethylaniline **17**

Over our quest of finding a suitable *ortho*-substituted arylboronate catalyst, we also became interested in the dimethylaniline analogue **17**. Making use of the readily available aniline **16** generated in the attempted imine synthesis above, reductive amination using either NaBH<sub>3</sub>CN or NaBH<sub>4</sub> (Scheme 4-10) only led to decomposition of the starting material.



**Scheme 4-10.** Attempted reductive amination to generate **17**.

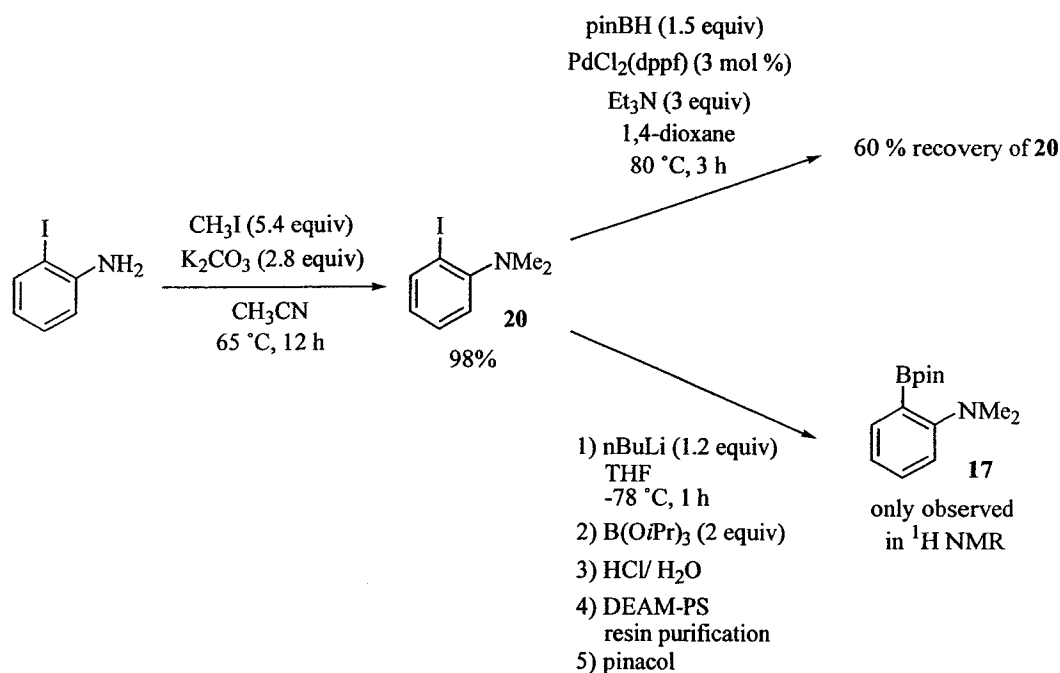
Nucleophilic substitution using different deprotonating agents in the presence of excess methyl iodide were then tried with mixed results (Table 4-1). While potassium hydroxide, sodium carbonate and tri-*n*-butylamine all led to decomposition of the starting material (Entries 1-3), PMP provided the monomethylated **18** (Entry 4) and 2,6-lutidine gave the trimethylammonium salt **19** (Entry 5) in 21 % and 28 % yield, respectively. Further reaction of **18** with PMP and methyl iodide at elevated temperature only disintegrated the monomethylated material. Demethylation was also attempted on **19** using sodium methoxide in methanol but without success.

**Table 4-1.** Attempted synthesis of **17** via nucleophilic substitution.

Entry	Conditions <sup>a</sup>	Product	Entry	Conditions <sup>a</sup>	Product <sup>b</sup>
1	KOH DMF rt, 1 h	Decomposition of starting material	4	PMP, DMF rt (2 h) then 65 °C (30 min)	 <b>18</b> 21 %
2	Na <sub>2</sub> CO <sub>3</sub> EtOH 75 °C, 16 h	Decomposition of starting material	5	2,6-lutidine DMF rt, 16 h	 <b>19</b> 28 %
3	tri- <i>n</i> -butylamine DMF rt, 16 h	Decomposition of starting material			

<sup>a</sup> All deprotonating agents were used in excess. <sup>b</sup> Isolated yields.

Starting over without the boronic ester moiety (Scheme 4-1), 2-iodoaniline was quantitatively converted to the corresponding dimethyl analogue **20**.<sup>8</sup> With **20** in hand, both palladium coupling and lithium-halogen exchange were tried but neither provided an efficient route for our target compound **17**. While only starting material was recovered from the palladium coupling, the boronic acid intermediate generated from the lithium-halogen exchange was again found to be more soluble in aqueous extracts. Employing the DEAM-PS resin, the purification was disappointingly inefficient (see Experimental 4.6.4.4). Meanwhile, since the preliminary model reaction studies (Section 4.4) only revealed modest results for the desired catalytic effects, no further optimization was undertaken.



Scheme 4-11. Last attempts to generate **17** from 2-iodoaniline.

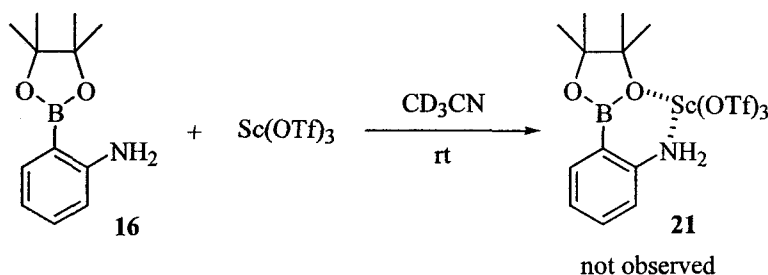
## 4.3 Results from Various NMR Experiments

### 4.3.1 Varying the amount of Lewis acid

Settling with the use of arylboronate **16** as a model substrate while varying the amount of Lewis acid (Table 4-2), the first series of NMR experiments were performed at room temperature in  $\text{CD}_3\text{CN}$ , where both substrate and catalyst are soluble. Referred to as the “magic Lewis acid” among our group,  $\text{Sc}(\text{OTf})_3$  was tested in all of the cases where an external metal was required. Unfortunately, complex **21** was never observed. With Entries 1 and 2 serving as controls, no significant change in chemical shifts was observed for either the fluorine or boron atom when the arylboronate and  $\text{Sc}(\text{OTf})_3$  were both present (Entries 3-6). In contrast,  $^1\text{H}$  and  $^{13}\text{C}$  NMR spectra revealed noticeable chemical shift differences upon addition of both catalytic and stoichiometric amount of the Lewis acid. In all cases, the aromatic as well as the amine proton signals were shifted downfield, while the pinacolate proton signal remained to be a sharp singlet residing at the

usual 1.3 to 1.4 ppm region. Furthermore, no trace of free amine was observed even when only a “catalytic” amount of  $\text{Sc}(\text{OTf})_3$  was used (0.25 and 0.5 equivalent for Entries 3 and 4, respectively). In retrospect, this last surprising result might have been overlooked and one possible explanation could be that the scandium metal, which can have as many as nine ligands, binds to more than one arylboronate molecules at a time.

**Table 4-2.** NMR experiments varying the amount of Lewis acid.



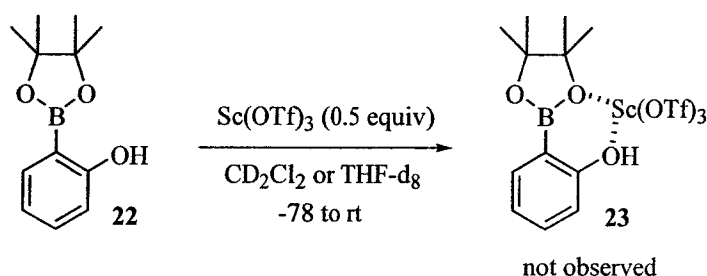
Entry	Amount of <b>16</b> (mg)	Amount of $\text{Sc}(\text{OTf})_3$	Chemical shift for $^{11}\text{B}$ (ppm)	Chemical shift for $^{19}\text{F}$ (ppm)
1	30	-	31	-
2	-	10 mg	-	-79.1
3	30	0.25 equiv	30.3	-79.6
4	30	0.5 equiv	29.9	-79.5
5	30	1 equiv	29.9	-79.2
6	30	2 equiv	29.9	-79.1

#### 4.3.2 Lowering the experimental temperature

Based on the results obtained from the room-temperature NMR experiments, the metal seemingly only binds to the less electronegative nitrogen without interacting with any of the two pinacolate oxygen atoms. However, since the desired interaction between an oxygen and the metal might be an equilibrium process occurring at a rate much too fast to be observed at ambient temperature,

we decided to cool down the NMR sample. Using 0.5 equivalent of  $\text{Sc}(\text{OTf})_3$  in the noncoordinating solvent  $\text{CD}_2\text{Cl}_2$ , the experiment temperature was systematically changed from  $-78\text{ }^\circ\text{C}$  to room temperature. Unfortunately, only similar results as the previous ambient-temperature experiments were obtained at all subzero temperatures investigated.

Changing substrate to the commercially available phenol **22** (Scheme 4-12), we hoped to promote the desired complexation (**23**) by making the two chelating groups electronically more similar but the results of the VT NMR experiments were only disappointing. Deuterated THF was also tried as solvent but it did not provide any promising data.



**Scheme 4-12.** VT NMR experiment with phenol **22**.

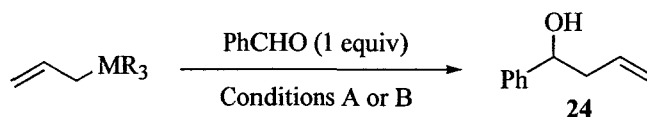
#### 4.4 Model Reaction Study

Despite all the negative results, simple allylsilylation and allylstannation were nevertheless conducted as model reactions (Table 4-3) because the concept of synergistic activation might still be valid provided that the most potent Lewis acidic species formed in the reaction mixture was the one generated from complex **23**. In the presence of 0.5 equivalent of catalyst at  $-78\text{ }^\circ\text{C}$  for 60 hours (Condition A), none of the allylsilylation led to the desired product (Entries 1-3). In order to discern any catalytic effect that might arise from mixing arylboronate **22** and  $\text{Sc}(\text{OTf})_3$  together, Entries 1, 2, 4 and 5 were served as control experiments.

In all the allylstannation cases using 20 mol % of catalyst (Condition B), the aldehyde substrate was still present after 2 hours at  $-40\text{ }^\circ\text{C}$  according to TLC

analysis. Upon stirring at room temperature for 1 hour, however, TLC indicated that all of the aldehyde had been consumed in Entries 4 and 6 where homoallylic alcohol **24** was indeed isolated after flash chromatography as the only identifiable product in 28 % and 68 % yield, respectively. According to the increased yield in Entry 6 compared to Entry 4, there seemed to be a small synergetic effect when both arylboronate **22** and Sc(OTf)<sub>3</sub> were present. To further investigate this intriguing result, more work in terms of extending the substrate scope and deducing the exact nature of the cooperative acceleration is warranted.

**Table 4-3.** Model reaction study.



Entry	MR <sub>3</sub>	Conditions	Catalyst	Product
1	SiMe <sub>3</sub>	A <sup>a</sup>	Sc(OTf) <sub>3</sub>	not observed
2	SiMe <sub>3</sub>	A <sup>a</sup>	<b>22</b>	not observed
3	SiMe <sub>3</sub>	A <sup>a</sup>	<b>22</b> + Sc(OTf) <sub>3</sub>	not observed
4	SnBu <sub>3</sub>	B <sup>b</sup>	Sc(OTf) <sub>3</sub>	28% <sup>c</sup>
5	SnBu <sub>3</sub>	B <sup>b</sup>	<b>22</b>	not observed
6	SnBu <sub>3</sub>	B <sup>b</sup>	<b>22</b> + Sc(OTf) <sub>3</sub>	68% <sup>c</sup>

<sup>a</sup> Conditions A: 0.5 equiv catalyst, THF, -78 °C, 60 h. <sup>b</sup> Conditions B: 20 mol % catalyst, CH<sub>3</sub>CN, -40 °C for 2 h then rt for 1 h. <sup>c</sup> Isolated yields.

## 4.5 Conclusion And Future Work

To summarize, this was a challenging project! After laborious attempts, all of the original *ortho*-substituted arylboronate targets were found to be either difficult to synthesize efficiently or unstable. Tested with the aniline and phenol analogues **16** and **22**, the desired complexation was not observed according to various NMR experiments. While allylsilylation did not lead to any desired product under the model reaction conditions, allylstannation did generate the corresponding homoallylic alcohol adduct in the presence of a catalytic amount of arylboronate **22** and Sc(OTf)<sub>3</sub>. However, since the yield obtained from the apparently accelerated allylstannation was only modest even at room temperature, time and effort were diverted toward other projects described in this thesis.

In terms of future work, it would be very interesting to find out whether any practical level of stereinduction could be obtained by employing a chiral analogue of arylboronate **22** in the same allylstannation studied in Section 4.4. The use of alkylboronates in lieu of aryl ones and, as demonstrated in Chapter 2, triflic acid as an alternative to scandium triflate are also worth examining. On a side note, the results obtained in this chapter did spring out a related project taken up by another group member later on where an intramolecular activation variant via hydrogen bonding was investigated.<sup>7</sup>

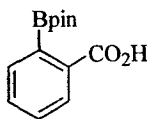
## 4.6 Experimental

### 4.6.1 General

The general experimental procedures described in Section 2.7.1 also apply here, with the following additions. Pyridine and CH<sub>3</sub>CN were distilled over CaH<sub>2</sub> before use. Ethanolamine, Et<sub>3</sub>N and CCl<sub>4</sub> were purified by Kugelrohr distillation prior to use. Boronic acid immobilization using DEAM-PS resin was done by agitation inside polypropylene filter vessels while resin washing operations were carried out on a vortexer.<sup>6</sup>

## 4.6.2 Toward the synthesis of arylboronic ester 5

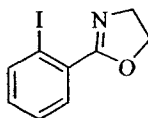
### 4.6.2.1 2-(4,4,5,5-Tetramethyl-1,3,2-dioxaborolan-2-yl)benzoic acid (10)



A suspension of (2-carboxylphenyl)boronic acid (103 mg, 0.62 mmol) in THF (5 mL) was treated with pinacol (73 mg, 0.62 mmol). The resulting solution was stirred at rt for 12 h followed by solvent evaporation to give pinacol ester **10** (153 mg, 0.617 mmol, 99 %).

$^1\text{H}$  NMR (300 MHz,  $\text{CDCl}_3$ ):  $\delta$  8.06 (d, 1H,  $J = 7.7$  Hz), 7.55 (m, 2H), 7.46 (m, 1H), 1.42 (s, 12H);  $^{13}\text{C}$  NMR (125 MHz,  $\text{CDCl}_3$ ):  $\delta$  173.2, 135.6, 132.7, 132.5, 132.3, 129.7, 129.1, 84.2, 24.8; IR ( $\text{CHCl}_3$  cast film,  $\text{cm}^{-1}$ ): 3250-2250 (broad), 1681, 1599, 1569, 1306, 1143, 757; HRMS (EI,  $m/z$ ) Calcd for  $\text{C}_{13}\text{H}_{17}^{11}\text{BO}_4$ : 248.12199. Found: 248.12182.

### 4.6.2.2 2-(2-Iodophenyl)-4,5-dihydro-oxazole (12)<sup>2b</sup>



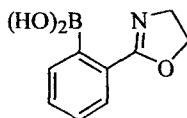
To a solution of 2-iodobenzoic acid (2.0 g, 8.1 mmol) in 1:1 pyridine/ $\text{CH}_3\text{CN}$  (12 mL), freshly distilled ethanolamine (0.49 mL, 8.1 mmol),  $\text{Et}_3\text{N}$  (3.4 mL, 24 mmol) and  $\text{CCl}_4$  (2.3 mL, 24 mmol) were added sequentially. The clear yellow solution was treated with  $\text{PPh}_3$  (6.4 g, 24 mmol) in 1:1 pyridine/ $\text{CH}_3\text{CN}$  (10 mL) using a dropping funnel over 20 min. and the resulting dark red mixture was stirred at rt for 24 h. The reaction solvent was then evaporated. Water (40 mL) was added to the crude mixture and extracted with  $\text{Et}_2\text{O}$  ( $3 \times 40$  mL). The combined organic phase was first washed with saturated  $\text{CuSO}_3(\text{aq})$  ( $3 \times 30$  mL) to remove pyridine and then washed with brine (30 mL). The resulting organic phase was dried with anhydrous  $\text{MgSO}_4$ , filtered and concentrated. Flash chromatography (started with 8 %  $\text{EtOAc}$ /petroleum ether



then gradually increased to 50 %) gave aryl iodide **12** (0.92 g, 3.4 mmol, 42 %) as a brown liquid.

$^1\text{H}$  NMR (300 MHz,  $\text{CDCl}_3$ ):  $\delta$  7.95 (dd, 1H,  $J = 7.8, 1.3$  Hz), 7.65 (dd, 1H,  $J = 7.8, 1.8$  Hz), 7.38 (td, 1H,  $J = 7.6, 1.3$  Hz), 7.11 (td, 1H,  $J = 7.6, 1.8$  Hz), 4.47 (t, 2H,  $J = 9.4$  Hz), 4.12 (t, 2H,  $J = 9.4$  Hz);  $^{13}\text{C}$  NMR (100 MHz,  $\text{CDCl}_3$ ):  $\delta$  164.4, 140.2, 133.2, 131.3, 130.4, 127.5, 94.4, 67.5, 55.0; IR (microscope,  $\text{cm}^{-1}$ ): 3419, 2971, 2901, 1656, 1470, 1354, 1243, 1089, 393; HRMS (EI,  $m/z$ ) Calcd for  $\text{C}_9\text{H}_8\text{ONI}$ : 272.96506. Found: 272.96527.

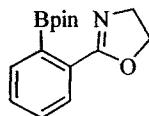
#### 4.6.2.3 [2-(4,5-Dihydro-oxazol-2-yl)-phenyl]boronic acid (**13**)



To a solution of aryl iodide **12** (101 mg, 0.37 mmol) in THF (2 mL) at  $-78$   $^{\circ}\text{C}$ ,  $n\text{BuLi}$  (1.4 M in hexane, 0.34 mL, 0.48 mmol) was added dropwise and the resulting mixture was stirred at  $-78$   $^{\circ}\text{C}$  for 90 min. followed by addition of  $\text{B}(\text{O}i\text{Pr})_3$  (0.43 mL, 1.8 mmol). After stirring for 30 min. at  $-78$   $^{\circ}\text{C}$ , the reaction mixture was stirred at rt for another 30 min. The reaction mixture was then neutralized by dropwise addition of HCl (1 M) followed by extraction with EtOAc ( $2 \times 10$  mL). The aqueous phase which contained the boronic acid product was submitted to solvent evaporation. The crude boronic acid was redissolved in anhydrous THF followed by immobilization using DEAM-PS resin (0.6 g) for 1 h. The resin was rinsed with anhydrous THF (5 mL) and the boronic acid was then cleaved by 5 %  $\text{H}_2\text{O}/\text{THF}$  wash ( $4 \times 5$  mL). Boronic acid **13** (24 mg, 0.12 mmol, 32 %) was obtained after solvent evaporation.

$^1\text{H}$  NMR (300 MHz,  $\text{CDCl}_3$ ):  $\delta$  7.59 (d, 1H,  $J = 7.4$  Hz), 7.44 (d, 1H,  $J = 7.0$  Hz), 7.30 (td, 1H,  $J = 7.4, 1.1$  Hz), 7.20 (td, 1H,  $J = 7.4, 1.1$  Hz), 4.89 (s, 2H), 3.66 (t, 2H,  $J = 5.2$  Hz), 3.42 (t, 2H,  $J = 5.2$  Hz).

#### 4.6.2.4 2-[2-(4,4,5,5-Tetramethyl-1,3,2-dioxaborolan-2-yl)-phenyl]-4,5-dihydro-oxazole (5)

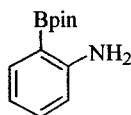


To a solution of boronic acid **13** (52.8 mg, 0.276 mmol) in THF (2.5 mL), pinacol (31.4 mg, 0.266 mmol) was added. The resulting solution was stirred at rt for 12 h followed by solvent evaporation. Flash chromatography (8 % MeOH/CH<sub>2</sub>Cl<sub>2</sub>) gave pinacol ester **5** (7 mg, 0.02 mmol, 7 %).

<sup>1</sup>H NMR (300 MHz, CDCl<sub>3</sub>): δ 7.62 (m, 1H), 7.47 (m, 2H), 7.24 (m, 1H), 3.62 (t, 2H, *J* = 5.0 Hz), 3.47 (t, 2H, *J* = 5.0 Hz), 1.36 (s, 12H).

#### 4.6.3 Toward the synthesis of arylboronic ester 7

##### 4.6.3.1 2-(4,4,5,5-Tetramethyl-1,3,2-dioxaborolan-2-yl) phenylamine (16)

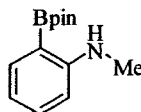


A solution of 2-nitrophenylboronic ester (0.5 g, 2 mmol) in EtOH (20 mL) was hydrogenated at 50 psi with 10 % Pd/C (50 mg) for 12 h. The mixture was then filtered through Celite<sup>®</sup> 545 with EtOH rinse followed by solvent removal. Flash chromatography (25 % EtOAc/hexane) gave aniline **16** (295 mg, 1.35 mmol, 68 %) as a yellowish solid.

<sup>1</sup>H NMR (300 MHz, CDCl<sub>3</sub>): δ 7.61 (dd, 1H, *J* = 7.4, 1.6 Hz), 7.21 (m, 1H), 6.67 (td, 1H, *J* = 7.3, 0.9 Hz), 6.59 (d, 1H, *J* = 8.1 Hz), 4.72 (broad s, 2H), 1.34 (s, 12H); <sup>13</sup>C NMR (100 MHz, CDCl<sub>3</sub>): δ 153.6, 136.7, 132.7, 116.8, 114.7, 83.4, 24.9; IR (microscope, cm<sup>-1</sup>): 3488, 3385, 2995, 1956, 1930, 1568, 1458, 1348, 1136, 960, 852; HRMS (EI, *m/z*) Calcd for C<sub>12</sub>H<sub>18</sub><sup>11</sup>BNO<sub>2</sub>: 219.14307. Found: 219.14296.

#### 4.6.4 Toward the synthesis of arylboronic ester 17

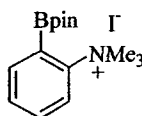
##### 4.6.4.1 Methyl-[2-(4,4,5,5-tetramethyl-1,3,2-dioxaborolan-2-yl)-phenyl] amine (18)



To a solution of aniline **16** (108 mg, 0.493 mmol) in DMF (4 mL), PMP (0.9 mL, 5 mmol) and CH<sub>3</sub>I (0.61 mL, 10 mmol) were added. The resulting solution was stirred at rt for 2 h and heated to 65 °C for 30 min. The reaction solvent was then evaporated. The residue was redissolved in EtOAc (15 mL), washed with NH<sub>4</sub>Cl<sub>(aq)</sub> (2 × 3 mL), water (2 × 3 mL) and brine (3 mL). The organic phase was dried with anhydrous Na<sub>2</sub>SO<sub>4</sub>, filtered and concentrated. Flash chromatography (20 % EtOAc/hexane) gave monomethylated aniline **18** (24 mg, 0.10 mmol, 21 %) as the only identifiable product.

<sup>1</sup>H NMR (300 MHz, CDCl<sub>3</sub>): δ 7.65 (dd, 1H, *J* = 7.4, 1.8 Hz), 7.34 (m, 1H), 6.64 (td, 1H, *J* = 7.3, 1.0 Hz), 6.56 (d, 1H, *J* = 8.4 Hz), 5.74 (broad s, 1H), 2.87 (s, 3H), 1.35 (s, 12H).

##### 4.6.4.2 Trimethyl-[2-(4,4,5,5-tetramethyl-1,3,2-dioxaborolan-2-yl)-phenyl] ammonium iodide (19)

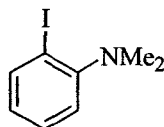


To a solution of aniline **16** (80.1 mg, 0.366 mmol) in DMF (1 mL), 2,6-lutidine (85 μL, 0.73 mmol) and CH<sub>3</sub>I (114 μL, 1.83 mmol) were added. The resulting solution was stirred at rt for 12 h followed by addition of Et<sub>2</sub>O to induce precipitate formation. The precipitate was isolated by vacuum filtration and recrystallized with EtOH to give ammonium salt **19** (39 mg, 0.10 mmol, 28 %) as a white solid.

<sup>1</sup>H NMR (300 MHz, CD<sub>3</sub>OD): δ 8.03 (dd, 1H, *J* = 7.7, 2.1 Hz), 7.91 (d, 1H, *J* = 8.6 Hz), 7.72 (m, 1H), 7.61 (td, 1H, *J* = 7.4, 0.8 Hz), 3.77 (s, 9H), 1.44 (s,

12H);  $^{13}\text{C}$  NMR (125 MHz,  $\text{CDCl}_3$ ):  $\delta$  145.2, 139.8, 133.9, 130.8, 128.4, 121.1, 87.1, 58.3, 25.0, 22.1; IR (microscope,  $\text{cm}^{-1}$ ): 2980, 1605, 1475, 1433, 1327, 1140, 1048, 961, 849, 774; HRMS (ES,  $m/z$ ) Calcd for  $\text{C}_{15}\text{H}_{25}\text{BNO}_2$ : 262.19729. Found: 262.19754.

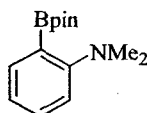
#### 4.6.4.3 (2-Iodophenyl)-dimethylamine (**20**)



To a solution of 2-iodoaniline (2 g, 9 mmol) in  $\text{CH}_3\text{CN}$  (15 mL),  $\text{K}_2\text{CO}_3$  (3.5 g, 25 mmol) and  $\text{CH}_3\text{I}$  (3 mL, 48 mmol) were added. The resulting dark purple mixture was refluxed at 65 °C for 12 h. Cooled to rt, ice-cold water (60 mL) was added. The mixture was extracted with benzene (3  $\times$  40 mL) and the combined organic phase was dried with anhydrous  $\text{MgSO}_4$ , filtered and concentrated. Flash chromatography (20 % EtOAc/hexane) gave **20** (2.19 g, 8.86 mmol, 98 %) as an orange liquid.

$^1\text{H}$  NMR (300 MHz,  $\text{CDCl}_3$ ):  $\delta$  7.85 (dd, 1H,  $J = 7.8, 1.5$  Hz), 7.32 (m, 1H), 7.11 (d, 1H,  $J = 8.2$  Hz), 6.77 (m, 1H), 2.78 (s, 6H);  $^{13}\text{C}$  NMR (100 MHz,  $\text{CDCl}_3$ ):  $\delta$  154.8, 140.0, 128.9, 124.8, 120.3, 97.1, 44.8; IR (microscope,  $\text{cm}^{-1}$ ): 2941, 2827, 1580, 1470, 1316, 1158, 1013, 945; HRMS (EI,  $m/z$ ) Calcd for  $\text{C}_8\text{H}_{10}\text{NI}$ : 246.98579. Found: 246.98567.

#### 4.6.4.4 Dimethyl-[2-(4,4,5,5-tetramethyl-1,3,2-dioxaborolan-2-yl)-phenyl] amine (**17**)

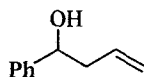


To a solution of aryl iodide **20** (103 mg, 0.417 mmol) in THF (2 mL) at -78 °C,  $n\text{BuLi}$  (1.6 M in hexane, 0.31 mL, 0.50 mmol) was added dropwise and the resulting mixture was stirred at -78 °C for 1 h. The lithiated intermediate was then cannulated into a -78 °C solution of  $\text{B}(\text{O}i\text{Pr})_3$  (0.2 mL, 0.9 mmol) in THF (2 mL). After stirring for 1 h at -78 °C, the reaction mixture was warmed up to rt and

neutralized by dropwise addition of HCl (1 M). After solvent evaporation under high vacuum over night, the crude boronic acid was redissolved in anhydrous THF followed by immobilization using DEAM-PS resin (0.5 g) for 1 h. The resin was rinsed with anhydrous THF (3 × 5 mL). Without the cleavage step with 5 % H<sub>2</sub>O/THF wash, however, the boronic acid was found in the anhydrous THF rinse. The still impure boronic acid (24.5 mg) was treated with pinacol (14 mg, 0.12 mmol) in THF (2 mL) at rt for 30 min. The crude boronic ester **17** (10.9 mg) was obtained after solvent evaporation as an analytical sample without further purification.

<sup>1</sup>H NMR (300 MHz, CDCl<sub>3</sub>): δ 7.66 (d, 1H, *J* = 7.2 Hz), 7.32 (m, 1H), 6.90 (m, 2H), 2.91 (s, 6H), 1.37 (s, 12H).

#### 4.6.5 Model allylstannation: preparation of *rac*-1-phenyl-3-buten-1-ol (**24**)



A solution of Sc(OTf)<sub>3</sub> (49 mg, 0.10 mmol) and phenol **22** (21 μL, 0.10 mmol) in CH<sub>3</sub>CN (1 mL) was stirred at -40 °C for 10 min. Benzaldehyde (51 μL, 0.50 mmol) and allyltributyltin (153 μL, 0.50 mmol) were then added sequentially. The resulting mixture was stirred at -40 °C for 2 h then at rt for another 1 h. The reaction was quenched by addition of NaHCO<sub>3(aq)</sub> (2 mL) and extracted with CH<sub>2</sub>Cl<sub>2</sub> (3 × 5 mL). The combined organic phase was dried with anhydrous MgSO<sub>4</sub>, filtered and concentrated. Flash chromatography (20 % EtOAc/hexane) gave homoallylic alcohol **24** (50.5 mg, 0.341 mmol, 68 %) as the only identifiable product which possessed identical spectroscopic characteristics to those reported in the literature.<sup>9</sup>

## 4.7 References

1. Rauniyar, V.; Hall, D. G. *J. Am. Chem. Soc.* **2004**, *126*, 4518-4519.
2. a) Vorbrüggen, H.; Kroliekiewicz, K. *Tetrahedron* **1993**, *49*, 9353-9372. b) Peer, M.; de Jong, J.C.; Kiefer, M.; Langer, T.; Rieck, H.; Schell, H. *Tetrahedron* **1996**, *52*, 7547-7583.
3. Boger, D. L.; Keim, H.; Oberhauser, B.; Schreiner, E. P.; Foster, C. A. *J. Am. Chem. Soc.* **1999**, *121*, 6197-6205.
4. a) Ishiyama, T.; Murata, M.; Miyaura, N. *J. Org. Chem.* **1995**, *60*, 7508-7510. b) Ishiyama, T.; Itoh, Y.; Kitano, T.; Miyaura, N. *Tetrahedron Lett.* **1997**, *38*, 3447-3450.
5. Vyskocil, S.; Meca, L.; Tislerova, I.; Cisarova, I.; Polasek, M.; Harutyunyan, S. R.; Belokon, Y. N.; Stead, R. M. J.; Farrugia, L.; Lockhart, S. C.; Mitchell, W. L.; Kocovsky, P. *Chem. Eur. J.* **2002**, *8*, 4633-4648.
6. Gravel, M.; Thompson, K. A.; Zak, M.; Bérubé, C.; Hall, D. G. *J. Org. Chem.* **2002**, *67*, 3-15.
7. Owokalu, F.; Hall, D. G. Unpublished results.
8. Bunnett, J. F.; Mitchel, E. *Tetrahedron* **1985**, *41*, 4119-4132.
9. Kobayashi, S.; Nishio, K. *J. Org. Chem.* **1994**, *59*, 6620-6628.

## Chapter 5 Thesis Conclusions

---

This thesis investigates various boronate activation strategies and their practical applications in carbonyl allylation reactions. Over the course of these studies, Brønsted acid- and Lewis acid-catalyzed allylboration were examined. Using *ortho*-substituted arylboronates, the concept of Lewis acid activation of a Lewis acid was further explored on allylsilylations and allylstannations.

*The most significant result that emerges from this thesis is the novel Brønsted acid-catalyzed allylboration protocol amenable to the most difficult, electronically deactivated allylboronate and aldehyde substrates.*<sup>1</sup> Circumventing the use of metal ions, this method employs a simple and cheap catalyst, triflic acid, and its usefulness was highlighted in the stereodivergent synthesis of all four diastereomers of eupomatilone-6. Starting from a common allylboronate, the syntheses were accomplished in only four or five steps with up to 43 % overall yield. With five X-ray crystallographic structures obtained, the ambiguity of the original stereochemical assignments was brought to an end.

In addition to the key TfOH-catalyzed allylboration, our synthetic route also featured a number of remarkable observations, including the unexpected activation of the 2-bromo-3,4,5-trimethoxybenzaldehyde via a postulated, steric-induced deconjugation, the subtle reagent-controlled diastereoselective hydrogenation of the  $\alpha$ -*exo*-methylene lactone intermediates, and the success of a challenging case of Suzuki biaryl coupling utilizing Buchwald's conditions. This work has opened up a new avenue for catalyzing allylboration of carbonyl compounds. Expanding the aldehyde substrate scope and probing the exact mechanism underlying the Brønsted acid-catalyzed allylboration would certainly

---

<sup>1</sup> Yu, S. H.; Ferguson, M. J.; McDonald, R.; Hall, D. G. *J. Am. Chem. Soc.* **2005**, *127*, 12808-12809.

be illuminating to the development of an asymmetric variant and would potentially lead to completely new methodologies.

In an attempt to access homoallylic alcohol products both efficiently and enantioselectively, we revisited the Lewis acid-catalyzed allylboration previously reported by our group. 2-Alkoxy carbonyl and 2-*O*-protected ether allylboronates, both unsubstituted at the 3-position, were tested here as substrates. With the presence of an electron-withdrawing, deactivating ester functionality, the allylboration using 2-alkoxy carbonyl allylboronates only provided disappointing yields and low stereoselectivities in general. Focusing on the more electron-rich 2-*O*-protected ether allylboronates, an efficient synthetic route was developed for the achiral substrates. Preliminary results indicated that protection with a benzyl group was not suitable, since no allylboration adduct was observed in the subsequent reactions. Using triisopropylsilyl ether as the protecting group, the corresponding Sc(OTf)<sub>3</sub>-catalyzed allylborations indeed proceeded smoothly at -78 °C with both aromatic and aliphatic aldehydes. Toward the goal of generating the desired chiral allylboronate analogue, a wide range of different methods, including diboron coupling, Pt-catalyzed borylation, lithium-halogen exchange, Grignard addition, hydrostannation, diol exchange and others, were tried but unfortunately without success. As a result, the enantioselectivity of the subsequent asymmetric allylboration could not be assessed.

Lastly, turning our attention to other classes of carbonyl allylation reactions, the idea of intermolecular Lewis acid activation of a Lewis acid was examined. By combining two mildly Lewis acidic species, namely *ortho*-substituted arylboronates and Sc(OTf)<sub>3</sub>, we intended to generate *in situ* a stronger Lewis acidic entity to catalyze allylsilylation and allylstannation. This first project was proved to be quite challenging.

After laborious attempts, all of the original arylboronate targets were found to be either difficult to synthesize efficiently or unstable. The desired boronate-metal complexation was not observed based on various NMR



experiments using simpler arylboronate analogues. Last but not least, allylsilylation did not lead to any desired product under the model reaction conditions. Despite all the negative results, the homoallylic alcohol adduct was generated from model allylstannations and more importantly, a small synergetic effect was observed. While only 28 % of the desired alcohol product was obtained when  $\text{Sc}(\text{OTf})_3$  was used as the sole catalyst, the yield was increased to 68 % in the presence of both 2-hydroxyphenylboronic acid pinacol ester and  $\text{Sc}(\text{OTf})_3$ . This promising result could potentially lead to an enantioselective Lewis acid-assisted Lewis acid-catalyzed allylstannation protocol. As one result in research always generates further questions, could TfOH serve as a better alternative to  $\text{Sc}(\text{OTf})_3$  in these allylstannations as well?

## Appendices: X-Ray Crystallography Reports

---

<b>Appendix A</b>	Structure Report for Lactone <b>20</b> (Chapter 2).....	123
<b>Appendix B</b>	Structure Report for Lactone <b>21</b> (Chapter 2).....	131
<b>Appendix C</b>	Structure Report for Lactone <b>24</b> (Chapter 2).....	139
<b>Appendix D</b>	Structure Report for Lactone 3,4- <i>epi</i> - <b>15</b> (Chapter 2).....	147
<b>Appendix E</b>	Structure Report for Lactone 4- <i>epi</i> - <b>15</b> (Chapter 2).....	157

# Appendix A Structure Report for Lactone 20 (Chapter 2)

**XCL Code:** DGH0503

**Date:** 7 April 2005

**Compound:** (3*RS*,4*RS*,5*RS*)-5-(2-Bromo-3,4,5-trimethoxyphenyl)-3,4-dimethyldihydrofuran-2(3*H*)-one

**Formula:** C<sub>15</sub>H<sub>19</sub>BrO<sub>5</sub>

**Supervisor:** D. G. Hall

**Crystallographer:**

M. J. Ferguson

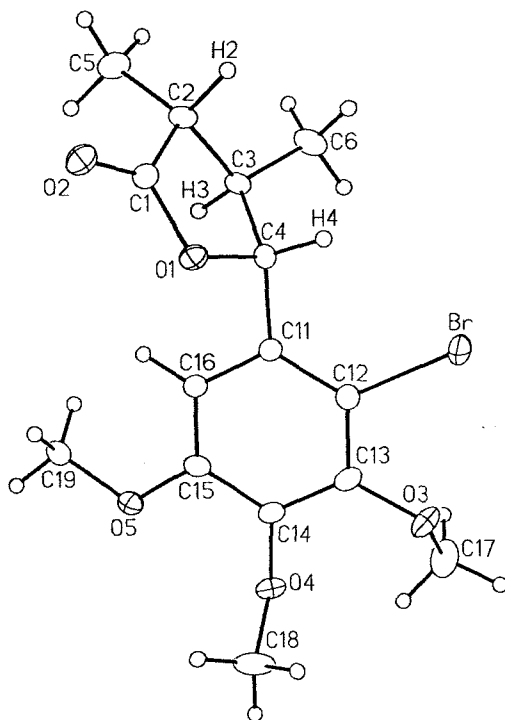


**Figure 1.** Perspective view of the (3*R*,4*R*,5*R*)-5-(2-bromo-3,4,5-trimethoxyphenyl)-3,4-dimethyldihydrofuran-2(3*H*)-one molecule showing the atom labelling scheme. Non-hydrogen atoms are represented by Gaussian ellipsoids at the 20% probability level. Hydrogen atoms are shown with arbitrarily small thermal parameters. The 3*S*, 4*S*, 5*S* enantiomer is also present in the crystal lattice.

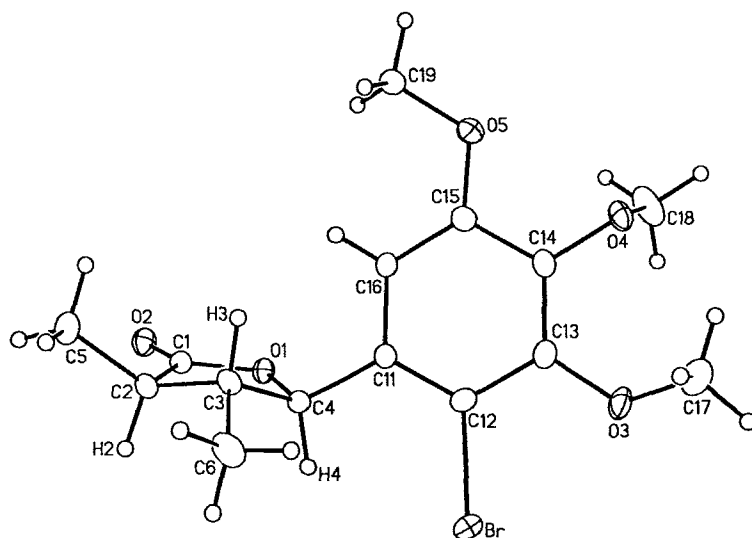


**Figure 2.** Alternate view of the molecule more clearly emphasizing the stereochemistry of the dimethyl-dihydrofuranone group.

### List of Tables

**Table 1.** Crystallographic Experimental Details

**Table 2.** Atomic Coordinates and Equivalent Isotropic Displacement Parameters

**Table 3.** Selected Interatomic Distances

**Table 4.** Selected Interatomic Angles

**Table 5.** Torsional Angles

**Table 6.** Anisotropic Displacement Parameters

**Table 7.** Derived Atomic Coordinates and Displacement Parameters for Hydrogen Atoms

**Table 1.** Crystallographic Experimental Details*A. Crystal Data*

formula	C <sub>15</sub> H <sub>19</sub> BrO <sub>5</sub>
formula weight	359.21
crystal dimensions (mm)	0.58 × 0.46 × 0.39
crystal system	monoclinic
space group	<i>P</i> 2 <sub>1</sub> / <i>n</i> (an alternate setting of <i>P</i> 2 <sub>1</sub> / <i>c</i> [No. 14])
unit cell parameters <sup>a</sup>	
<i>a</i> (Å)	9.2892 (8)
<i>b</i> (Å)	10.5046 (9)
<i>c</i> (Å)	16.1275 (14)
β (deg)	96.1980 (10)
<i>V</i> (Å <sup>3</sup> )	1564.5 (2)
<i>Z</i>	4
ρ <sub>calcd</sub> (g cm <sup>-3</sup> )	1.525
μ (mm <sup>-1</sup> )	2.645

*B. Data Collection and Refinement Conditions*

diffractometer	Bruker PLATFORM/SMART 1000 CCD <sup>b</sup>
radiation (λ [Å])	graphite-monochromated Mo Kα (0.71073)
temperature (°C)	-80
scan type	ω scans (0.3°) (20 s exposures)
data collection 2θ limit (deg)	52.86
total data collected	11751 (-11 ≤ <i>h</i> ≤ 11, -13 ≤ <i>k</i> ≤ 13, -20 ≤ <i>l</i> ≤ 20)
independent reflections	3215 ( <i>R</i> <sub>int</sub> = 0.0245)
number of observed reflections ( <i>NO</i> )	2739 [ <i>F</i> <sub>o</sub> <sup>2</sup> ≥ 2α( <i>F</i> <sub>o</sub> <sup>2</sup> )]
structure solution method	direct methods ( <i>SHELXS-86</i> <sup>c</sup> )
refinement method	full-matrix least-squares on <i>F</i> <sup>2</sup> ( <i>SHELXL-93</i> <sup>d</sup> )
absorption correction method	multi-scan ( <i>SADABS</i> )
range of transmission factors	0.4252–0.3091
data/restraints/parameters	3215 [ <i>F</i> <sub>o</sub> <sup>2</sup> ≥ -3α( <i>F</i> <sub>o</sub> <sup>2</sup> )] / 0 / 190
goodness-of-fit ( <i>S</i> ) <sup>e</sup>	1.072 [ <i>F</i> <sub>o</sub> <sup>2</sup> ≥ -3α( <i>F</i> <sub>o</sub> <sup>2</sup> )]
final <i>R</i> indices <sup>f</sup>	
<i>R</i> <sub>1</sub> [ <i>F</i> <sub>o</sub> <sup>2</sup> ≥ 2α( <i>F</i> <sub>o</sub> <sup>2</sup> )]	0.0323
<i>wR</i> <sub>2</sub> [ <i>F</i> <sub>o</sub> <sup>2</sup> ≥ -3α( <i>F</i> <sub>o</sub> <sup>2</sup> )]	0.0876
largest difference peak and hole	0.492 and -0.413 e Å <sup>-3</sup>

<sup>a</sup>Obtained from least-squares refinement of 7115 reflections with 4.64° < 2θ < 52.68°.

<sup>b</sup>Programs for diffractometer operation, data collection, data reduction and absorption correction were those supplied by Bruker.

(continued)

**Table 1.** Crystallographic Experimental Details (continued)

<sup>c</sup>Sheldrick, G. M. *Acta Crystallogr.* **1990**, *A46*, 467–473.

<sup>d</sup>Sheldrick, G. M. *SHELXL-93*. Program for crystal structure determination. University of Göttingen, Germany, 1993.

$eS = [\sum w(F_o^2 - F_c^2)^2 / (n - p)]^{1/2}$  ( $n$  = number of data;  $p$  = number of parameters varied;  $w = [\sigma^2(F_o^2) + (0.0481P)^2 + 0.5690P]^{-1}$  where  $P = [\text{Max}(F_o^2, 0) + 2F_c^2]/3$ ).

$fR_1 = \sum ||F_o| - |F_c|| / \sum |F_o|$ ;  $wR_2 = [\sum w(F_o^2 - F_c^2)^2 / \sum w(F_o^4)]^{1/2}$ .

**Table 2.** Atomic Coordinates and Equivalent Isotropic Displacement Parameters

Atom	<i>x</i>	<i>y</i>	<i>z</i>	$U_{eq}, \text{Å}^2$
Br	0.18953(3)	0.41740(3)	0.234375(16)	0.05295(12)*
O1	0.06351(16)	0.09658(13)	0.37778(9)	0.0329(3)*
O2	0.0760(2)	-0.09420(14)	0.43684(11)	0.0446(4)*
O3	-0.0462(2)	0.60473(15)	0.24138(10)	0.0494(4)*
O4	-0.25809(18)	0.62012(15)	0.35530(10)	0.0418(4)*
O5	-0.26458(17)	0.44493(16)	0.47356(11)	0.0434(4)*
C1	0.1273(2)	0.0103(2)	0.43144(12)	0.0332(4)*
C2	0.2645(2)	0.0643(2)	0.47665(13)	0.0352(5)*
C3	0.2470(2)	0.2075(2)	0.46259(13)	0.0335(4)*
C4	0.1488(2)	0.21395(19)	0.37961(12)	0.0315(4)*
C5	0.2926(3)	0.0210(3)	0.56725(15)	0.0521(6)*
C6	0.3886(2)	0.2780(3)	0.46048(18)	0.0529(6)*
C11	0.0445(2)	0.32448(19)	0.37066(12)	0.0307(4)*
C12	0.0467(2)	0.4181(2)	0.31045(13)	0.0337(4)*
C13	-0.0536(2)	0.5185(2)	0.30396(12)	0.0350(5)*
C14	-0.1580(2)	0.5229(2)	0.35908(13)	0.0345(5)*
C15	-0.1598(2)	0.43029(19)	0.42174(13)	0.0338(5)*
C16	-0.0599(2)	0.3321(2)	0.42683(13)	0.0324(4)*
C17	-0.0587(4)	0.7367(3)	0.2588(2)	0.0653(8)*
C18	-0.3882(3)	0.5931(3)	0.3042(2)	0.0692(9)*
C19	-0.2560(2)	0.3655(2)	0.54526(14)	0.0403(5)*

Anisotropically-refined atoms are marked with an asterisk (\*). The form of the anisotropic displacement parameter is:  $\exp[-2\pi^2(h^2a^{*2}U_{11} + k^2b^{*2}U_{22} + l^2c^{*2}U_{33} + 2klb^{*c^*}U_{23} + 2hla^{*c^*}U_{13} + 2hka^{*b^*}U_{12})]$ .

**Table 3.** Selected Interatomic Distances (Å)

Atom1	Atom2	Distance	Atom1	Atom2	Distance
Br	C12	1.902(2)	C2	C3	1.528(3)
O1	C1	1.346(2)	C2	C5	1.526(3)
O1	C4	1.464(2)	C3	C4	1.538(3)
O2	C1	1.203(3)	C3	C6	1.512(3)
O3	C13	1.364(3)	C4	C11	1.509(3)
O3	C17	1.421(3)	C11	C12	1.384(3)
O4	C14	1.378(3)	C11	C16	1.399(3)
O4	C18	1.416(3)	C12	C13	1.404(3)
O5	C15	1.358(3)	C13	C14	1.385(3)
O5	C19	1.421(3)	C14	C15	1.404(3)
C1	C2	1.509(3)	C15	C16	1.384(3)

**Table 4.** Selected Interatomic Angles (deg)

Atom1	Atom2	Atom3	Angle	Atom1	Atom2	Atom3	Angle
C1	O1	C4	110.77(15)	C4	C11	C12	123.77(19)
C13	O3	C17	119.3(2)	C4	C11	C16	117.70(18)
C14	O4	C18	114.00(18)	C12	C11	C16	118.53(19)
C15	O5	C19	116.94(16)	Br	C12	C11	120.96(16)
O1	C1	O2	120.7(2)	Br	C12	C13	117.30(15)
O1	C1	C2	110.34(18)	C11	C12	C13	121.7(2)
O2	C1	C2	128.92(19)	O3	C13	C12	117.9(2)
C1	C2	C3	103.19(16)	O3	C13	C14	123.2(2)
C1	C2	C5	113.5(2)	C12	C13	C14	118.87(19)
C3	C2	C5	116.13(19)	O4	C14	C13	120.83(19)
C2	C3	C4	102.47(16)	O4	C14	C15	119.0(2)
C2	C3	C6	114.00(18)	C13	C14	C15	120.14(19)
C4	C3	C6	113.26(19)	O5	C15	C14	115.43(18)
O1	C4	C3	104.46(16)	O5	C15	C16	124.63(19)
O1	C4	C11	107.82(15)	C14	C15	C16	119.9(2)
C3	C4	C11	115.57(17)	C11	C16	C15	120.77(19)

**Table 5.** Torsional Angles (deg)

Atom1	Atom2	Atom3	Atom4	Angle	Atom1	Atom2	Atom3	Atom4	Angle
C4	O1	C1	O2	-177.44(19)	O1	C4	C11	C16	54.3(2)
C4	O1	C1	C2	0.9(2)	C3	C4	C11	C12	117.8(2)
C1	O1	C4	C3	-18.9(2)	C3	C4	C11	C16	-62.1(2)
C1	O1	C4	C11	-142.36(17)	C4	C11	C12	Br	-2.1(3)
C17	O3	C13	C12	-136.2(3)	C4	C11	C12	C13	179.28(19)
C17	O3	C13	C14	46.1(3)	C16	C11	C12	Br	177.83(15)
C18	O4	C14	C13	91.7(3)	C16	C11	C12	C13	-0.8(3)
C18	O4	C14	C15	-90.5(3)	C4	C11	C16	C15	-179.40(18)
C19	O5	C15	C14	-170.38(19)	C12	C11	C16	C15	0.7(3)
C19	O5	C15	C16	10.3(3)	Br	C12	C13	O3	3.1(3)
O1	C1	C2	C3	17.5(2)	Br	C12	C13	C14	-179.16(15)
O1	C1	C2	C5	144.0(2)	C11	C12	C13	O3	-178.24(19)
O2	C1	C2	C3	-164.3(2)	C11	C12	C13	C14	-0.5(3)
O2	C1	C2	C5	-37.8(3)	O3	C13	C14	O4	-2.7(3)
C1	C2	C3	C4	-27.4(2)	O3	C13	C14	C15	179.53(19)
C1	C2	C3	C6	-150.1(2)	C12	C13	C14	O4	179.61(18)
C5	C2	C3	C4	-152.19(19)	C12	C13	C14	C15	1.9(3)
C5	C2	C3	C6	85.0(3)	O4	C14	C15	O5	0.9(3)
C2	C3	C4	O1	28.4(2)	O4	C14	C15	C16	-179.79(19)
C2	C3	C4	C11	146.64(18)	C13	C14	C15	O5	178.64(18)
C6	C3	C4	O1	151.63(18)	C13	C14	C15	C16	-2.0(3)
C6	C3	C4	C11	-90.1(2)	O5	C15	C16	C11	179.99(19)
O1	C4	C11	C12	-125.8(2)	C14	C15	C16	C11	0.7(3)



**Table 6. Anisotropic Displacement Parameters ( $U_{ij}$ , Å<sup>2</sup>)**

Atom	$U_{11}$	$U_{22}$	$U_{33}$	$U_{23}$	$U_{13}$	$U_{12}$
Br	0.05578(18)	0.06185(19)	0.04474(16)	0.01891(11)	0.02150(12)	0.00932(12)
O1	0.0340(8)	0.0347(8)	0.0286(7)	-0.0001(6)	-0.0036(6)	-0.0002(6)
O2	0.0528(10)	0.0347(9)	0.0456(9)	0.0006(7)	0.0022(8)	0.0017(7)
O3	0.0778(13)	0.0387(9)	0.0310(8)	0.0082(7)	0.0027(8)	0.0092(8)
O4	0.0428(9)	0.0405(8)	0.0392(8)	-0.0032(7)	-0.0079(7)	0.0128(7)
O5	0.0342(8)	0.0505(9)	0.0465(9)	0.0061(8)	0.0094(7)	0.0104(7)
C1	0.0375(11)	0.0351(11)	0.0271(10)	-0.0025(8)	0.0043(8)	0.0069(9)
C2	0.0313(10)	0.0422(12)	0.0314(10)	-0.0024(9)	0.0000(8)	0.0097(9)
C3	0.0271(10)	0.0400(11)	0.0323(10)	-0.0056(9)	-0.0021(8)	0.0054(8)
C4	0.0290(10)	0.0360(11)	0.0300(10)	0.0012(8)	0.0048(8)	0.0008(8)
C5	0.0519(15)	0.0654(17)	0.0360(12)	0.0073(12)	-0.0091(11)	0.0118(13)
C6	0.0288(12)	0.0565(15)	0.0718(18)	-0.0058(13)	-0.0023(11)	-0.0028(10)
C11	0.0281(10)	0.0344(10)	0.0287(10)	0.0000(8)	-0.0013(8)	-0.0008(8)
C12	0.0327(10)	0.0412(11)	0.0271(10)	0.0006(8)	0.0029(8)	-0.0024(9)
C13	0.0403(12)	0.0360(11)	0.0266(10)	0.0010(8)	-0.0068(8)	-0.0001(9)
C14	0.0347(11)	0.0348(11)	0.0317(10)	-0.0023(9)	-0.0074(8)	0.0052(9)
C15	0.0269(10)	0.0392(11)	0.0341(11)	-0.0025(9)	-0.0020(8)	0.0011(8)
C16	0.0287(10)	0.0360(11)	0.0321(10)	0.0050(8)	0.0013(8)	0.0004(8)
C17	0.091(2)	0.0423(14)	0.0654(18)	0.0033(13)	0.0190(16)	-0.0121(14)
C18	0.0499(16)	0.0708(19)	0.079(2)	-0.0167(16)	-0.0269(15)	0.0238(14)
C19	0.0315(11)	0.0493(13)	0.0406(12)	0.0016(10)	0.0065(9)	0.0008(10)

The form of the anisotropic displacement parameter is:

$$\exp[-2\pi^2(h^2a^2U_{11} + k^2b^2U_{22} + l^2c^2U_{33} + 2klb*c*U_{23} + 2hla*c*U_{13} + 2hka*b*U_{12})]$$

**Table 7.** Derived Atomic Coordinates and Displacement Parameters for Hydrogen Atoms

Atom	<i>x</i>	<i>y</i>	<i>z</i>	$U_{eq}, \text{\AA}^2$
H2	0.3475	0.0350	0.4469	0.042
H3	0.1941	0.2443	0.5078	0.040
H4	0.2096	0.2141	0.3321	0.038
H5A	0.3092	-0.0712	0.5691	0.063
H5B	0.2084	0.0414	0.5965	0.063
H5C	0.3782	0.0648	0.5943	0.063
H6A	0.4428	0.2764	0.5161	0.064
H6B	0.3689	0.3664	0.4436	0.064
H6C	0.4458	0.2368	0.4204	0.064
H16	-0.0623	0.2691	0.4689	0.039
H17A	-0.0487	0.7860	0.2082	0.078
H17B	0.0176	0.7614	0.3026	0.078
H17C	-0.1537	0.7535	0.2777	0.078
H18A	-0.4537	0.6662	0.3043	0.083
H18B	-0.4345	0.5181	0.3259	0.083
H18C	-0.3665	0.5763	0.2471	0.083
H19A	-0.3366	0.3849	0.5777	0.048
H19B	-0.1640	0.3808	0.5796	0.048
H19C	-0.2614	0.2761	0.5279	0.048

# Appendix B Structure Report for Lactone 21 (Chapter 2)

XCL Code: DGH0502

Date: 6 April 2005

Compound: (3*RS*,4*SR*,5*SR*)-5-(2-Bromo-3,4,5-trimethoxyphenyl)-3,4-dimethyldihydrofuran-2(3*H*)-one

Formula: C<sub>15</sub>H<sub>19</sub>BrO<sub>5</sub>

Supervisor: D. G. Hall

Crystallographer:

R. McDonald

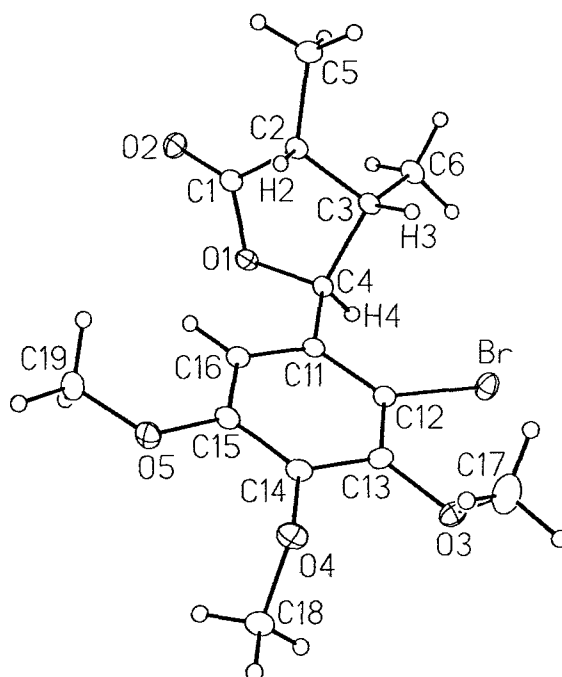


**Figure 1.** Perspective view of the (3*R*,4*S*,5*S*)-5-(2-bromo-3,4,5-trimethoxyphenyl)-3,4-dimethyldihydrofuran-2(3*H*)-one molecule showing the atom labelling scheme. Non-hydrogen atoms are represented by Gaussian ellipsoids at the 20% probability level. Hydrogen atoms are shown with arbitrarily small thermal parameters. The 3*S*,4*R*,5*R* enantiomer is also present in the crystal lattice.

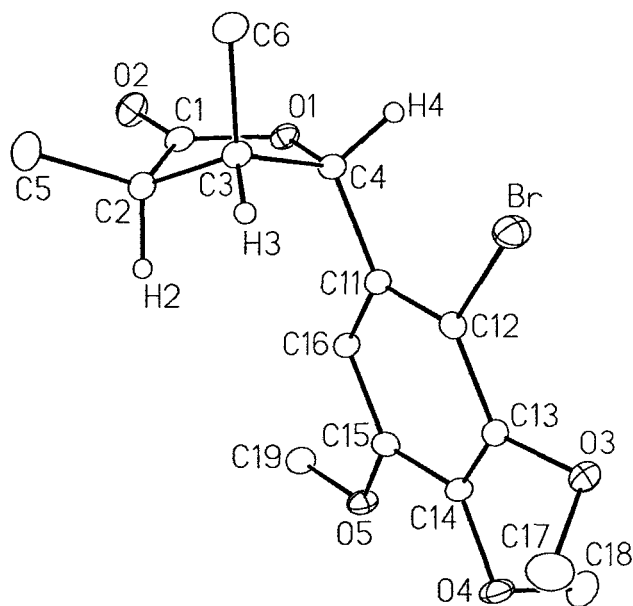


**Figure 2.** Alternate view of the molecule more clearly emphasizing the stereochemistry of the dimethyldihydrofuranone group.

### List of Tables

**Table 1.** Crystallographic Experimental Details

**Table 2.** Atomic Coordinates and Equivalent Isotropic Displacement Parameters

**Table 3.** Selected Interatomic Distances

**Table 4.** Selected Interatomic Angles

**Table 5.** Torsional Angles

**Table 6.** Anisotropic Displacement Parameters

**Table 7.** Derived Atomic Coordinates and Displacement Parameters for Hydrogen Atoms

**Table 1.** Crystallographic Experimental Details*A. Crystal Data*

formula	C <sub>15</sub> H <sub>19</sub> BrO <sub>5</sub>
formula weight	359.21
crystal dimensions (mm)	0.38 × 0.28 × 0.24
crystal system	monoclinic
space group	<i>P</i> 2 <sub>1</sub> / <i>c</i> (No. 14)
unit cell parameters <sup>a</sup>	
<i>a</i> (Å)	7.9639 (3)
<i>b</i> (Å)	23.3702 (8)
<i>c</i> (Å)	8.5236 (3)
β (deg)	99.8561 (6)
<i>V</i> (Å <sup>3</sup> )	1562.98 (10)
<i>Z</i>	4
ρ <sub>calcd</sub> (g cm <sup>-3</sup> )	1.527
μ (mm <sup>-1</sup> )	2.648

*B. Data Collection and Refinement Conditions*

diffractometer	Bruker PLATFORM/SMART 1000 CCD <sup>b</sup>
radiation (λ [Å])	graphite-monochromated Mo Kα (0.71073)
temperature (°C)	-80
scan type	ω scans (0.2°) (20 s exposures)
data collection 2θ limit (deg)	52.74
total data collected	11429 (-9 ≤ <i>h</i> ≤ 9, -29 ≤ <i>k</i> ≤ 29, -10 ≤ <i>l</i> ≤ 10)
independent reflections	3190 ( <i>R</i> <sub>int</sub> = 0.0223)
number of observed reflections ( <i>NO</i> )	2830 [ <i>F</i> <sub>o</sub> <sup>2</sup> ≥ 2α( <i>F</i> <sub>o</sub> <sup>2</sup> )]
structure solution method	direct methods ( <i>SHELXS-86</i> <sup>c</sup> )
refinement method	full-matrix least-squares on <i>F</i> <sup>2</sup> ( <i>SHELXL-93</i> <sup>d</sup> )
absorption correction method	multi-scan ( <i>SADABS</i> )
range of transmission factors	0.5690–0.4327
data/restraints/parameters	3190 [ <i>F</i> <sub>o</sub> <sup>2</sup> ≥ -3α( <i>F</i> <sub>o</sub> <sup>2</sup> )] / 0 / 190
goodness-of-fit ( <i>S</i> ) <sup>e</sup>	1.036 [ <i>F</i> <sub>o</sub> <sup>2</sup> ≥ -3α( <i>F</i> <sub>o</sub> <sup>2</sup> )]
final <i>R</i> indices <sup>f</sup>	
<i>R</i> <sub>1</sub> [ <i>F</i> <sub>o</sub> <sup>2</sup> ≥ 2α( <i>F</i> <sub>o</sub> <sup>2</sup> )]	0.0252
<i>wR</i> <sub>2</sub> [ <i>F</i> <sub>o</sub> <sup>2</sup> ≥ -3α( <i>F</i> <sub>o</sub> <sup>2</sup> )]	0.0677
largest difference peak and hole	0.470 and -0.339 e Å <sup>-3</sup>

<sup>a</sup>Obtained from least-squares refinement of 7661 reflections with 5.16° < 2θ < 52.74°.

<sup>b</sup>Programs for diffractometer operation, data collection, data reduction and absorption correction were those supplied by Bruker.

(continued)

**Table 1.** Crystallographic Experimental Details (continued)

<sup>c</sup>Sheldrick, G. M. *Acta Crystallogr.* **1990**, *A46*, 467–473.

<sup>d</sup>Sheldrick, G. M. *SHELXL-93*. Program for crystal structure determination. University of Göttingen, Germany, 1993.

$eS = [\sum w(F_o^2 - F_c^2)^2 / (n - p)]^{1/2}$  ( $n$  = number of data;  $p$  = number of parameters varied;  $w = [\sigma^2(F_o^2) + (0.0386P)^2 + 0.5019P]^{-1}$  where  $P = [\text{Max}(F_o^2, 0) + 2F_c^2]/3$ ).

$fR_1 = \sum ||F_o| - |F_c|| / \sum |F_o|$ ;  $wR_2 = [\sum w(F_o^2 - F_c^2)^2 / \sum w(F_o^4)]^{1/2}$ .

**Table 2.** Atomic Coordinates and Equivalent Isotropic Displacement Parameters

Atom	<i>x</i>	<i>y</i>	<i>z</i>	<i>U</i> <sub>eq</sub> , Å <sup>2</sup>
Br	-0.26165(2)	0.213621(8)	-0.01483(2)	0.03864(8)*
O1	-0.23468(15)	0.04045(5)	0.23378(14)	0.0287(3)*
O2	-0.19947(19)	-0.00677(6)	0.46431(17)	0.0420(3)*
O3	0.06609(17)	0.22365(6)	-0.14428(16)	0.0365(3)*
O4	0.34886(16)	0.15328(6)	-0.09131(16)	0.0388(3)*
O5	0.34604(15)	0.05637(6)	0.07201(15)	0.0343(3)*
C1	-0.1927(2)	0.03758(7)	0.3949(2)	0.0296(4)*
C2	-0.1428(2)	0.09634(7)	0.4596(2)	0.0289(4)*
C3	-0.2439(2)	0.13505(7)	0.3325(2)	0.0273(3)*
C4	-0.2359(2)	0.09973(7)	0.1808(2)	0.0256(3)*
C5	-0.1644(3)	0.10539(9)	0.6315(2)	0.0423(5)*
C6	-0.4281(2)	0.14482(8)	0.3545(2)	0.0364(4)*
C11	-0.0802(2)	0.11277(7)	0.10672(18)	0.0250(3)*
C12	-0.0736(2)	0.16276(7)	0.01988(19)	0.0260(3)*
C13	0.0685(2)	0.17646(7)	-0.04811(19)	0.0274(3)*
C14	0.2065(2)	0.13957(8)	-0.0277(2)	0.0291(4)*
C15	0.2036(2)	0.08940(7)	0.0605(2)	0.0278(4)*
C16	0.0606(2)	0.07610(7)	0.1271(2)	0.0266(3)*
C17	0.1669(3)	0.27011(10)	-0.0725(3)	0.0555(6)*
C18	0.3495(3)	0.12830(10)	-0.2433(2)	0.0465(5)*
C19	0.3461(2)	0.00356(8)	0.1554(2)	0.0367(4)*

Anisotropically-refined atoms are marked with an asterisk (\*). The form of the anisotropic displacement parameter is:  $\exp[-2\pi^2(h^2a^{*2}U_{11} + k^2b^{*2}U_{22} + l^2c^{*2}U_{33} + 2klb^{*c^*}U_{23} + 2hla^{*c^*}U_{13} + 2hka^{*b^*}U_{12})]$ .

**Table 3.** Selected Interatomic Distances (Å)

Atom1	Atom2	Distance	Atom1	Atom2	Distance
Br	C12	1.8951(16)	C2	C3	1.530(2)
O1	C1	1.358(2)	C2	C5	1.519(2)
O1	C4	1.457(2)	C3	C4	1.545(2)
O2	C1	1.199(2)	C3	C6	1.528(2)
O3	C13	1.372(2)	C4	C11	1.515(2)
O3	C17	1.425(3)	C11	C12	1.389(2)
O4	C14	1.3756(19)	C11	C16	1.399(2)
O4	C18	1.422(2)	C12	C13	1.394(2)
O5	C15	1.362(2)	C13	C14	1.385(2)
O5	C19	1.424(2)	C14	C15	1.395(3)
C1	C2	1.508(2)	C15	C16	1.391(2)

**Table 4.** Selected Interatomic Angles (deg)

Atom1	Atom2	Atom3	Angle	Atom1	Atom2	Atom3	Angle
C1	O1	C4	110.37(12)	C4	C11	C12	119.98(15)
C13	O3	C17	114.02(15)	C4	C11	C16	121.40(15)
C14	O4	C18	113.28(15)	C12	C11	C16	118.60(15)
C15	O5	C19	117.12(13)	Br	C12	C11	120.64(12)
O1	C1	O2	121.17(16)	Br	C12	C13	117.84(13)
O1	C1	C2	109.20(14)	C11	C12	C13	121.50(15)
O2	C1	C2	129.63(17)	O3	C13	C12	120.25(15)
C1	C2	C3	101.87(14)	O3	C13	C14	120.33(15)
C1	C2	C5	114.42(15)	C12	C13	C14	119.23(16)
C3	C2	C5	117.88(15)	O4	C14	C13	119.71(16)
C2	C3	C4	100.65(13)	O4	C14	C15	119.95(16)
C2	C3	C6	113.69(15)	C13	C14	C15	120.32(15)
C4	C3	C6	111.12(14)	O5	C15	C14	115.10(15)
O1	C4	C3	104.32(13)	O5	C15	C16	125.03(16)
O1	C4	C11	110.98(13)	C14	C15	C16	119.87(16)
C3	C4	C11	113.27(13)	C11	C16	C15	120.48(16)

**Table 5.** Torsional Angles (deg)

Atom1	Atom2	Atom3	Atom4	Angle	Atom1	Atom2	Atom3	Atom4	Angle
C4	O1	C1	O2	173.10(16)	O1	C4	C11	C16	-14.8(2)
C4	O1	C1	C2	-6.42(17)	C3	C4	C11	C12	-76.20(19)
C1	O1	C4	C3	-17.15(16)	C3	C4	C11	C16	102.12(18)
C1	O1	C4	C11	105.17(15)	C4	C11	C12	Br	-2.6(2)
C17	O3	C13	C12	106.9(2)	C4	C11	C12	C13	179.16(15)
C17	O3	C13	C14	-78.1(2)	C16	C11	C12	Br	179.00(12)
C18	O4	C14	C13	-95.2(2)	C16	C11	C12	C13	0.8(2)
C18	O4	C14	C15	86.5(2)	C4	C11	C16	C15	-178.81(15)
C19	O5	C15	C14	-177.50(15)	C12	C11	C16	C15	-0.5(2)
C19	O5	C15	C16	1.6(2)	Br	C12	C13	O3	-3.7(2)
O1	C1	C2	C3	27.32(17)	Br	C12	C13	C14	-178.68(12)
O1	C1	C2	C5	155.66(15)	C11	C12	C13	O3	174.57(15)
O2	C1	C2	C3	-152.15(18)	C11	C12	C13	C14	-0.4(2)
O2	C1	C2	C5	-23.8(3)	O3	C13	C14	O4	6.4(2)
C1	C2	C3	C4	-35.30(15)	O3	C13	C14	C15	-175.26(15)
C1	C2	C3	C6	83.57(17)	C12	C13	C14	O4	-178.59(15)
C5	C2	C3	C4	-161.40(15)	C12	C13	C14	C15	-0.3(2)
C5	C2	C3	C6	-42.5(2)	O4	C14	C15	O5	-1.9(2)
C2	C3	C4	O1	32.58(15)	O4	C14	C15	C16	178.90(15)
C2	C3	C4	C11	-88.22(16)	C13	C14	C15	O5	179.75(15)
C6	C3	C4	O1	-88.13(16)	C13	C14	C15	C16	0.6(3)
C6	C3	C4	C11	151.06(15)	O5	C15	C16	C11	-179.29(15)
O1	C4	C11	C12	166.84(14)	C14	C15	C16	C11	-0.2(2)



**Table 6.** Anisotropic Displacement Parameters ( $U_{ij}$ , Å<sup>2</sup>)

Atom	$U_{11}$	$U_{22}$	$U_{33}$	$U_{23}$	$U_{13}$	$U_{12}$
Br	0.03048(11)	0.03827(13)	0.04806(13)	0.01041(8)	0.00921(8)	0.00584(7)
O1	0.0306(6)	0.0264(6)	0.0312(6)	-0.0048(5)	0.0113(5)	-0.0061(5)
O2	0.0524(8)	0.0314(7)	0.0444(8)	0.0059(6)	0.0152(7)	-0.0011(6)
O3	0.0376(7)	0.0367(7)	0.0353(7)	0.0072(5)	0.0068(6)	-0.0086(5)
O4	0.0294(6)	0.0473(8)	0.0440(8)	-0.0020(6)	0.0184(6)	-0.0097(6)
O5	0.0258(6)	0.0365(7)	0.0428(7)	0.0025(6)	0.0125(5)	0.0019(5)
C1	0.0258(8)	0.0319(9)	0.0331(9)	-0.0015(7)	0.0110(7)	-0.0006(7)
C2	0.0286(8)	0.0309(9)	0.0285(9)	-0.0028(7)	0.0082(7)	-0.0024(7)
C3	0.0262(8)	0.0278(9)	0.0295(8)	-0.0041(7)	0.0089(7)	-0.0017(6)
C4	0.0238(8)	0.0257(8)	0.0282(8)	-0.0025(6)	0.0069(6)	-0.0020(6)
C5	0.0542(12)	0.0440(12)	0.0296(10)	-0.0040(8)	0.0095(9)	-0.0034(9)
C6	0.0314(9)	0.0402(11)	0.0405(10)	-0.0059(8)	0.0144(8)	0.0025(8)
C11	0.0245(8)	0.0288(9)	0.0224(8)	-0.0041(6)	0.0057(6)	-0.0034(6)
C12	0.0237(8)	0.0291(9)	0.0249(8)	-0.0025(6)	0.0032(6)	0.0001(6)
C13	0.0286(8)	0.0302(9)	0.0230(8)	-0.0008(7)	0.0036(7)	-0.0071(7)
C14	0.0252(8)	0.0361(10)	0.0274(8)	-0.0038(7)	0.0085(7)	-0.0083(7)
C15	0.0239(8)	0.0317(9)	0.0284(8)	-0.0060(7)	0.0058(7)	-0.0015(6)
C16	0.0258(8)	0.0285(9)	0.0267(8)	-0.0022(7)	0.0078(6)	-0.0024(6)
C17	0.0536(13)	0.0338(11)	0.0756(17)	0.0062(11)	0.0016(12)	-0.0132(10)
C18	0.0456(12)	0.0589(14)	0.0401(11)	0.0058(10)	0.0217(9)	0.0109(10)
C19	0.0315(9)	0.0346(10)	0.0456(11)	0.0016(8)	0.0108(8)	0.0045(7)

The form of the anisotropic displacement parameter is:

$$\exp[-2\pi^2(h^2a^2U_{11} + k^2b^2U_{22} + l^2c^2U_{33} + 2klb*c*U_{23} + 2hla*c*U_{13} + 2hka*b*U_{12})]$$

**Table 7.** Derived Atomic Coordinates and Displacement Parameters for Hydrogen Atoms

Atom	<i>x</i>	<i>y</i>	<i>z</i>	<i>U</i> <sub>eq</sub> , Å <sup>2</sup>
H2	-0.0192	0.1017	0.4546	0.035
H3	-0.1840	0.1725	0.3281	0.033
H4	-0.3411	0.1069	0.1007	0.031
H5A	-0.1259	0.1440	0.6657	0.051
H5B	-0.0964	0.0770	0.6995	0.051
H5C	-0.2848	0.1010	0.6404	0.051
H6A	-0.4295	0.1667	0.4523	0.044
H6B	-0.4841	0.1078	0.3619	0.044
H6C	-0.4888	0.1662	0.2632	0.044
H16	0.0587	0.0419	0.1868	0.032
H17A	0.1589	0.3022	-0.1476	0.067
H17B	0.2860	0.2579	-0.0446	0.067
H17C	0.1252	0.2822	0.0239	0.067
H18A	0.4546	0.1389	-0.2813	0.056
H18B	0.2510	0.1422	-0.3186	0.056
H18C	0.3432	0.0866	-0.2348	0.056
H19A	0.4546	-0.0162	0.1555	0.044
H19B	0.2523	-0.0205	0.1028	0.044
H19C	0.3314	0.0110	0.2654	0.044

## Appendix C Structure Report for Lactone 24 (Chapter 2)

XCL Code: DGH0506

Date: 5 May 2005

Compound: (3*S*,4*R*,5*S*)-5-(2-Bromo-3,4,5-trimethoxyphenyl)-3,4-dimethyldihydrofuran-2(3*H*)-one

Formula: C<sub>15</sub>H<sub>19</sub>BrO<sub>5</sub>

Supervisor: D. G. Hall

Crystallographer:  
M. J. Ferguson

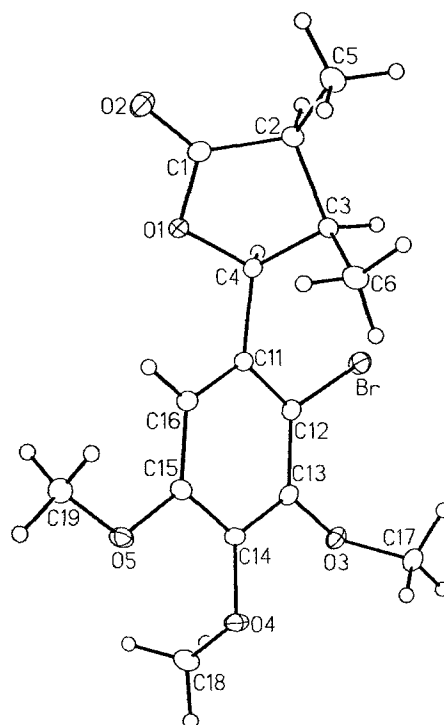


**Figure 1.** Perspective view of the (3*S*,4*R*,5*S*)-5-(2-bromo-3,4,5-trimethoxyphenyl)-3,4-dimethyldihydrofuran-2(3*H*)-one molecule showing the atom labelling scheme. Non-hydrogen atoms are represented by Gaussian ellipsoids at the 20% probability level. Hydrogen atoms are shown with arbitrarily small thermal parameters. The 3*R*, 4*S*, 5*R* enantiomer is also present in the crystal lattice.

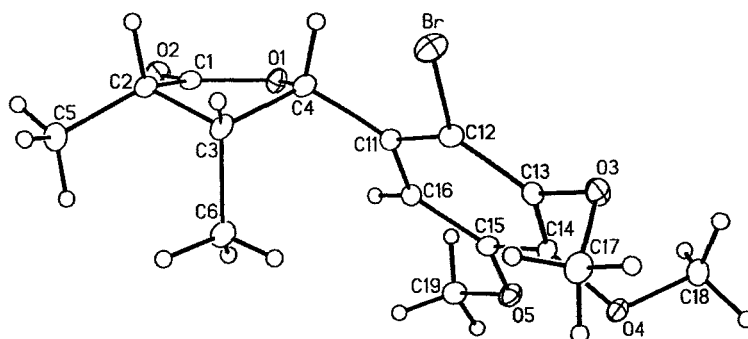


**Figure 2.** Alternate view of the molecule more clearly emphasizing the stereochemistry of the dimethyldihydrofuranone group.

### List of Tables

**Table 1.** Crystallographic Experimental Details

**Table 2.** Atomic Coordinates and Equivalent Isotropic Displacement Parameters

**Table 3.** Selected Interatomic Distances

**Table 4.** Selected Interatomic Angles

**Table 5.** Torsional Angles

**Table 6.** Anisotropic Displacement Parameters

**Table 7.** Derived Atomic Coordinates and Displacement Parameters for Hydrogen Atoms

**Table 1.** Crystallographic Experimental Details

<i>A. Crystal Data</i>	
formula	C <sub>15</sub> H <sub>19</sub> BrO <sub>5</sub>
formula weight	359.21
crystal dimensions (mm)	0.55 × 0.50 × 0.21
crystal system	monoclinic
space group	<i>P</i> 2 <sub>1</sub> / <i>c</i> (No. 14)
unit cell parameters <sup>a</sup>	
<i>a</i> (Å)	10.2249 (6)
<i>b</i> (Å)	9.8448 (6)
<i>c</i> (Å)	15.8781 (10)
β (deg)	105.3820 (10)
<i>V</i> (Å <sup>3</sup> )	1541.07 (16)
<i>Z</i>	4
ρ <sub>calcd</sub> (g cm <sup>-3</sup> )	1.548
μ (mm <sup>-1</sup> )	2.686
<i>B. Data Collection and Refinement Conditions</i>	
diffractometer	Bruker PLATFORM/SMART 1000 CCD <sup>b</sup>
radiation (λ [Å])	graphite-monochromated Mo Kα (0.71073)
temperature (°C)	-80
scan type	ω scans (0.3°) (20 s exposures)
data collection 2θ limit (deg)	52.78
total data collected	11618 (-12 ≤ <i>h</i> ≤ 12, -12 ≤ <i>k</i> ≤ 12, -19 ≤ <i>l</i> ≤ 19)
independent reflections	3154 ( <i>R</i> <sub>int</sub> = 0.0236)
number of observed reflections ( <i>NO</i> )	2830 [ <i>F</i> <sub>o</sub> <sup>2</sup> ≥ 2α( <i>F</i> <sub>o</sub> <sup>2</sup> )]
structure solution method	direct methods ( <i>SHELXS-86</i> <sup>c</sup> )
refinement method	full-matrix least-squares on <i>F</i> <sup>2</sup> ( <i>SHELXL-93</i> <sup>d</sup> )
absorption correction method	multi-scan ( <i>SADABS</i> )
range of transmission factors	0.6024–0.3197
data/restraints/parameters	3154 [ <i>F</i> <sub>o</sub> <sup>2</sup> ≥ -3α( <i>F</i> <sub>o</sub> <sup>2</sup> )] / 0 / 190
goodness-of-fit ( <i>S</i> ) <sup>e</sup>	1.078 [ <i>F</i> <sub>o</sub> <sup>2</sup> ≥ -3α( <i>F</i> <sub>o</sub> <sup>2</sup> )]
final <i>R</i> indices <sup>f</sup>	
<i>R</i> <sub>1</sub> [ <i>F</i> <sub>o</sub> <sup>2</sup> ≥ 2α( <i>F</i> <sub>o</sub> <sup>2</sup> )]	0.0266
<i>wR</i> <sub>2</sub> [ <i>F</i> <sub>o</sub> <sup>2</sup> ≥ -3α( <i>F</i> <sub>o</sub> <sup>2</sup> )]	0.0685
largest difference peak and hole	0.660 and -0.589 e Å <sup>-3</sup>

<sup>a</sup>Obtained from least-squares refinement of 4455 reflections with 5.32° < 2θ < 52.78°.

<sup>b</sup>Programs for diffractometer operation, data collection, data reduction and absorption correction were those supplied by Bruker.

(continued)

**Table 1.** Crystallographic Experimental Details (continued)<sup>c</sup>Sheldrick, G. M. *Acta Crystallogr.* **1990**, *A46*, 467–473.<sup>d</sup>Sheldrick, G. M. *SHELXL-93*. Program for crystal structure determination. University of Göttingen, Germany, 1993.
$$eS = [\sum w(F_o^2 - F_c^2)^2 / (n - p)]^{1/2} \quad (n = \text{number of data; } p = \text{number of parameters varied; } w = [\sigma^2(F_o^2) + (0.0336P)^2 + 0.8303P]^{-1} \text{ where } P = [\text{Max}(F_o^2, 0) + 2F_c^2] / 3).$$

$$fR_1 = \sum |F_o| - |F_c| / \sum |F_o|; \quad wR_2 = [\sum w(F_o^2 - F_c^2)^2 / \sum w(F_o^4)]^{1/2}.$$
**Table 2.** Atomic Coordinates and Equivalent Isotropic Displacement Parameters

Atom	x	y	z	$U_{eq}, \text{Å}^2$
Br	0.42004(2)	0.17530(2)	0.665301(14)	0.03750(8)*
O1	0.04610(12)	0.12166(13)	0.43801(9)	0.0285(3)*
O2	-0.06929(14)	-0.01044(15)	0.33013(9)	0.0378(3)*
O3	0.47498(13)	0.47724(14)	0.67381(8)	0.0312(3)*
O4	0.34498(14)	0.67948(12)	0.56128(9)	0.0326(3)*
O5	0.12099(14)	0.62338(13)	0.43479(9)	0.0316(3)*
C1	0.03617(18)	0.01621(18)	0.38147(12)	0.0272(4)*
C2	0.17099(19)	-0.05507(18)	0.39701(12)	0.0278(4)*
C3	0.27265(18)	0.05276(18)	0.44579(13)	0.0295(4)*
C4	0.18313(17)	0.12950(18)	0.49523(12)	0.0264(4)*
C5	0.1949(2)	-0.1166(2)	0.31479(14)	0.0380(5)*
C6	0.3288(2)	0.1435(2)	0.38581(17)	0.0438(5)*
C11	0.21891(17)	0.27644(18)	0.51652(12)	0.0246(4)*
C12	0.32614(18)	0.31057(18)	0.58744(12)	0.0260(4)*
C13	0.36790(18)	0.44526(18)	0.60415(11)	0.0255(4)*
C14	0.29875(18)	0.54820(17)	0.55036(12)	0.0250(4)*
C15	0.18592(18)	0.51546(18)	0.48128(12)	0.0253(4)*
C16	0.14856(18)	0.38077(18)	0.46393(11)	0.0247(4)*
C17	0.60202(19)	0.4795(2)	0.65055(14)	0.0364(4)*
C18	0.2944(2)	0.7570(2)	0.62181(13)	0.0349(4)*
C19	0.0062(2)	0.5949(2)	0.36286(13)	0.0333(4)*

Anisotropically-refined atoms are marked with an asterisk (\*). The form of the anisotropic displacement parameter is:  $\exp[-2\pi^2(h^2a^{*2}U_{11} + k^2b^{*2}U_{22} + l^2c^{*2}U_{33} + 2klb^{*c^{*}}U_{23} + 2hla^{*c^{*}}U_{13} + 2hka^{*b^{*}}U_{12})]$ .

**Table 3.** Selected Interatomic Distances (Å)

Atom1	Atom2	Distance	Atom1	Atom2	Distance
Br	C12	1.8958(18)	C2	C3	1.543(3)
O1	C1	1.359(2)	C2	C5	1.517(3)
O1	C4	1.456(2)	C3	C4	1.551(3)
O2	C1	1.196(2)	C3	C6	1.525(3)
O3	C13	1.371(2)	C4	C11	1.508(2)
O3	C17	1.442(2)	C11	C12	1.389(3)
O4	C14	1.371(2)	C11	C16	1.397(3)
O4	C18	1.427(2)	C12	C13	1.397(2)
O5	C15	1.362(2)	C13	C14	1.391(3)
O5	C19	1.431(2)	C14	C15	1.402(3)
C1	C2	1.508(3)	C15	C16	1.387(2)

**Table 4.** Selected Interatomic Angles (deg)

Atom1	Atom2	Atom3	Angle	Atom1	Atom2	Atom3	Angle
C1	O1	C4	110.10(14)	C4	C11	C12	120.41(16)
C13	O3	C17	112.21(14)	C4	C11	C16	121.03(16)
C14	O4	C18	114.52(14)	C12	C11	C16	118.52(16)
C15	O5	C19	117.29(14)	Br	C12	C11	120.88(13)
O1	C1	O2	120.93(17)	Br	C12	C13	117.81(14)
O1	C1	C2	110.04(15)	C11	C12	C13	121.31(16)
O2	C1	C2	129.01(17)	O3	C13	C12	120.65(16)
C1	C2	C3	103.11(14)	O3	C13	C14	119.68(16)
C1	C2	C5	113.23(16)	C12	C13	C14	119.66(16)
C3	C2	C5	117.77(16)	O4	C14	C13	120.45(16)
C2	C3	C4	100.36(14)	O4	C14	C15	120.01(16)
C2	C3	C6	113.87(17)	C13	C14	C15	119.43(16)
C4	C3	C6	113.65(15)	O5	C15	C14	115.23(15)
O1	C4	C3	104.94(14)	O5	C15	C16	124.69(17)
O1	C4	C11	109.07(14)	C14	C15	C16	120.08(16)
C3	C4	C11	116.10(14)	C11	C16	C15	120.87(17)

**Table 5. Torsional Angles (deg)**

Atom1	Atom2	Atom3	Atom4	Angle	Atom1	Atom2	Atom3	Atom4	Angle
C4	O1	C1	O2	178.00(17)	O1	C4	C11	C16	-20.1(2)
C4	O1	C1	C2	-0.63(19)	C3	C4	C11	C12	-79.6(2)
C1	O1	C4	C3	21.44(18)	C3	C4	C11	C16	98.1(2)
C1	O1	C4	C11	146.46(14)	C4	C11	C12	Br	-5.6(2)
C17	O3	C13	C12	91.7(2)	C4	C11	C12	C13	174.77(16)
C17	O3	C13	C14	-89.3(2)	C16	C11	C12	Br	176.59(13)
C18	O4	C14	C13	-88.7(2)	C16	C11	C12	C13	-3.0(3)
C18	O4	C14	C15	95.3(2)	C4	C11	C16	C15	-176.89(16)
C19	O5	C15	C14	179.19(15)	C12	C11	C16	C15	0.9(3)
C19	O5	C15	C16	-0.1(2)	Br	C12	C13	O3	1.2(2)
O1	C1	C2	C3	-20.38(19)	Br	C12	C13	C14	-177.80(13)
O1	C1	C2	C5	-148.74(16)	C11	C12	C13	O3	-179.20(15)
O2	C1	C2	C3	161.13(19)	C11	C12	C13	C14	1.8(3)
O2	C1	C2	C5	32.8(3)	O3	C13	C14	O4	6.4(2)
C1	C2	C3	C4	30.98(17)	O3	C13	C14	C15	-177.46(15)
C1	C2	C3	C6	-90.80(18)	C12	C13	C14	O4	-174.57(15)
C5	C2	C3	C4	156.46(17)	C12	C13	C14	C15	1.5(3)
C5	C2	C3	C6	34.7(2)	O4	C14	C15	O5	-6.8(2)
C2	C3	C4	O1	-32.13(17)	O4	C14	C15	C16	172.50(15)
C2	C3	C4	C11	-152.61(16)	C13	C14	C15	O5	177.03(15)
C6	C3	C4	O1	89.81(19)	C13	C14	C15	C16	-3.6(3)
C6	C3	C4	C11	-30.7(2)	O5	C15	C16	C11	-178.30(16)
O1	C4	C11	C12	162.13(15)	C14	C15	C16	C11	2.4(3)



**Table 6.** Anisotropic Displacement Parameters ( $U_{ij}$ , Å<sup>2</sup>)

Atom	$U_{11}$	$U_{22}$	$U_{33}$	$U_{23}$	$U_{13}$	$U_{12}$
Br	0.03194(12)	0.03283(12)	0.04157(13)	0.00949(8)	-0.00105(8)	-0.00061(8)
O1	0.0216(6)	0.0247(6)	0.0393(7)	-0.0048(5)	0.0081(5)	-0.0018(5)
O2	0.0292(7)	0.0459(8)	0.0377(7)	-0.0081(6)	0.0078(6)	-0.0080(6)
O3	0.0240(6)	0.0399(8)	0.0292(7)	-0.0066(6)	0.0061(5)	-0.0059(6)
O4	0.0388(8)	0.0241(7)	0.0397(8)	-0.0080(5)	0.0186(6)	-0.0097(5)
O5	0.0369(7)	0.0218(6)	0.0337(7)	0.0032(5)	0.0051(6)	-0.0005(5)
C1	0.0293(10)	0.0247(9)	0.0303(9)	0.0015(7)	0.0126(8)	-0.0055(7)
C2	0.0309(9)	0.0205(8)	0.0335(10)	0.0019(7)	0.0113(8)	-0.0008(7)
C3	0.0250(9)	0.0212(9)	0.0428(11)	-0.0006(8)	0.0100(8)	0.0007(7)
C4	0.0230(9)	0.0225(8)	0.0333(10)	0.0016(7)	0.0067(7)	-0.0020(7)
C5	0.0410(11)	0.0318(10)	0.0439(12)	-0.0044(9)	0.0159(9)	0.0030(9)
C6	0.0452(12)	0.0305(10)	0.0682(16)	-0.0075(10)	0.0368(12)	-0.0067(9)
C11	0.0232(8)	0.0231(8)	0.0293(9)	-0.0013(7)	0.0099(7)	-0.0020(7)
C12	0.0239(9)	0.0254(9)	0.0287(9)	0.0033(7)	0.0071(7)	0.0012(7)
C13	0.0225(8)	0.0305(9)	0.0248(9)	-0.0046(7)	0.0086(7)	-0.0043(7)
C14	0.0284(9)	0.0214(8)	0.0286(9)	-0.0035(7)	0.0138(7)	-0.0050(7)
C15	0.0278(9)	0.0233(8)	0.0278(9)	0.0017(7)	0.0126(7)	0.0005(7)
C16	0.0244(8)	0.0247(9)	0.0253(9)	-0.0018(7)	0.0072(7)	-0.0012(7)
C17	0.0248(9)	0.0384(11)	0.0463(12)	-0.0067(9)	0.0098(8)	-0.0043(8)
C18	0.0446(12)	0.0262(10)	0.0344(10)	-0.0039(8)	0.0115(9)	0.0015(8)
C19	0.0358(10)	0.0323(10)	0.0301(10)	0.0047(8)	0.0058(8)	0.0002(8)

The form of the anisotropic displacement parameter is:

$$\exp[-2\pi^2(h^2a^2U_{11} + k^2b^2U_{22} + l^2c^2U_{33} + 2klb*c*U_{23} + 2hla*c*U_{13} + 2hka*b*U_{12})]$$

**Table 7.** Derived Atomic Coordinates and Displacement Parameters for Hydrogen Atoms

Atom	<i>x</i>	<i>y</i>	<i>z</i>	$U_{eq}, \text{\AA}^2$
H2	0.1713	-0.1311	0.4388	0.033
H3	0.3493	0.0070	0.4888	0.035
H4	0.1861	0.0798	0.5506	0.032
H5A	0.1227	-0.1820	0.2899	0.046
H5B	0.2828	-0.1632	0.3292	0.046
H5C	0.1948	-0.0445	0.2722	0.046
H6A	0.3912	0.2102	0.4209	0.053
H6B	0.2538	0.1909	0.3451	0.053
H6C	0.3774	0.0877	0.3529	0.053
H16	0.0741	0.3592	0.4156	0.030
H17A	0.6756	0.5022	0.7022	0.044
H17B	0.5978	0.5479	0.6051	0.044
H17C	0.6190	0.3900	0.6286	0.044
H18A	0.3320	0.8491	0.6259	0.042
H18B	0.3213	0.7136	0.6794	0.042
H18C	0.1953	0.7615	0.6017	0.042
H19A	-0.0302	0.6802	0.3342	0.040
H19B	-0.0638	0.5490	0.3842	0.040
H19C	0.0341	0.5361	0.3209	0.040

# Appendix D Structure Report for 3,4-*epi*-15 (Chapter 2)

XCL Code: DGH0507

Date: 11 May 2005

Compound: (3*SR*, 4*SR*, 5*SR*)-5-[2-{1,3-benzodioxol-5-yl}-3,4,5-trimethoxyphenyl]-3,4-dimethyldihydrofuran-2(3*H*)-one

Formula: C<sub>22</sub>H<sub>24</sub>O<sub>7</sub>

Supervisor: D. G. Hall

Crystallographer:

M. J. Ferguson

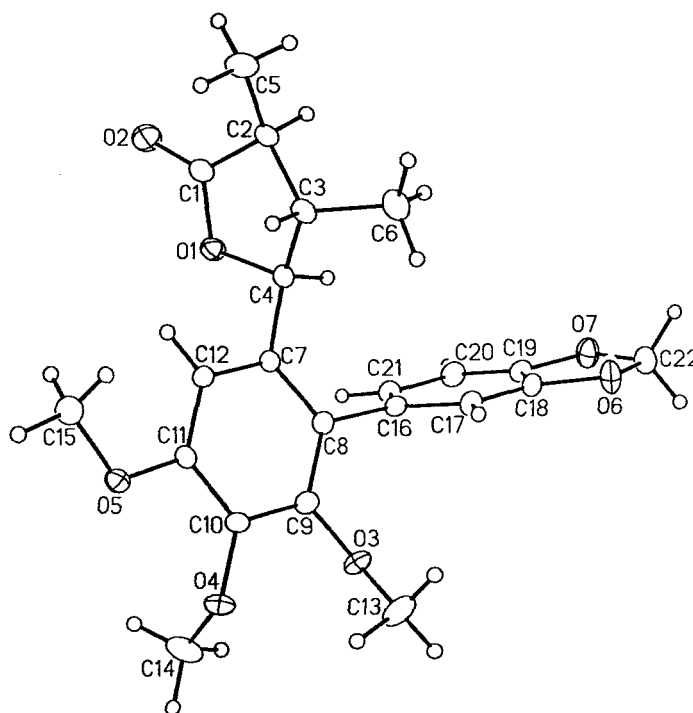


**Figure 1.** Perspective view of the (3*S*, 4*S*, 5*S*)-5-[2-{1,3-benzodioxol-5-yl}-3,4,5-trimethoxyphenyl]-3,4-dimethyldihydrofuran-2(3*H*)-one molecule showing the atom labelling scheme. Non-hydrogen atoms are represented by Gaussian ellipsoids at the 20% probability level. Hydrogen atoms are shown with arbitrarily small thermal parameters. The 3*R*, 4*R*, 5*R* enantiomer is also present in the crystal lattice.

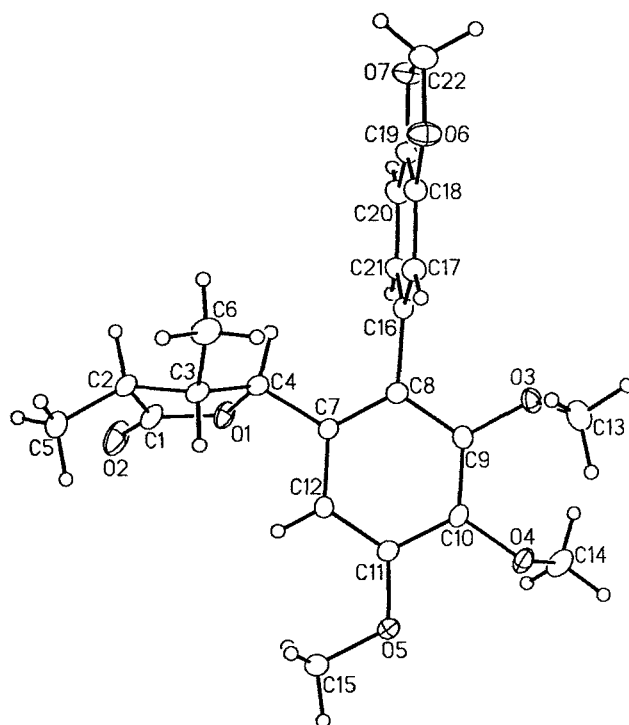


**Figure 2.** Alternate view of the molecule more clearly emphasizing the stereochemistry of the dimethylhydrofuranone group.

### List of Tables

**Table 1.** Crystallographic Experimental Details

**Table 2.** Atomic Coordinates and Equivalent Isotropic Displacement Parameters

**Table 3.** Selected Interatomic Distances

**Table 4.** Selected Interatomic Angles

**Table 5.** Torsional Angles

**Table 6.** Anisotropic Displacement Parameters

**Table 7.** Derived Atomic Coordinates and Displacement Parameters for Hydrogen Atoms

**Table 1.** Crystallographic Experimental Details

<i>A. Crystal Data</i>	
formula	C <sub>22</sub> H <sub>24</sub> O <sub>7</sub>
formula weight	400.41
crystal dimensions (mm)	0.41 × 0.12 × 0.07
crystal system	monoclinic
space group	<i>P</i> 2 <sub>1</sub> / <i>c</i> (No. 14)
unit cell parameters <sup>a</sup>	
<i>a</i> (Å)	7.8495 (9)
<i>b</i> (Å)	33.138 (4)
<i>c</i> (Å)	7.8963 (9)
β (deg)	102.652 (2)
<i>V</i> (Å <sup>3</sup> )	2004.1 (4)
<i>Z</i>	4
ρ <sub>calcd</sub> (g cm <sup>-3</sup> )	1.327
μ (mm <sup>-1</sup> )	0.099
<i>B. Data Collection and Refinement Conditions</i>	
diffractometer	Bruker PLATFORM/SMART 1000 CCD <sup>b</sup>
radiation (λ [Å])	graphite-monochromated Mo Kα (0.71073)
temperature (°C)	-80
scan type	ω scans (0.3°) (20 s exposures)
data collection 2θ limit (deg)	53.00
total data collected	14816 (-9 ≤ <i>h</i> ≤ 9, -41 ≤ <i>k</i> ≤ 41, -9 ≤ <i>l</i> ≤ 9)
independent reflections	4122 ( <i>R</i> <sub>int</sub> = 0.0827)
number of observed reflections ( <i>NO</i> )	2302 [ <i>F</i> <sub>o</sub> <sup>2</sup> ≥ 2α( <i>F</i> <sub>o</sub> <sup>2</sup> )]
structure solution method	direct methods ( <i>SHELXS-86</i> <sup>c</sup> )
refinement method	full-matrix least-squares on <i>F</i> <sup>2</sup> ( <i>SHELXL-93</i> <sup>d</sup> )
absorption correction method	multi-scan ( <i>SADABS</i> )
range of transmission factors	0.9931–0.9606
data/restraints/parameters	4122 [ <i>F</i> <sub>o</sub> <sup>2</sup> ≥ -3α( <i>F</i> <sub>o</sub> <sup>2</sup> )] / 0 / 262
goodness-of-fit ( <i>S</i> ) <sup>e</sup>	0.995 [ <i>F</i> <sub>o</sub> <sup>2</sup> ≥ -3α( <i>F</i> <sub>o</sub> <sup>2</sup> )]
final <i>R</i> indices <sup>f</sup>	
<i>R</i> <sub>1</sub> [ <i>F</i> <sub>o</sub> <sup>2</sup> ≥ 2α( <i>F</i> <sub>o</sub> <sup>2</sup> )]	0.0514
<i>wR</i> <sub>2</sub> [ <i>F</i> <sub>o</sub> <sup>2</sup> ≥ -3α( <i>F</i> <sub>o</sub> <sup>2</sup> )]	0.1322
largest difference peak and hole	0.207 and -0.198 e Å <sup>-3</sup>

<sup>a</sup>Obtained from least-squares refinement of 2296 reflections with 4.92° < 2θ < 51.68°.

<sup>b</sup>Programs for diffractometer operation, data collection, data reduction and absorption correction were those supplied by Bruker.

(continued)

**Table 1.** Crystallographic Experimental Details (continued)

<sup>c</sup>Sheldrick, G. M. *Acta Crystallogr.* **1990**, *A46*, 467–473.

<sup>d</sup>Sheldrick, G. M. *SHELXL-93*. Program for crystal structure determination. University of Göttingen, Germany, 1993.

$$e_S = [\Sigma w(F_o^2 - F_c^2)^2 / (n - p)]^{1/2} \quad (n = \text{number of data; } p = \text{number of parameters varied; } w = [\sigma^2(F_o^2) + (0.0529P)^2 + 0.3500P]^{-1} \text{ where } P = [\text{Max}(F_o^2, 0) + 2F_c^2]/3).$$

$$f_{R1} = \Sigma ||F_o| - |F_c|| / \Sigma |F_o|; \quad wR2 = [\Sigma w(F_o^2 - F_c^2)^2 / \Sigma w(F_o^4)]^{1/2}.$$

**Table 2.** Atomic Coordinates and Equivalent Isotropic Displacement Parameters

Atom	<i>x</i>	<i>y</i>	<i>z</i>	<i>U</i> <sub>eq</sub> , Å <sup>2</sup>
O1	0.2282(2)	0.29112(5)	0.3066(2)	0.0462(5)*
O2	0.3942(3)	0.23642(6)	0.3639(3)	0.0842(8)*
O3	-0.2332(2)	0.42676(5)	0.0429(2)	0.0405(4)*
O4	-0.3248(2)	0.38016(5)	-0.2614(2)	0.0429(5)*
O5	-0.1323(2)	0.31645(5)	-0.3060(2)	0.0414(5)*
O6	0.2841(3)	0.50303(5)	0.4639(2)	0.0537(5)*
O7	0.2328(3)	0.48295(5)	0.7291(2)	0.0527(5)*
C1	0.3841(4)	0.27199(9)	0.3341(4)	0.0523(8)*
C2	0.5270(3)	0.30125(8)	0.3255(3)	0.0447(7)*
C3	0.4285(3)	0.33641(8)	0.2248(3)	0.0386(6)*
C4	0.2506(3)	0.33402(7)	0.2721(3)	0.0347(6)*
C5	0.6712(4)	0.28354(10)	0.2485(4)	0.0707(10)*
C6	0.5146(4)	0.37744(8)	0.2636(4)	0.0519(7)*
C7	0.0970(3)	0.34766(7)	0.1339(3)	0.0309(6)*
C8	0.0030(3)	0.38221(7)	0.1544(3)	0.0319(6)*
C9	-0.1379(3)	0.39319(7)	0.0186(3)	0.0320(6)*
C10	-0.1853(3)	0.36977(7)	-0.1298(3)	0.0324(6)*
C11	-0.0843(3)	0.33618(7)	-0.1507(3)	0.0321(6)*
C12	0.0544(3)	0.32536(7)	-0.0195(3)	0.0327(6)*
C13	-0.2405(4)	0.45819(8)	-0.0821(4)	0.0612(9)*
C14	-0.4885(3)	0.36842(11)	-0.2310(4)	0.0633(9)*
C15	-0.0122(4)	0.28701(9)	-0.3412(3)	0.0528(8)*
C16	0.0536(3)	0.40870(7)	0.3115(3)	0.0320(6)*
C17	0.1414(3)	0.44473(7)	0.2980(3)	0.0364(6)*
C18	0.1937(3)	0.46730(7)	0.4454(3)	0.0362(6)*
C19	0.1621(3)	0.45545(7)	0.6020(3)	0.0372(6)*
C20	0.0749(3)	0.42074(8)	0.6192(3)	0.0417(7)*
C21	0.0195(3)	0.39732(8)	0.4696(3)	0.0366(6)*
C22	0.3024(4)	0.51449(8)	0.6409(4)	0.0508(7)*

Anisotropically-refined atoms are marked with an asterisk (\*). The form of the anisotropic displacement parameter is:  $\exp[-2\pi^2(h^2a^{*2}U_{11} + k^2b^{*2}U_{22} + l^2c^{*2}U_{33} + 2klb^{*c^*}U_{23} + 2hla^{*c^*}U_{13} + 2hka^{*b^*}U_{12})]$ .

**Table 3. Selected Interatomic Distances (Å)**

Atom1	Atom2	Distance	Atom1	Atom2	Distance
O1	C1	1.353(3)	C3	C4	1.524(3)
O1	C4	1.465(3)	C3	C6	1.520(3)
O2	C1	1.201(3)	C4	C7	1.507(3)
O3	C9	1.377(3)	C7	C8	1.391(3)
O3	C13	1.427(3)	C7	C12	1.396(3)
O4	C10	1.378(3)	C8	C9	1.410(3)
O4	C14	1.412(3)	C8	C16	1.500(3)
O5	C11	1.368(3)	C9	C10	1.386(3)
O5	C15	1.425(3)	C10	C11	1.397(3)
O6	C18	1.372(3)	C11	C12	1.376(3)
O6	C22	1.425(3)	C16	C17	1.394(3)
O7	C19	1.379(3)	C16	C21	1.385(3)
O7	C22	1.429(3)	C17	C18	1.369(3)
C1	C2	1.496(4)	C18	C19	1.371(3)
C2	C3	1.523(3)	C19	C20	1.360(3)
C2	C5	1.515(4)	C20	C21	1.400(3)



**Table 4.** Selected Interatomic Angles (deg)

Atom1	Atom2	Atom3	Angle	Atom1	Atom2	Atom3	Angle
C1	O1	C4	110.1(2)	O3	C9	C8	117.5(2)
C9	O3	C13	115.70(18)	O3	C9	C10	121.1(2)
C10	O4	C14	113.91(19)	C8	C9	C10	121.3(2)
C11	O5	C15	115.97(18)	O4	C10	C9	121.3(2)
C18	O6	C22	105.86(19)	O4	C10	C11	119.2(2)
C19	O7	C22	105.34(19)	C9	C10	C11	119.4(2)
O1	C1	O2	120.7(3)	O5	C11	C10	115.8(2)
O1	C1	C2	110.5(2)	O5	C11	C12	124.6(2)
O2	C1	C2	128.8(3)	C10	C11	C12	119.7(2)
C1	C2	C3	102.7(2)	C7	C12	C11	121.0(2)
C1	C2	C5	113.6(3)	C8	C16	C17	118.9(2)
C3	C2	C5	115.2(2)	C8	C16	C21	121.2(2)
C2	C3	C4	102.7(2)	C17	C16	C21	119.9(2)
C2	C3	C6	115.3(2)	C16	C17	C18	117.7(2)
C4	C3	C6	112.8(2)	O6	C18	C17	127.9(2)
O1	C4	C3	104.45(19)	O6	C18	C19	110.0(2)
O1	C4	C7	108.42(18)	C17	C18	C19	122.0(2)
C3	C4	C7	115.9(2)	O7	C19	C18	110.1(2)
C4	C7	C8	121.5(2)	O7	C19	C20	128.1(2)
C4	C7	C12	118.1(2)	C18	C19	C20	121.8(2)
C8	C7	C12	120.3(2)	C19	C20	C21	117.0(2)
C7	C8	C9	118.1(2)	C16	C21	C20	121.6(2)
C7	C8	C16	121.8(2)	O6	C22	O7	108.4(2)
C9	C8	C16	120.0(2)				

**Table 5.** Torsional Angles (deg)

Atom1	Atom2	Atom3	Atom4	Angle	Atom1	Atom2	Atom3	Atom4	Angle
C4	O1	C1	O2	-179.6(3)	C12	C7	C8	C16	-175.2(2)
C4	O1	C1	C2	1.7(3)	C4	C7	C12	C11	179.9(2)
C1	O1	C4	C3	17.6(2)	C8	C7	C12	C11	-2.2(3)
C1	O1	C4	C7	141.8(2)	C7	C8	C9	O3	178.03(19)
C13	O3	C9	C8	121.7(2)	C7	C8	C9	C10	1.7(3)
C13	O3	C9	C10	-61.9(3)	C16	C8	C9	O3	-5.1(3)
C14	O4	C10	C9	-81.6(3)	C16	C8	C9	C10	178.6(2)
C14	O4	C10	C11	101.8(3)	C7	C8	C16	C17	102.2(3)
C15	O5	C11	C10	168.9(2)	C7	C8	C16	C21	-75.7(3)
C15	O5	C11	C12	-10.3(3)	C9	C8	C16	C17	-74.5(3)
C22	O6	C18	C17	178.7(3)	C9	C8	C16	C21	107.5(3)
C22	O6	C18	C19	-2.5(3)	O3	C9	C10	O4	2.8(3)
C18	O6	C22	O7	4.6(3)	O3	C9	C10	C11	179.3(2)
C22	O7	C19	C18	3.5(3)	C8	C9	C10	O4	179.0(2)
C22	O7	C19	C20	-177.6(3)	C8	C9	C10	C11	-4.5(3)
C19	O7	C22	O6	-5.0(3)	O4	C10	C11	O5	1.3(3)
O1	C1	C2	C3	-20.2(3)	O4	C10	C11	C12	-179.5(2)
O1	C1	C2	C5	-145.3(2)	C9	C10	C11	O5	-175.4(2)
O2	C1	C2	C3	161.2(3)	C9	C10	C11	C12	3.9(3)
O2	C1	C2	C5	36.2(4)	O5	C11	C12	C7	178.6(2)
C1	C2	C3	C4	29.4(2)	C10	C11	C12	C7	-0.6(3)
C1	C2	C3	C6	152.5(2)	C8	C16	C17	C18	-176.8(2)
C5	C2	C3	C4	153.4(2)	C21	C16	C17	C18	1.2(3)
C5	C2	C3	C6	-83.5(3)	C8	C16	C21	C20	176.4(2)
C2	C3	C4	O1	-29.0(2)	C17	C16	C21	C20	-1.5(4)
C2	C3	C4	C7	-148.2(2)	C16	C17	C18	O6	178.6(2)
C6	C3	C4	O1	-153.7(2)	C16	C17	C18	C19	0.0(4)
C6	C3	C4	C7	87.1(3)	O6	C18	C19	O7	-0.6(3)
O1	C4	C7	C8	130.4(2)	O6	C18	C19	C20	-179.7(2)
O1	C4	C7	C12	-51.9(3)	C17	C18	C19	O7	178.2(2)
C3	C4	C7	C8	-112.6(3)	C17	C18	C19	C20	-0.8(4)
C3	C4	C7	C12	65.2(3)	O7	C19	C20	C21	-178.4(2)
C4	C7	C8	C9	179.4(2)	C18	C19	C20	C21	0.5(4)
C4	C7	C8	C16	2.6(3)	C19	C20	C21	C16	0.7(4)
C12	C7	C8	C9	1.7(3)					

**Table 6.** Anisotropic Displacement Parameters ( $U_{ij}$ , Å<sup>2</sup>)

Atom	$U_{11}$	$U_{22}$	$U_{33}$	$U_{23}$	$U_{13}$	$U_{12}$
O1	0.0386(10)	0.0398(11)	0.0550(12)	0.0143(9)	-0.0014(8)	-0.0023(8)
O2	0.0703(16)	0.0443(13)	0.116(2)	0.0197(13)	-0.0272(13)	0.0053(12)
O3	0.0501(11)	0.0365(10)	0.0367(10)	0.0090(8)	0.0134(8)	0.0147(9)
O4	0.0343(10)	0.0578(12)	0.0333(9)	0.0097(8)	0.0008(8)	0.0090(9)
O5	0.0414(11)	0.0432(11)	0.0343(10)	-0.0041(8)	-0.0033(8)	0.0058(9)
O6	0.0732(14)	0.0403(11)	0.0470(12)	-0.0055(9)	0.0121(10)	-0.0194(10)
O7	0.0721(14)	0.0444(11)	0.0413(11)	-0.0096(9)	0.0118(9)	-0.0074(10)
C1	0.0450(18)	0.0444(18)	0.0546(18)	0.0056(14)	-0.0173(14)	0.0032(14)
C2	0.0339(15)	0.0502(17)	0.0428(16)	-0.0081(13)	-0.0071(12)	0.0031(13)
C3	0.0340(14)	0.0455(16)	0.0332(14)	-0.0027(12)	0.0003(11)	-0.0046(12)
C4	0.0359(14)	0.0310(14)	0.0340(14)	-0.0012(11)	0.0010(11)	-0.0032(11)
C5	0.0456(18)	0.091(3)	0.067(2)	-0.0221(19)	-0.0062(15)	0.0203(18)
C6	0.0495(17)	0.0564(19)	0.0494(17)	-0.0002(14)	0.0098(13)	-0.0147(15)
C7	0.0305(13)	0.0293(13)	0.0317(13)	0.0025(10)	0.0043(10)	-0.0024(11)
C8	0.0359(14)	0.0295(13)	0.0302(13)	0.0040(11)	0.0073(11)	-0.0027(11)
C9	0.0337(14)	0.0288(13)	0.0355(14)	0.0067(11)	0.0122(11)	0.0010(11)
C10	0.0290(13)	0.0364(14)	0.0302(13)	0.0086(11)	0.0028(11)	0.0024(11)
C11	0.0307(13)	0.0314(14)	0.0323(14)	0.0016(11)	0.0027(11)	-0.0043(11)
C12	0.0319(14)	0.0282(13)	0.0365(14)	0.0012(11)	0.0040(11)	0.0018(11)
C13	0.091(2)	0.0406(17)	0.0529(18)	0.0139(14)	0.0176(17)	0.0224(17)
C14	0.0363(17)	0.105(3)	0.0448(17)	0.0019(17)	0.0014(13)	0.0044(17)
C15	0.0530(18)	0.0594(19)	0.0419(16)	-0.0128(14)	0.0013(13)	0.0078(15)
C16	0.0301(13)	0.0308(13)	0.0347(14)	0.0006(11)	0.0065(11)	0.0023(11)
C17	0.0439(16)	0.0328(14)	0.0327(14)	0.0044(11)	0.0087(11)	-0.0015(12)
C18	0.0386(15)	0.0271(13)	0.0420(15)	0.0010(11)	0.0068(12)	-0.0027(11)
C19	0.0422(15)	0.0347(14)	0.0342(14)	-0.0042(12)	0.0075(12)	0.0077(12)
C20	0.0498(17)	0.0433(16)	0.0358(15)	0.0032(12)	0.0178(12)	0.0023(13)
C21	0.0381(14)	0.0349(14)	0.0378(15)	0.0001(12)	0.0103(11)	-0.0011(12)
C22	0.0549(18)	0.0446(17)	0.0510(18)	-0.0091(14)	0.0075(14)	-0.0053(14)

The form of the anisotropic displacement parameter is:

$$\exp[-2\pi^2(h^2a^2U_{11} + k^2b^2U_{22} + l^2c^2U_{33} + 2klb*c*U_{23} + 2hla*c*U_{13} + 2hka*b*U_{12})]$$

**Table 7.** Derived Atomic Coordinates and Displacement Parameters for Hydrogen Atoms

Atom	<i>x</i>	<i>y</i>	<i>z</i>	<i>U</i> <sub>eq</sub> , Å <sup>2</sup>
H2	0.5794	0.3106	0.4460	0.054
H3	0.4129	0.3308	0.0979	0.046
H4	0.2539	0.3498	0.3807	0.042
H5A	0.7595	0.3043	0.2454	0.085
H5B	0.6221	0.2741	0.1304	0.085
H5C	0.7253	0.2608	0.3201	0.085
H6A	0.6272	0.3775	0.2291	0.062
H6B	0.5333	0.3830	0.3882	0.062
H6C	0.4389	0.3983	0.1986	0.062
H12	0.1222	0.3024	-0.0336	0.039
H13A	-0.3106	0.4806	-0.0535	0.073
H13B	-0.2940	0.4478	-0.1978	0.073
H13C	-0.1221	0.4677	-0.0809	0.073
H14A	-0.5812	0.3767	-0.3294	0.076
H14B	-0.5067	0.3814	-0.1248	0.076
H14C	-0.4911	0.3390	-0.2177	0.076
H15A	-0.0589	0.2746	-0.4546	0.063
H15B	0.0050	0.2662	-0.2510	0.063
H15C	0.0997	0.3000	-0.3421	0.063
H17	0.1641	0.4533	0.1903	0.044
H20	0.0525	0.4127	0.7278	0.050
H21	-0.0429	0.3730	0.4768	0.044
H22A	0.2385	0.5400	0.6483	0.061
H22B	0.4271	0.5189	0.6953	0.061

# Appendix E      Structure Report      for      4-*epi*-15 (Chapter 2)

**XCL Code:** DGH0509

**Date:** 22 June 2005

**Compound:** 5-(2-(1,3-Benzodioxol-5-yl)-3,4,5-trimethoxyphenyl)-3,4-dimethyldihydrofuran-2(3*H*)-one (*racemate*)

**Formula:** C<sub>22</sub>H<sub>24</sub>O<sub>7</sub>

**Supervisor:** D. G. Hall

**Crystallographer:**

R. McDonald

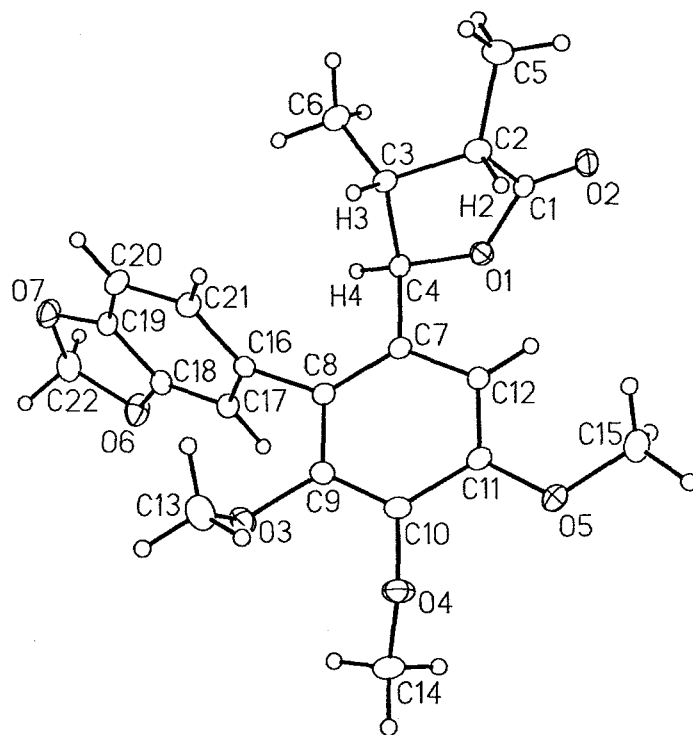


**Figure 1.** Perspective view of the 5-(2-(1,3-benzodioxol-5-yl)-3,4,5-trimethoxyphenyl)-3,4-dimethyldihydrofuran-2(3*H*)-one molecule showing the atom labelling scheme. Non-hydrogen atoms are represented by Gaussian ellipsoids at the 20% probability level. Hydrogen atoms are shown with arbitrarily small thermal parameters.

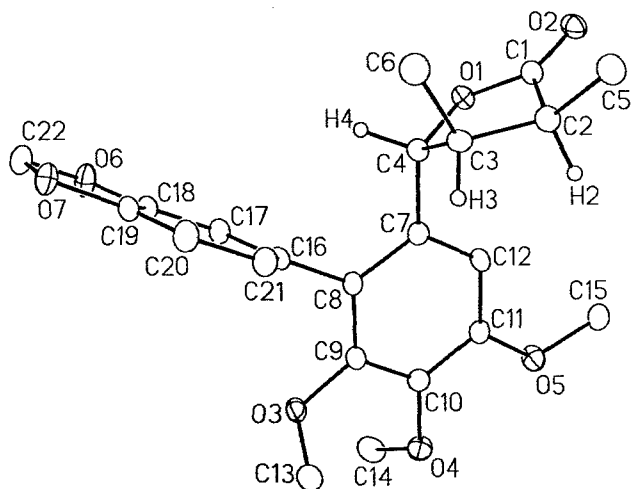


**Figure 2.** View of the molecule more clearly illustrating the relative stereochemistries of the stereogenic centers (note: this compound has crystallized in a centrosymmetric space group, therefore both enantiomers are present in equal abundance in the crystal lattice).

### List of Tables

**Table 1.** Crystallographic Experimental Details

**Table 2.** Atomic Coordinates and Equivalent Isotropic Displacement Parameters

**Table 3.** Selected Interatomic Distances

**Table 4.** Selected Interatomic Angles

**Table 5.** Torsional Angles

**Table 6.** Anisotropic Displacement Parameters

**Table 7.** Derived Atomic Coordinates and Displacement Parameters for Hydrogen Atoms

**Table 1. Crystallographic Experimental Details**

<i>A. Crystal Data</i>	
formula	C <sub>22</sub> H <sub>24</sub> O <sub>7</sub>
formula weight	400.41
crystal dimensions (mm)	0.39 × 0.28 × 0.06
crystal system	triclinic
space group	$P\bar{1}$ (No. 2)
unit cell parameters <sup>a</sup>	
<i>a</i> (Å)	7.6045 (10)
<i>b</i> (Å)	8.7072 (12)
<i>c</i> (Å)	15.590 (2)
$\alpha$ (deg)	75.876 (2)
$\beta$ (deg)	82.717 (2)
$\gamma$ (deg)	80.088 (2)
<i>V</i> (Å <sup>3</sup> )	982.3 (2)
<i>Z</i>	2
$\rho_{\text{calcd}}$ (g cm <sup>-3</sup> )	1.354
$\mu$ (mm <sup>-1</sup> )	0.101
<i>B. Data Collection and Refinement Conditions</i>	
diffractometer	Bruker PLATFORM/SMART 1000 CCD <sup>b</sup>
radiation ( $\lambda$ [Å])	graphite-monochromated Mo K $\alpha$ (0.71073)
temperature (°C)	-80
scan type	$\omega$ scans (0.3°) (15 s exposures)
data collection $2\theta$ limit (deg)	52.78
total data collected	7493 ( $-9 \leq h \leq 9, -10 \leq k \leq 10, -19 \leq l \leq 18$ )
independent reflections	3994 ( $R_{\text{int}} = 0.0362$ )
number of observed reflections ( <i>NO</i> )	2428 [ $F_o^2 \geq 2\sigma(F_o^2)$ ]
structure solution method	direct methods ( <i>SHELXS-86</i> <sup>c</sup> )
refinement method	full-matrix least-squares on $F^2$ ( <i>SHELXL-93</i> <sup>d</sup> )
absorption correction method	Gaussian integration (face-indexed)
range of transmission factors	0.9940–0.9617
data/restraints/parameters	3994 [ $F_o^2 \geq -3\sigma(F_o^2)$ ] / 0 / 262
goodness-of-fit ( <i>S</i> ) <sup>e</sup>	1.012 [ $F_o^2 \geq -3\sigma(F_o^2)$ ]
final <i>R</i> indices <sup>f</sup>	
$R_1$ [ $F_o^2 \geq 2\sigma(F_o^2)$ ]	0.0498
$wR_2$ [ $F_o^2 \geq -3\sigma(F_o^2)$ ]	0.1378
largest difference peak and hole	0.438 and -0.174 e Å <sup>-3</sup>

<sup>a</sup>Obtained from least-squares refinement of 2016 reflections with  $4.87^\circ < 2\theta < 51.64^\circ$ .

(continued)

**Table 1.** Crystallographic Experimental Details (continued)

<sup>b</sup>Programs for diffractometer operation, data collection, data reduction and absorption correction were those supplied by Bruker.

<sup>c</sup>Sheldrick, G. M. *Acta Crystallogr.* **1990**, *A46*, 467–473.

<sup>d</sup>Sheldrick, G. M. *SHELXL-93*. Program for crystal structure determination. University of Göttingen, Germany, 1993.

<sup>e</sup> $S = [\sum w(F_o^2 - F_c^2)^2 / (n - p)]^{1/2}$  ( $n$  = number of data;  $p$  = number of parameters varied;  $w = [\sigma^2(F_o^2) + (0.0572P)^2 + 0.2908P]^{-1}$  where  $P = [\text{Max}(F_o^2, 0) + 2F_c^2]/3$ ).

<sup>f</sup> $R_1 = \sum ||F_o| - |F_c|| / \sum |F_o|$ ;  $wR_2 = [\sum w(F_o^2 - F_c^2)^2 / \sum w(F_o^4)]^{1/2}$ .



**Table 2.** Atomic Coordinates and Equivalent Isotropic Displacement Parameters

Atom	<i>x</i>	<i>y</i>	<i>z</i>	<i>U</i> <sub>eq</sub> , Å <sup>2</sup>
O1	-0.3151(2)	-0.05912(19)	0.33279(10)	0.0349(4)*
O2	-0.4989(2)	-0.1428(2)	0.45120(12)	0.0459(5)*
O3	0.2138(2)	0.3820(2)	0.14179(11)	0.0403(4)*
O4	-0.0333(2)	0.61311(19)	0.20419(11)	0.0464(5)*
O5	-0.3115(2)	0.53286(19)	0.31594(12)	0.0467(5)*
O6	0.2686(2)	-0.0989(2)	-0.02005(12)	0.0516(5)*
O7	0.5073(2)	-0.2536(2)	0.05329(12)	0.0476(5)*
C1	-0.3533(3)	-0.1106(3)	0.42091(16)	0.0345(6)*
C2	-0.1908(3)	-0.1100(3)	0.46798(16)	0.0395(6)*
C3	-0.0375(3)	-0.1291(3)	0.39787(15)	0.0335(6)*
C4	-0.1260(3)	-0.0412(3)	0.31210(15)	0.0313(5)*
C5	-0.1879(4)	-0.2263(3)	0.55829(17)	0.0497(7)*
C6	0.0365(4)	-0.3034(3)	0.39649(19)	0.0507(7)*
C7	-0.1042(3)	0.1334(3)	0.28148(15)	0.0305(5)*
C8	0.0435(3)	0.1760(3)	0.22303(14)	0.0301(5)*
C9	0.0667(3)	0.3372(3)	0.19888(15)	0.0328(5)*
C10	-0.0551(3)	0.4545(3)	0.22909(15)	0.0351(6)*
C11	-0.2009(3)	0.4104(3)	0.28844(15)	0.0340(6)*
C12	-0.2243(3)	0.2504(3)	0.31438(15)	0.0334(6)*
C13	0.3478(4)	0.4187(4)	0.1877(2)	0.0554(8)*
C14	-0.0702(4)	0.6865(3)	0.11451(18)	0.0526(8)*
C15	-0.4490(4)	0.4940(3)	0.38324(19)	0.0505(7)*
C16	0.1732(3)	0.0580(3)	0.18258(14)	0.0299(5)*
C17	0.1476(3)	0.0434(3)	0.09780(15)	0.0349(6)*
C18	0.2675(3)	-0.0637(3)	0.06104(15)	0.0336(6)*
C19	0.4089(3)	-0.1551(3)	0.10491(16)	0.0355(6)*
C20	0.4390(3)	-0.1436(3)	0.18747(16)	0.0408(6)*
C21	0.3179(3)	-0.0346(3)	0.22575(16)	0.0375(6)*
C22	0.4174(4)	-0.2219(3)	-0.02590(19)	0.0495(7)*

Anisotropically-refined atoms are marked with an asterisk (\*). The form of the anisotropic displacement parameter is:  $\exp[-2\pi^2(h^2a^{*2}U_{11} + k^2b^{*2}U_{22} + l^2c^{*2}U_{33} + 2klb^{*c^*}U_{23} + 2hla^{*c^*}U_{13} + 2hka^{*b^*}U_{12})]$ .

**Table 3.** Selected Interatomic Distances (Å)

Atom1	Atom2	Distance	Atom1	Atom2	Distance
O1	C1	1.347(3)	C3	C4	1.542(3)
O1	C4	1.460(3)	C3	C6	1.529(3)
O2	C1	1.199(3)	C4	C7	1.510(3)
O3	C9	1.387(3)	C7	C8	1.396(3)
O3	C13	1.436(3)	C7	C12	1.397(3)
O4	C10	1.373(3)	C8	C9	1.398(3)
O4	C14	1.429(3)	C8	C16	1.495(3)
O5	C11	1.361(3)	C9	C10	1.386(3)
O5	C15	1.407(3)	C10	C11	1.395(3)
O6	C18	1.371(3)	C11	C12	1.388(3)
O6	C22	1.428(3)	C16	C17	1.399(3)
O7	C19	1.381(3)	C16	C21	1.389(3)
O7	C22	1.432(3)	C17	C18	1.365(3)
C1	C2	1.517(3)	C18	C19	1.372(3)
C2	C3	1.510(3)	C19	C20	1.366(3)
C2	C5	1.521(3)	C20	C21	1.393(3)

**Table 4.** Selected Interatomic Angles (deg)

Atom1	Atom2	Atom3	Angle	Atom1	Atom2	Atom3	Angle
C1	O1	C4	110.83(18)	O3	C9	C8	119.2(2)
C9	O3	C13	111.91(18)	O3	C9	C10	118.9(2)
C10	O4	C14	113.5(2)	C8	C9	C10	121.9(2)
C11	O5	C15	117.85(19)	O4	C10	C9	121.7(2)
C18	O6	C22	106.27(19)	O4	C10	C11	118.9(2)
C19	O7	C22	105.82(18)	C9	C10	C11	119.3(2)
O1	C1	O2	121.3(2)	O5	C11	C10	115.3(2)
O1	C1	C2	108.9(2)	O5	C11	C12	125.1(2)
O2	C1	C2	129.8(2)	C10	C11	C12	119.5(2)
C1	C2	C3	102.85(19)	C7	C12	C11	120.8(2)
C1	C2	C5	112.5(2)	C8	C16	C17	118.12(19)
C3	C2	C5	119.5(2)	C8	C16	C21	122.3(2)
C2	C3	C4	101.60(18)	C17	C16	C21	119.6(2)
C2	C3	C6	113.9(2)	C16	C17	C18	117.7(2)
C4	C3	C6	111.5(2)	O6	C18	C17	128.0(2)
O1	C4	C3	104.77(17)	O6	C18	C19	110.1(2)
O1	C4	C7	110.68(17)	C17	C18	C19	121.9(2)
C3	C4	C7	114.41(19)	O7	C19	C18	109.9(2)
C4	C7	C8	119.00(19)	O7	C19	C20	128.0(2)
C4	C7	C12	120.8(2)	C18	C19	C20	122.1(2)
C8	C7	C12	120.1(2)	C19	C20	C21	116.7(2)
C7	C8	C9	118.3(2)	C16	C21	C20	122.0(2)
C7	C8	C16	122.9(2)	O6	C22	O7	107.90(19)
C9	C8	C16	118.8(2)				

**Table 5.** Torsional Angles (deg)

Atom1	Atom2	Atom3	Atom4	Angle	Atom1	Atom2	Atom3	Atom4	Angle
C4	O1	C1	O2	-175.1(2)	C12	C7	C8	C16	-177.5(2)
C4	O1	C1	C2	7.5(2)	C4	C7	C12	C11	177.9(2)
C1	O1	C4	C3	13.7(2)	C8	C7	C12	C11	1.2(3)
C1	O1	C4	C7	-110.1(2)	C7	C8	C9	O3	179.2(2)
C13	O3	C9	C8	-105.4(2)	C7	C8	C9	C10	-2.0(3)
C13	O3	C9	C10	75.7(3)	C16	C8	C9	O3	-3.2(3)
C14	O4	C10	C9	73.4(3)	C16	C8	C9	C10	175.6(2)
C14	O4	C10	C11	-108.5(2)	C7	C8	C16	C17	95.7(3)
C15	O5	C11	C10	-173.0(2)	C7	C8	C16	C21	-85.2(3)
C15	O5	C11	C12	7.5(3)	C9	C8	C16	C17	-81.7(3)
C22	O6	C18	C17	-178.1(3)	C9	C8	C16	C21	97.3(3)
C22	O6	C18	C19	1.3(3)	O3	C9	C10	O4	-0.2(3)
C18	O6	C22	O7	-2.0(3)	O3	C9	C10	C11	-178.3(2)
C22	O7	C19	C18	-1.3(3)	C8	C9	C10	O4	-179.0(2)
C22	O7	C19	C20	178.7(3)	C8	C9	C10	C11	2.9(3)
C19	O7	C22	O6	2.0(3)	O4	C10	C11	O5	0.6(3)
O1	C1	C2	C3	-26.0(2)	O4	C10	C11	C12	-179.8(2)
O1	C1	C2	C5	-155.9(2)	C9	C10	C11	O5	178.7(2)
O2	C1	C2	C3	156.9(2)	C9	C10	C11	C12	-1.7(3)
O2	C1	C2	C5	27.1(4)	O5	C11	C12	C7	179.2(2)
C1	C2	C3	C4	32.3(2)	C10	C11	C12	C7	-0.3(3)
C1	C2	C3	C6	-87.7(2)	C8	C16	C17	C18	179.4(2)
C5	C2	C3	C4	157.7(2)	C21	C16	C17	C18	0.3(3)
C5	C2	C3	C6	37.7(3)	C8	C16	C21	C20	-179.5(2)
C2	C3	C4	O1	-28.7(2)	C17	C16	C21	C20	-0.5(4)
C2	C3	C4	C7	92.6(2)	C16	C17	C18	O6	179.4(2)
C6	C3	C4	O1	92.9(2)	C16	C17	C18	C19	0.2(4)
C6	C3	C4	C7	-145.7(2)	O6	C18	C19	O7	0.0(3)
O1	C4	C7	C8	-151.41(19)	O6	C18	C19	C20	-180.0(2)
O1	C4	C7	C12	31.9(3)	C17	C18	C19	O7	179.4(2)
C3	C4	C7	C8	90.5(2)	C17	C18	C19	C20	-0.6(4)
C3	C4	C7	C12	-86.2(3)	O7	C19	C20	C21	-179.5(2)
C4	C7	C8	C9	-176.8(2)	C18	C19	C20	C21	0.5(4)
C4	C7	C8	C16	5.7(3)	C19	C20	C21	C16	0.1(4)
C12	C7	C8	C9	-0.1(3)					

**Table 6.** Anisotropic Displacement Parameters ( $U_{ij}$ , Å<sup>2</sup>)

Atom	$U_{11}$	$U_{22}$	$U_{33}$	$U_{23}$	$U_{13}$	$U_{12}$
O1	0.0310(9)	0.0387(10)	0.0334(10)	-0.0038(7)	-0.0044(7)	-0.0055(7)
O2	0.0371(10)	0.0394(11)	0.0564(12)	-0.0087(9)	0.0084(9)	-0.0049(8)
O3	0.0437(10)	0.0396(10)	0.0339(10)	-0.0046(8)	0.0063(8)	-0.0088(8)
O4	0.0648(12)	0.0287(10)	0.0407(10)	-0.0008(8)	-0.0003(9)	-0.0064(8)
O5	0.0462(11)	0.0303(10)	0.0547(12)	-0.0072(8)	0.0084(9)	0.0060(8)
O6	0.0445(11)	0.0726(14)	0.0408(11)	-0.0278(10)	-0.0048(8)	0.0051(9)
O7	0.0441(11)	0.0485(11)	0.0482(11)	-0.0194(9)	0.0025(9)	0.0060(8)
C1	0.0330(14)	0.0273(13)	0.0374(14)	-0.0044(10)	0.0023(11)	0.0032(10)
C2	0.0445(15)	0.0355(14)	0.0360(14)	-0.0044(11)	-0.0058(12)	-0.0024(11)
C3	0.0341(13)	0.0255(12)	0.0386(14)	-0.0022(10)	-0.0064(11)	-0.0029(10)
C4	0.0272(12)	0.0309(13)	0.0332(13)	-0.0055(10)	-0.0003(10)	-0.0015(10)
C5	0.0591(18)	0.0435(16)	0.0404(16)	0.0002(12)	-0.0066(13)	-0.0029(13)
C6	0.0530(17)	0.0385(16)	0.0516(17)	-0.0037(13)	-0.0025(14)	0.0069(13)
C7	0.0318(13)	0.0293(13)	0.0275(12)	-0.0036(10)	-0.0052(10)	0.0011(10)
C8	0.0311(12)	0.0316(13)	0.0246(12)	-0.0035(10)	-0.0043(10)	0.0006(10)
C9	0.0350(13)	0.0344(14)	0.0265(13)	-0.0025(10)	-0.0029(10)	-0.0042(11)
C10	0.0434(14)	0.0277(13)	0.0308(13)	-0.0015(10)	-0.0030(11)	-0.0034(11)
C11	0.0360(13)	0.0287(13)	0.0325(13)	-0.0033(10)	-0.0042(11)	0.0036(10)
C12	0.0304(12)	0.0318(13)	0.0321(13)	-0.0012(10)	0.0019(10)	-0.0007(10)
C13	0.0510(17)	0.0593(19)	0.0590(19)	-0.0176(15)	0.0058(15)	-0.0187(14)
C14	0.0557(18)	0.0358(15)	0.0551(18)	0.0103(13)	-0.0087(14)	-0.0027(13)
C15	0.0519(17)	0.0439(16)	0.0531(18)	-0.0196(14)	0.0116(14)	0.0007(13)
C16	0.0294(12)	0.0296(13)	0.0276(13)	-0.0023(10)	0.0003(10)	-0.0042(10)
C17	0.0313(13)	0.0409(15)	0.0304(13)	-0.0061(11)	-0.0030(10)	-0.0023(11)
C18	0.0321(13)	0.0408(14)	0.0292(13)	-0.0105(11)	0.0009(10)	-0.0075(11)
C19	0.0302(13)	0.0317(14)	0.0409(15)	-0.0082(11)	0.0052(11)	-0.0005(10)
C20	0.0357(14)	0.0429(15)	0.0378(15)	-0.0056(12)	-0.0062(11)	0.0079(11)
C21	0.0373(14)	0.0425(15)	0.0297(13)	-0.0066(11)	-0.0059(11)	0.0021(11)
C22	0.0464(16)	0.0548(18)	0.0515(17)	-0.0271(14)	0.0039(13)	-0.0038(13)

The form of the anisotropic displacement parameter is:

$$\exp[-2\pi^2(h^2a^2U_{11} + k^2b^2U_{22} + l^2c^2U_{33} + 2klb^*c^*U_{23} + 2hla^*c^*U_{13} + 2hka^*b^*U_{12})]$$

**Table 7.** Derived Atomic Coordinates and Displacement Parameters for Hydrogen Atoms

Atom	<i>x</i>	<i>y</i>	<i>z</i>	<i>U</i> <sub>eq</sub> , Å <sup>2</sup>
H2	-0.1987	-0.0001	0.4785	0.047
H3	0.0610	-0.0723	0.4057	0.040
H4	-0.0748	-0.0972	0.2636	0.038
H5A	-0.2969	-0.1989	0.5956	0.060
H5B	-0.0826	-0.2194	0.5867	0.060
H5C	-0.1822	-0.3356	0.5507	0.060
H6A	0.1362	-0.3067	0.3502	0.061
H6B	-0.0584	-0.3559	0.3840	0.061
H6C	0.0791	-0.3591	0.4543	0.061
H12	-0.3233	0.2202	0.3550	0.040
H13A	0.4494	0.4493	0.1453	0.066
H13B	0.3889	0.3243	0.2332	0.066
H13C	0.2967	0.5074	0.2158	0.066
H14A	-0.0512	0.7987	0.1008	0.063
H14B	-0.1948	0.6811	0.1070	0.063
H14C	0.0102	0.6300	0.0742	0.063
H15A	-0.5178	0.5926	0.3968	0.061
H15B	-0.3964	0.4273	0.4367	0.061
H15C	-0.5285	0.4352	0.3631	0.061
H17	0.0501	0.1058	0.0668	0.042
H20	0.5376	-0.2067	0.2173	0.049
H21	0.3347	-0.0233	0.2831	0.045
H22A	0.5003	-0.1867	-0.0787	0.059
H22B	0.3752	-0.3201	-0.0316	0.059